

T
HV-91
SHA

A STUDY ON SALTWATER TRANSPORT TOWARDS A PUMPING WELL

A THESIS

submitted in fulfilment of the
requirements for the award of the degree
of
DOCTOR OF PHILOSOPHY
in
HYDROLOGY



By

MOSTAFA ELERAKY ELSAYED SHALABEY



DEPARTMENT OF HYDROLOGY
UNIVERSITY OF ROORKEE
ROORKEE-247 667 (INDIA)

JULY, 1991

CANDIDATE'S DECLARATION

I hereby certify that the work which is being presented in the thesis entitled **A STUDY ON SALTWATER TRANSPORT TOWARDS A PUMPING WELL** in fulfilment of the requirement for the award of the Degree of Doctor of Philosophy, submitted in the Department of Hydrology, University of Roorkee, is an authentic record of my own work carried out during a period from ^{JULY} December 1988 to July 1991 under the supervision of Dr. Deepak Kashyap. *M.E. Shalabey*

The matter embodied in this thesis has not been submitted by me for the award of any other degree.

M.E. Shalabey

(MOSTAFA ELERAKY ELSAYED SHALABEY)

This is to certify that the above statement made by the candidate is correct to the best of our knowledge.

Dated *July, 15*, 1991

Deepak Kashyap

(DEEPAK KASHYAP)
Reader in Hydrology
Department of Hydrology
University of Roorkee
Roorkee(India)

The Ph.D. viva-voca examination of Mr. Mostafa Eleraky Elsayed Shalabey, research scholar has been held on

Signature of Guide(s)

Signature of External Examiner(s)

AKNOWLEDGEMENTS

I express my deep sense of gratitude to Dr. Deepak Kashyap, Reader, Deptt. of Hydrology, University of Roorkee, Roorkee, for his keen interest, guidance and encouragement throughout the course of the present study.

This research venture could be taken up and sustained, only due to the whole hearted cooperation of Dr. Deepak Kashyap.

I wish to express my gratitude to Dr. D.K. Srivastava, Prof and Head, Dept. of Hydrology, University of Roorkee, for making available, facilities of the department.

I wish to express my gratitude to Dr. B.S. Mathur, Prof., Dept. of Hydrology, University of Roorkee, for his cooperation throughout the course of study.

I am thankful to Dr. D.C. Singhal, Dr. Ranvir Singh, Dr. N.K. Goel and H. Joshi, Readers, Dept. of Hydrology, for their cooperation throughout the course of study.

I am thankful to staff of the computer centre for their courteous and prompt assistance.

I offer my heartfelt thanks and deep regards to my Egyptian Government for the financial support during my entire period of stay in India.

I am thankful to India Government for the Financial support during my entire period of stay in India.

I am thankful to Head and all staff members in my Department, Irrigation and Hydraulic, Faculty of Engineering, Alexandria University, Egypt.

I am thankful to my father, my mother, my wife father, my wife mother and my brother Mohamed.

Finally, I am thankful to my wife, my son Alaa, my son Emad, and my daughter Hend.

M. E. Shalabey

(MOSTAFA ELERAKY ELSAYED SHALABEY)



SYNOPSIS

The available analytical solutions for upconing of saltwater interface are based upon many restrictive assumptions which may not always be satisfied. In the present study, an attempt has been made to develop a numerical model for simulation of saltwater transport occurring in consequence of pumping water from a partially penetrating well. The well is assumed to tap only the freshwater zone and saltwater is assumed to occur below the well screen. The model, accounting for both convective and diffusive components of saltwater transport, is based upon a numerical solution of the differential equations governing the pressure distribution and the mass transport in a two-dimensional axi-symmetric flow domain. While calculating the pressure distribution, the variation of the specific weight and dynamic viscosity of fluid due to time and space variation of saltwater concentration is accounted for. The pressure distribution is computed by the finite difference employing iterative alternating direction implicit explicit (IADIE) scheme. To avoid numerical dispersion, computation of the total saltwater transport is accomplished in three stages. First, the convective transport is computed by the method of characteristics. The necessary velocities are calculated from the precomputed pressure distribution. Subsequently, the diffusive transport is computed by the finite difference employing iterative alternating direction implicit explicit (IADIE) scheme. Finally, the two transports are integrated to get the total transport.

Thus, the proposed model basically simulates the vertical and radial movement of the saltwater during and subsequent to the closure of

pumping. Such a simulation leads to estimates of spatially and temporally distributed saltwater concentration in the aquifer and temporally distributed saltwater concentration in the pumped water. Further, the fractional saltwater settlement [i.e., the fraction of saltwater lifted (during the pumping), settling down to the initial position of the interface] at different discrete times since the closure of the pumpage may also be estimated.

The model has been implicitly validated by comparing its response with Bear and Dagan's analytical solution.

The model results have been compared with the field data from Ashqelon region, Isreal reported by Schmorak and Mercado (1969). Reproduction of the entire upconing data points (including the ones not honouring the analytical solution) is quite well.

The model can be employed to determine the permissible discharge and the pumping schedules for wells underlain by saltwater. A possible procedure for such a design has been illustrated.

INDEX

CHAPTER	PARA	DESCRIPTION	PAGE
NUMBER	NUMBER		
		List of Symbols	x
		List of Figures	xvi
		List of Tables	xix
I		INTRODUCTION	
	1.1	General	1
	1.2	Present Study	2
II		LITERATURE REVIEW	
	2.1	Introduction	4
	2.2	Research Work Upto 1930	4
	2.2.1	Macrolevel Planning	4
	2.3	Research Work From 1930 to 1940	5
	2.3.1	Macrolevel Planning	5
	2.3.2	Microlevel Planning	7
	2.4	Research Work From 1940-1960	7
	2.4.1	Macrolevel Planning	7
	2.5	Research Work After 1960	8
	2.5.1	Upconing	8
	2.5.1.1	Upconing Below a Horizontal Infinite Drain.	8
	2.5.1.2	Upconing Below a Point Sink	12
	2.5.1.3	Upconing Below a Well	13
	2.5.2	Two - Three Dimensional Flow Analyses.	16

CHAPTER	PARA	DESCRIPTION	PAGE
	NUMBER	NUMBER	16
	2.5.2.1	Two-Dimensional Analysis	16
	2.5.2.1.1	Two-Dimensional Flow in a vertical Plane	16
	2.5.2.1.1.1	Macrolevel Planning	16
	2.5.2.1.2	Two-Dimensional Horizontal Flow	24
	2.5.2.1.2.1	Macrolevel Planning	24
	2.5.2.2	Three-Dimensional Flow Analysis	25
	2.5.2.2.1	Macrolevel Planning	25
	2.5.3	Field Experiments	26
	2.5.3.1	Macrolevel Planning	26
	2.5.3.2	Microlevel Planning	26
III		THE MODEL DEVELOPMENT	
	3.1	The Problem	27
	3.2	Governing Equations	27
	3.2.1	Differential Equation Governing Two-Dimensional (r-z plane) Unsteady State Axi-Symmetric Mass Transport.	27
	3.2.2	Differential Equation Governing Two- Dimensional (r-z plane) Unsteady State Axi-Symmetric Radial Flow of Fluid with Time and Space Variant Specific Weight and Viscosity.	29
	3.3	The Solution	30
	3.3.1	Solution Strategy	30
	3.3.2	Coordinate System	30
	3.3.3	Convective Transport	30

CHAPTER NUMBER	PARA NUMBER	DESCRIPTION	PAGE
	3.3.3.1	Method of Characteristics	30
	3.3.3.1.1	Simulation of Convective Transport	32
	3.3.3.1.1.1	Model Description	32
	3.3.3.1.1.2	Positioning of Take-off Points	33
	3.3.3.1.1.3	Upward Lifting of Take off Points	36
	3.3.3.1.1.4	Convection of Moving Point	37
	3.3.3.1.1.5	Finite Difference Grid	38
	3.3.3.1.1.6	Estimation of Saltwater Concentration	38
	3.3.4	Total Transport	40
	3.3.4.1	Differential Equation	40
	3.3.4.1.1	Finite Difference Solution	41
	3.3.4.1.2	IADIE Method	41
	3.3.4.1.2.1	Discretization of Concentration and Convective Transport	42
	3.3.4.1.2.2	Computation of Discretized Convective Transport	43
	3.3.4.1.2.3	IADIE Formulation	43
	3.3.4.1.3	The Dispersion Coefficient	56
	3.3.4.1.4	Convergence Criteria	57
	3.3.4.1.5	Integration of Diffusive Transport with the moving points.	57
	3.3.5	Computation of Velocity Distribution	58
	3.3.5.1	Simulation of Pressure Distribution	59
	3.3.5.1.1	Specific Weight Variation	61
	3.3.5.1.2	The Dynamic Viscosity Equation	61
	3.3.5.1.3	The Specific Storage Equation	62

CHAPTER	PARA	DESCRIPTION	PAGE
NUMBER	NUMBER		
	3.3.5.1.4	Time and Space Steps	64
	3.3.5.1.5	Finite Difference Solution	66
	3.3.5.1.6	IADIE Formulation	66
	3.3.5.1.7	Convergence Criteria	88
	3.3.5.1.8	Computation of Nodal Velocities	89
	3.3.5.1.9	Computation of Moving Point Velocities	90
	3.3.6	Total Saltwater Lifted into Suspension	94
	3.3.7	Entry of Saltwater in the Pumped Well	95
	3.3.8	Settlement of Saltwater Interface	97
	3.4	Computer Code	97
IV		MODEL VALIDATION	
	4.1	Comparison With An Analytical Solution	101
	4.1.1	Results	102
	4.2	Comparison with Field Data	109
	4.2.1	Experimental Setup	109
	4.2.2	Reported Parameters	110
	4.2.3	Comparison with Model Results	112
	4.2.3.1	Model Operation	112
	4.2.3.1.1	Pressure Simulation	112
	4.2.3.1.2	Simulation of Saltwater Transport	113
	4.2.3.2	Upconed Interface Positions	113
	4.2.3.3	Saltwater Concentration in Pumped Water.	127
V		MODEL OPERATION	
	5.1	Influence of the Variation of Fluid Properties on the Solution	138

CHAPTER NUMBER	PARA NUMBER	DESCRIPTION	PAGE
	5.2	Well Design	141
	5.2.1	Model Capability	141
	5.2.2	Design Parameter	141
	5.2.3	Model Operation	143
	5.2.3.1	Pressure Simulation	143
	5.2.3.2	Simulation of Saltwater Transport	144
	5.2.4	Model Results	145
VI		CONCLUSION	152
	ANNEXURE-A	Numerical Dispersion	156
	B	Computer Code	160
	C	Output of the Model as a Sample	187
		REFERENCES	212

LIST OF SYMBOLS

SYMBOL	DESCRIPTION	DIMENSION
A	Initial thickness of freshwater domain	[L]
AR_j	Area assigned to each take off point	[L ²]
B	Initial thickness of saltwater domain	[L]
$C_{i,j,k+1}^*$	The finally converged total saltwater concentration at the node (i,j) at discrete time t_{k+1}	[1]
CC_{ijk}	Saltwater concentration at any node (i,j) at discrete time t_k due to convective transport.	[1]
CP_k	Saltwater concentration in the pumped water at discrete time t_k	[1]
d	Strip thickness	[L]
D	Vertical distance between well bottom and initial position of the interface	[L]
$D_{r_{ij}}$	Diffusive coefficient in the radial direction at node (i,j)	[L ² T ⁻¹]
$D_{z_{ij}}$	Diffusive coefficient in the vertical direction at node (i,j).	[L ² T ⁻¹]
H	Total thickness of the aquifer	[L]
J_1	A subset of the moving points, Comprises of all moving points lying in the domain of node (i,j) at discrete time t_k	[1]
J_2	A subset of the moving points, Comprises of all moving points which enter into the domain of the node (i,j) during the time step (t_k to t_{k+1}).	[1]

SYMBOL	DESCRIPTION	DIMENSION
J_3	A subset of the moving points, Comprises of all moving points which move out of the domain of the node (i, j) during the time step (t_k to t_{k+1}).	[1]
J_4	A subset of the moving points, Comprises of all moving points lying in the domain of saltwater node (i, j) at discrete time t_{k+1} .	[1]
J_5	Number of take off points lifted into suspension during the time step (t_k to t_{k+1})	[1]
J_6	A subset of the moving points, Comprises of all moving points which have entered into pumped well till the discrete time t_k .	[1]
J_7	A subset of the moving points, Comprises of all moving points which have reached or fallen below the initial position of the interface during the period t^* to t_k .	[1]
$k_{r,ij}$	Intrinsic permeability in the radial direction at node (i, j).	[L ²]
$k_{z,ij}$	Intrinsic permeability in the vertical direction at node (i, j).	[L ²]
L_p	Length of well	[L]
L_s	Length of screen	[L]
NC	Number of pressure columns	[1]
NCS	Number of columns for saltwater simulation	[1]
NR	Number of pressure rows	[1]
NRB	Number of rows upto bottom of blind pipe	[1]

SYMBOL	DESCRIPTION	DIMENSION
NRS	Number of rows upto initial position of the interface.	[1]
NRW	Number of rows upto bottom of screen	[1]
P_{ijk}	Water pressure at pressure node (i,j) at discrete time t_k	[FL ⁻²]
q_{ijk}^*	The volume of saltwater entering the domain of node(i,j) due to convection in r and z directions per unit volume of water in the domain, per unit time [pre-computed rate of the net convective transport (inflow :+ve, outflow : -ve)]	[T ⁻¹]
q_r	Darcy's velocity in the radial direction.	[LT ⁻¹]
q_z	Darcy's velocity in the vertical direction	[LT ⁻¹]
Q	Discharge rate	[L ³ T ⁻¹]
r	Radial distance from the centre of well	[L]
r_w	Radius of well	[L]
R_{mk}	Radial coordinate of m th moving point at discrete time t_k .	[L]
S_s	Specific storage	[L]
SW_k	Average drawdown ,corresponding to freshwater, in the well screen at discrete time t_k	[L]
t	Time	[T]
t^*	Pumpage time	[T]
U_{ijk}	Radial seepage velocity at pressure node (i,j) at discrete time t_k	[LT ⁻¹]

SYMBOL	DESCRIPTION	DIMENSION
$U(R_m, Z_m, t_k)$	Radial velocity of m^{th} moving point at discrete time t_k	$[L T^{-1}]$
V_{ijk}	Vertical seepage velocity at pressure node (i, j) at discrete time t_k	$[L T^{-1}]$
$V(XS_j, Z_j, t_k)$	Vertical velocity of j^{th} take off point at discrete time t_k	$[L T^{-1}]$
$V(R_m, Z_m, t_k)$	Vertical velocity of m^{th} moving point at discrete time t_k	$[L T^{-1}]$
V_c	Saltwater volume lifted into suspension due to convection	$[L^3]$
V_d	Saltwater volume lifted into suspension due to diffusion.	$[L^3]$
VL_m	Volume of m^{th} moving point	$[L^3]$
VLX_{ij}	Volume of soil-water discretized by node (i, j)	$[L^3]$
VOL	Volume of j^{th} take off point	$[L^3]$
VS_k	Cumulative volume of saltwater entered into the pumped well till the discrete time t_k	$[L^3]$
VSL_k	Cumulative volume of saltwater settled down till discrete time t_k	$[L^3]$
V_t	Total volume of saltwater lifted into suspension in the time step Δt	$[L^3]$
XF_i	Radial coordinate of pressure nodal point (i, j)	$[L]$
XL_j	Radial coordinate of the upstream face of the j^{th} take off point.	$[L]$
XS_j	Radial coordinate of the j^{th} take off point.	$[L]$

SYMBOL	DESCRIPTION	DIMENSION
XU_j	Radial coordinate of the downstream face of the j^{th} take off point.	[L]
z	Vertical coordinate above any datum	[L]
Z_{jk}	Vertical coordinate of j^{th} take off point at discrete time t_k	[L]
ZF_i	Vertical coordinate of pressure nodal point (i,j)	[L]
α	Reciprocal of the bulk modulus of elasticity of aquifer skeleton	[1]
α_L	Longitudinal dispersivity of the aquifer.	[L]
α_T	Transverse dispersivity of the aquifer	[L]
β	Reciprocal of the bulk modulus of elasticity of water.	[1]
ΔC_{ij}	Change of concentration, at node (i,j), due to the diffusive transport.	[1]
Δr_j	Radial spacing between pressure nodes (i,j) and (i,j+1)	[L]
Δr_{sj}	Radial spacing between the j^{th} and $(j+1)^{\text{th}}$ take off points.	[L]
Δt	Time step for pressure simulation from t_k to t_{k+1}	[T]
Δt_s	Time step for saltwater simulation	[T]
Δt_s^m	Maximum desirable time step for simulation of saltwater transport	[T]
ΔV_{ij}	Addition or abstraction of saltwater volume due to diffusive transport at node (i,j).	[L ³]

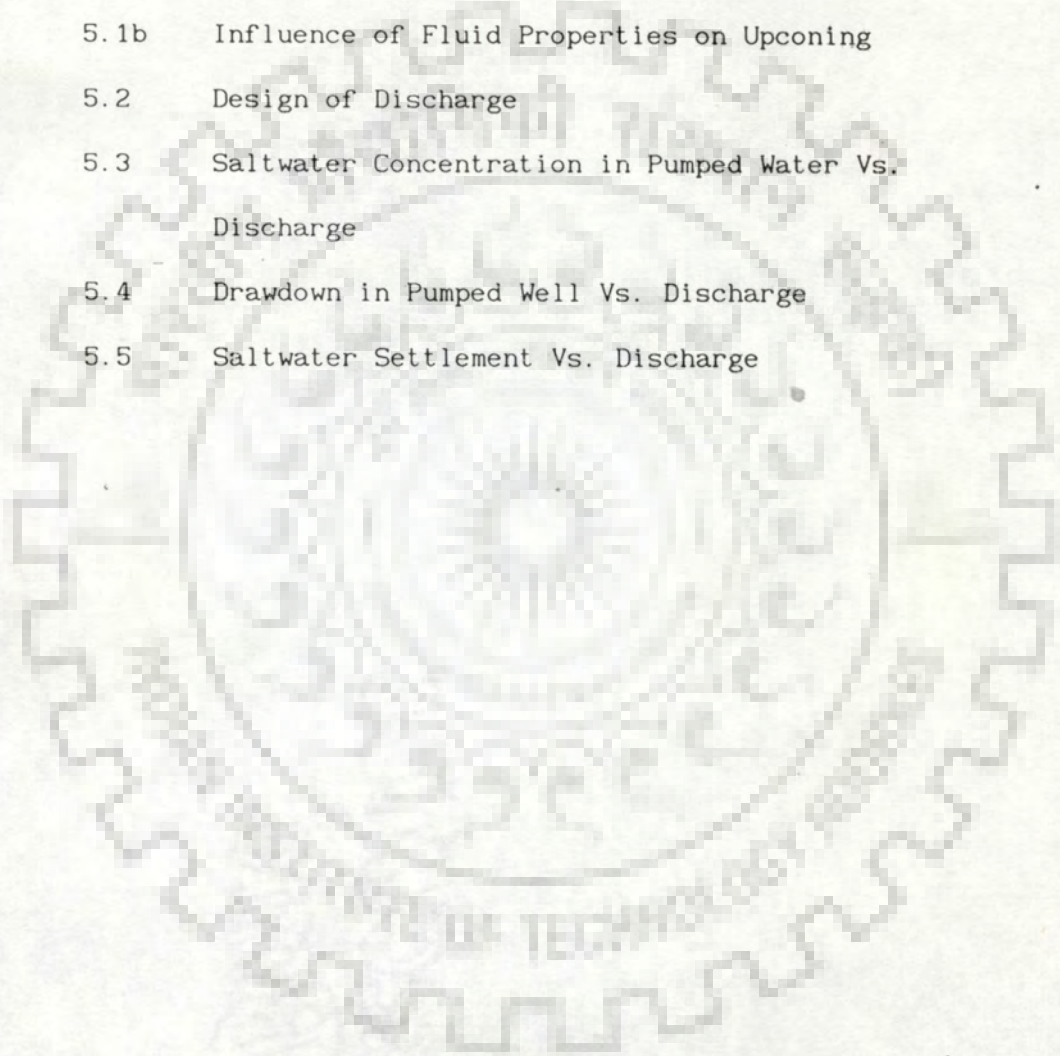
SYMBOL	DESCRIPTION	DIMENSION
Δz_i	Vertical distance between node (i,j) and (i+1,j).	[L]
ϵ	Pre-stipulated convergence factor for pressure simulation.	[FL ⁻²]
ϵ_1	Pre-stipulated convergence factor for saltwater simulation.	[1]
ϕ	Aquifer porosity	[1]
γ_{ij}	Specific weight of water at pressure node (i,j)	[FL ⁻³]
γ_f	Specific weight of freshwater	[FL ⁻³]
$\gamma(C)$	Specific weight of water having C units of volume of saltwater per unit total volume.	[FL ⁻³]
γ_s	Specific weight of saltwater	[FL ⁻³]
μ_{ij}	Dynamic viscosity of water at pressure node (i,j).	[FTL ⁻²]
$\mu(0)$	Dynamic viscosity of freshwater	[FTL ⁻²]
$\mu(C)$	Dynamic viscosity of water having C units of saltwater per unit total volume	[FTL ⁻²]

LIST OF FIGURES

NUMBER	DESCRIPTION	PAGE
2.1	Ghyben-Herzberg Interface	6
2.2	Shapes of Upconed Interface Under a Drain	10
3.1	Saltwater Upconing Beneath a Pumping Well	28
3.2a	Take Off Points	31
3.2b	Positioning of Take Off Points	34
3.3	Lifting of Take Off Points	35
3.4	Finite Difference Mesh and Boundaries for Simulation of Saltwater Transport	39
3.5	Boundary Nodes for Simulation of Saltwater Transport	47
3.6a	Oswald Viscometer	63
3.6b	Variation of Viscosity With Saltwater Concentration	63
3.7	Finite Difference Mesh and Boundaries for Pressure Simulation.	67
3.8	Boundary Nodes for Pressure Simulation	74
3.9	Interpolation to Calculate Velocities of Moving Points.	91
3.10	Time Steps	94
4.1	Pumping Well	103
4.2a	Influence of Screen Length on Upconing (Time = 405 min , $Q=0.002 \text{ m}^3/\text{min}$)	104
4.2.b	Influence of Screen Length on Upconing (Time = 973 min , $Q=0.002 \text{ m}^3/\text{min}$)	105
4.3.a	Influence of Saltwater Layer Thickness on Upconing (Time 405 min , $Q=0.002 \text{ m}^3/\text{min}$)	106

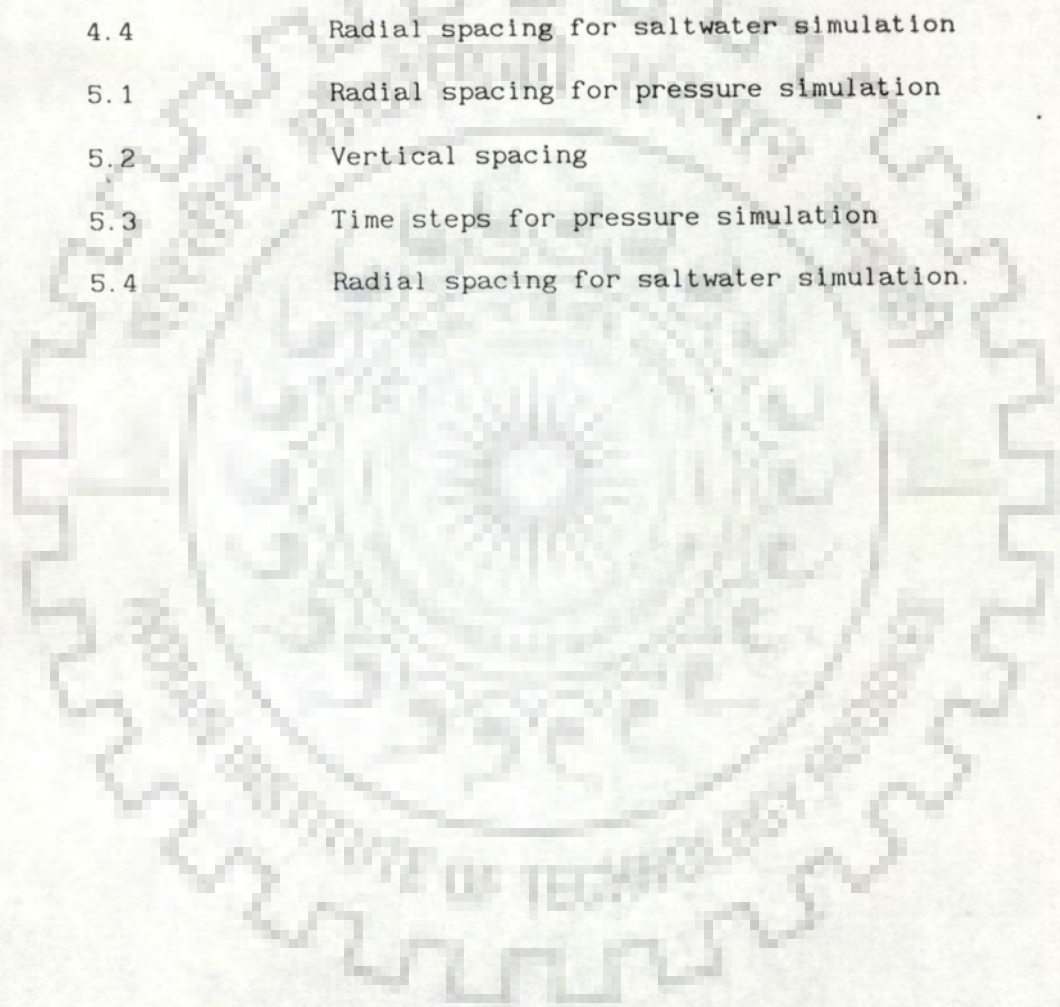
NUMBER	DESCRIPTION	PAGE
4.3.b	Influence of Saltwater Layer Thickness on Upconing (Time 973 min , $Q=0.002 \text{ m}^3/\text{min}$)	107
4.4	Influence of Z/D on Upconing ($Q=0.002 \text{ m}^3/\text{min}$)	108
4.5	Layout of Pumping and Observation wells	111
4.6	Position of Moving Points (Test A, Time=2.93 days)	114
4.7	Position of Moving Points (Test A, Time=8 days)	115
4.8	Upconing and Settlement Vs. Time (Test A, $r=4.5 \text{ ms}$)	119
4.9	Upconing and Settlement Vs. Time (Test B, $r=4.5 \text{ ms}$)	120
4.10	Upconing and Settlement Vs. Time (Test A, $r=12.4 \text{ ms}$)	121
4.11	Upconing and Settlement Vs. Time (Test B, $r=12.4 \text{ ms}$)	122
4.12	Upconing and Settlement Vs. Time (Test A, $r=16.7 \text{ ms}$)	123
4.13	Upconing and Settlement Vs. Time (Test B, $r=16.7 \text{ ms}$)	124
4.14	Upconing and Settlement Vs. Time (Test A, $r=33.9 \text{ ms}$)	125
4.15	Upconing and Settlement Vs. Time (Test B, $r=33.9 \text{ ms}$)	126
4.16	Position of the Interface (Test A, time =8 days)	128
4.17	Position of the Interface (Test A, time=30 days)	129
4.18	Position of the Interface (Test A, time=62 days)	130
4.19	Position of the Interface (Test B, time=16 days)	131
4.20	Position of the Interface (Test B, time=57 days)	132
4.21	Time Variation of Cumulative Saltwater Entered into Pumping Well (Test A)	133
4.22	Time Variation of Cumulative Saltwater Entered into Pumping Well (Test B)	134
4.23	Relation Between Saltwater Concentration and Salt Concentration	135

NUMBER	DESCRIPTION	PAGE
4.24	Saltwater Concentration in Pumped Water Vs. Time (Test A).	136
4.25	Saltwater Concentration in Pumped Water Vs. Time (Test B)	137
5.1a	Influence of Fluid Properties on Upconing	139
5.1b	Influence of Fluid Properties on Upconing	140
5.2	Design of Discharge	142
5.3	Saltwater Concentration in Pumped Water Vs. Discharge	149
5.4	Drawdown in Pumped Well Vs. Discharge	150
5.5	Saltwater Settlement Vs. Discharge	151



LIST OF TABLES

NUMBER	DESCRIPTION	PAGE
3.1	Number of time steps	65
4.1	Radial spacing for pressure simulation	116
4.2	Vertical spacing	117
4.3	Time steps for pressure simulation	117
4.4	Radial spacing for saltwater simulation	118
5.1	Radial spacing for pressure simulation	146
5.2	Vertical spacing	146
5.3	Time steps for pressure simulation	147
5.4	Radial spacing for saltwater simulation.	147



CHAPTER I

INTRODUCTION

1.1 GENERAL

In many aquifers, freshwater may be underlain by saltwater. The ground water of such aquifers can be pumped through partially penetrating wells tapping only the upper part of the freshwater zone. However, the partial penetration induces vertically upward velocity to the saltwater, drawing the saltwater into the freshwater zone of the aquifer. Such a convective transport of the saltwater is termed as "upconing". Apart from the upconing, there is some upward movement of the saltwater due to diffusion. An indiscriminately long duration of pumping can lead to entry of saltwater into the well. Subsequent to the closure of pumpage, the heavier saltwater, lifted into the freshwater zone during pumping, starts settling down.

Planning of groundwater development in coastal aquifers may have two distinct aspects i.e., control of saltwater intrusion to an acceptable extent and control of the saltwater concentration in the pumped water to a permissible level. The first aspect involves designing such a regional pumping/recharge pattern which keeps the interface between the freshwater and saltwater at a pre-assigned large enough depth.

The second aspect, to which the present study is related, involves designing the well system for implementing the evolved pumping pattern. The wells as well as their pumping schedules have to be so designed that the localized vertically upward transport of the saltwater [comprising of the convective transport (upconing) and the diffusive

transport] below a pumping well does not lead to an excessive saltwater concentration in the pumped water.

The available analytical solutions of the upconing [e.g., Muskat's approximate solution, solution based upon Dupuit's assumptions (Bear, 1979); Method of small perturbation (Dagan and Bear, 1968); and Bear and Dagan's analytical solution (Schmorak and Mercado, 1969)] permit estimation of only the convective upconing below a point sink/horizontal drain (and not a well) in an incompressible aquifer (i.e., specific storage = 0) provided the upconing does not exceed a threshold value (varying from 0.25 to 0.5 times the vertical distance between the point sink/drain and the initial position of the interface).

1.2 PRESENT STUDY

In the present study, an attempt has been made to develop a numerical model for simulation of saltwater transport occurring in consequence of pumping water from a partially penetrating well. The well is assumed to tap only the freshwater zone and saltwater is assumed to occur below the well screen. The model, accounting for both convective and diffusive components of saltwater transport, is based upon a numerical solution of the differential equations governing the pressure distribution and the mass transport in a two - dimensional axisymmetric flow domain. While calculating the pressure distribution, the variation of the specific weight and dynamic viscosity of fluid due to time and space variation of saltwater concentration is accounted for. The pressure distribution is computed by the finite difference. To avoid numerical dispersion, computation of the total saltwater transport is accomplished in three stages. First, the convective transport is computed by the method of characteristics. The necessary velocities are

calculated from the precomputed pressure distribution. Subsequently, the diffusive transport is computed by the finite difference. Finally, the two transports are integrated to get the total transport. The model is capable of simulating the upward saltwater transport during pumping; entry of saltwater into the well and its settlement on closure of the pumpage.

The saltwater transport, as computed by the proposed model, is found to converge to the analytical's solution as the ideal conditions assumed therein are approached. However, under non-ideal conditions, the numerical solution varies significantly from the analytical solution. The numerical model has reproduced, the field data reported by Schmorak and Mercado (1969) quite well.

The model can be employed to determine the permissible discharge and the pumping schedules for wells underlain by saltwater. A possible procedure for such a design has been illustrated.

CHAPTER II

LITERATURE REVIEW

2.1 INTRODUCTION

Planning of groundwater development in coastal aquifers may have two distinct aspects i.e., control of saltwater intrusion to an acceptable extent and control of the saltwater concentration in the pumped water to a permissible level. The first aspect involves designing such a regional pumping/recharge pattern (distributed in space and time) which keeps the interface between the freshwater and saltwater at a preassigned large enough depth. This may be viewed as Regional or Macrolevel Planning. The second aspect essentially involves designing the well system for implementing the evolved pumping pattern. The wells as well as their pumping schedules have to be so designed that the localized vertically upward transport of saltwater [(comprising of the convective transport (upconing) and the diffusive transport] below a pumping well does not lead to an excessive saltwater concentration in the pumped water. This may be viewed as Microlevel Planning.

The reported research work in these two aspects is described in the following paragraphs.

2.2 RESEARCH WORK UPTO 1930

2.2.1 Macrolevel Planning

The equation given by Badon and Ghyben in 1888 and by Herzberg in 1901 (Bear, 1979) permits an estimation of the position of the saltwater-freshwater interface. The interface is assumed to be sharp

(the sharp interface assumes that the fresh water - saltwater system is composed of two completely immiscible fluids). The equation, based upon the assumptions of static equilibrium and hydrostatic pressure distribution in the fresh water region with stationary seawater, is as follows;

$$Z = \frac{\rho_f}{\rho_s - \rho_f} h \quad \dots\dots(2.1)$$

Where Z is the depth of the interface below mean sea level at any location, h is the height of the water table above the interface at the same location, and ρ_s and ρ_f are the densities of saltwater and freshwater respectively (refer Fig.2.1). Substituting $\rho_f = 1.0 \text{ gm/cm}^3$ and $\rho_s = 1.025 \text{ gm/cm}^3$, the Ghyben - Herzberg relationship indicates that $Z = 40 h$, i.e., the depth of a stationary interface below sea level is 40 times the height of the fresh water table above it.

2.3 RESEARCH WORK FROM 1930 TO 1940

2.3.1 Macrolevel Planning

Hubbert (1940) used the dynamics of the interface to derive an equation governing the depth of interface by assuming the freshwater head (h_f) and saltwater head (h_s) as follows;

$$h_f = \frac{p}{\rho_f g} + Z \quad \dots\dots(2.2)$$

$$h_s = \frac{p}{\rho_s g} + Z \quad \dots\dots(2.3)$$

Where p is the fluid pressure at a point at which the head is measured, g is the gravity acceleration, Z is the elevation (above datum) of the point.

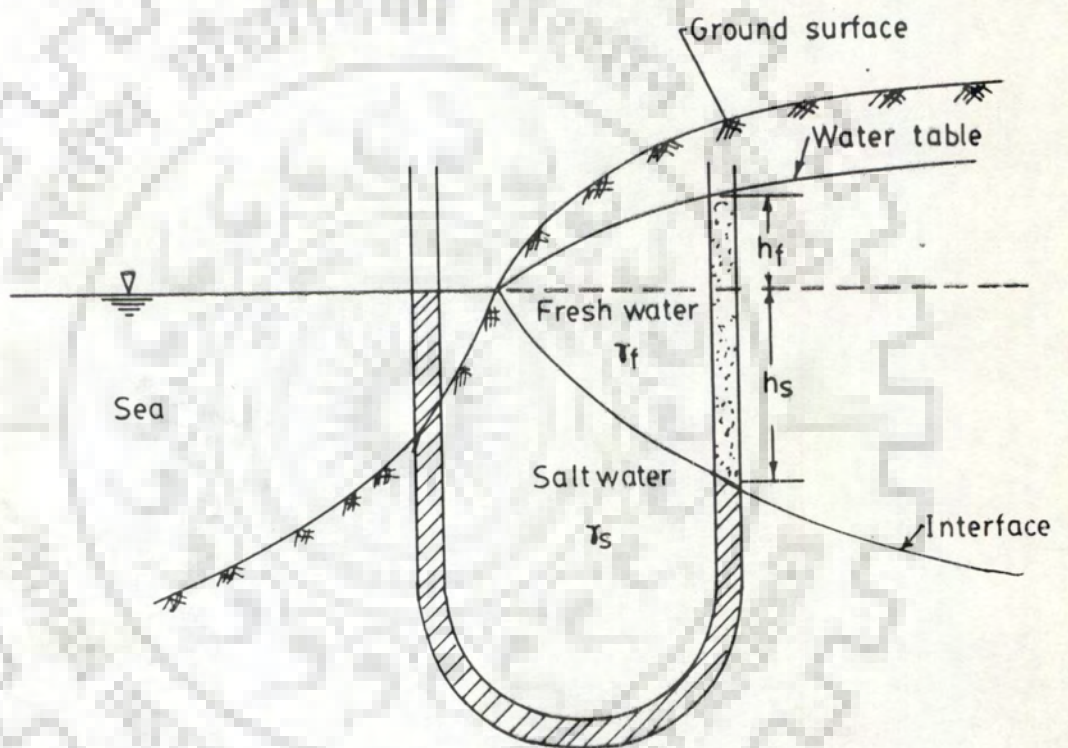


Fig (2.1) Ghyben - Herzberg Interface (Bear 1979)

From equations (2.2) and (2.3) the elevation (Z) at a point on the interface can be written as follows;

$$Z = \frac{\rho_f}{(\rho_f - \rho_s)} h_f - \frac{\rho_s}{(\rho_f - \rho_s)} h_s \quad \dots\dots(2.4)$$

This equation is an improvement over the Ghyben - Herzberg's equation because it relates the freshwater and saltwater heads on the interface to it's position, whereas the Ghyben - Herzberg equation relates the head at the water table to the position of the interface.

2.3.2 Microlevel Planning

Muskat and Wyckoff (Muskat, 1937) presented the earliest known solution for brine upconing below an oil well using a sharp interface.

2.4 RESEARCH WORK FROM 1940-1960

During these years, a large number of studies related to the ground water management in coastal aquifers, were carried out. Most of these studies still form the basis for understanding the mechanisms of saltwater transport. The proposed models were generally validated by comparing their solutions with field data.

2.4.1 Macrolevel Planning

Strigfield et al. (1941) studied the saltwater intrusion in the coastal area of Georgia and Northeastern Florida.

Several relationships were developed during these years. Glover (1959) developed the following equation to describe the sharp interface under steady flow condition:

$$\Delta\gamma^2 - \frac{2q}{\Delta\gamma K} x - \frac{q^2}{\Delta\gamma^2 K^2} y = 0.0 \quad (2.5)$$

Where q is the freshwater discharge per unit length of shore, K is the

hydraulic conductivity of the medium, $\Delta\gamma = (\rho_s - \rho_f)/\rho_f$, ρ_s and ρ_f are the densities of saltwater and freshwater, respectively, x is the distance from the shore, and y is the depth from mean sea level.

Cooper (1959) developed a hypothesis to describe the dispersion of salts produced by reciprocative motion of the saltwater front in a coastal aquifer and defined the amount of mixing.

Henry (1959) developed a few theoretical equations for determining the shape and location of the interface under various conditions. He assumed that the flow is steady and two-dimensional, the freshwater and saltwater are immiscible, and there is no fingering.

Kohout (1960) studied the saltwater movement in the Biscayne aquifer along the coast of the Miami area, Florida. He concluded that, over a period of nearly 20 years, the saltwater front in this area was dynamically stable at a position seaward of that computed according to the Ghyben Herzberg formula.

Luszczynski and Swarzenski (1960) studied the position and Chloride concentration of the saltwater body in the Magothy formation in the Cedarhurst-Woodmere area of southwestern Nassau county, Long Island, N.Y.

2.5 RESEARCH WORK AFTER 1960

The research work reported after 1960 can be classified into the following topics

- 1 Upconing
- 2 Two-three dimensional flow analyses
- 3 Field experiments

2.5.1 Upconing

The reported upconing solutions can be classified into the following categories

- 1 Upconing below a horizontal infinite drain
(line sink of infinite length)
- 2 Upconing below a point sink
- 3 Upconing below a well (finite vertical sink)

2.5.1.1 Upconing Below a Horizontal Infinite Drain

(Line Sink of Infinite Length)

Bear and Dagan (1964b) presented solutions describing the shape and position of an interface between two immiscible liquids of different densities under different conditions (refer Fig:2.2), using the hodograph method. Other solutions have been given by several investigators (Bear, 1979). The solutions hold good provided the rise of interface is small in comparison to the distance between the initial position of the interface and the drain. Dagan and Bear (1968) presented solutions for time dependent interface upconing below a infinite drain in an aquifer of finite and infinite thickness. The solutions account for the anisotropy and the influence of fluid properties on hydraulic conductivity. The solutions are based upon the method of small perturbations. Dagan and Bear (1968) determined the range of validity of these solutions by means of experiments on a sand box model. They concluded that the approximate solutions hold good provided the upconing does not exceed one third of the initial distance between the interface and the drain.

The equations are as follows;

For finite thickness

$$Z = \frac{\mu_f q}{\pi \Delta\gamma (k_x k_z)^{1/2}} \int_0^{\infty} \frac{1}{\lambda} \frac{\cosh [\lambda(a-d)]}{\sinh(\lambda a)}$$

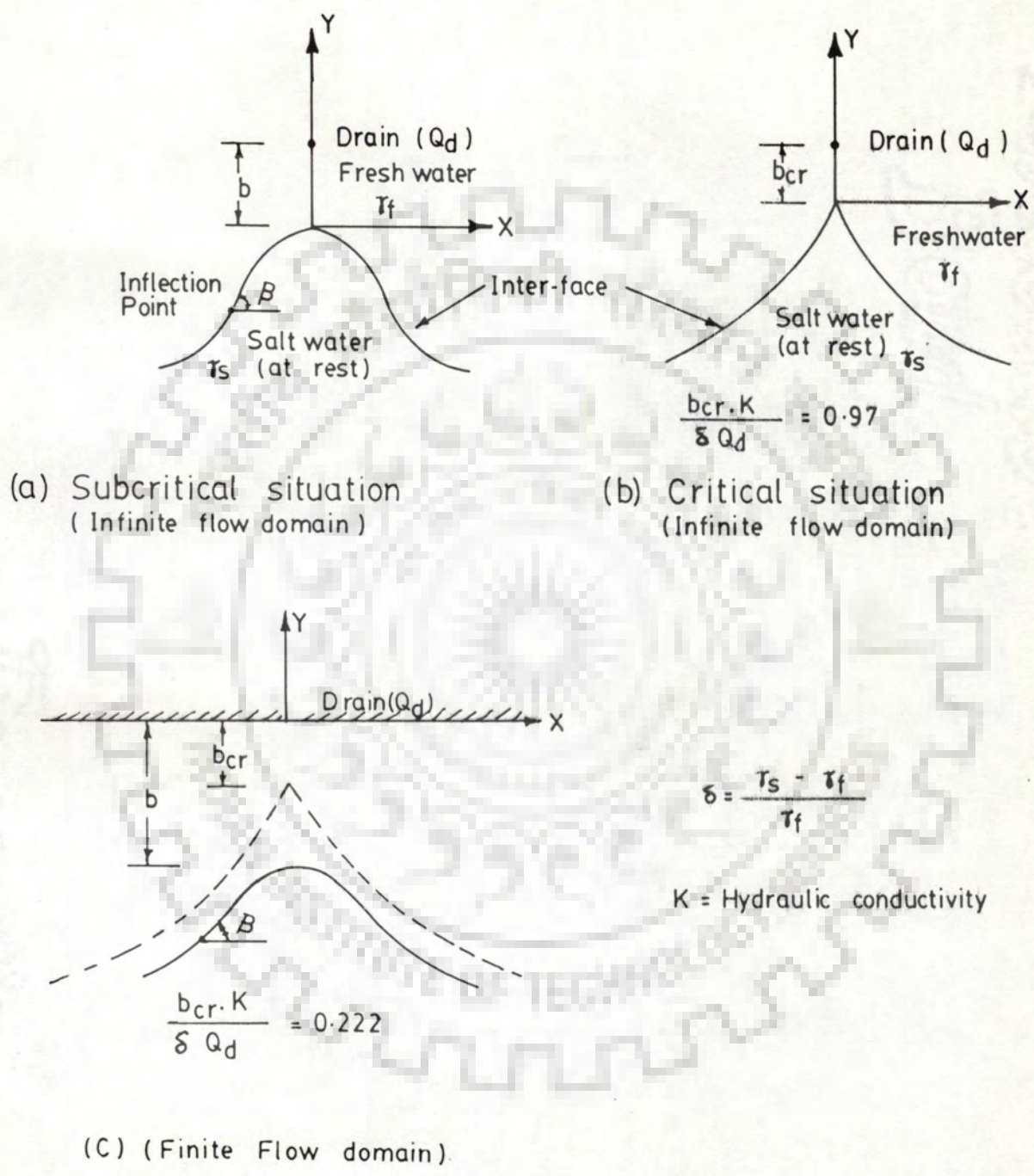


Fig (2.2) Shapes of Upconed Interface Under a Drain
(Bear and dagan, 1964 b)

$$\left\{ 1 - \exp\left(\frac{-\lambda k_z \Delta\gamma}{\phi [\mu_f \cotgh(\lambda a) + \mu_s \cotgh(\lambda b)]} t \right) \right\} \cos\left[\lambda \left(\frac{k_z}{k_x} \right)^{1/2} x \right] d\lambda \quad \dots\dots\dots (2.6)$$

For infinite thickness

$$Z = \frac{\mu_f q}{2\pi \Delta\gamma (k_x k_z)^{1/2}} \ln \frac{\left(\frac{k_z}{k_x} \right)^2 x^2 - \left[\frac{k_z \Delta\gamma t}{\phi (\mu_f + \mu_s)} + d \right]^2}{\left(\frac{k_z}{k_x} \right)^2 x^2 + d^2} \quad \dots\dots\dots (2.7)$$

Where Z is the vertical upward rise above the initial position of the interface, a and b are the initial thickness of freshwater and saltwater zones in the aquifer respectively, q is the drain discharge, $\Delta\gamma = \gamma_s - \gamma_f$, γ_s and γ_f are the saltwater and freshwater specific weights respectively, ϕ is the aquifer porosity, μ_f and μ_s are the freshwater and saltwater dynamic viscosities respectively, x is the horizontal distance from the drain, d is the vertical distance between the initial position of the interface and bottom of drain, λ is Fourier function, and k_x and k_z are the intrinsic permeabilities in the horizontal and vertical directions respectively.

Ackermann and Chang (1971) presented graphically the effect of pumping rate on the interface and freshwater/saltwater heads assuming immiscibility of fluids. They determined the validity of their results by means of experiments on an electric analog model.

Kembloski (1985) presented a new implicit approximation of the sharp interface motion under drain as a sequence of quasi-steady states (Bear, 1979). He compared his results with experimental data reported by Dagan and Bear (1968).

2.5.1.2 Upconing Below a Point Sink

Dagan and Bear (1968) presented a solution for time dependent interface upconing below a point sink in an isotropic aquifer of finite thickness. The solution accounts for the influence of fluid properties on hydraulic conductivity. The solution is based upon the method of small perturbations. Dagan and Bear (1968) determined the range of validity of this solution by means of experiments on a sand box model. They concluded that the approximate solution holds good provided the upconing does not exceed one third of the initial distance between the interface and point sink.

The equation is as follows

$$Z = \frac{\mu_f Q}{2\pi\Delta\gamma(k_x k_z)^{1/2}} \int_0^{\infty} \frac{\cosh[\lambda(a-d)]}{\sinh(\lambda a)} [1 - \exp\left(\frac{-\lambda k_z \Delta\gamma t}{\phi [\mu_f \cotgh(\lambda a) + \mu_s \cotgh(\lambda b)]}\right)] J_0(\lambda r) d\lambda \quad \dots (2.8)$$

Where Z is the vertical upward rise above the initial position of the interface, Q is the point sink discharge, r is the radial distance from the point sink, J_0 is the Bessel's function, a and b are the initial thickness of freshwater and saltwater zones in the aquifer respectively, $\Delta\gamma = \gamma_s - \gamma_f$, γ_s and γ_f are the saltwater and freshwater specific weights respectively, ϕ is the aquifer porosity, μ_f and μ_s are the freshwater and saltwater dynamic viscosities respectively, d is the vertical distance between the initial position of interface and bottom of drain, λ is Fourier function, and k_x and k_z are the intrinsic permeabilities in the horizontal and vertical directions respectively.

2.5.1.3 Upconing Below a Well (Finite Vertical Sink)

Bennett et al. (1968) used an electric analog model to study brine upconing beneath freshwater wells in the Punjab Region of West Pakistan to determine permissible pumping rates for partially penetrating wells. Their results give a good indication of maximum production rates for a wide range of cases.

Bear and Dagan (Schmorak and Mercado, 1969) presented a solution for time dependent interface upconing below a partially penetrating well in an aquifer of infinite thickness. The solution accounts for anisotropy and ignores the influence of fluid properties on hydraulic conductivity. The solution (equation 4.1, chap. 4) is based upon the method of small perturbations. Dagan and Bear (1968) determined the range of validity of this solution by means of experiments on a sand box model. They concluded that the approximate solution holds good provided the upconing does not exceed one third of the initial distance between the interface and bottom of well.

Sahni (1973) presented numerical and experimental models for upconing below a partially penetrating skimming well, using a finite difference iterative technique for numerical model. He reported that the numerical model results showed better agreement than the Muskat's analysis with the results of experiments conducted by him (Sahni).

Haubold (1975) found that the Muskat's analytical solution achieves a close match to the Hele-Shaw model results when $Z/D \leq 0.5$ (Z is the interface rise and D is the distance between initial position of interface and bottom of well).

The reported numerical solutions (e.g. Chandler and McWhorter, 1975) are based upon estimation of the steady state piezometric head distribution.

Rubin and Pinder (1977) described the upconing below a pumping well taking into account the miscibility of the two fluid.

Diersch et al.(1984) used a finite element model for estimating upconing below a pumping well. The effects of diffusive transport and density dependence were accounted for in this study.

Srimal (1985) and Cat (1986) simulated the movement of saltwater below partially a penetrating well tapping a confined aquifer by using the method of characteristics. However, these studies were not conclusive because the variation of specific weight over the space and time (caused by varying saltwater concentration) was not accounted for.

Wirojanagud et al.(1985) presented two axi - symmetric models, assuming an abrupt interface. In the first model, he used the finite element method with an iterative scheme for solving the steady state equation. The other model accounts for diffusive transport and it's results were compared with the analytical solution for the fully penetrating well. He further used the technique of dimensional analysis for designing the depth of well and pumpage rate.

Reilly et al.(1987) developed a numerical finite - element model assuming a sharp interface. They validated the results with the results reported by Bennett et al.(1968). Further, they employed the model to estimate the maximum permissible discharge from Truro well field.

Reilly and Goodman (1987) presented a numerical solution for diffusive transport employing finite element. They used the sharp interface method and the fluid - density dependent solute transport method to simulate saltwater upconing beneath a pumping well. They compared the sharp interface results with those of a variable-density diffusive transport model. They found that even for stable

upconing, significant quantities of saltwater will be pumped and that the development of a transition zone is mainly dependent on the transverse dispersivity. They simulated the upconing at Test Site No.4, Truro, Cape Cod, Massachusetts.

Hoque (1987) presented a numerical model for simulation of saltwater upconing in confined, unconfined, homogeneous / heterogeneous and isotropic / anisotropic aquifers using the block - centered finite difference method. He used line successive overrelaxation technique (LSOR) and banded algorithm to solve the matrix equations. He found that the results of his model were close to Bear and Dagan's analytical solution (Schmorak and Mercado, 1969) for small distances from the well. For large distances, the deviation was quite large.

McElwee and Kemblowski (1990) developed an approximate model of saltwater upconing in aquifers using explicit, implicit and Crank-Nicolson procedures, assuming validity of Dupuit - Forchheimer's assumptions. The model accounts for vertical diffusive transport. They further, presented a complete steady state analytical solution (equations 2.9 to 2.11) assuming constant hydraulic conductivity and stationary saltwater.

$$\phi_s = [1 - \alpha^{-1}] \phi_f(0) + \alpha Z_b(0) \quad \dots (2.9)$$

$$[\phi_f(x) - \phi_s]^2 = -\alpha N x^2 / [1 + \alpha] K_f + 2 [\phi_f(0) - \phi_s]$$

$$(\partial \phi_f / \partial x)_{x=0} x + [\alpha / (1 + \alpha)]^2 [\phi_f(0) - Z_b(0)]^2 \quad \dots (2.10)$$

$$Z_b(x) = [(1 + \alpha) / \alpha] \phi_s - (1 / \alpha) \phi_f(x) \quad \dots (2.11)$$

Where ϕ_s is the saltwater piezometric head $= Z + \frac{p}{\gamma_s}$, Z is the vertical coordinate, p is the pressure, γ_s is the specific weight of saltwater, $\alpha = \gamma_s - \gamma_f$, γ_f is the specific weight of freshwater, $\phi_f(0)$ is the freshwater piezometric head at $x = 0$, X is the horizontal distance from well, $Z_b(0)$ is the elevation of the transition zone bottom at $x = 0$, $\phi_f(X)$ is the freshwater piezometric head at any distance X , N is discharge (negative) or recharge (positive), K_f is the hydraulic conductivity for freshwater, and $Z_b(x)$ is the elevation of the transition zone bottom at any distance x .

2.5.2 Two - Three Dimensional Flow Analyses

2.5.2.1 Two - Dimensional Flow Analysis

The reported research on two dimensional flow analysis can be divided into

1. Two - dimensional flow in a vertical plane
2. Two - dimensional horizontal flow

2.5.2.1.1 Two - Dimensional Flow in a Vertical Plane

Such flow analysis accounts for the role of the vertical hydraulic gradients in the saltwater transport.

2.5.2.1.1.1 Macrolevel Planning

Rumer and Harleman (1963) presented an equation for the convective and dispersive movement of the interface. They conducted laboratory experiments and found a good agreement between their solution and experimental results.

Ackermann and Sridurongkatum (1964) presented an analytical solution for the freshwater intrusion due to seepage from a canal into a salinized aquifer. They further validated the solution by an electric analog model.

Bear and Dagan (1964a) presented solutions of the transient

movement of an abrupt interface in an isotropic, homogeneous confined coastal aquifer. The solutions are based on the Dupuit - Forchheimer's assumptions and neglect diffusive transport and water compressibility. The authors have validated their solutions by a Hele-Shaw model.

Charmonman (1965) presented a solution of the pattern of freshwater flow in an unconfined aquifer. Though, the solution is valid for unconfined aquifers only, the author has shown that it may as well be applied to confined aquifers also.

Columbus (1965) developed an analytical steady state solution of saltwater intrusion in an unconfined aquifer. He validated the solution by a viscous flow model. The solution holds good even when the Dupuit - Forchheimer's assumptions are not satisfied.

Rumber and Shiau (1968) presented an equation for the position of the interface under isotropic and nonhomogenous, and anisotropic and nonhomogenous conditions. They found the results to compare well with Henry's solutions reported in 1964 (Rumber and Shiau, 1968) for both confined and unconfined aquifers when the depth of the aquifer is less than the length of saltwater intrusion.

Hantush (1968) simulated unsteady movement of freshwater in a thick saline unconfined aquifer under different boundary conditions.

Bruch (1970) presented results of a series of dispersion experiments in a two - dimensional porous medium.

Shechter and Schwarz (1970) arrived at the optimal design of coastal collector wells, with respect to the economic engineering and hydrologic considerations.

Pinder and Cooper (1970) presented a numerical solution for the position of the saltwater front in coastal aquifers. They used the method of characteristics, assuming that: the dynamic viscosity, the

dispersion coefficient and porosity are constant with space and time, and the effect of release of water from storage is negligible on the saltwater front movement.

Shamir and Dagan (1971) presented a finite difference numerical solution, assuming a shallow sharp interface and horizontal flow (Dupuit - Forchheimer's assumptions). The model results are reported to be in good agreement with analytical solutions but only in a fair agreement with Hele-Shaw model.

Bennett and Giusti (1971) used an electric analog model for the simulation of the interface in a coastal aquifer near Ponce, Puerto Rico.

Collins et al. (1972) employed Hele-Shaw model to simulate fresh and saltwater motion in aquifers of Long Island, N.Y.

Lee and Cheng (1974) presented a finite element model for simulating saltwater intrusion in coastal aquifers, assuming the seepage velocity perpendicular to seepage surface. The results compared well with the solutions of Henry, 1960 (Lee and Chang, 1974) and Pinder and Cooper (1970), and also with the field data from Biscayne aquifer at Cutler area, Florida (Kohout, 1960).

Mualem and Bear (1974) studied the shape of the interface under steady state conditions, assuming a thin horizontal semipervious layer in a coastal aquifer. The solution is based upon Dupuit-Forchheimer's assumptions. The authors employed Hele-Shaw model and field data for validation of their solution.

Many Hele-Shaw models were developed and used by various investigators for different objectives i.e., by Bear and Dagan (1964a), Columbus (1965) to validate their solutions, by Chahill (1968, 1973), Dagan and Bear (1968) to determine the range of validity of their

analytical solutions, by Kashef(1970) to study saltwater intrusion, by Collins et al. (1971, 1972) to study the interface of Long Island, N.Y., by Mercer et al. (1980) to validate their numerical solutions under the Dupuit -Forchheimer's assumptions, and by Gupta (1985) to validate his analytical and numerical solutions for saltwater interface in an unconfined aquifer.

Kashef and Smith(1975) presented a numerical model for growth of saltwater zone due to well discharge. they presented their numerical results in figures under several conditions.

Vandenberg (1975) arrived at the optimal pumpage to avoid the saltwater intrusion into the pumped well. The aquifer was treated as confined, thin, homogeneous and isotropic, and semi-infinite in areal extent.

Wang and Cheng (1975) presented a finite element model for simulating the dispersion of pollutants in a semi-infinite aquifer.

Segol et al.(1975) presented a Galerkin - finite element model for simulating the saltwater front movement.

Nutbrown (1976) estimated optimal pumpage from an unconfined coastal aquifer by a simple analytical model incorporating a number of parameters.

Vappicha and Nagaraja (1976) presented analytical and numerical solutions using the quasi-steady state principle with three different boundary conditions. They assumed a sharp interface, homogeneous, isotropic aquifer and ignored the compressibility of the aquifer and water. The authors have validated their solution by a viscous model.

Segol and Pinder (1976) used a Galerkin - finite element approximation to simulate the movement of the interface in the Cutler

area of the Biscayne aquifer near Miami, Florida, adopting Cooper and Pinder's approach (i.e., zero storage coefficient) (1970). They found their results to match well with the field data.

Tresoff et al. (1976) presented a finite - difference model to simulate water table and ground water flow in two dimensions using line successive over relaxation (LSOR).

Van der Veer (1977a) presented a steady state analytical solution for the position of the interface in a coastal aquifer, assuming the saltwater to be at rest. He compared the results with the results of Badon Ghyben and Herzberg's solution. He found that the interface and the phreatic surface are straight lines for some special cases. Van der Veer (1977b) presented an analytical solution for the position of the steady state interface in a coastal aquifer, accounting for the movement of saltwater.

Van der Veer (1978) presented an exact solution for two - dimensional ground water flow, assuming a semi - pervious boundary.

Konikow and Bredehoeff (1978) presented a model for two - dimensional solute transport and dispersion in ground water. The solution is based upon the method of characteristics. The change in concentration over time due to convective transport and diffusive transport are estimated. They assumed that there are no vertical variations in concentration and head; and ignored the effect of fluid density and viscosity gradients on flow.

Panigrahi et al. (1980) presented a finite difference numerical solution for saltwater intrusion in unconfined coastal aquifer of infinite extent.

Bear and Kapuler (1981) presented a finite difference numerical model for the movement of an interface in a layered coastal

aquifer.

Van dam and Sikkema (1982) presented, a solution of the shape of interface in a semi - confined aquifer, assuming the saltwater to be at rest. The solution is based upon Dupuit - Forchheimer's assumptions. Sikkema and Van dam (1982) presented an analytical solution for the interface in a semi confined aquifer considering the geohydrological terms, assuming the saltwater to be at rest.

Volker and Rushton (1982) presented two models for steady - state saltwater intrusion in coastal aquifer assuming miscible and immiscible fluids. The boundary integral method has been used, for an abrupt interface while a finite - difference method has been used in the dispersive model.

Basak and Rajagopalan (1982) presented an unsteady state analytical solution for the length of saltwater intrusion in a coastal aquifer, using non-Darcy flow, Dupuit - Forchheimer's assumptions and Ghyben - Herzberg approximation.

Frind (1982a) presented a Galerkin finite element model for simulation of long term transient density - dependent transport in groundwater assuming the fluid to be incompressible. The author validated his solution by comparing the results with segol et al. (1975), Pinder and Cooper (1970), Henry, 1964 (Frind, 1982a), and Lee Cheng (1974).

Frind (1982 b) presented a finite element model for simulating saltwater intrusion in a confined aquifer overlain by a leaky aquitard.

Kashef (1983a) expressed some selected analytical solutions (for the position of the interface) in simple equations in terms of the Ghyben - Herzberg form. He compared these solutions with the Ghyben - Herzberg solution. He concluded that, for using the Ghyben - Herzberg

solution in field , the free surface location may be determined by recording water levels in series of observation wells or even by recording one level in one observation well.

Polo and Ramis (1983) presented a numerical solution for a sharp interface motion with the Dupuit - Forchheimer's assumptions. They found a good agreement between their results and analytical solutions presented by Verruijt, 1968 (Polo and Ramis, 1983), by Keulegan, 1954 (Polo and Ramis, 1983), by Vappoicha and Nagaraja, 1975 (Polo and Ramis, 1983), and by Vappicha and Nagaraja (1976).

Gupta (1983) presented a finite element numerical model for steady state interface upconing beneath a coastal infiltration gallery.

Khaleel, R., and Reddell, D.L. (1985) presented a numerical model based upon method of characteristics , for convective and diffusive transport in a saturated - unsaturated porous medium. They used a three-way linear interpolation scheme to assign seepage velocities to the moving points. They reported a agreement of their results with i) analytical solution presented by Harleman and Rumer (1963); ii) field data presented by Warrick et al. (1971); iii) numerical solution presented by Van Genuchten in 1978 (Khaleel and Reddell, 1985).

Mehnert and Jennincs (1985) presented a numerical model for saltwater intrusion, assuming miscible fluids and variable hydraulic conductivity.

Isaacs (1985) presented an analytical solution for the interface toe position using dimensional analysis for a one dimensional unconfined coastal aquifer. The author validated his solution by comparing the results with numerical solution presented by him.

Bear et al. (1985) developed an analytical solution for the interface toe by the successive steady state method. The authors

validated his solution by comparing the results with other numerical solutions presented by Shamir and Dagan (1971), by Kapuler, 1972 (Bear et al., 1985), and by Shapiro et al., 1983, (Bear et al., 1985)

McElwee (1985) presented a model for saltwater intrusion into a river, assuming a steady state sharp interface. He found that, as the river stage rises, the saltwater intrusion declines and vice versa.

Gupta (1985a) used analytical and numerical models based upon diffusive transport to simulate saltwater movement in the Nakhon Luang aquifer, Bangkok, Thailand.

Gupta (1985b) developed analytical and numerical solutions for the free surface fluctuation and the saltwater interface under various boundary conditions. The results compared well with the Hele-Shaw results.

Isaacs and Hunt (1986) presented an analytical solution for the position of the interface in a coastal aquifer. The results compared well with the Shamir and Dagan's numerical solution (1971).

Gupta and Gaikwad (1987) presented a numerical model, based upon Dupuit - Forchheimer's assumptions and Ghyben - Herzberg approximation, for interface upconing due to a horizontal well in an unconfined aquifer. They found a good agreement between their results and analytical solutions and also with Hele-Shaw model results.

Appelo and Willemsen (1987) presented a combined geochemical/mixing cell model to simulate concentration changes due to sea water intrusions.

Voss and Souza (1987) presented a Galerkin finite element model for a variable density flow and solute transport in a regional aquifer system containing a narrow freshwater saltwater transition zone.

Sherif et al. (1988) presented a finite element model for

saltwater intrusion in the Nile Delta aquifer, Egypt. The results compared well with the models of Rouve et al., 1980 (Sherif et al., 1988), and of Kawatani, 1980 (Sherif et al., 1988).

Detournay and Strack (1988) presented a steady state analytical solution for the saltwater intrusion in a coastal aquifer. The solution is based upon hodograph method.

Reilly (1990) simulated dispersion in a two-layered coastal aquifer system using a density-dependent solute-transport formulation based upon Fick's law. He found that for a good simulation either the dispersion formulation should be flow - direction - dependent or the dispersivities must change spatially.

2.5.2.1.2 Two-Dimensional Horizontal Flow

2.5.2.1.2.1 Macrolevel Planning

Mercer et al. (1980) presented a finite difference model for sharp interface motion. The solution is based upon the Dupuit-Forchheimer's assumptions. The authors validated their solution by comparing the simulated results with the analytical solution presented by Keulagan, 1954 (Mercer et al., 1980), Hele - Shaw model conducted by Bear and Dagan (1964a), and field area near Kahului, Maui, Hawaii.

Andrews (1981) presented a hydrologic and water quality model for the horizontal movement of saltwater in the Costa de Hermosillo, Mexico. The model ignored the density effects which are very important for the freshwater and saltwater equilibrium.

Kishi et al. (1982) presented a finite element model for the areal steady state position of the interface in a coastal aquifer. They applied their model to the confined groundwater in the estuary of the Naka river, Tokushima Prefecture, Japan. The model results are reported

to be in close agreement with the results obtained from deep wells.

Inouchi et al. (1985) developed a Galerkin finite element model for a two - dimensional unsteady interface in a confined aquifer. The solution is based upon two equations accounting for very rapid and very slow variations of the interface with time. The model results compared well with the field data.

Contractor and Srivastava (1990) presented a finite element model for the two dimensional areal position of the saltwater interface in the Northern Guan aquifer. The model results are in a close agreement with analytical solutions presented by Van der Veer, 1976 (Contractor and Srivastava, 1990), and by Sa da Costa and Wilson, 1979 (Contractor and Srivastava, 1990). However, the results compare well with only one of the sets of reported field data.

Ledoux et al. (1990) presented a finite difference model to simulate the position of the interface. The results are in a good agreement with the analytical solution presented by Issacs and Hunt (1986), and by Hantush (1968).

2.5.2.2 Three Dimensional Flow Analysis

2.5.2.2.1 Macrolevel Planning

Shamir and Harleman (1967) presented a finite difference model for dispersion in steady state three - dimensional flow in porous mediums.

Strack (1976) presented an analytical solution for the position of the interface. The solution is based upon Dupuit - Forchheimer's assumptions.

- Kishi and Fukuo (1977) presented a numerical model for a three - dimensional steady interface.

Huyakorn et al. (1987) presented a three - dimensional finite

element model to simulate saltwater intrusion in single and multiple coastal aquifers. The solution is based upon the Picard sequential solution algorithm with a special provision to enhance the convergence.

Kakinuma et al. (1988) presented a three - dimensional diffusive transport numerical model to simulate saltwater intrusion in confined aquifers in the estuaries of the Naka and Kiki rivers in Japan. The solution is based upon a constant as well as a velocity - dependent dispersion coefficient.

Bush (1988) simulated saltwater flow in the Floridan aquifer system beneath the north end of Hilton Head Island and Port Royal Sound.

2.5.3 Field Experiments

2.5.3.1 Macrolevel Planning.

Kashef (1983a) described saltwater intrusion in the Nile Delta, Egypt. He discussed various techniques for water resources management. He used two methods to study the saltwater intrusion into the Delta.

Johnston (1983) monitored the interface in the Tertiary limestone aquifer, Southeast Atlantic outer-continental shelf of the U.S.A.

2.5.3.2 Microlevel Planning

Schmorak and Mercado (1969) carried out field investigation on wells in Ashqelon region in a coastal plane of Israel to check the validity of Bear and Dagan's analytical solution (Schmorak and Mercado, 1969) and to study the salinization of pumped well. They conclude that the theoretical estimates are in agreement with field results up to a critical rise which may be $1/3$ to $1/2$ of the distance between initial position of interface and bottom of well.

CHAPTER-III

THE MODEL DEVELOPMENT

3.1 THE PROBLEM

The fresh water in many aquifers may be underlain by saltwater. The entry of saltwater in a pumped well tapping one of such aquifers can possibly be avoided by providing adequate "cushion" between bottom of the screen and the freshwater - saltwater interface. However, the resulting partial penetration induces vertically upward velocity to the saltwater. An indiscriminate pumping can draw the saltwater into the pumped well.

The present study is aimed at developing a numerical model for simulation of the convective and diffusive saltwater transport in a confined aquifer occurring in consequence of pumping water from a partially penetrating well underlain by saltwater (Fig.3.1). The transport comprises of upward lifting of saltwater into the freshwater zone, subsequent entry into the pumped well, and finally downward settlement after the closure of pumpage.

3.2 GOVERNING EQUATIONS

The physical process leading to the saltwater transport can be described by the following equations.

3.2.1 Differential Equation Governing Two - Dimensional (r-z plane) Unsteady State Axi - Symmetric Mass Transport.

The differential equation is as follows (Bear, 1979)

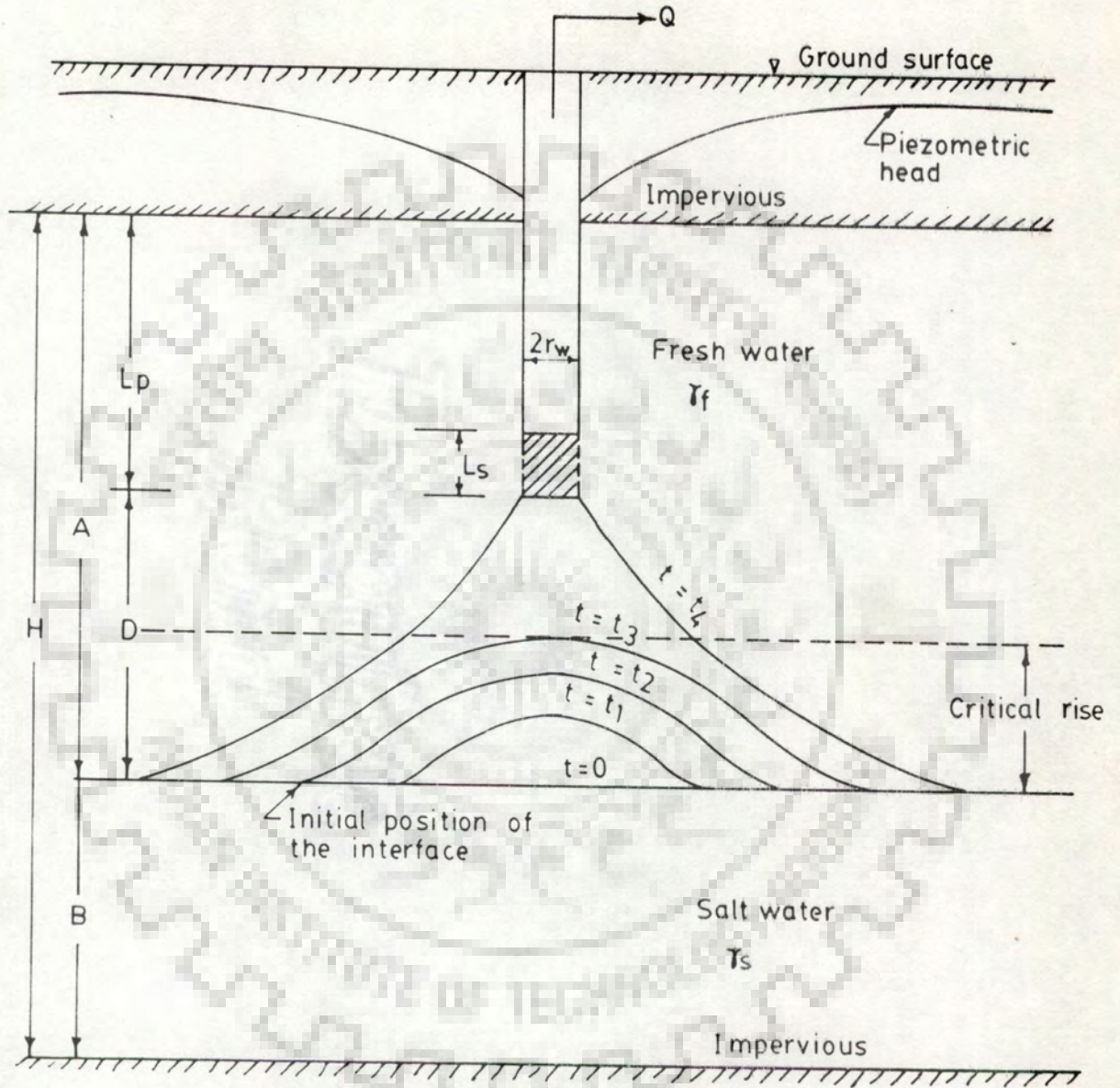


Fig (3.1) Salt water Upconing Beneath a Pumping Well

$$\frac{D_r}{r} \frac{\partial}{\partial r} \left(r \frac{\partial C}{\partial r} \right) + D_z \frac{\partial^2 C}{\partial z^2} - \frac{q_r}{\phi} \frac{\partial C}{\partial r} - \frac{q_z}{\phi} \frac{\partial C}{\partial z} = \frac{\partial C}{\partial t} \quad \dots (3.1.a)$$

$$q_r = - \frac{k_r}{\mu} \left[\frac{\partial p}{\partial r} + \gamma \frac{\partial z}{\partial r} \right] \quad \dots (3.1.b)$$

$$q_z = - \frac{k_z}{\mu} \left[\frac{\partial p}{\partial z} + \gamma \right] \quad \dots (3.1.c)$$

$$C = C(r, z, t)$$

$$\mu = \mu(C)$$

$$\gamma = \gamma(C)$$

Where $C(L)$ is the concentration of saltwater, $r(L)$ is the radial distance from the centre of the well, $z(L)$ is the vertical coordinate above any datum, $t(T)$ is the time, $D_r (L^2 T^{-1})$ and $D_z (L^2 T^{-1})$ are the diffusive coefficients in the radial and vertical directions respectively, $p(FL^{-2})$ is the water pressure, $k_r (L^2)$ and $k_z (L^2)$ are the intrinsic permeabilities in the radial and vertical directions respectively, $\gamma (FL^{-3})$ is the specific weight of water, $\mu (FTL^{-2})$ is the dynamic viscosity of water, $\phi(1)$ is the porosity of aquifer, and $q_r (LT^{-1})$ and $q_z (LT^{-1})$ are the Darcy's velocities in the r and z directions respectively.

3.2.2 Differential Equation Governing Two -Dimensional (r - z plane) Unsteady State Axi-Symmetric Radial Flow of a Fluid With Time and Space Variant Specific Weight and Viscosity.

The differential equation is as follows (Bear, 1979).

$$\frac{k_r}{\mu r} \left(\frac{\partial p}{\partial r} \right) + \frac{\partial}{\partial r} \left(\frac{k_r}{\mu} \frac{\partial p}{\partial r} \right) + \frac{\partial}{\partial z} \left[\frac{k_z}{\mu} \left(\frac{\partial p}{\partial z} + \gamma \right) \right] = \frac{S_s}{\gamma} \frac{\partial p}{\partial t} \quad \dots (3.3)$$

$$p = p(r, z, t)$$

$$S_s = S_s(\gamma)$$

Where S_s (1) is the specific storage.

3.3 THE SOLUTION

The first two terms on the left side of equation (3.1) represent the 'moderation' of concentration due to diffusive transport and the last two terms represent the concentration variation due to the convective transport. The spatial variation of the pressure, governing the convective transport (refer eqns. 3.1b and 3.1c), is described by equation 3.3. A complete solution of the two coupled differential equation by finite difference is subject to errors on account of numerical dispersion (refer annexure-A).

3.3.1 Solution Strategy

In the present model the convective transport in a finite time step is first computed by the method of characteristics. Subsequently the total transport in the time step is computed by solving equation (3.1) for a known initial concentration distribution and the pre-computed convective transport, using a finite difference scheme.

3.3.2 Coordinate System

The r-z space, in the present study, is represented by a coordinate system shown in Fig. (3.2a). Thus, the radial coordinate (r) of a point represents its radial distance from the centre of the well and the vertical coordinate (z) represents its vertical distance from the lower impervious layer.

3.3.3 Convective Transport

The convective component is computed by the method of characteristics. A brief description of the method is as follows.

3.3.3.1 Method of Characteristics

The method of characteristics has been adopted to avoid the

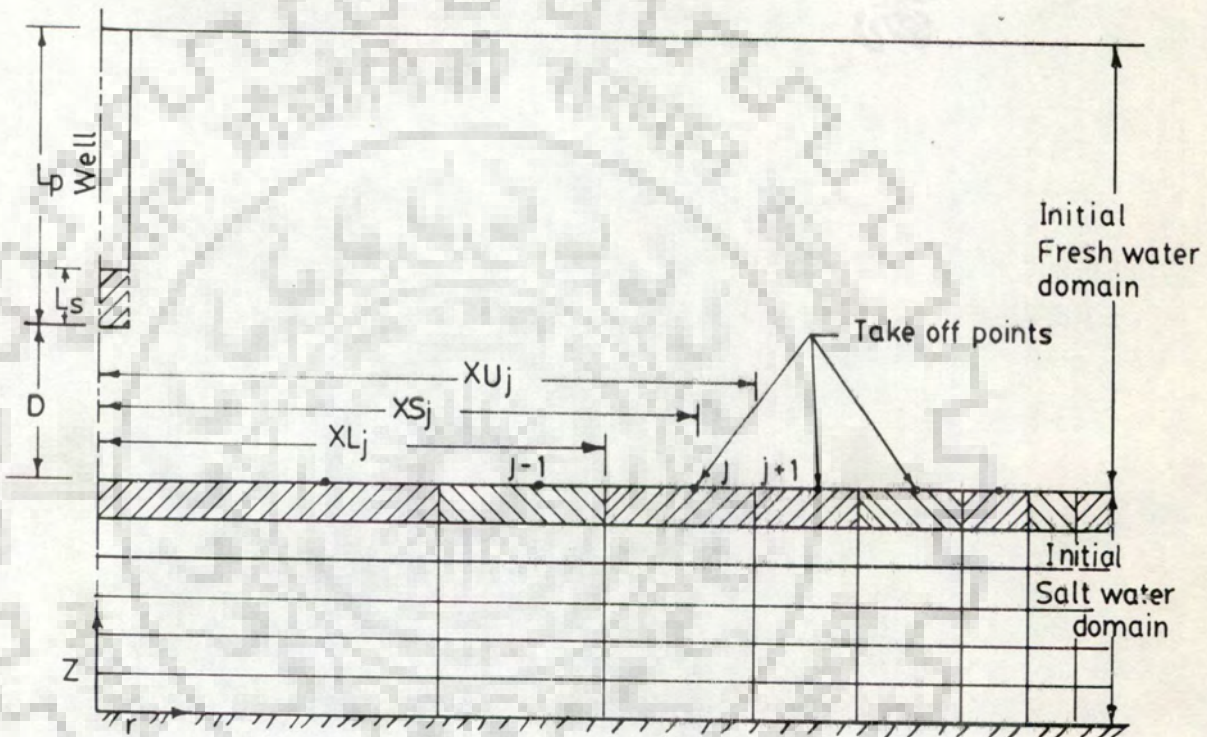


Fig (3.2 a) Take off Points

numerical dispersion encountered^{re} in solving the equation of mass transport (equation 3.1). The method is based upon solution of an equivalent set of differential equations, known as characteristic equations. The characteristic equations of equation (3.1) are as follows

$$\frac{dr}{dt} = \frac{q_r}{\phi} \quad \dots\dots\dots(3.4.a)$$

$$\frac{dz}{dt} = \frac{q_z}{\phi} \quad \dots\dots\dots(3.4.b)$$

$$\frac{dC}{dt} = \frac{D_r}{r} \frac{\partial}{\partial r} \left(r \frac{\partial C}{\partial r} \right) + \frac{D_z}{z} \frac{\partial^2 C}{\partial z^2} \quad \dots\dots\dots(3.4.c)$$

Equations 3.4(a) and 3.4(b) describe the convective transport, while equation 3.4(c) describes the diffusive transport.

3.3.3.1.1 Simulation of Convective Transport

Convective transport is simulated by solving equations 3.4(a) and 3.4(b) by the method of characteristics. The computational details are as follows

3.3.3.1.1.1 Model Description

The initial saltwater domain is discretized by a finite number of horizontal strips of uniform thickness (refer Fig,3.2a). The top of the uppermost strip represents the initial position of the interface between the saltwater and freshwater. Each strip is divided into a finite number of non-uniform substrips. Each substrip of the top strip is viewed as a take off point i.e., on the verge of being lifted into the fresh water zone. A take off point is assumed to move vertically upwards until it's entire thickness moves just above the initial position of the interface. At this stage the point is assumed to have "taken off" and a new take off point (from the underlying substrip)

is assumed to take its place. There after the "taken off" point is redefined as a moving point having both radial and vertical components of velocity. (Fig.3.3).

3.3.3.1.1.2 Positioning of Take Off Points

The uppermost strip is discretized by a finite (say n) number of take off points in such a way that each take off point discretizes an equal volume (say Vol) of saltwater and the last take off point remains practically stationary. Thus,

$$\frac{\text{Vol}}{\phi} = 3.14 (XU_j^2 - XL_j^2) d \quad \dots\dots\dots (3.5)$$

$$j = 1, \dots\dots\dots n$$

Where $XU_j(L)$ and $XL_j(L)$ are respectively the radial coordinates of the downstream and upstream faces of the domain of j^{th} take off point (refer Fig.3.2a), and $d(L)$ is the strip thickness. The j^{th} take off point is assumed to be positioned at the centre of gravity of the stretched space domain (refer Fig. 3.2b) discretized by it. Thus, its radial coordinate (XS_j) is generated by taking moments of the areas around o (refer Fig.3.2b).

Thus,

$$\pi(XU_j + XL_j)(XU_j - XL_j)XS_j = \pi(XU_j - XL_j)^2 \left(\frac{2}{3} XU_j - \frac{2}{3} XL_j + XL_j \right)$$

$$+ 2\pi XL_j (XU_j - XL_j) \left(\frac{1}{2} XU_j - \frac{1}{2} XL_j + XL_j \right)$$

$$(XU_j^2 - XL_j^2)XS_j = \frac{2}{3} XU_j^3 - \frac{4}{3} XU_j^2 XL_j + \frac{2}{3} XU_j XL_j^2 + \frac{1}{3} XU_j^2 XL_j$$

$$- \frac{2}{3} XU_j XL_j^2 + \frac{1}{3} XL_j^3 + XU_j^2 XL_j - XL_j^3$$

$$(XU_j^2 - XL_j^2)XS_j = \frac{2}{3} (XU_j^3 - XL_j^3)$$

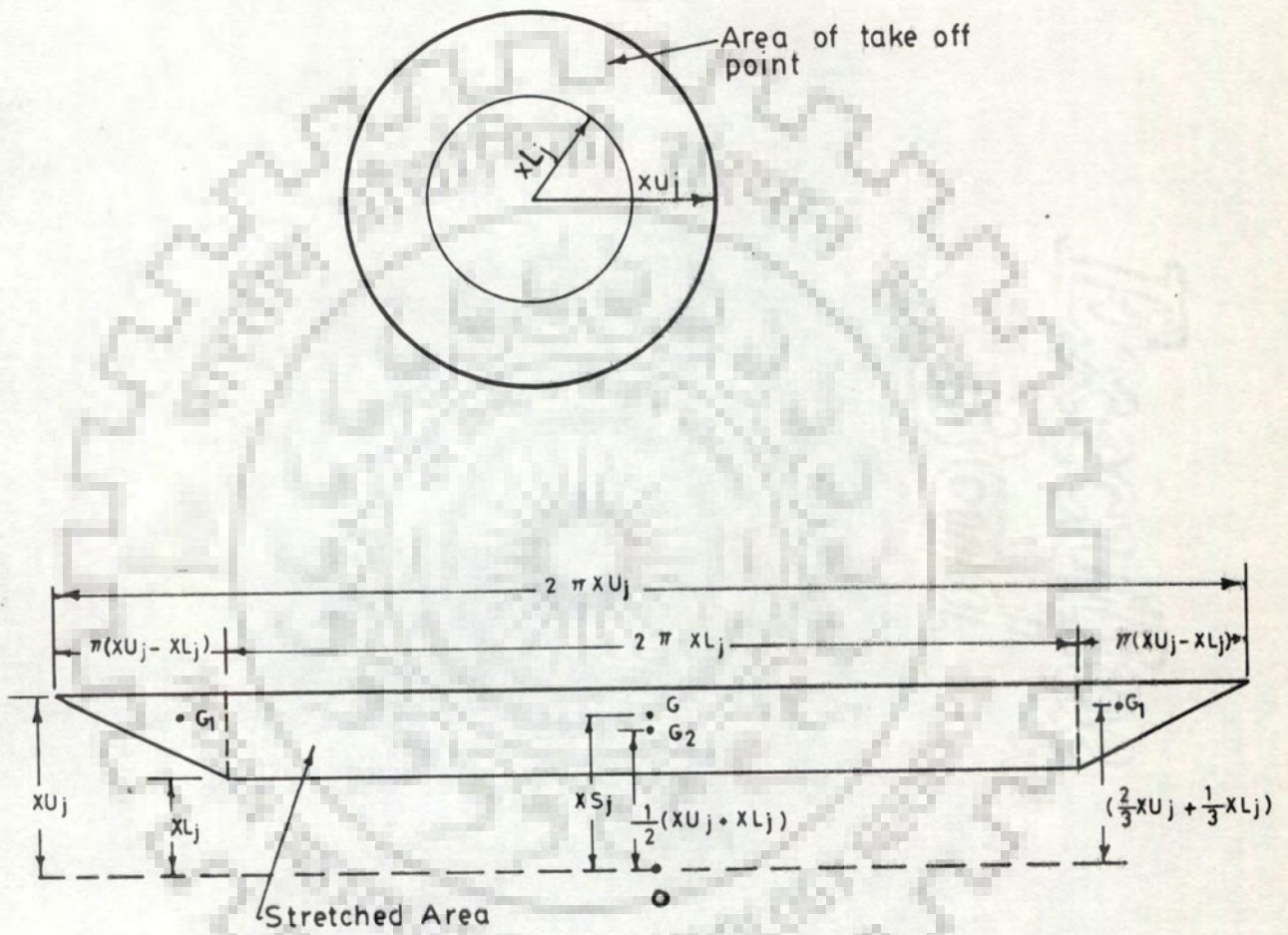


Fig (3.2 b) Positioning of Take off Points

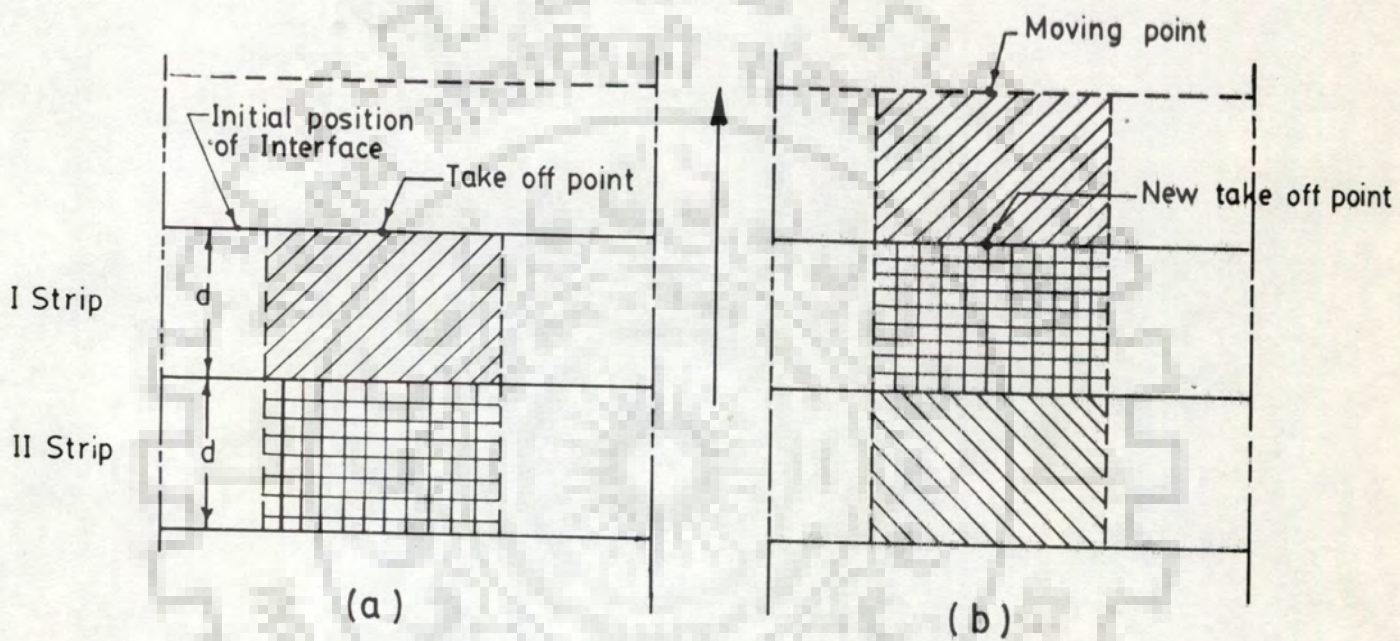


Fig. (3.3) Lifting of Take off Points

(a) Before lifting

(b) After lifting

$$XS_j = \frac{2 (XU_j^3 - XL_j^3)}{3 (XU_j^2 - XL_j^2)} \dots\dots\dots(3.6)$$

For a stipulated value of Vol and a known value of the radius of well (r_w), the domains of the take off points are generated as follows

$$XL_1 = r_w$$

$$XU_1 = \left(\frac{Vol}{\phi d} + XL_1^2 \right)^{1/2}$$

$$XL_2 = XU_1$$

$$XU_2 = \left(\frac{Vol}{\phi d} + XL_2^2 \right)^{1/2}$$

$$XL_j = XU_{j-1}$$

$$XU_j = \left(\frac{Vol}{\phi d} + XL_j^2 \right)^{1/2}$$

$$XL_n = XU_{n-1}$$

$$XU_n = \left(\frac{Vol}{\phi d} + XL_n^2 \right)^{1/2}$$

Further, the corresponding radial coordinates of the take off points are computed in accordance with the equation (3.6). Finally, the radial spacing (Δrs_j) between the j^{th} and $(j+1)^{th}$ take off points is computed as follows

$$\Delta rs_j = XS_{j+1} - XS_j \dots\dots\dots(3.7)$$

3.3.3.1.1.3 Upward Lifting of Take Off Points

Since a take off point is assumed to move vertically upwards, it's radial coordinate remains constant while it's vertical coordinate

j increases. Let Z_{jk} be the vertical coordinate of the j^{th} take off point at the k^{th} discrete time t_k . Thus $Z_{j,k+1}$ i.e., it's vertical coordinate at t_{k+1} can be written as follow:

$$Z_{j,k+1} = Z_{j,k} + (t_{k+1} - t_k) V(XS_j, Z_{jk}, t_k) \dots\dots\dots (3.8)$$

[$Z_{j,0} = B$, where B is the initial saltwater thickness (refer Fig.(3.1))]

Where XS_j is the radial coordinate of j^{th} take off point, $V(XS_j, Z_{jk}, t_k)$ is the vertical velocity of water at the space point (XS_j, Z_{jk}) and time t_k .

Since n^{th} take off point is assumed to be stationary,

$$V(XS_n, B, t_k) = 0 \text{ (for all } k\text{'s)} \dots\dots\dots (3.9.a)$$

and $Z_{n,k+1} = B \dots\dots\dots (3.9.b)$

When the vertical distance moved by j^{th} take off point equals (or just exceeds) the thickness of strip (d) [i.e., $(Z_{j,k+1} - Z_{j,0}) \geq d$], the entire saltwater volume represented by it would have gone into suspension. At this stage, the j^{th} take off point is assumed to have taken off and is termed as moving point. It's subsequent movement in suspension is governed by the velocity distribution in the flow domain above the initial position of the interface.

As a take off point takes off, the saltwater substrip lying just below it, is assumed to move up and take it's position in the topmost strip. This is termed as the new j^{th} take off point (Fig.3.3).

3.3.3.1.1.4 Convection of Moving Point

Each moving point is assigned a new position at the end of the time step in accordance with the following equations.

$$R_{m,k+1} = R_{mk} - (t_{k+1} - t_k)U(R_m, Z_m, t_k) \quad \dots\dots(3.10)$$

$$Z_{m,k+1} = Z_{mk} + (t_{k+1} - t_k)V(R_m, Z_m, t_k) \quad \dots\dots(3.11)$$

Where $R_{m,k+1}$ and $Z_{m,k+1}$ are respectively the radial and vertical coordinates of the m^{th} moving point at $(k+1)^{\text{th}}$ time; and $U(R_m, Z_m, t_k)$ and $V(R_m, Z_m, t_k)$ are respectively the radial and vertical velocities at the space point (R_m, Z_m) at k^{th} time.

3.3.3.1.1.5 Finite Difference Grid

For arriving at a spatial distribution of saltwater concentration at various discrete times, a finite-differences grid (refer Fig.3.4) is superposed over the transport domain. The domain is bounded by initial position of the interface on the lower side, upper boundary of the flow domain on the upper side, well on the downstream side and zero lift boundary (i.e. a column passing through the last take off point) on the upstream side (refer Fig.3.4). A column is passed through each take off point. Rows are positioned uniformly between the lower and upper boundaries. Thus, the entire domain is discretized by a finite number of nodal points. Each nodal point, represented by its row and column numbers, discretizes the soil-water domain lying closest to it (Fig.3.4).

3.3.3.1.1.6 Estimation of Saltwater Concentration

The saltwater concentration (CC_{ijk}) at any node (i,j) at a discrete time t_k will be as follows

$$CC_{ijk} = \frac{\sum_{m \in J_1} VL_m}{\phi VLX_{ij}} \quad \dots\dots(3.12)$$

Where J_1 , a subset of the moving points, comprises of the moving points

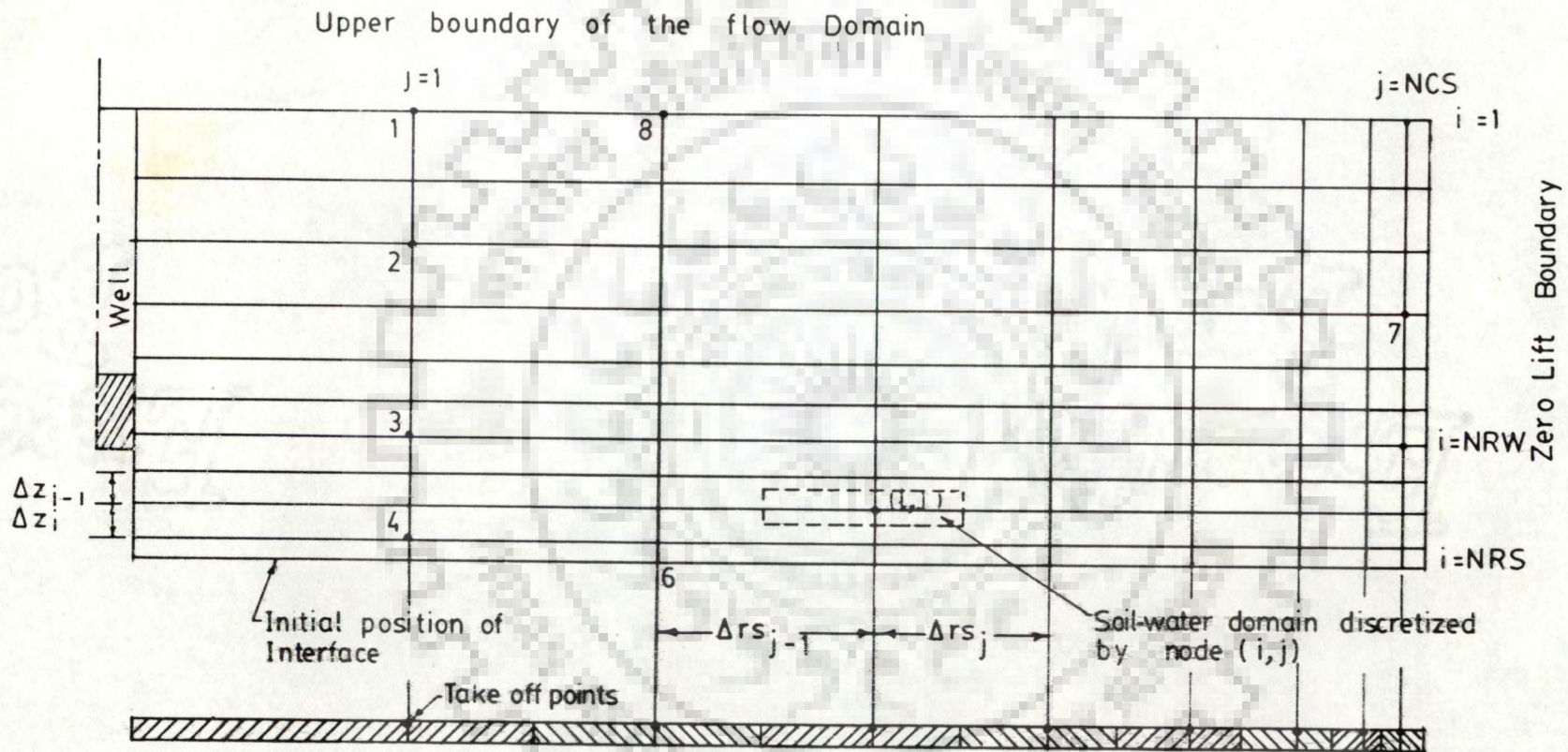


Fig (3.4) Finite Difference Mesh and Boundaries for Simulation of Saltwater Transport

lying in the domain of node (i, j) at discrete time t_k ; VL_m is the volume of saltwater discretized by m^{th} moving point (under pure convective transport; VL_m for all m 's will be equal to Vol . However, there is a redistribution of the saltwater among moving points due to diffusion. This aspect shall be dealt with in the subsequent solution), $V LX_{ij}$ is the volume of soil-water discretized by node (i, j) , and ϕ is the porosity of the aquifer.

$$V LX_{ij} = 3.14(XU_j^2 - XL_j^2) \left(\frac{Z_{i-1} + Z_{i+1}}{2} \right) \quad \dots (3.13)$$

3.3.4 Total Transport

The total transport of saltwater is computed by solving equation 3.4(c) governing the diffusive transport and treating the precalculated convective transport as a known saltwater input (or abstraction).

3.3.4.1 Differential Equation

Equation 3.4(c) is modified as follows to represent the total transport.

$$\frac{D_r}{r} \frac{\partial}{\partial r} \left(r \frac{\partial C}{\partial r} \right) + D_z \frac{\partial^2 C}{\partial z^2} + q^* = \frac{\partial c}{\partial t} \quad \dots (3.14)$$

Where C is the resultant saltwater concentration accounting for convective as well as diffusive transport, D_r and D_z are the diffusion coefficients in r and z directions respectively, and q^* (T^{-1}) is the volume of saltwater entering the domain of node (i, j) due to convection in r and z directions per unit volume of water in the domain per unit time [the pre-computed rate of the net convective transport (inflow :

+ve ,outflow : -ve)].

3.3.4.1.1 Finite Difference Solution

Equation (3.14) is written in terms of the finite differences over the grid described earlier and solved by iterative alternating direction implicit explicit (IADIE) scheme . Thus, the space above the initial position of the interface is discretized by a finite number of nodes lying at the intersection of rows and columns (Fig.3.4). Similarly, the time domain is discretized by a finite number of discrete times.

3.3.4.1.2 IADIE Method

A replacement of spatial and temporal derivatives in equation 3.14 by finite differences leads to a determinate system of linear equations. The iterative alternating direction implicit explicit (IADIE) method for solving the system of linear equations requires a memory far smaller than required by any standard numerical method like Gauss elimination . Consider an area to be discretized by N rows and M columns, implying $N*M$ nodes. Thus the solution by Gauss elimination will require a memory of $(N*M)^2$ for storing the coefficient matrix. This memory requirement may become prohibitively large even for moderate values of N and M . This illustrates the necessity of devising some alternative procedures which utilize the sparseness of the coefficient matrix. It can be easily verified that the system of equations will be pentagonal i.e., each row of the coefficient matrix will have only five non-zero elements, one located at the diagonal, one just prior and one following the diagonal. The position of the remaining two non-zero elements will be governed by the adopted numbering system of nodes. No algorithm is available which can utilise this pattern of sparseness of

matrix. However, an efficient algorithm i.e., Thomas' algorithm is available for solving a tridiagonal system (i.e., a system in which only the diagonal element, one element prior and one element following it are non-zero and rest are all zeros) of equations. The algorithm reduces the memory requirement for storing the coefficient matrix drastically i.e., from square of the number of equations to three times the number of equations.

In the IADIE formulation, the pentagonal system of equations is reduced to a tridiagonal system by writing the spatial derivatives implicitly in one direction (say along r direction or along a row) and explicitly in other direction (i.e., along z direction or along a column). The resulting system of equations is tridiagonal in nature. After all row equations have been processed row by row (employing Thomas' algorithm) the directions of the implicit and explicit derivatives are reversed i.e., the solution is obtained column-wise. After all column equations have been processed column by column, the above process is repeated till the convergence is achieved. Thus, the solution of $N \times M$ number of equations is accomplished by repeated alternate solutions of N and M number of tridiagonal system of equations. The memory requirement for storing the coefficient matrix is thus reduced from $(N \times M)^2$ to $3N$ and $3M$, which is indeed a drastic reduction.

3.3.4.1.2.1 Discretization of Concentration and Convective Transport

The continuous variations of C and q^* with respect to z, r and t are discretized by subscripting them. The first, second and the third subscripts represent respectively the row number (discretized z), column number (discretized r) and the discrete time. The superscript of C represents the iteration number.

3.3.4.1.2.2 Computation of Discretized Convective Transport

The convective transport q^* is evaluated as follows

$$q_{ijk}^* = \left(\sum_{m \in J_2} VL_m - \sum_{m \in J_3} VL_m \right) / [\phi VLX_{ij}(t_{k+1} - t_k)] \quad \dots\dots\dots (3.15)$$

Where J_2 and J_3 are subsets of the moving points, including respectively all such moving points which enter into and move out of the domain of the node (i, j) during the time step $(t_k$ to $t_{k+1})$.

3.3.4.1.2.3 IADIE Formulation

As discussed earlier the IADIE formulation comprises of two stages

Stage I (Implicit in r-direction and Explicit in Z-direction)

Interior Nodes

Consider an interior node (i, j) , a time increment from t_k to t_{k+1} and l^{th} iteration. Writing the spatial derivatives of C with respect to r implicitly and with respect to z explicitly, equation (3.14) is expressed in terms of finite-differences as follows (refer Fig. 3.4).

$$D_{r, ij} \left[\frac{(C_{i, j+1, k+1}^{(l)} - C_{i, j, k+1}^{(l)}) (XS_{j+1} + XS_j)}{\Delta r_s_j \cdot 2} - \frac{(C_{i, j, k+1}^{(l)} - C_{i, j-1, k+1}^{(l)}) (XS_j + XS_{j-1})}{\Delta r_s_{j-1} \cdot 2} \right] + D_{z, i, j} \left[\frac{(C_{i+1, j, k+1}^{(l-1)} - C_{i, j, k+1}^{(l-1)})}{\Delta z_i} - \frac{(C_{i, j, k+1}^{(l-1)} - C_{i-1, j, k+1}^{(l-1)})}{\Delta z_{i-1}} \right]$$

$$\frac{2}{(\Delta z_i + \Delta z_{i-1})} - a_{ijk}^* = \frac{(C_{i,j,k+1}^{(l)} - C_{ijk})}{\Delta t_s} \dots\dots\dots (3.16)$$

Where Δr_{s_j} is the radial distance between node (i,j) and node (i,j+1), XS_j is the radial coordinate of the node (i,j), Δt_s is the time step and C_{ijk} is the initial concentration at the beginning of the time step Δt_s . Subsequently the term $C_{i,j,k+1}^{(l-1)}$ in the explicit derivative is replaced by the implicit term $C_{i,j,k+1}^{(l)}$. This has been found to lead to a much faster convergence, possibly because of the strengthening of the diagonal term BB_j (refer equation 3.18) without disturbing the tridiagonal nature of the system of equations. The same approach has been used subsequently for writing down all the explicit finite differences.

Equation (3.16) is rearranged as follows:

$$\begin{aligned} & C_{i,j-1,k+1}^{(l)} \left[\frac{2 D_{r_{i,j}}}{XS_j (\Delta r_{s_{j-1}} + \Delta r_{s_j})} \frac{(XS_j + XS_{j-1})}{2 \Delta r_{s_{j-1}}} \right] \\ & + C_{i,j,k+1}^{(l)} \left[\frac{2 D_{r_{i,j}}}{XS_j (\Delta r_{s_{j-1}} + \Delta r_{s_j})} \left(- \frac{XS_{j+1} + XS_j}{2 \Delta r_{s_j}} - \frac{XS_j + XS_{j-1}}{2 \Delta r_{s_{j-1}}} \right) \right] \\ & + \frac{2 D_{z_{i,j}}}{\Delta z_i + \Delta z_{i-1}} \left(- \frac{1}{\Delta z_i} - \frac{1}{\Delta z_{i-1}} \right) - \frac{1}{\Delta t_s} \Big] \\ & + C_{i,j+1,k+1}^{(l)} \left[\frac{2 D_{r_{i,j}}}{XS_j (\Delta r_{s_{j-1}} + \Delta r_{s_j})} \frac{XS_{j+1} + XS_j}{2 \Delta r_{s_j}} \right] \end{aligned}$$

$$\begin{aligned}
 = - & \frac{2 D_{z_{i,j}}}{\Delta z_i + \Delta z_{i-1}} \left[\frac{C_{i+1,j,k+1}^{(\ell-1)}}{\Delta z_i} + \frac{C_{i-1,j,k+1}^{(\ell-1)}}{\Delta z_{i-1}} \right] \\
 & + q_{ijk}^* - \frac{C_{ijk}}{\Delta t_s} \dots\dots\dots (3.17)
 \end{aligned}$$

For a given interior row (i.e., i=2,.....NRS-1) equation (3.17) is of the form

$$AA_j C_{i,j-1,k+1} + BB_j C_{i,j,k+1} + CC_j C_{i,j+1,k+1} = DD_j \quad (3.18)$$

j=2,.....NCS-1)

Where NRS is the number of rows up to the initial position of the interface, and NCS is the number of columns up to zero lift boundary (refer Fig.3.4).

Boundary Nodes

For any interior row (say i=i* ; NRS>i*>1) equation (3.18) can be written at each interior column (i.e., j=2,NCS-1). This provides (NCS-2)equations. However, the unknowns [C^(ℓ)_{i*,j,k+1}, j=1,...NCS] along the i*th row are NCS in number. [C_{i*,j,k} are known from the preceding time step or initial conditions; C^(ℓ-1)_{i*-1,j,k+1}, C^(ℓ-1)_{i*+1,j,k+1} from the preceding iteration]. This deficit is fulfilled by writing the boundary conditions at (i*,1)and(i*,NCS). For the first and the NRSth rows (i.e., i=1 and i=NRS),all the NCS equations are written exclusively from the boundary conditions. The resulting system of NCS equations are solved sequentially (i=1,.....NRS) for the unknowns. Thus, solution can proceed row-wise leading to a substantial reduction of the memory requirement.

The boundary conditions are assigned as follows

Interior Rows ($i^* = 2, \dots, \text{NRS}-1$)

As described earlier, the boundary condition equations are written at $j=1$ and $j=\text{NCS}$.

The boundary at $j=\text{NCS}$ represents the 'zero lift' condition (refer 3.3.3.1.1.5). Thus, due to absence of vertical convection, the saltwater-concentration along this column will be quite small and has been assumed to be zero. Thus, at a node (i^*, NCS) the boundary condition is expressed as follows (refer Fig. 3.5-7)

$$C_{i^*, \text{NCS}, k+1}^{(k)} = 0.0 \quad \dots (3.19)$$

The boundary at $j=1$ is divided in three parts i.e., below the well ($\text{NRS} > i^* > \text{NRW}$); across the screen ($\text{NRB} < i^* \leq \text{NRW}$) [(NRW is the number of rows up to the well bottom, and NRB is the number of rows up to the bottom of blind pipe) (refer Fig.3.4)] and across the blind pipe ($1 < i^* \leq \text{NRB}$) (refer Fig. 3.4).

At any node ($i^*, 1$; $i^* = \text{NRW}+1, \dots, \text{NRS}-1$) lying below the well the boundary condition is derived from the saltwater balance as follows (refer Fig. 3.5-4)

$$S_1 + S_3 + S_4 + q^* = \frac{\partial c}{\partial t}$$

$$2D_r \frac{C_{i^*, j+1, k+1}^{(k)} - C_{i^*, j, k+1}^{(k)}}{\Delta r_s j} = \frac{XU_1}{(XU_1^2 - r_w^2)}$$

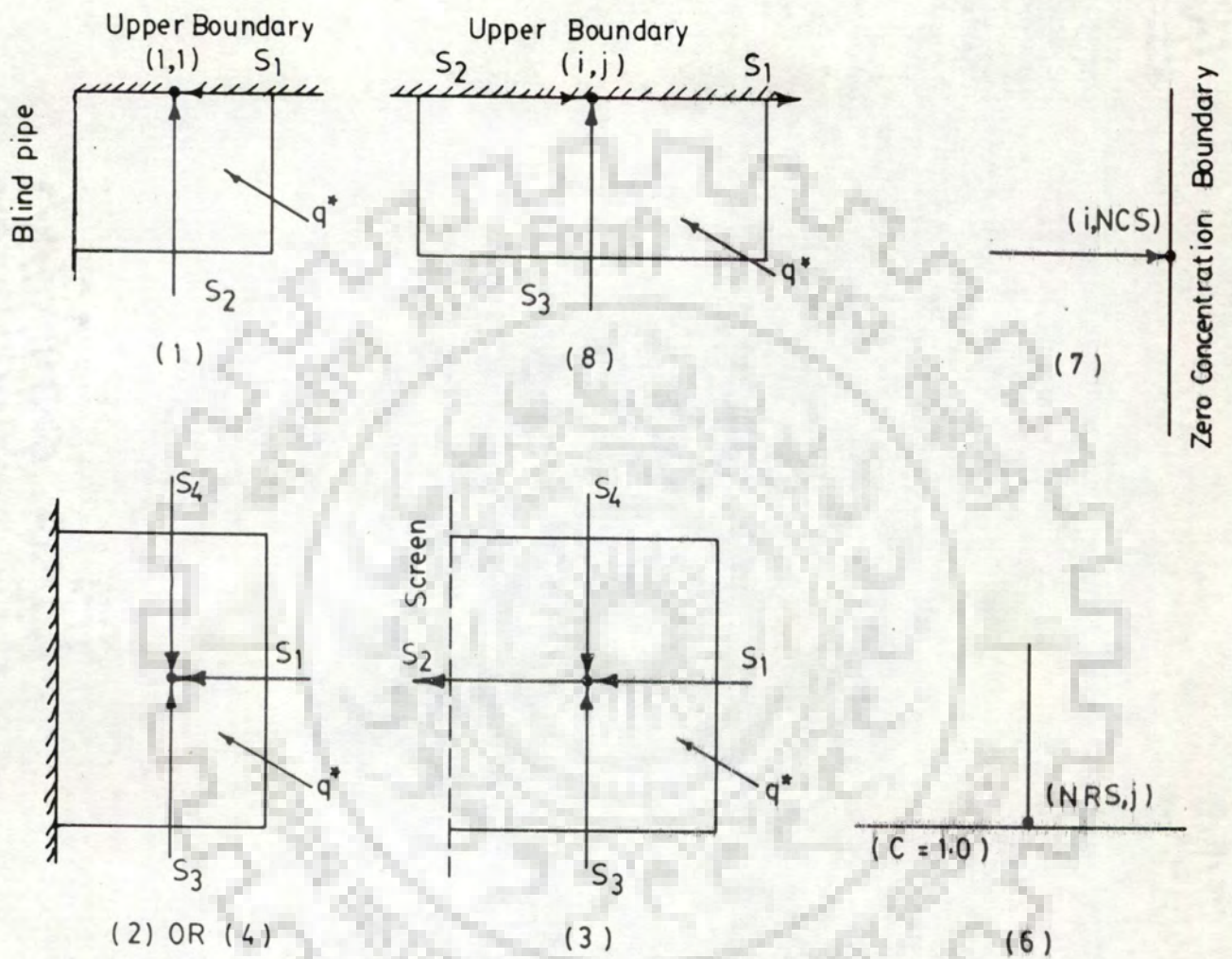


Fig (3.5) Boundary Nodes for Simulation of Saltwater Transport

$$\begin{aligned}
 & + D_z \left[\frac{C_{i^*-1,j,k+1}^{(l-1)} - C_{i^*,j,k+1}^{(l)}}{\Delta z_{i^*-1}} + \frac{C_{i^*+1,j,k+1}^{(l-1)} - C_{i^*,j,k+1}^{(l)}}{\Delta z_{i^*}} \right] \\
 & \frac{2}{\Delta z_{i^*-1} + \Delta z_{i^*}} + q_{i^*jk}^* = \frac{C_{i^*,j,k+1}^{(l)} - C_{i^*,j,k}^*}{\Delta t_s} \dots\dots\dots (3.20)
 \end{aligned}$$

At any node $(i^*, 1; i^* = \text{NRB}+1, \dots, \text{NRW})$ lying across the screen the boundary condition is derived from the saltwater balance as follows (refer Fig. 3.5-3)

$$\begin{aligned}
 S_1 - S_2 + S_3 + S_4 + q^* &= \frac{\partial C}{\partial t} \\
 2D_r \left(\frac{C_{i^*,j+1,k+1}^{(l)} - C_{i^*,j,k+1}^{(l)}}{\Delta r_{s_j}} - \frac{C_{i^*,j,k+1}^{(l)} - C_P}{X S_1 - r_w} \right) \frac{X U_1}{X U_1^2 - r_w^2} \\
 + D_z \left[\frac{C_{i^*-1,j,k+1}^{(l-1)} - C_{i^*,j,k+1}^{(l)}}{\Delta z_{i^*-1}} + \frac{C_{i^*+1,j,k+1}^{(l-1)} - C_{i^*,j,k+1}^{(l)}}{\Delta z_{i^*}} \right] \\
 \frac{2}{\Delta z_{i^*-1} + \Delta z_{i^*}} + q_{i^*jk}^* &= \frac{C_{i^*,j,k+1}^{(l)} - C_{i^*,j,k}^*}{\Delta t_s} \dots\dots\dots (3.21)
 \end{aligned}$$

Where C_P is the saltwater concentration in the pumped water at the discrete time t_k .

At any node $(i^*, 1; i^* = 2, \dots, \text{NRB})$ lying across the blind pipe the boundary condition is derived from the saltwater balance as follows (refer Fig. 3.5-2)

$$S_1 + S_3 + S_4 + q^* = \frac{\partial c}{\partial t}$$

$$\begin{aligned}
 & - 2D_r \frac{C_{i^*, j+1, k+1}^{(l)} - C_{i^*, j, k+1}^{(l)}}{\Delta r s_j} \frac{XU_1}{(XU_1^2 - r_w^2)} \\
 & + D_z \frac{C_{i^*, j, k+1}^{(l-1)} - C_{i^*, j, k+1}^{(l)}}{\Delta z_{i^*-1}} + \frac{C_{i^*, j+1, k+1}^{(l-1)} - C_{i^*, j, k+1}^{(l)}}{\Delta z_{i^*}} \\
 & \frac{2}{\Delta z_{i^*-1} + \Delta z_{i^*}} + q_{i^* jk} = \frac{C_{i^*, j, k+1}^{(l)} - C_{i^*, j, k}^{(l)}}{\Delta t_s} \dots\dots (3.22)
 \end{aligned}$$

Boundary Rows (i=1, i=NRS)

The upper boundary of the flow transport domain is represented by i=1. The boundary condition is derived from saltwater balance at (1,1); (1, j; j=2,NCS-1) and (1, NCS)

Node (1,1) (refer Fig. 3.5-1)

$$\begin{aligned}
 S_1 + S_2 + q^* &= \frac{\partial c}{\partial t} \\
 D_r \frac{C_{i, j+1, k+1}^{(l)} - C_{i, j, k+1}^{(l)}}{\Delta r s_j} &+ \frac{2 XU_1}{(XU_1^2 - r_w^2)} + 2D_z \frac{C_{i+1, j, k+1}^{(l-1)} - C_{i, j, k+1}^{(l)}}{(\Delta z_1)^2} \\
 + q_{ijk}^* &= \frac{C_{i, j, k+1}^{(l)} - C_{i, j, k}^{(l)}}{\Delta t_s} \dots (3.23)
 \end{aligned}$$

Nodes 1, j; j=2,NCS-1 (refer Fig. 3.5-8)

$$S_3 - S_1 + S_2 + q^* = \frac{\partial c}{\partial t}$$

$$\begin{aligned}
 & 2 D_{r_{ij}} \frac{C_{i,j-1,k+1}^{(l)} - C_{i,j,k+1}^{(l)}}{\Delta r_{s_{j-1}}} \left(\frac{XU_{j-1}}{XU_j^2 - XU_{j-1}^2} \right) \\
 & - 2 D_{r_{ij}} \frac{C_{i,j,k+1}^{(l)} - C_{i,j+1,k+1}^{(l)}}{\Delta r_{s_j}} \left(\frac{XU_j}{XU_{j+1}^2 - XU_j^2} \right) \\
 & + 2 D_{z_{ij}} \frac{C_{i+1,j,k+1}^{(l-1)} - C_{i,j,k+1}^{(l)}}{(\Delta z_i)^2} + q_{ijk} \\
 & = \frac{C_{i,j,k+1}^{(l)} - C_{i,j,k}^{(l)}}{\Delta t_s} \dots \dots \dots (3.24)
 \end{aligned}$$

Nodes 1, NCS (refer Fig. 3.5-7)

$$C_{i,j,K+1}^{(l)} = 0.0 \dots \dots \dots (3.25)$$

The lower boundary of the flow transport domain is represented by $i=NRS$. The boundary condition at $(NRS, j; j=1, \dots, NCS)$ (refer Fig. 3.5-6) is as follows

$$C_{i,j,k+1}^{(l)} = 1.0 \text{ (i.e., saltwater reservoir)} \dots \dots \dots (3.26)$$

For known boundary conditions ; C_{ijk} (from the preceding time step or initial conditions); and $C_{i-1,j,k+1}^{(l-1)}$, and $C_{i+1,j,k+1}^{(l-1)}$ (from the preceding iteration ; $C_{i-1,j,k+1}^{(0)} = C_{i-1,j,k}^{(0)}$, $C_{i,j,k+1}^{(0)} = C_{i,j,k}^{(0)}$, $C_{i+1,j,k+1}^{(0)} = C_{i+1,j,k}^{(0)}$) equation (3.18) is solved for $[C_{i,j,k+1}^{(l)}, j=1, NCS]$ successively for each row by Thomas' algorithm.



StageII (explicit in r-direction and implicit in z-direction)

Interior Nodes

Consider an interior node(i,j), a time increment from t_k to t_{k+1} and l^{th} iteration. Writing the spatial derivatives of C with respect to r explicitly and with respect to z implicitly, equation (3.14) is expressed in terms of finite-differences as follows(refer Fig. 3.4).

$$\begin{aligned}
 & \frac{D_{r_{i,j}}}{XS_j} \left[\frac{(C_{i,j+1,k+1}^{(l-1)} - C_{i,j,k+1}^{(l)})}{\Delta r_{s_j}} \frac{(XS_{j+1} + XS_j)}{2} \right. \\
 & \left. - \frac{(C_{i,j,k+1}^{(l)} - C_{i,j-1,k+1}^{(l-1)})}{\Delta r_{s_{j-1}}} \frac{(XS_j + XS_{j-1})}{2} \right] \frac{2}{(\Delta r_{s_j} + \Delta r_{s_{j-1}})} \\
 & + D_{z_{i,j}} \left[\frac{(C_{i+1,j,k+1}^{(l)} - C_{i,j,k+1}^{(l)})}{\Delta z_i} - \frac{(C_{i,j,k+1}^{(l)} - C_{i-1,j,k+1}^{(l)})}{\Delta z_{i-1}} \right] \\
 & \frac{2}{(\Delta z_i + \Delta z_{i-1})} - q_{ijk}^* \\
 & = \frac{C_{i,j,k+1}^{(l)} - C_{ijk}}{\Delta t_s} \dots\dots\dots (3.25)
 \end{aligned}$$

Equation (3.25) is rearranged as follows:

$$C_{i-1,j,k+1}^{(l)} \left[\frac{2D_{z_{i,j}}}{\Delta z_i + \Delta z_{i-1}} \left(\frac{1}{\Delta z_{i-1}} \right) \right]$$

$$\begin{aligned}
 &+ C_{i,j,k+1}^{(\ell)-} \left[\frac{2 D_{r,i,j}}{X S_j (\Delta r s_{j-1} + \Delta r s_j)} \left(- \frac{X S_{j+1} + X S_j}{2 \Delta r s_j} - \frac{X S_j + X S_{j-1}}{2 \Delta r s_{j-1}} \right) \right. \\
 &\quad + \frac{2 D_{z,i,j}}{\Delta z_i + \Delta z_{i-1}} \left(- \frac{1}{\Delta z_i} - \frac{1}{\Delta z_{i-1}} \right) \\
 &\quad \left. - \frac{1}{\Delta t_s} \right] + C_{i+1,j,k+1}^{(\ell)} \left[- \frac{2 D_{z,i,j}}{(\Delta z_i + \Delta z_{i-1})} \right. \\
 &\quad \left. \left(\frac{1}{\Delta z_{i-1}} \right) \right] \\
 &= - \frac{2 D_{r,i,j}}{X S_j (\Delta r s_j + \Delta r s_{j-1})} \left[\frac{X S_{j+1} + X S_j}{2 \Delta r s_j} C_{i,j+1,k+1}^{(\ell-1)} \right. \\
 &\quad \left. + \frac{X S_j + X S_{j-1}}{2 \Delta r s_{j-1}} C_{i,j-1,k+1}^{(\ell-1)} \right] + q_{ijk}^* - \frac{C_{ijk}}{\Delta t_s} \quad (3.26)
 \end{aligned}$$

For a given interior column (i.e., $j=2, \dots, NCS-1$) equation (3.26) is of the form

$$AA_i C_{i-1,j,k+1} + BB_i C_{i,j,k+1} + CC_i C_{i+1,j,k+1} = DD_i \quad (3.27)$$

$i=2, \dots, (NRS-1)$

Boundary Nodes

For any interior column (say $j=j^*$; $NCS > j^* > 1$) equation (3.27) can be written at each interior row (i.e., $i=2, NRS-1$). This provides $(NRS-2)$ equations. However, the unknowns $[C_{i,j^*,k+1}^{(\ell)}, j=1, \dots, NRS]$ along the j^* th column are NRS in number. $[C_{i,j^*,k}^*]$ are known from the preceding

time step or initial conditions ; $C_{i,j-1,k+1}^{(\ell-1)}$, $C_{i,j+1,k+1}^{(\ell-1)}$ from the preceding iteration]. This deficit is fulfilled by writing the boundary conditions at $(1, j^*)$ and (NRS, j^*) . For the first and the NCS^{th} column (i.e., $j=1$ and $j=NCS$), all the NRS equations are written exclusively from the boundary conditions. The resulting system of NRS equations are solved sequentially ($j=1, \dots, NCS$) for the unknowns. Thus, solution can proceed column-wise leading to a substantial reduction of the memory requirement.

The boundary conditions are assigned as follows

Interior Columns ($j^* = 2, \dots, NCS-1$)

As described earlier, the boundary condition equations are written at $i=1$ and $i=NRS$.

The boundary at $i=NRS$ represented the initial position of the interface. Thus, at a node (NRS, j^*) the boundary condition is expressed as follows (refer Fig. 3.5-6)

$$C_{NRS, j^*, k+1}^{(\ell)} = 1.0 \text{ (i.e., saltwater reservoir)} \quad \dots (3.28)$$

The upper boundary of the flow transport domain is represented by $i=1$. The boundary condition is derived from saltwater balance at $(1, j^*; j^* = 2, \dots, NCS-1)$ (refer Fig. 3.5-8)

Nodes $1, j^*; j^* = 2, \dots, NCS-1$

$$S_3 - S_1 + S_2 + q = \frac{\partial c}{\partial t}$$

$$2 D_r \frac{C_{i, j^*-1, k+1}^{(\ell-1)} - C_{i, j^*, k+1}^{(\ell)}}{\Delta r_{j^*-1}} \left(\frac{XU_{j^*-1}}{XU_{j^*}^2 - XU_{j^*-1}^2} \right)$$

$$\begin{aligned}
 & -2 D_r \frac{c_{i,j,k+1}^{(\ell)} - c_{i,j+1,k+1}^{(\ell-1)}}{\Delta r_{ij} \Delta r_s} \left(\frac{XU_j}{XU_{j+1}^2 - XU_j^2} \right) \\
 & + 2 D_z \frac{c_{i+1,j,k+1}^{(\ell)} - c_{i,j,k+1}^{(\ell)}}{(\Delta Z_i)^2} + q_{ij,k}^* \\
 & = \frac{c_{i,j,k+1}^{(\ell)} - c_{i,j,k}^{(\ell)}}{\Delta t_s} \dots \dots \dots (3.29)
 \end{aligned}$$

Boundary Columns (j=1, j=NCS)

The boundary at j=1 is divided in five parts i.e., at interface(i=NRS); below the well (NRS > i > NRW); across the screen (NRB < i ≤ NRW); across the blind pipe (1 < i ≤ NRB); and at first row (i=1)(refer Fig. 3.4).

At node (NRS,1) the boundary condition is represented by the initial position of the interface as follows(refer Fig.3.5-6)

$$c_{NRS,1,k+1}^{(\ell)} = 1.0 \text{ (i.e., saltwater reservoir) } \dots \dots (3.30)$$

At any node (i,1 ; i= NRW+1,....NRS-1) lying below the well the boundary condition is derived from the saltwater balance as follows (refer Fig. 3.5-4)

$$\begin{aligned}
 S_1 + S_3 + S_4 + q^* &= \frac{\partial c}{\partial t} \\
 2D_r \frac{c_{i,j+1,k+1}^{(\ell-1)} - c_{i,j,k+1}^{(\ell)}}{r_{ij} \Delta r_s} &= \frac{XU_1}{(XU_1^2 - r_w^2)}
 \end{aligned}$$

$$\begin{aligned}
 & + D_{z_{ij}} \left[\frac{C_{i-1,j,k+1}^{(l)} - C_{i,j,k+1}^{(l)}}{\Delta z_{i-1}} + \frac{C_{i+1,j,k+1}^{(l)} - C_{i,j,k+1}^{(l)}}{\Delta z_i} \right] \\
 & \frac{2}{\Delta z_{i-1} + \Delta z_i} + q_{ijk}^* = \frac{C_{i,j,k+1}^{(l)} - C_{i,j,k}^{(l)}}{\Delta t_s} \dots\dots\dots (3.31)
 \end{aligned}$$

At any node (i,1 ; i= NRB+1,....NRW) lying across the screen the boundary condition is derived from the saltwater balance as follows (refer Fig. 3.5-3)

$$\begin{aligned}
 S_1 - S_2 + S_3 + S_4 + q &= \frac{\partial C}{\partial t} \\
 2D_{r_{ij}} \left(\frac{C_{i,j+1,k+1}^{(l-1)} - C_{i,j,k+1}^{(l)}}{\Delta r_{sj}} - \frac{C_{i,j,k+1}^{(l)} - CP_k}{XS_1 - r_w} \right) & \frac{XU_1}{XU_1^2 - r_w^2} \\
 + D_{z_{ij}} \left[\frac{C_{i-1,j,k+1}^{(l)} - C_{i,j,k+1}^{(l)}}{\Delta z_{i-1}} + \frac{C_{i+1,j,k+1}^{(l)} - C_{i,j,k+1}^{(l)}}{\Delta z_i} \right] \\
 \frac{2}{\Delta z_{i-1} + \Delta z_i} + q_{ijk}^* &= \frac{C_{i,j,k+1}^{(l)} - C_{i,j,k}^{(l)}}{\Delta t_s} \dots\dots\dots (3.32)
 \end{aligned}$$

Where CP_k is the saltwater concentration in the pumped water at the discrete time t_k .

At any node (i,1; i=2,NRB) lying across the blind pipette boundary condition is derived from the saltwater balance as follows (refer Fig. 3.5-2)

$$S_1 + S_3 + S_4 + q^* = \frac{\partial c}{\partial t}$$

$$\begin{aligned}
& 2D_{r_{ij}} \frac{C_{i,j+1,k+1}^{(\ell-1)} - C_{i,j,k+1}^{(\ell)}}{\Delta r_{s_j}} - \frac{XU_1}{(XU_1^2 - r_w^2)} \\
& + D_{z_{ij}} \left[\frac{C_{i-1,j,k+1}^{(\ell)} - C_{i,j,k+1}^{(\ell)}}{\Delta z_{i-1}} + \frac{C_{i+1,j,k+1}^{(\ell)} - C_{i,j,k+1}^{(\ell)}}{\Delta z_i} \right] \\
& \frac{2}{\Delta z_{i-1} + \Delta z_i} + q_{ijk}^* = \frac{C_{i,j,k+1}^{(\ell)} - C_{i,j,k}^{(\ell)}}{\Delta t_s} \dots (3.33)
\end{aligned}$$

Node (1,1) (refer Fig. 3.5-1)

$$\begin{aligned}
& S_1 + S_2 + q^* = \frac{\partial c}{\partial t} \\
& D_{r_{ij}} \frac{C_{i,j+1,k+1}^{(\ell-1)} - C_{i,j,k+1}^{(\ell)}}{\Delta r_{s_j}} - \frac{2 XU_1}{(XU_1^2 - r_w^2)} + 2D_{z_{ij}} \frac{C_{i+1,j,k+1}^{(\ell)} - C_{i,j,k+1}^{(\ell)}}{(\Delta z_i)^2} \\
& + q_{ijk}^* = \frac{C_{i,j,k+1}^{(\ell)} - C_{i,j,k}^{(\ell)}}{\Delta t_s} \dots (3.34)
\end{aligned}$$

For known boundary conditions; C_{ijk} (from the preceding time step or initial conditions); and $C_{i,j-1,k+1}^{(\ell-1)}$ and $C_{i,j+1,k+1}^{(\ell-1)}$ (from the preceding iteration; $C_{i,j-1,k+1}^{(0)} = C_{i,j-1,k}$, $C_{i,j,k+1}^{(0)} = C_{i,j,k}$, $C_{i,j+1,k+1}^{(0)} = C_{i,j+1,k}$) equation (3.27) is solved for $[C_{i,j,k+1}^{(\ell)}, i=1, NRS]$ successively for each column by Thomas' algorithm.

3.3.4.1.3 The Dispersion Coefficient

In the present model the values of the dispersion coefficients are computed in accordance with the following equations (Scheidegger, 1961)

$$D_{r_{ij}} = \alpha_L U_{ij} \quad \dots\dots\dots(3.35)$$

and

$$D_{z_{ij}} = \alpha_T V_{ij} \quad \dots\dots\dots(3.36)$$

Where α_L and α_T are longitudinal and transverse dispersivities respectively, U_{ij} and V_{ij} are components of velocity in the longitudinal and transverse directions respectively.

3.3.4.1.4 Convergence Criteria

The differences of the $C_{i,j,k+1}^{(l)}$ values obtained in two successive iterations for all the nodes are summed up. This sum is then compared with a prestipulated convergence factor (say $\epsilon 1$). The iterations are continued until this sum attains a value less than $\epsilon 1$ i.e.,

$$\sum_j \sum_i | C_{i,j,k+1}^{(l)} - C_{i,j,k+1}^{(l-1)} | < \epsilon 1 \quad (3.37)$$

$$C_{i,j,k+1}^* = C_{i,j,k+1}^{(l)}$$

Where $C_{i,j,k+1}^*$ is the finally converged total concentration (i.e., concentration due to convection as well as diffusion) at the node (i,j) at discrete time t_{k+1} .

3.3.4.1.5 Integration of Diffusive Transport with the Moving Points

The finite difference solution described in the preceding solution provides the total concentration, $(C_{i,j,k+1}^*)$ at time t_{k+1} . The change of concentration (ΔC_{ij}) due to the diffusive transport is obtained as follows

$$\Delta C_{ij} = C_{i,j,k+1}^* - CC_{i,j,k+1} \quad \dots (3.38)$$

Where $CC_{i,j,k+1}$ is the concentration at node (i,j) at discrete time t_{k+1} accounting for only convection during the period t_k to t_{k+1} (refer equation 3.12).

ΔC_{ij} can be positive or zero or negative. A positive ΔC_{ij} implies addition of saltwater in the domain of the node (i,j) during the time step, and vice versa. The corresponding addition or abstraction (ΔV_{ij}) of saltwater volume is given by the following equation

$$\Delta V_{ij} = \Delta C_{ij} VLX_{ij} \phi \quad \dots (3.39)$$

This volume is accounted for by modifying appropriately the volumes of all the moving points lying in the domain of the node (i,j) at time t_{k+1} . This moderation of the moving point volumes is accomplished as follows.

If there are n moving points in the domain of nodal point (i,j) at t_{k+1} , the volume of each moving point (VL_m) is modified as follows

$$VL_m = VL_m + VL_m \frac{\Delta V_{ij}}{\sum_{m \in J_4} VL_m} \quad \dots (3.40)$$

Where J_4 , a subset of the moving points, comprises of all moving points lying in the domain of saltwater node (i,j) at discrete time t_{k+1} .

However, if there is no moving point in the domain, a new moving point is generated. This moving point is stationed at the node (i,j) and is assigned a volume equal to ΔV_{ij} .

3.3.5 Computation of Velocity Distribution

It is necessary to compute velocity distribution in space and time for assigning velocities of the take off and moving points.

Further, velocities need to be known for estimating the diffusion coefficients. The velocities at any discrete time are computed by first simulating the pressure distribution in space and subsequently by differentiating the pressure with respect to r and z coordinates.

3.3.5.1 Simulation of Pressure Distribution

The distribution of pressure in space and time is arrived at by solving equation 3.4. The equation can be expanded to the following form,

$$\begin{aligned} & \frac{k_r}{\mu r} \frac{\partial p}{\partial r} + \frac{k_r}{\mu} \frac{\partial^2 p}{\partial r^2} + \frac{1}{\mu} \frac{\partial p}{\partial r} \frac{\partial k_r}{\partial r} - \frac{k_r}{\mu} \frac{\partial p}{\partial r} \frac{\partial \mu}{\partial r} + \frac{k_z}{\mu} \frac{\partial^2 p}{\partial z^2} \\ & + \frac{1}{\mu} \frac{\partial p}{\partial z} \frac{\partial k_z}{\partial z} - \frac{k_z}{\mu} \frac{\partial p}{\partial z} \frac{\partial \mu}{\partial z} + \frac{k_z}{\mu} \frac{\partial \gamma}{\partial z} + \frac{\gamma}{\mu} \frac{\partial k_z}{\partial z} - \frac{k_z \gamma}{\mu} \frac{\partial \mu}{\partial z} \\ & = \frac{S_s}{\gamma} \frac{\partial p}{\partial t} \end{aligned} \quad \dots\dots\dots (3.41)$$

where $p = p(r, z, t)$

$\mu = \mu(C)$ [or $\mu(r, z, t)$ since $C = C(r, z, t)$]

$S_s = S_s(C)$ [or $S_s(r, z, t)$ since $C = C(r, z, t)$]

$\gamma = \gamma(C)$ [or $\gamma(r, z, t)$ since $C = C(r, z, t)$]

This equation is solved numerically by using IADIE. A finite difference grid is superposed over the entire flow domain. This grid has to be necessarily different from the finite difference grid used for computing diffusion transport. In order to discriminate between the two grids, the grid for pressure computations is qualified as 'pressure'. Thus, the rows and columns of the finite difference grid for simulation of pressure shall be hence forth called as 'pressure row' and 'pressure column' respectively.

Transformation of r Coordinate

The r coordinate is transformed to a new radial coordinate a as follows

Defining $a = \log_e r$

$$\text{or } \frac{\partial a}{\partial r} = \frac{1}{r}$$

$$\begin{aligned} \text{therefore } & \frac{k_r}{\mu r} \left(\frac{\partial p}{\partial r} \right) + \frac{\partial}{\partial r} \left(\frac{k_r}{\mu} \frac{\partial p}{\partial r} \right) \\ &= \frac{k_r}{\mu r^2} \frac{\partial p}{\partial a} + \frac{\partial}{r \partial a} \left(\frac{k_r}{\mu r} \frac{\partial p}{\partial a} \right) \\ &= \frac{1}{r^2} \frac{k_r}{\mu} \frac{\partial p}{\partial a} - \frac{1}{r^3} \frac{\partial r}{\partial a} \frac{k_r}{\mu} \frac{\partial p}{\partial a} \\ &+ \frac{1}{r^3} \frac{\partial}{\partial a} \left(\frac{k_r}{\mu} \frac{\partial p}{\partial a} \right) \\ &= \frac{1}{r^2} \frac{\partial}{\partial a} \left(\frac{k_r}{\mu} \frac{\partial p}{\partial a} \right) \dots \dots \dots (3.42) \end{aligned}$$

Thus equation (3.3) becomes

$$\frac{1}{r^2} \frac{\partial}{\partial a} \left(\frac{k_r}{\mu} \frac{\partial p}{\partial a} \right) + \frac{\partial}{\partial z} \left[\frac{k_z}{\mu} \left(-\frac{\partial p}{\partial z} + \gamma \right) \right] = \frac{S_s}{\gamma} \frac{\partial p}{\partial t} \quad (3.43)$$

Further, equation 3.43 can be expanded to the following form

$$\begin{aligned} & \frac{k_r}{r^2 \mu} \frac{\partial^2 p}{\partial a^2} + \frac{1}{\mu r^2} \frac{\partial p}{\partial a} \frac{\partial k_r}{\partial a} - \frac{k_r}{\mu r^2} \frac{\partial p}{\partial a} \frac{\partial \mu}{\partial a} + \frac{k_z}{\mu} \frac{\partial^2 p}{\partial z^2} \\ &+ \frac{1}{\mu} \frac{\partial p}{\partial z} \frac{\partial k_z}{\partial z} - \frac{k_z}{2} \frac{\partial p}{\partial z} \frac{\partial \mu}{\partial z} + \frac{k_z}{\mu} \frac{\partial \gamma}{\partial z} \\ &+ \frac{\gamma}{\mu} \frac{\partial k_z}{\partial z} - \frac{k_z \gamma}{\mu} \frac{\partial \mu}{\partial z} = \frac{S_s}{\gamma} \frac{\partial p}{\partial t} \dots \dots (3.44) \end{aligned}$$

The change of variable from r to a is known to control the

truncation errors in the finite differences solution (Rushton, 1979).

3.3.5.1.1 Specific Weight Variation

The variation of specific weight (γ) with saltwater concentration (C) is assumed to be governed by the following equation (Frind, 1982a).

$$\gamma(C) = \gamma(0) \left[1 + C \left(\frac{\gamma_s}{\gamma(0)} - 1 \right) \right] \quad \dots (3.45)$$

Where $\gamma(C)$ is the specific weight of water having C units of volume of salt water per unit total volume ($0 \leq C \leq 1$), $\gamma(0)$ is the specific weight of fresh water, and γ_s is the specific weight of saltwater.

3.3.5.1.2 The Dynamic Viscosity Equation

An experiment was carried out to obtain the relationship between μ and C using Ostwald Viscometer (refer Fig. 3.6a) (Garde and Mirajgaoker, 1983). This is a capillary tube viscometer in which the weight of liquid causes the flow. The liquid was first drawn through the capillary tube into the bulb well above the mark a. It was then allowed to drain back and the time (henceforth referred as flow time) required for the flow of the liquid from point a to point b was recorded.

Experiment was conducted on eleven samples of saline water having different saltwater concentrations ($0 \leq C \leq 1$). The flow time $[t(C)]$ for each sample was recorded. From proportionality, the relative viscosity $\left[\frac{\mu(C)}{\mu(0)} \right]$, is obtained as follows (Garde and Mirajgaoker, 1983).

$$\begin{aligned} \frac{\mu(C)}{\mu(0)} &= \frac{\gamma(C)}{\gamma(0)} \frac{t(C)}{t(0)} \\ &= \left[1 + C \left(\frac{\gamma_s}{\gamma(0)} - 1 \right) \right] \frac{t(C)}{t(0)} \quad (3.46a) \end{aligned}$$

Where $\mu(C)$ is the dynamic viscosity of saline water having a saltwater

concentration C ; $\mu(0)$ is the dynamic viscosity of freshwater ($C=0$); $t(C)$ is the flow time for the saline water having saltwater concentration C ; and $t(0)$ is the flow time for the freshwater ($C=0$).

The relative viscosity of each sample was computed from equation (3.46a). The plot of relative viscosity vs. the concentration is shown in Fig.(3.6b). The plot indicates a linear relation between relative viscosity and the saltwater concentration. The equation of the best straight line passing through the data points is as follows

$$\frac{\mu(C)}{\mu(0)} = (1.0 + 0.02825614 C) \quad \dots (3.46b)$$

3.3.5.1.3 The Specific Storage Equation

The specific storage, which is a function of the elasticity of water and the aquifer skeleton, is given by the following equation (Jacob, 1950)

$$\frac{S_s(C)}{\gamma(C)} = \frac{S_s(0)}{\gamma(0)} = \phi \beta \left(1 + \frac{\alpha}{\phi \beta} \right) \quad \dots (3.47)$$

Where β is reciprocal of the bulk modulus of elasticity of water, α is reciprocal of the bulk modulus of elasticity of aquifer skeleton, $S_s(C)$ is the specific storage of aquifer having C units of volume of saltwater per unit total volume of water, and $S_s(0)$ is the specific storage of aquifer having freshwater.

Assuming, ϕ , α and β to be constant.

$$\frac{S_s(C)}{\gamma(C)} = \frac{S_s(0)}{\gamma(0)} = \text{constant} \quad \dots (3.48)$$

$$\text{Thus } S_s(C) = S_s(0) \frac{\gamma(C)}{\gamma(0)}$$

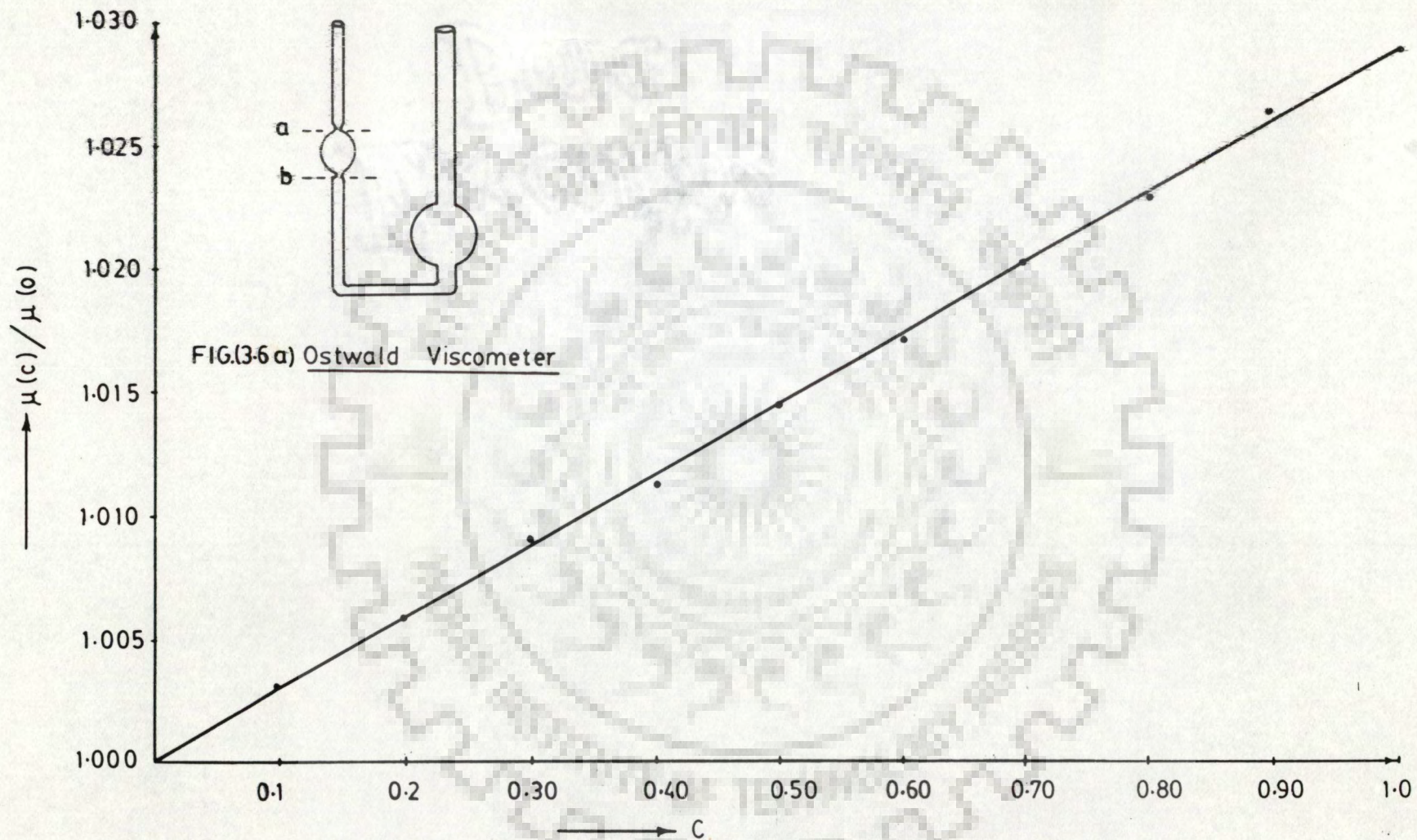


Fig. (3-6 b) Variation of Viscosity with Saltwater Concentration

$$= S_s (0) \left[1 + C \left(\frac{\gamma_s}{\gamma(0)} - 1 \right) \right] \quad \dots (3.49)$$

3.3.5.1.4 Time and Space Steps

Time Step: At the initial stage of pumping, the drawdowns increase very rapidly. The rate of increase of drawdowns decreases as the pumping continues. Thus, to control the truncation error in the finite - difference approximation of $\partial h / \partial t$, it is necessary to use ^avery small time step at the beginning of the pumpage. However, to restrict the computer time and the ^oroundoff error, the time step should be increased gradually, as the pumping continues.

Radial Space Step: The piezometric gradient in the lateral direction in the vicinity of the pumped well, is steep. The gradient decreases as the pumping continues. Thus, to control the truncation error in the finite difference approximate of $\partial h / \partial r$, $\partial^2 h / \partial r^2$ it is necessary to use very small radial space steps in the vicinity of the well face. However, to restrict the computer time and ^oroundoff error, the radial space steps should be increased gradually, as the radial distance increases.

Vertical Space Step: Close to the interface, the change of concentration in the vertical direction is very steep. Thus, to control the truncation error in the finite difference approximate of $\partial c / \partial z$ and $\partial^2 c / \partial z^2$, it is necessary to use very small vertical space steps in the vicinity of the interface. However, to restrict the computer time and roundoff error, the vertical space steps should be increased gradually, as the vertical distance increases from the interface .

Rushton and Chan Criteria: Rushton and Chan (1976) suggested an algorithm for assigning radial space steps and time steps for one dimensional axi - symmetric flow towards a fully penetrating well. They suggested division of every tenfold increase in radial distance as well

as time by an appropriate number of steps of equal logarithmic increase. The suggested initial time and distance are $0.1(r_w^2 S/4T)$ and (r_w) respectively (T is the transmissibility and S is the storage coefficient). Each tenfold increase in the radial distance is divided into six equal logarithmic steps. Each tenfold increase in the time is divided into decreasing number of equal logarithmic steps.

In the present study, each radial tenfold increase is divided in accordance with the Rushton and Chan's criteria. Thus, the change of $\log r$ in any space step is taken as $(1/6)$. The corresponding step of a is given as follows,

$$\begin{aligned} a &= \ln r = 2.3 \log r \\ \Delta a &= 2.3 \Delta (\log r) \\ &= \frac{2.3}{6} \\ &= 0.383 \end{aligned}$$

Each tenfold increase in time is divided into larger (i.e., larger than what is suggested by Rushton and Chan) number of equal logarithmic steps (refer Table 3.1). This was found to be necessary to speed up the rate of convergence of IADIE Scheme.

Table (3.1) Number of time steps.

$\frac{4tT}{r_w^2 S}$	Number of time steps suggested by Rushton and Chan (1976)	Number of time steps used in the present study
0.1-1	60	90
1-10	45	65
10-100	30	45
> 100	6	7

3.3.5.1.5 Finite Difference Solution

Equation (3.44) is written in terms of finite differences and solved by iterative alternating direction implicit-explicit (IADIE) scheme explained earlier. The space is discretized by a finite number of pressure nodes lying at the intersection of pressure rows and pressure columns (Fig.3.7). Similarly, the time domain is discretized by a finite number of discrete times. The spacing between the pressure rows and pressure columns and the time steps are assigned in accordance with the criteria described in the preceding paragraph.

3.3.5.1.6 IADIE Formulation

The two stages of IADIE to solve equation (3.44) are as follows

Stage I (Implicit in r-direction and Explicit in z-direction)

Interior Nodes

Consider an interior pressure node (i, j) , a time increment from t_k to t_{k+1} and l^{th} iteration. Writing the spatial derivatives of p with respect to r implicitly and with respect to z explicitly, equation (3.44) is expressed in terms of finite-differences as follows (refer Fig. 3.7).

$$\left[\frac{(p_{i,j+1,k+1}^{(l)} - p_{i,j,k+1}^{(l)})}{\Delta a} - \frac{(p_{i,j,k+1}^{(l)} - p_{i,j-1,k+1}^{(l)})}{\Delta a} \right] \frac{1}{\Delta a} \frac{1}{r_j^2} \\ \frac{(k_{r_{i,j-1}} + k_{r_{ij}})/2}{(\mu_{i,j-1} + \mu_{ij})/2} + \left[\frac{(p_{i,j+1,k+1}^{(l)} - p_{i,j,k+1}^{(l)})}{\Delta a} \right. \\ \left. \frac{(k_{r_{i,j+1,k}} - k_{r_{ijk}})}{\Delta a} + \frac{(p_{i,j,k+1}^{(l)} - p_{i,j-1,k+1}^{(l)})}{\Delta a} \frac{(k_{r_{ijk}} - k_{r_{i,j-1,k}})}{\Delta a} \right]$$

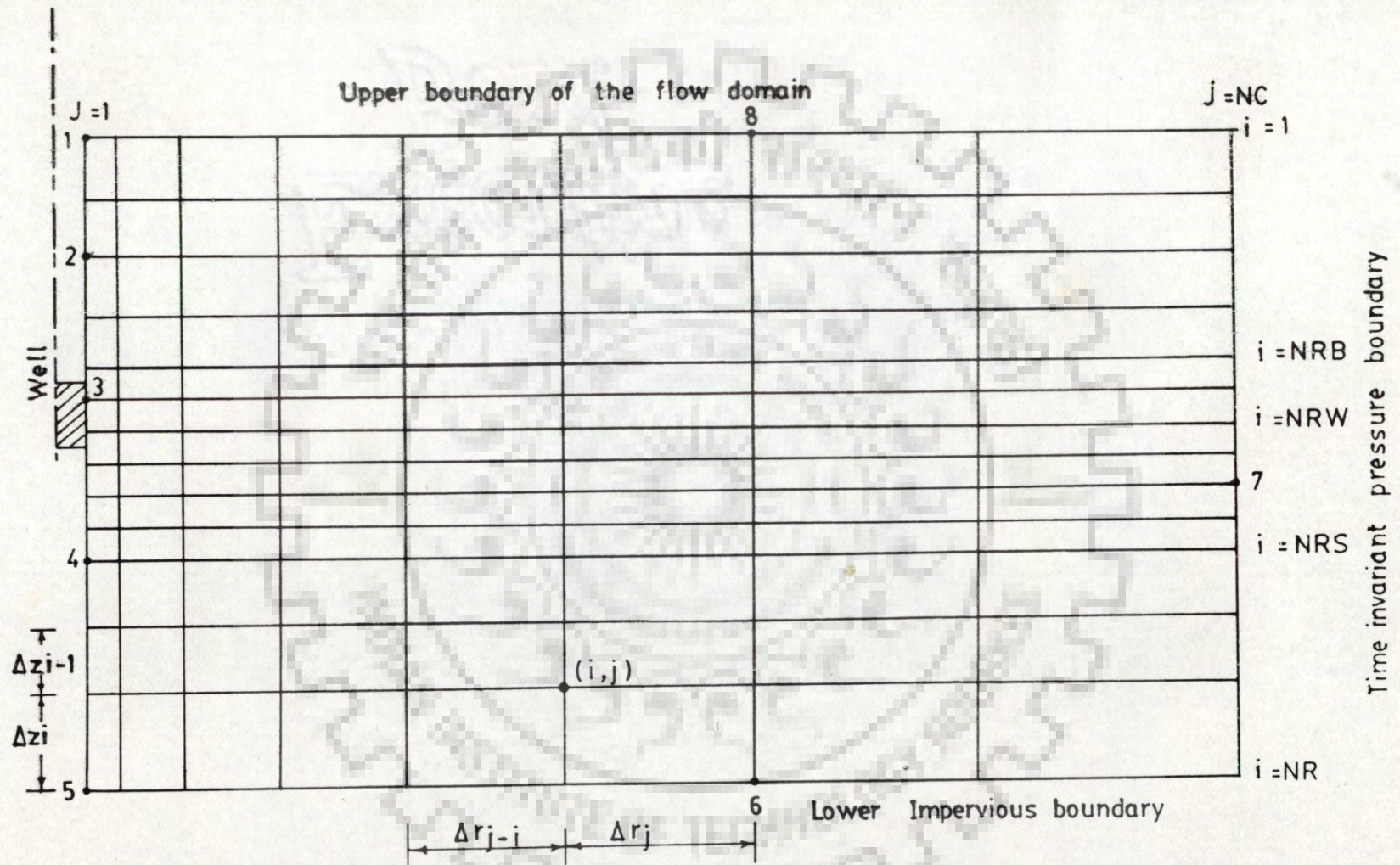


Fig (3.7) Finite Difference Mesh and Boundaries for Pressure Simulation

$$\frac{1}{r_j^2} \frac{1}{(\mu_{i,j} + \mu_{i,j-1})} \frac{(p_{i,j+1,k+1}^{(\ell)} - p_{i,j,k+1}^{(\ell)})}{\Delta a} + \frac{(\mu_{i,j+1,k} - \mu_{ijk})}{\Delta a} + \frac{(p_{i,j,k+1}^{(\ell)} - p_{i,j-1,k+1}^{(\ell)})}{\Delta a} \frac{(\mu_{ijk} - \mu_{i,j-1,k})}{\Delta a}]$$

$$\frac{1}{2r_j^2} \frac{(k_{r_{ij}} + k_{r_{i,j-1}})/2}{[(\mu_{i,j} + \mu_{i,j-1})/2]^2} + [\frac{(p_{i-1,j,k+1}^{(\ell-1)} - p_{i,j,k+1}^{(\ell-1)})}{\Delta z_{i-1}}$$

$$\frac{(p_{i,j,k+1}^{(\ell-1)} - p_{i+1,j,k+1}^{(\ell-1)})}{\Delta z_i}] \frac{1}{\Delta z_i} \frac{(k_{z_{ij}} + k_{z_{i-1,j}})/2}{(\mu_{ij} + \mu_{i-1,j})/2} +$$

$$[\frac{(p_{i-1,j,k+1}^{(\ell-1)} - p_{i,j,k+1}^{(\ell-1)})}{\Delta z_{i-1}} \frac{(k_{z_{i-1,j,k}} - k_{z_{ijk}})}{\Delta z_{i-1}} +$$

$$\frac{(p_{i,j,k+1}^{(\ell-1)} - p_{i+1,j,k+1}^{(\ell-1)})}{\Delta z_i} \frac{(k_{z_{ijk}} - k_{z_{i+1,j,k}})}{\Delta z_i}] \frac{1}{2(\mu_{ij} + \mu_{i-1,j})/2}$$

$$- [\frac{(p_{i-1,j,k+1}^{(\ell-1)} - p_{i,j,k+1}^{(\ell-1)})}{\Delta z_{i-1}} \frac{(\mu_{i-1,j,k} - \mu_{ijk})}{\Delta z_{i-1}}$$

$$+ \frac{(p_{i,j,k+1}^{(\ell-1)} - p_{i+1,j,k+1}^{(\ell-1)})}{\Delta z_i} \frac{(\mu_{ijk} - \mu_{i+1,j,k})}{\Delta z_i}] \frac{(k_{z_{ij}} + k_{z_{i-1,j}})/2}{2[(\mu_{ij} + \mu_{i-1,j})/2]^2}$$

$$+ [\frac{(\gamma_{i-1,j,k} - \gamma_{ijk})}{\Delta z_{i-1}} + \frac{(\gamma_{ijk} - \gamma_{i+1,j,k})}{\Delta z_i}] \frac{(k_{z_{ij}} + k_{z_{i-1,j}})/2}{2(\mu_{ij} + \mu_{i-1,j})/2}$$

$$+ [\frac{(k_{z_{i-1,j,k}} - k_{z_{ijk}})}{\Delta z_{i-1}} + \frac{(k_{z_{ijk}} - k_{z_{i+1,j,k}})}{\Delta z_i}] \frac{(\gamma_{ij} + \gamma_{i-1,j})/2}{2(\mu_{ij} + \mu_{i-1,j})/2}$$

$$- \left[\frac{(\mu_{i-1,j,k}^{-\mu_{ijk}})}{\Delta z_{i-1}} + \frac{(\mu_{ijk}^{-\mu_{i+1,j,k}})}{\Delta z_i} \right] \frac{(k_{z_{i,j}} + k_{z_{i-1,j}})/2}{2[(\mu_{ij} + \mu_{i-1,j})/2]^2} \\ \frac{(\gamma_{ij} + \gamma_{i-1,j})}{2} = \left[\frac{(p_{i,j,k+1}^{(\ell)} - p_{ijk})}{\Delta t} \right] \frac{S_{s_{ij}}}{\gamma_{ij}} \quad \dots\dots (3.50)$$

Where r_j is the radial distance of the j^{th} pressure column from the centre of the well, $p_{i,j,k}$ is the pressure at the beginning of the time interval at pressure node (i,j) , $p_{i,j,k+1}^{(\ell)}$ is the pressure at the end of the time interval at pressure node (i,j) , $k_{r_{ij}}$ and $k_{z_{ij}}$ are the intrinsic permeabilities in the radial and vertical directions at pressure node (i,j) respectively, $\mu_{i,j}$ is the dynamic viscosity at pressure node (i,j) , $\gamma_{i,j}$ is the specific weight at pressure node (i,j) , $S_{s_{ij}}$ is the specific storage at pressure node (i,j) , Δt is the time step, Δr_j is the radial distance between pressure node (i,j) and pressure node $(i,j+1)$, Δz_i is the vertical distance between pressure node (i,j) and pressure node $(i+1,j)$, and

$$\Delta z_1 = \frac{(\Delta z_i + \Delta z_{i-1})}{2}$$

Subsequently the term $p_{i,j,k+1}^{(\ell-1)}$ in the explicit derivative is replaced by the implicit term $p_{i,j,k+1}^{(\ell)}$. This has been found to lead to a much faster convergence, possibly because of the strengthening of the diagonal term B_j (refer equation 3.52) without disturbing the tridiagonal nature of the system of equations. The same approach has been used subsequently for writing down all the explicit finite differences equations.

Equation (3.50) is rearranged as follows,

$$p_{i,j-1,k+1}^{(\ell)} \left[\frac{1}{\Delta a^2} - \frac{1}{r_j^2} \frac{(k_{r_{ij}} + k_{r_{i,j-1}})}{(\mu_{ij} + \mu_{i,j-1})} - \frac{(k_{r_{ijk}} - k_{r_{i,j-1,k}})}{\Delta a^2} \right. \\ \left. \frac{1}{r_j^2} \frac{1}{(\mu_{ij} + \mu_{i,j-1})} + \frac{(\mu_{ijk} - \mu_{i,j-1,k})}{\Delta a^2} \frac{1}{2r_j^2} \frac{(k_{r_{ij}} + k_{r_{k,j-1}})^{1/2}}{[(\mu_{ij} + \mu_{i,j-1})/2]^2} \right]$$

$$+ p_{i,j,k+1}^{(\ell)} \left[\left(-\frac{2}{\Delta a^2} \right) \frac{1}{r_j^2} \frac{(k_{r_{ij}} + k_{r_{i,j-1}})}{(\mu_{ij} + \mu_{i,j-1})} \right.$$

$$\left. + \left(-\frac{k_{r_{i,j+1,k}}}{\Delta a^2} - \frac{k_{r_{ijk}}}{\Delta a^2} + \frac{k_{r_{ijk}} - k_{r_{i,j-1,k}}}{\Delta a^2} \right) \frac{1}{(\mu_{ij} + \mu_{i,j-1})} \frac{1}{r_j^2} \right.$$

$$\left. - \left(-\frac{\mu_{i,j+1,k} - \mu_{ijk}}{\Delta a^2} + \frac{\mu_{ijk} - \mu_{i,j-1,k}}{\Delta a^2} \right) \frac{1}{2r_j^2} \frac{(k_{r_{ij}} + k_{r_{i,j-1}})^{1/2}}{[(\mu_{ij} + \mu_{i,j-1})/2]^2} \right.$$

$$- \frac{S_{s_{ij}}}{\gamma_{ij} \Delta t} + \left(-\frac{1}{\Delta z_{i-1}} - \frac{1}{\Delta z_i} \right) \frac{(k_{z_{ij}} + k_{z_{i+1,j}})}{\Delta z_i (\mu_{ij} + \mu_{i-1,j})}$$

$$+ \left(-\frac{k_{z_{i-1,j,k}} - k_{z_{ijk}}}{\Delta z_{i-1}^2} + \frac{k_{z_{ijk}} - k_{z_{i+1,j,k}}}{\Delta z_i^2} \right) \frac{1}{(\mu_{ij} + \mu_{i+1,j})}$$

$$- \left(-\frac{\mu_{i-1,j,k} - \mu_{ijk}}{\Delta z_{i-1}^2} + \frac{k_{z_{ijk}} - k_{z_{i+1,j,k}}}{\Delta z_i^2} \right) \frac{(k_{z_{ij}} + k_{z_{i+1,j}})}{2[(\mu_{ij} + \mu_{i+1,j})/2]^2}$$

$$+ p_{i,j+1,k+1}^{(\ell)} \left[\frac{1}{\Delta a^2} - \frac{1}{r_j^2} \frac{(k_{r_{ij}} + k_{r_{i,j-1}})}{(\mu_{ij} + \mu_{i,j-1})} \right.$$

$$\left. + \frac{1}{\Delta a^2} (k_{r_{i,j+1,k}} - k_{r_{ijk}}) \frac{1}{r_j^2} \frac{1}{(\mu_{ij} + \mu_{i,j-1})} \right]$$

$$\begin{aligned}
& - \frac{(\mu_{i,j+1,k} - \mu_{ijk})}{\Delta a^2} \frac{1}{r_j^2} \frac{(k_{r_{ij}} + k_{r_{i,j-1}})/2}{[(\mu_{ij} + \mu_{i,j-1})/2]^2}] \\
& = - \left(\frac{p_{i-1,j,k+1}^{(\ell-1)}}{\Delta z_{i-1}} + \frac{p_{i+1,j,k+1}^{(\ell-1)}}{\Delta z_i} \right) \frac{(k_{z_{ij}} + k_{z_{i-1,j}})}{(\mu_{ij} + \mu_{i-1,j})} \\
& - \left(p_{i-1,j,k+1}^{(\ell-1)} \frac{k_{z_{i-1,j,k}} - k_{z_{ijk}}}{\Delta z_{i-1}^2} - p_{i+1,j,k+1}^{(\ell-1)} \frac{k_{z_{ijk}} - k_{z_{i+1,j,k}}}{\Delta z_i^2} \right) \\
& \frac{1}{(\mu_{ij} + \mu_{i-1,j})} + \left[\frac{p_{i-1,j,k+1}^{(\ell-1)} (\mu_{i-1,j,k} - \mu_{ijk})}{\Delta z_{i-1}^2} \right. \\
& \left. - \frac{p_{i+1,j,k+1}^{(\ell-1)} (\mu_{ijk} - \mu_{i+1,j,k})}{\Delta z_i^2} \right] \frac{(k_{z_{ij}} + k_{z_{i-1,j}})}{(\mu_{ij} + \mu_{i-1,j})^2} \\
& - \left[\frac{(\gamma_{i-1,j,k} - \gamma_{ijk})}{\Delta z_{i-1}} + \frac{(\gamma_{ijk} - \gamma_{i+1,j,k})}{\Delta z_i} \right] \frac{(k_{z_{ij}} + k_{z_{i-1,j}})}{2(\mu_{ij} + \mu_{i-1,j})} \\
& - \left[\frac{(k_{z_{i-1,j,k}} - k_{z_{ijk}})}{\Delta z_{i-1}} + \frac{(k_{z_{ijk}} - k_{z_{i+1,j,k}})}{\Delta z_i} \right] \frac{(\gamma_{ij} + \gamma_{i-1,j})}{2(\mu_{ij} + \mu_{i-1,j})} \\
& + \left[\frac{(\mu_{i-1,j,k} - \mu_{ijk})}{\Delta z_{i-1}} + \frac{(\mu_{ijk} - \mu_{i+1,j,k})}{\Delta z_i} \right] \\
& - \frac{(k_{z_{ij}} + k_{z_{i-1,j}}) (\gamma_{ij} + \gamma_{i-1,j})}{4(\mu_{ij} + \mu_{i-1,j})} - \frac{p_{ijk}}{\Delta t} \frac{S_{s_{ij}}}{\gamma_{ij}} \dots (3.51)
\end{aligned}$$

For a given interior pressure row (i.e., $i=2, NR-1$) equation (3.51) is of the form

$$A_j p_{i,j-1,k+1} + B_j p_{i,j,k+1} + C_j p_{i,j+1,k+1} = D_j \quad \dots (3.52)$$

$j=2, \dots, \dots, \text{NC}-1$)

Where NR is the number of pressure rows up to the lower impervious boundary, and NC is the number of pressure columns up to the time-invariant pressure boundary.

Boundary Pressure Nodes

For any interior pressure row ($i=i^*$; $\text{NR} > i^* > 1$) equation (3.52) can be written at each interior pressure column (i.e., $j=2, \text{NC}-1$). This provides $(\text{NC} - 2)$ equations. However, the unknowns $[p_{i^*,j,k+1}^{(l)}, j=1, \dots, \text{NC}]$ along the i^{th} pressure row are NC in number. $[p_{i^*,j,k+1}^{(l)}$ are known from the preceding time step or initial conditions $p_{i^*-1,j,k+1}^{(l-1)}, p_{i^*+1,j,k+1}^{(l-1)}$ from preceding iteration]. This deficit is fulfilled by writing the boundary conditions at $(i^*, 1)$ and (i^*, NC) . For the first and the NR^{th} pressure rows (i.e., $i=1$ and $i=\text{NR}$), all the NC equations are written exclusively from the boundary conditions. The resulting system of NC equations are solved sequentially ($i=1, \dots, \text{NR}$) for the unknowns. Thus, solution can proceed pressure row-wise leading to a substantial reduction of the memory requirement.

The boundary conditions are assigned as follows

Interior Pressure Rows ($i=i^*$; $i^*=2, \dots, \text{NR}-1$)

As described earlier, the boundary condition equations are written at $j=1$ and $j=\text{NC}$.

The boundary at $j=\text{NC}$ is assumed to represent a time-invariant pressure condition. Thus, at a pressure node (i^*, NC) the boundary condition is expressed as follows

$$p_{i^*, \text{NC}, k+1}^{(l)} = P_{i^*, \text{NC}, 0} \quad \dots (3.53)$$

The boundary at $j=1$ is divided in three parts i.e., below the

well ($NR > i^* > NRW$); across the screen ($NRB < i^* \leq NRW$) and across the blind pipe ($1 < i^* \leq NRB$) (refer Fig. 3.7).

At any pressure node lying below the well ($i^*, 1$; $i^* = NRW+1, \dots, NR-1$) the boundary condition is derived from the water balance as follows (refer Fig. 3.8-4)

$$\begin{aligned}
 S_1 + S_2 + S_3 &= \frac{S_s}{\gamma} \frac{\partial p}{\partial t} \frac{(\Delta z_{i-1}^* + \Delta z_i^*)}{2} [\pi(r_w + \Delta r_j/2)^2 - \pi r_w^2] \\
 &+ \frac{k_{r_{i,j}}}{\mu_{i,j}} \frac{(p_{i^*,j+1,k+1}^{(l)} - p_{i^*,j,k+1}^{(l)})}{\Delta r_j} [2\pi(r_w + \Delta r_j/2) \frac{\Delta z_{i-1}^* + \Delta z_i^*}{2}] + \\
 &+ \frac{k_{z_{i,j}}}{\mu_{i,j}} \frac{(p_{i^*,j+1,k+1}^{(l-1)} - p_{i^*,j,k+1}^{(l)})}{\Delta z_i^*} [-\gamma_{i^*,j}] + \\
 &+ \frac{k_{z_{i-1,j}}}{\mu_{i-1,j}} \frac{(p_{i^*,j-1,k+1}^{(l-1)} - p_{i^*,j,k+1}^{(l)})}{\Delta z_{i-1}^*} [1 + \gamma_{i^*,j}] [\pi(r_w + \Delta r_j/2)^2 - \pi r_w^2] \\
 &= \frac{S_{s_{i,j}}}{\gamma_{i,j}} \frac{(p_{i^*,j,k+1}^{(l)} - p_{i^*,j,k}^{(l)})}{\Delta t} \frac{(\Delta z_{i-1}^* + \Delta z_i^*)}{2} [\pi(r_w + \Delta r_j/2)^2 - \pi r_w^2]
 \end{aligned} \dots\dots\dots (3.54)$$

At any pressure node ($i^*, 1$; $i^* = NRB+1, \dots, NRW$) lying across the screen the boundary condition is derived from the water balance as follows (refer Fig. 3.8-3)

$$\begin{aligned}
 S_2 + S_3 + S_1 \frac{Q}{NRW-0.5} &= \frac{S_s}{\gamma} \frac{\partial p}{\partial t} \frac{(\Delta z_{i-1}^* + \Delta z_i^*)}{2} [\pi(r_w + \Delta r_j/2)^2 - \pi r_w^2] \\
 &+ \frac{k_{r_{i,j}}}{\mu_{i,j}} \frac{(p_{i^*,j+1,k+1}^{(l)} - p_{i^*,j,k+1}^{(l)})}{\Delta r_j} [2\pi(r_w + \Delta r_j/2) \frac{\Delta z_{i-1}^* + \Delta z_i^*}{2}] +
 \end{aligned}$$

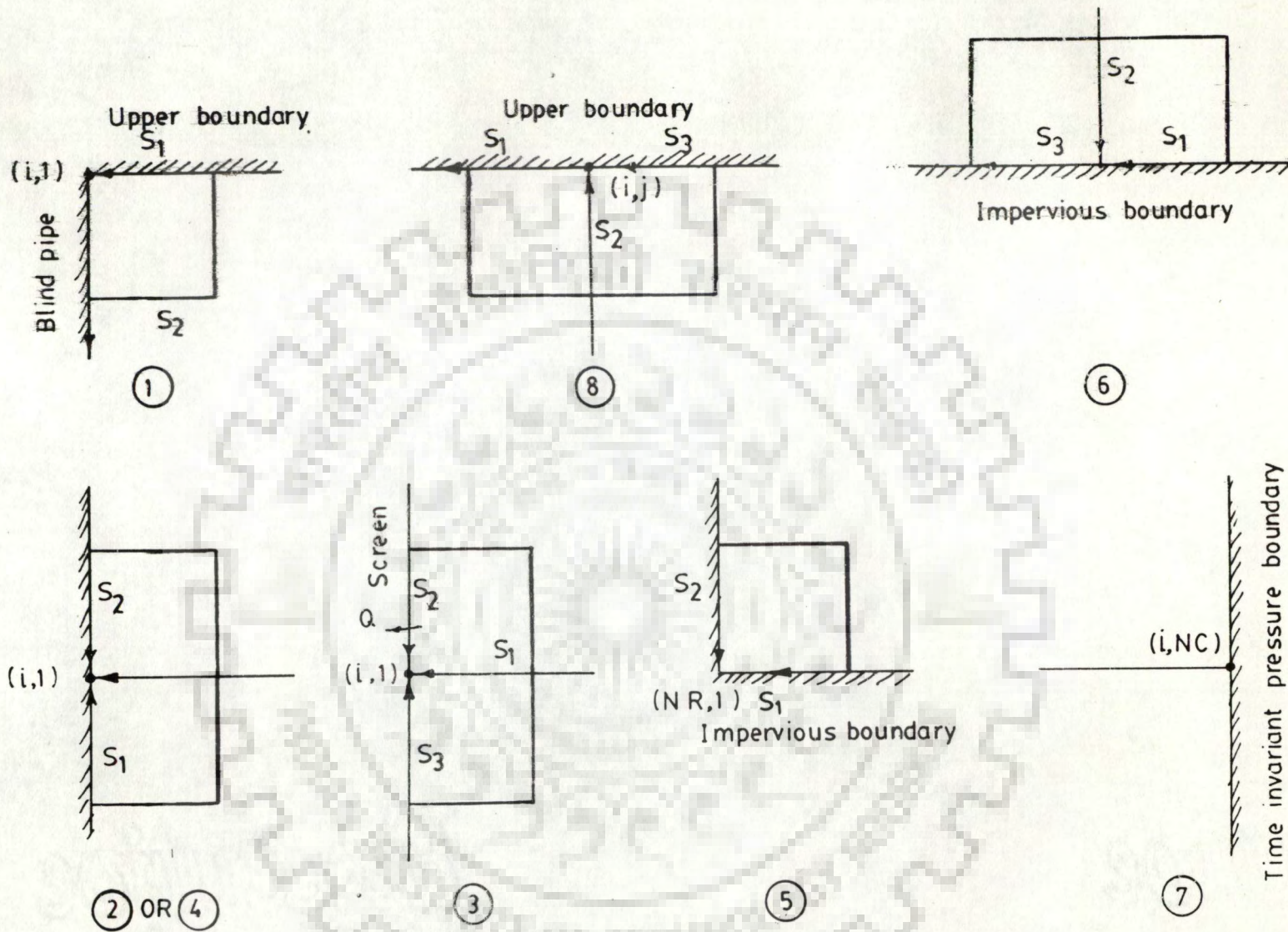


Fig (3.8) Boundary Nodes for Pressure Simulation

$$\begin{aligned}
& \left\{ \frac{k_{z i j}^*}{\mu_{i j}^*} \left[\frac{(p_{i+1, j, k+1}^{(l-1)} - p_{i, j, k+1}^{(l)})}{\Delta z_i^*} \right] - \gamma_{i j}^* \right\} - \frac{Q}{NRW - 0.5} + \\
& \frac{k_{z i-1, j}^*}{\mu_{i-1, j}^*} \left[\frac{(p_{i-1, j, k+1}^{(l-1)} - p_{i, j, k+1}^{(l)})}{\Delta z_{i-1}^*} \right] + \gamma_{i j}^* \left\} [\pi(r_w + \Delta r_j/2)^2 - \pi r_w^2] \right. \\
& = \frac{S_{s i j}^*}{\gamma_{i j}^*} \frac{(p_{i, j, k+1}^{(l)} - p_{i, j, k}^{(l)}) (\Delta z_{i-1}^* + \Delta z_i^*)}{\Delta t} \left(\frac{i-1}{2} \frac{i}{2} \right) [\pi(r_w + \Delta r_j/2)^2 - \pi r_w^2] \\
& \dots \dots \dots (3.55)
\end{aligned}$$

At any pressure node ($i^*=1; i^*=2, \dots, NRB$) lying across the blind pipe the boundary condition is derived from the water balance as follows (refer Fig. 3.8-2)

$$\begin{aligned}
S_1 + S_2 + S_3 &= \frac{S_s}{\gamma} \frac{\partial p}{\partial t} \left(\frac{i-1}{2} \frac{i}{2} \right) (\Delta z_{i-1}^* + \Delta z_i^*) [\pi(r_w + \Delta r_j/2)^2 - \pi r_w^2] \\
& \frac{k_{r i j}^*}{\mu_{i j}^*} \left[\frac{(p_{i, j+1, k+1}^{(l)} - p_{i, j, k+1}^{(l)})}{\Delta r_j} \right] [2\pi(r_w + \Delta r_j/2) \frac{\Delta z_{i-1}^* + \Delta z_i^*}{2}] + \\
& \left\{ \frac{k_{z i j}^*}{\mu_{i j}^*} \left[\frac{(p_{i+1, j, k+1}^{(l-1)} - p_{i, j, k+1}^{(l)})}{\Delta z_i^*} \right] - \gamma_{i j}^* \right\} + \\
& \frac{k_{z i-1, j}^*}{\mu_{i-1, j}^*} \left[\frac{(p_{i-1, j, k+1}^{(l-1)} - p_{i, j, k+1}^{(l)})}{\Delta z_{i-1}^*} \right] + \gamma_{i j}^* \left\} [\pi(r_w + \Delta r_j/2)^2 - \pi r_w^2] \right. \\
& = \frac{S_{s i j}^*}{\gamma_{i j}^*} \frac{(p_{i, j, k+1}^{(l)} - p_{i, j, k}^{(l)}) (\Delta z_{i-1}^* + \Delta z_i^*)}{\Delta t} \left(\frac{i-1}{2} \frac{i}{2} \right) [\pi(r_w + \Delta r_j/2)^2 - \pi r_w^2] \\
& \dots \dots \dots (3.56)
\end{aligned}$$

Boundary Pressure Rows ($i=1, i=NR$)

The upper boundary of the flow transport domain is represented by $i=1$. The boundary condition is derived from water balance at $(1,1); (1,j; j=2, \dots, NC-1)$ and $(1,NC)$

Pressure Node $(1,1)$ (refer Fig. 3.8-1)

$$\begin{aligned}
 S_1 - S_2 &= \frac{S_s}{\gamma} \frac{\partial p}{\partial t} \frac{\Delta z_1}{2} [\pi(r_w + \Delta r_j/2)^2 - \pi r_w^2] \\
 &+ \frac{k_{r_{ij}}}{\mu_{ij}} \left[\frac{(p_{i,j+1,k+1}^{(l)} - p_{i,j,k+1}^{(l)})}{\Delta r_j} \right] [2\pi(r_w + \Delta r_j/2)] \frac{\Delta z_1}{2} - \\
 &+ \frac{k_{z_{ij}}}{\mu_{ij}} \left[\frac{(p_{i,j,k+1}^{(l)} - p_{i+1,j,k+1}^{(l)})}{\Delta z_1} \right] + \gamma_{ij} [\pi(r_w + \Delta r_j/2)^2 - \pi r_w^2] + \\
 &= \frac{S_{s_{ij}}}{\gamma_{ij}} \frac{(p_{i,j,k+1}^{(l)} - p_{i,j,k}^{(l)})}{\Delta t} \frac{\Delta z_1}{2} [\pi(r_w + \Delta r_j/2)^2 - \pi r_w^2] \dots (3.57)
 \end{aligned}$$

Pressure Nodes $1,j; j=2, \dots, NC-1$ (refer Fig. 3.8-8)

$$\begin{aligned}
 S_1 - S_3 - S_2 &= \frac{S_s}{\gamma} \frac{\partial p}{\partial t} \frac{\Delta z_1}{2} \pi [(r_{j+1} - \Delta r_j/2)^2 - (r_j - \Delta r_{j-1}/2)^2] \\
 &+ \frac{k_{r_{ij}}}{\mu_{ij}} \left[\frac{(p_{i,j+1,k+1}^{(l)} - p_{i,j,k+1}^{(l)})}{\Delta r_j} \right] (r_{j+1} - \Delta r_j/2) - \\
 &+ \frac{k_{r_{i,j-1}}}{\mu_{i,j-1}} \left[\frac{(p_{i,j,k+1}^{(l)} - p_{i,j-1,k+1}^{(l)})}{\Delta r_{j-1}} \right] (r_j - \Delta r_{j-1}/2) \pi \frac{\Delta z_1}{2} -
 \end{aligned}$$

$$\frac{k_{z_{ij}}}{\mu_{1j}} \left[\frac{(p_{i,j,k+1}^{(l)} - p_{i+1,j,k+1}^{(l-1)})}{\Delta z_i} + \gamma_{ij} \right] \pi [(r_{j+1} - \Delta r_j/2)^2 - (r_j - \Delta r_{j-1}/2)^2] = \frac{S_{s_{ij}}}{\gamma_{ij}} \frac{(p_{i,j,k+1}^{(l)} - p_{i,j,k}^{(l)})}{\Delta t} \frac{\Delta z_i}{2} \dots (3.58)$$

Pressure Nodes 1, NC(refer Fig 3.8-7)

$$p_{i,NC,k+1}^{(l)} = p_{i,NC,0} \dots (3.59)$$

The lower boundary of the flow transport domain is represented by $i=NR$. The boundary condition at $(NR,1)$; $(NR,j; j=2, \dots, NC-1)$ and (NR,NC)

Pressure Node(NR,1)(refer Fig. 3.8-5)

$$S_1 + S_2 = \frac{S_s}{\gamma} \frac{\partial p}{\partial t} \frac{\Delta z_{i-1}}{2} \left[\pi (r_w + \Delta r_j/2)^2 - \pi r_w^2 \right] + \frac{k_{r_{ij}}}{\mu_{ij}} \left[\frac{(p_{i,j+1,k+1}^{(l)} - p_{i,j,k+1}^{(l)})}{\Delta r_j} \right] \left[2\pi (r_w + \Delta r_j/2) \right] \frac{\Delta z_{i-1}}{2} + \frac{k_{z_{i-1,j}}}{\mu_{i-1,j}} \left[\frac{(p_{i-1,j,k+1}^{(l-1)} - p_{i,j,k+1}^{(l)})}{\Delta z_{i-1}} + \gamma_{ij} \right] \left[\pi (r_w + \Delta r_j/2)^2 - \pi r_w^2 \right] = \frac{S_{s_{1j}}}{\gamma_{1j}} \frac{(p_{i,j,k+1}^{(l)} - p_{i,j,k}^{(l)})}{\Delta t} \frac{\Delta z_{i-1}}{2} \left[\pi (r_w + \Delta r_j/2)^2 - \pi r_w^2 \right] \dots (3.60)$$

Pressure Nodes(NR, j; j=2,.....NC-1)(refer Fig.3.8-6)

$$\begin{aligned}
 S_1 - S_3 - S_2 &= \frac{S_s}{\gamma} \frac{\partial p}{\partial t} \frac{\Delta z_{i-1}}{2} \pi [(r_{j+1} - \Delta r_j / 2)^2 - (r_j - \Delta r_{j-1} / 2)^2] \\
 &\left\{ \frac{k_{r_{ij}}}{\mu_{ij}} \left[\frac{(p_{i,j+1,k+1}^{(l)} - p_{i,j,k+1}^{(l)})}{\Delta r_j} \right] (r_{j+1} - \Delta r_j / 2) - \right. \\
 &\frac{k_{r_{i,j-1}}}{\mu_{i,j-1}} \left[\frac{(p_{i,j,k+1}^{(l)} - p_{i,j-1,k+1}^{(l)})}{\Delta r_{j-1}} \right] (r_j - \Delta r_{j-1} / 2) \left. \right\} \pi \frac{\Delta z_{i-1}}{2} \\
 &\frac{k_{z_{i-1,j}}}{\mu_{i-1,j}} \left[\frac{(p_{i,j,k+1}^{(l)} - p_{i-1,j,k+1}^{(l-1)})}{\Delta z_{i-1}} \right] - \alpha_{ij} \left. \right] \pi [(r_{j+1} - \Delta r_j / 2)^2 - \\
 &(r_j - \Delta r_{j-1} / 2)^2] = \frac{S_{s_{ij}}}{\alpha_{ij}} \frac{(p_{i,j,k+1}^{(l)} - p_{i,j,k}^{(l)})}{\Delta t} \frac{\Delta z_{i-1}}{2} \\
 &\pi [(r_{j+1} - \Delta r_j / 2)^2 - (r_j - \Delta r_{j-1} / 2)^2] \dots (3.61)
 \end{aligned}$$

Pressure Node(NR, NC)

$$p_{i,NC,k+1}^{(l)} = p_{i,NC,0} \dots (3.62)$$

For known boundary conditions; p_{ijk} (from the preceding time step or initial conditions); and $p_{i-1,j,k+1}^{(l-1)}$, and $p_{i+1,j,k+1}^{(l-1)}$ (from the preceding iteration ; $p_{i-1,j,k+1}^{(0)} = p_{i-1,j,k}^{(0)}$, $p_{i,j,k+1}^{(0)} = p_{i,j,k}^{(0)}$, $p_{i+1,j,k+1}^{(0)} = p_{i+1,j,k}^{(0)}$) equation (3.52) is solved for $[p_{i,j,k+1}^{(l)}, j=1,NC]$ successively for each pressure row by Thomas' algorithm.

Stage II (Explicit in r-direction and Implicit in z-direction)

Interior Pressure Nodes

Consider an interior pressure node (i, j) , a time increment from t_k to t_{k+1} and l^{th} iteration. Writing the spatial derivatives of p with respect to r explicitly and with respect to z implicitly, equation (3.44) is expressed in terms of finite-differences as follows (refer Fig. 3.7).

$$\begin{aligned}
 & \left[\frac{(p_{i,j+1,k+1}^{(l-1)} - p_{i,j,k+1}^{(l)})}{\Delta a} - \frac{(p_{i,j,k+1}^{(l)} - p_{i,j-1,k+1}^{(l-1)})}{\Delta a} \right] \frac{1}{\Delta a} \frac{1}{r_j^2} \\
 & \frac{(k_{r_{i,j-1}} + k_{r_{ij}})/2}{(\mu_{i,j-1} + \mu_{ij})/2} + \left[\frac{(p_{i,j+1,k+1}^{(l-1)} - p_{i,j,k+1}^{(l)})}{\Delta a} \right. \\
 & \left. \frac{(k_{r_{i,j+1,k}} - k_{r_{ijk}})}{\Delta a} + \frac{(p_{i,j,k+1}^{(l)} - p_{i,j-1,k+1}^{(l-1)})}{\Delta a} \frac{(k_{r_{ijk}} - k_{r_{i,j-1,k}})}{\Delta a} \right] \\
 & \frac{1}{r_j^2} \frac{1}{(\mu_{ij} + \mu_{i,j-1})} - \left[\frac{(p_{i,j+1,k+1}^{(l-1)} - p_{i,j,k+1}^{(l)})}{\Delta a} \frac{(\mu_{i,j+1,k} - \mu_{ijk})}{\Delta a} \right. \\
 & \left. + \frac{(p_{i,j,k+1}^{(l)} - p_{i,j-1,k+1}^{(l-1)})}{\Delta a} \frac{(\mu_{ijk} - \mu_{i,j-1,k})}{\Delta a} \right] \frac{1}{r_j^2} \frac{(k_{r_{ij}} + k_{r_{i,j-1}})}{(\mu_{i,j} + \mu_{i,j-1})^2} \\
 & \left. + \left[\frac{(p_{i-1,j,k+1}^{(l)} - p_{i,j,k+1}^{(l)})}{\Delta z_{i-1}} - \frac{(p_{i,j,k+1}^{(l)} - p_{i+1,j,k+1}^{(l)})}{\Delta z_i} \right] \frac{1}{\Delta z_i} \right. \\
 & \left. \frac{(k_{z_{ij}} + k_{z_{i-1,j}})}{(\mu_{ij} + \mu_{i-1,j})} + \left[\frac{(p_{i-1,j,k+1}^{(l)} - p_{i,j,k+1}^{(l)})}{\Delta z_{i-1}} \frac{(k_{z_{i-1,j,k}} - k_{z_{ijk}})}{\Delta z_{i-1}} \right. \right.
 \end{aligned}$$

$$\begin{aligned}
& + \frac{{}^{(l)}P_{i,j,k+1} - {}^{(l)}P_{i+1,j,k+1}}{\Delta z_i} \frac{{}^{(k)}z_{ijk} - {}^{(k)}z_{i+1,j,k}}{\Delta z_i} \frac{1}{(\mu_{ij} + \mu_{i-1,j})} \\
& - \left[\frac{{}^{(l)}P_{i-1,j,k+1} - {}^{(l)}P_{i,j,k+1}}{\Delta z_{i-1}} \frac{(\mu_{i-1,j,k} - \mu_{ijk})}{\Delta z_{i-1}} \right. \\
& + \left. \frac{{}^{(l)}P_{i,j,k+1} - {}^{(l)}P_{i+1,j,k+1}}{\Delta z_i} \frac{(\mu_{ijk} - \mu_{i+1,j,k})}{\Delta z_i} \right] \\
& \frac{{}^{(k)}z_{ij} + {}^{(k)}z_{i-1,j}}{(\mu_{ij} + \mu_{i-1,j})^2} + \left[\frac{(\gamma_{i-1,j,k} - \gamma_{ijk})}{\Delta z_{i-1}} + \frac{(\gamma_{ijk} - \gamma_{i+1,j,k})}{\Delta z_i} \right] \\
& \frac{{}^{(k)}z_{ij} + {}^{(k)}z_{i-1,j}}{2(\mu_{ij} + \mu_{i-1,j})} + \left[\frac{{}^{(k)}z_{i-1,j,k} - {}^{(k)}z_{ijk}}{\Delta z_{i-1}} + \frac{{}^{(k)}z_{ijk} - {}^{(k)}z_{i+1,j,k}}{\Delta z_i} \right] \\
& \frac{(\gamma_{ij} + \gamma_{i-1,j})}{2(\mu_{ij} + \mu_{i-1,j})} - \left[\frac{(\mu_{i-1,j,k} - \mu_{ijk})}{\Delta z_{i-1}} + \frac{(\mu_{ijk} - \mu_{i+1,j,k})}{\Delta z_i} \right] \\
& \frac{{}^{(k)}z_{i,j} + {}^{(k)}z_{i-1,j}}{(\mu_{ij} + \mu_{i-1,j})^2} \frac{(\gamma_{ij} + \gamma_{i-1,j})}{2} \\
& = \left[\frac{{}^{(l)}P_{i,j,k+1} - {}^{(l)}P_{ijk}}{\Delta t} \right] \frac{S_{sij}}{\gamma_{ij}} \dots \dots \dots (3.63)
\end{aligned}$$

Equation (3.63) is rearranged as follows,

$$\begin{aligned}
& {}^{(l)}P_{i-1,j,k+1} \left[\frac{{}^{(k)}z_{ij} + {}^{(k)}z_{i-1,j}}{(\mu_{ij} + \mu_{i-1,j}) \Delta z_{i-1}} + \frac{{}^{(k)}z_{i-1,j,k} - {}^{(k)}z_{ijk}}{\Delta z_{i-1} (\mu_{ij} + \mu_{i-1,j})^2} \right. \\
& \left. - \frac{(\mu_{i-1,j,k} - \mu_{ijk}) ({}^{(k)}z_{ij} + {}^{(k)}z_{i-1,j})}{\Delta z_{i-1}^2 (\mu_{ij} + \mu_{i-1,j})^2} \right]
\end{aligned}$$

$$\begin{aligned}
& + p_{i,j,k+1}^{(l)} \left[\left(-\frac{1}{\Delta z_{i-1}} - \frac{1}{\Delta z_i} \right) \frac{1}{\Delta z_i} \frac{(k_{z_{ij}} + k_{z_{i-1,j}})}{(\mu_{ij} + \mu_{i-1,j})} + \right. \\
& \left(-\frac{(k_{z_{i-1,j,k}} - k_{z_{ijk}})}{\Delta z_{i-1}^2} + \frac{(k_{z_{ijk}} - k_{z_{i+1,j,k}})}{\Delta z_i^2} \right) \frac{1}{(\mu_{ij} + \mu_{i-1,j})} \\
& - \left(-\frac{\mu_{i-1,j,k} - \mu_{ijk}}{\Delta z_{i-1}^2} + \frac{\mu_{ijk} - \mu_{i+1,j,k}}{\Delta z_i^2} \right) \frac{(k_{z_{ij}} + k_{z_{i-1,j}})}{(\mu_{ij} + \mu_{i-1,j})^2} \\
& + \left(-\frac{2}{\Delta a^2} \right) \frac{(k_{r_{ij}} + k_{r_{i,j-1}})}{(\mu_{ij} + \mu_{i,j-1}) r_j^2} \\
& + \left(-\frac{k_{r_{i,j+1,k}} - k_{r_{ijk}}}{\Delta a^2} + \frac{k_{r_{ijk}} - k_{r_{i,j-1,k}}}{\Delta a^2} \right) \frac{1}{r_j^2 (\mu_{ij} + \mu_{i,j-1})} \\
& - \left(-\frac{\mu_{i,j+1,k} - \mu_{ijk}}{\Delta a^2} + \frac{\mu_{ijk} - \mu_{i,j-1,k}}{\Delta a^2} \right) \frac{(k_{r_{ij}} + k_{r_{i,j-1}})}{r_j^2 (\mu_{ij} + \mu_{i,j-1})^2} \\
& - \frac{S_{s_{ij}}}{\gamma_{ij} \Delta t} \Big] + \\
& p_{i+1,j,k+1}^{(l)} \left[\frac{1}{\Delta z_i \Delta z_i} \frac{(k_{z_{ij}} + k_{z_{i-1,j}})}{(\mu_{ij} + \mu_{i-1,j})} - \frac{(k_{z_{ijk}} - k_{z_{i+1,j,k}})}{\Delta z_i^2 (\mu_{ij} + \mu_{i-1,j})} \right. \\
& \left. + (\mu_{ijk} - \mu_{i+1,j,k}) \frac{(k_{z_{ijk}} + k_{z_{i-1,j,k}})}{\Delta z_i^2 (\mu_{ij} + \mu_{i-1,j})^2} \right]
\end{aligned}$$

$$\begin{aligned}
&= - \left(\frac{P_{i,j+1,k+1}^{(\ell-1)} + P_{i,j-1,k+1}^{(\ell-1)}}{\Delta a^2} \right) \frac{1}{r_j^2} \frac{(k_{r_{ij}} + k_{r_{i,j-1}})}{(\mu_{ij} + \mu_{i,j-1})} \\
&- \frac{1}{r_j^2} \left[\frac{P_{i,j+1,k+1}^{(\ell-1)}}{\Delta a^2} (k_{r_{i,j+1,k}} - k_{r_{ijk}}) - \frac{P_{i,j-1,k+1}^{(\ell-1)}}{\Delta a^2} \right. \\
&\left. (k_{r_{ijk}} - k_{r_{i,j-1,k}}) \right] \frac{1}{(\mu_{ij} + \mu_{i,j-1})} + \frac{1}{r_j^2} \left[\frac{P_{i,j+1,k+1}^{(\ell-1)}}{\Delta a^2} \right. \\
&\left. (\mu_{i,j+1,k} - \mu_{ijk}) - \frac{P_{i,j-1,k+1}^{(\ell-1)}}{\Delta a^2} (\mu_{ijk} - \mu_{i,j-1,k}) \right] \frac{(k_{r_{ij}} + k_{r_{i,j-1}})}{(\mu_{ij} + \mu_{i,j-1})^2} \\
&- \left[\frac{(\gamma_{i-1,j,k} - \gamma_{ijk})}{\Delta z_{i-1}} + \frac{(\gamma_{ijk} - \gamma_{i+1,j,k})}{\Delta z_i} \right] \frac{(k_{z_{ij}} + k_{z_{i-1,j}})}{2(\mu_{ij} + \mu_{i-1,j})} \\
&- \left[\frac{(k_{z_{i-1,j,k}} - k_{z_{ijk}})}{\Delta z_{i-1}} + \frac{(k_{z_{ijk}} - k_{z_{i+1,j,k}})}{\Delta z_i} \right] \frac{(\gamma_{ij} + \gamma_{i-1,j})}{2(\mu_{ij} + \mu_{i-1,j})} \\
&+ \left[\frac{(\mu_{i-1,j,k} - \mu_{ijk})}{\Delta z_{i-1}} + \frac{(\mu_{ijk} - \mu_{i+1,j,k})}{\Delta z_i} \right] \\
&\frac{(k_{z_{ij}} + k_{z_{i-1,j}})(\gamma_{ij} + \gamma_{i-1,j})}{2(\mu_{ij} + \mu_{i-1,j})^2} - \frac{P_{ijk} S_{s_{ij}}}{\gamma_{ij} \Delta t} \quad \dots (3.64)
\end{aligned}$$

For a given interior pressure column (i.e., $j=2, \dots, NC-1$) equation (3.64) is of the form

$$A_i P_{i-1,j,k+1} + B_i P_{i,j,k+1} + C_i P_{i+1,j,k+1} = D_i \quad \dots (3.65)$$

$i=2, \dots, NR-1$

Boundary Pressure Nodes

For any interior pressure column (say $j=j^*$; $NC > j^* > 1$) equation (3.65) can be written at each interior pressure row (i.e., $i=2, \dots, NR-1$). This provides $(NR-2)$ equations. However, the unknowns $[p_{i,j,k+1}^{(\ell)}, j=1, \dots, NR]$ along the j^{th} pressure column are NR in number. $[p_{i,j,k}^{(\ell-1)}$ are known from the preceding time step or initial conditions; $p_{i,j^*-1,k+1}^{(\ell-1)}, p_{i,j^*+1,k+1}^{(\ell-1)}$ from preceding iteration]. This deficit is fulfilled by writing the boundary conditions at $(1, j^*)$ and (NR, j^*) . For the first and the NC^{th} pressure column (i.e., $j=1$ and $j=NC$), all the NR equations are written exclusively from the boundary conditions. The resulting system of NR equations are solved sequentially ($j=1, \dots, NC$) for the unknowns. Thus, solution can proceed pressure column-wise leading to a substantial reduction of the memory requirement.

The boundary conditions are assigned as follows

Interior Pressure Columns ($j^* = 2, \dots, NC-1$)

As described earlier, the boundary condition equations are written at $i=1$ and $i=NR$.

The upper boundary of the flow transport domain is represented by $i=1$. The boundary condition is derived from water balance at $(1, j^*); j^* = 2, \dots, NC-1$ (refer Fig. 3.8-8)

$$S_1 - S_3 + S_2 = \frac{S_s}{\gamma} \frac{\partial p}{\partial t} \frac{\Delta z_1}{2} \pi \left[(r_{j+1}^* - \Delta r_j^*/2)^2 - (r_j^* - \Delta r_{j-1}^*/2)^2 \right]^2$$

$$\left\{ \frac{k_{r_{ij}^*}}{\mu_{ij}^*} \left[\frac{p_{i,j^*+1,k+1}^{(\ell-1)} - p_{i,j^*,k+1}^{(\ell)}}{\Delta r_j^*} \right] (r_{j+1}^* - \Delta r_j^*/2) - \right.$$

$$\begin{aligned}
& \frac{k_r}{\mu} \frac{i, j-1}{i, j-1} \left[\frac{(p^{(l)})_{i, j, k+1} - (p^{(l-1)})_{i, j-1, k+1}}{\Delta r_{j-1}} \right] (r_{j-1}^* - \Delta r_{j-1}^*/2) \pi \frac{\Delta z_i}{2} + \\
& \frac{k_z}{\mu} \frac{i, j}{i, j} \left[\frac{(p^{(l)})_{i+1, j, k+1} - (p^{(l)})_{i, j, k+1}}{\Delta z_i} \right] + \gamma_{ij} \pi [(r_{j+1}^* - \Delta r_j^*/2)^2 - \\
& (r_{j-1}^* - \Delta r_{j-1}^*/2)^2] = \frac{S_{s, ij}}{\gamma_{ij}} \frac{(p^{(l)})_{i, j, k+1} - (p^{(l)})_{i, j, k}}{\Delta t} \frac{\Delta z_i}{2} \\
& \pi [(r_{j+1}^* - \Delta r_j^*/2)^2 - (r_{j-1}^* - \Delta r_{j-1}^*/2)^2] \quad \dots (3.66)
\end{aligned}$$

The lower boundary of the flow transport domain is represented by $i=NR$. The boundary condition at $(NR, j; j=2, \dots, NC-1)$ is written as follows

Pressure Nodes $(NR, j; j=2, \dots, NC-1)$ (refer Fig. 3.8-6)

$$S_1 - S_3 - S_2 = \frac{S_s}{\gamma} \frac{\partial p}{\partial t} \frac{\Delta z_{NR-1}}{2} \pi [(r_{j+1}^* - \Delta r_j^*/2)^2 - (r_j^* - \Delta r_{j-1}^*/2)^2]$$

$$\left\{ \frac{k_r}{\mu} \frac{i, j}{i, j} \left[\frac{(p^{(l-1)})_{i, j+1, k+1} - (p^{(l)})_{i, j, k+1}}{\Delta r_j} \right] (r_{j+1}^* - \Delta r_j^*/2) - \right.$$

$$\left. \frac{k_r}{\mu} \frac{i, j-1}{i, j-1} \left[\frac{(p^{(l)})_{i, j, k+1} - (p^{(l-1)})_{i, j-1, k+1}}{\Delta r_{j-1}} \right] (r_j^* - \Delta r_{j-1}^*/2) \right\} \pi \frac{\Delta z_{i-1}}{2} -$$

$$\frac{k_z}{\mu} \frac{i-1, j}{i-1, j} \left[\frac{(p^{(l)})_{i, j, k+1} - (p^{(l)})_{i-1, j, k+1}}{\Delta z_{i-1}} \right] - \gamma_{ij} \pi [(r_{j+1}^* - \Delta r_j^*/2)^2 -$$

$$\left[\pi (r_{j+1}^* - \Delta r_j^* / 2)^2 - \pi (r_j^* - \Delta r_{j-1}^* / 2)^2 \right] = \frac{S_{s_{ij}}}{\gamma_{ij}} \frac{(p_{i,j,k+1}^{(l)} - p_{i,j,k}^{(l)})}{\Delta t} \frac{\Delta z_{NR-1}}{2} \quad \dots (3.67)$$

Boundary Pressure Columns ($j=1, j=NC$)

The boundary at $j=1$ is divided in five parts i.e., at last pressure row ($i=NR$); below the well ($NR > i > NRW$); across the screen ($NRB < i \leq NRW$); across the blind pipe ($1 < i \leq NRB$); and at first pressure row ($i=1$) (refer Fig. 3.7).

Pressure Node ($NR, 1$) (refer Fig. 3.8-5)

$$\begin{aligned} S_1 + S_2 &= \frac{S_s}{\gamma} \frac{\partial p}{\partial t} \frac{\Delta z_{i-1}}{2} \left[\pi (r_w + \Delta r_j / 2)^2 - \pi r_w^2 \right] \\ &+ \frac{k_{r_{ij}}}{\mu_{ij}} \left[\frac{(p_{i,j+1,k+1}^{(l-1)} - p_{i,j,k+1}^{(l)})}{\Delta r_j} \right] \left[2\pi (r_w + \Delta r_j / 2) \right] \frac{\Delta z_{i-1}}{2} + \\ &+ \frac{k_{z_{i-1,j}}}{\mu_{i-1,j}} \left[\frac{(p_{i-1,j,k+1}^{(l)} - p_{i,j,k+1}^{(l)})}{\Delta z_{i-1}} \right] + \gamma_{ij} \left[\pi (r_w + \Delta r_j / 2)^2 - \pi r_w^2 \right] \\ &= \frac{S_{s_{ij}}}{\gamma_{ij}} \frac{(p_{i,j,k+1}^{(l)} - p_{i,j,k}^{(l)})}{\Delta t} \frac{\Delta z_{i-1}}{2} \left[\pi (r_w + \Delta r_j / 2)^2 - \pi r_w^2 \right] \quad \dots (3.68) \end{aligned}$$

At any pressure node ($i, 1$; $i = NRW+1, \dots, NR-1$) lying below the well the boundary condition is derived from the water balance as follows (refer Fig. 3.8-4)

$$\begin{aligned}
S_1 + S_2 + S_3 &= \frac{S_s}{\gamma} \frac{\partial p}{\partial t} \frac{(\Delta z_{i-1} + \Delta z_i)}{2} \left[\pi(r_w + \Delta r_j/2)^2 - \pi r_w^2 \right] \\
&+ \frac{k_{r_{ij}}}{\mu_{ij}} \left[\frac{(p_{i,j+1,k+1}^{(l)} - p_{i,j,k+1}^{(l)})}{\Delta r_j} \right] \left[2\pi(r_w + \Delta r_j/2) \frac{\Delta z_{i-1} + \Delta z_i}{2} \right] + \\
&\left\{ \frac{k_{z_{ij}}}{\mu_{ij}} \left[\frac{(p_{i+1,j,k+1}^{(l)} - p_{i,j,k+1}^{(l)})}{\Delta z_i} \right] - \gamma_{ij} \right\} + \\
&\frac{k_{z_{i-1,j}}}{\mu_{i-1,j}} \left[\frac{(p_{i-1,j,k+1}^{(l)} - p_{i,j,k+1}^{(l)})}{\Delta z_{i-1}} \right] + \gamma_{ij} \left\} \left[\pi(r_w + \Delta r_j/2)^2 - \pi r_w^2 \right] \\
&= \frac{S_{s_{ij}}}{\gamma_{ij}} \frac{(p_{i,j,k+1}^{(l)} - p_{i,j,k}^{(l)}) (\Delta z_{i-1} + \Delta z_i)}{\Delta t} \left[\pi(r_w + \Delta r_j/2)^2 - \pi r_w^2 \right] \\
&\dots\dots\dots (3.69)
\end{aligned}$$

At any pressure node $(i, 1 ; i = \text{NRB}+1, \dots, \text{NRW})$ lying across the screen the boundary condition is derived from the water balance as follows (refer Fig. 3.8-3)

$$S_2 + S_3 + S_1 - \frac{Q}{\text{NRW} - 0.5} = \frac{S_s}{\gamma} \frac{\partial p}{\partial t} \frac{(\Delta z_{i-1} + \Delta z_i)}{2} \left[\pi(r_w + \Delta r_j/2)^2 - \pi r_w^2 \right]$$

$$\frac{k_{r_{ij}}}{\mu_{ij}} \left[\frac{(p_{i,j+1,k+1}^{(l)} - p_{i,j,k+1}^{(l)})}{\Delta r_j} \right] \left[2\pi(r_w + \Delta r_j/2) \frac{\Delta z_{i-1} + \Delta z_i}{2} \right] +$$

$$\left\{ \frac{k_{z_{ij}}}{\mu_{ij}} \left[\frac{(p_{i+1,j,k+1}^{(l)} - p_{i,j,k+1}^{(l)})}{\Delta z_i} \right] - \gamma_{ij} \right\} - \frac{Q}{\text{NRW} - 0.5} +$$

$$\begin{aligned}
& \frac{k_{z_{i-1,j}}}{\mu_{i-1,j}} \left[\frac{(p_{i-1,j,k+1}^{(\ell)} - p_{i,j,k+1}^{(\ell)})}{\Delta z_{i-1}} \right] + \gamma_{ij} \left] \left[\pi (r_w + \Delta r_j / 2)^2 - \pi r_w^2 \right] \right. \\
& = \frac{S_{s_{ij}}}{\gamma_{ij}} \frac{(p_{i,j,k+1}^{(\ell)} - p_{i,j,k}^{(\ell)}) (\Delta z_{i-1} + \Delta z_i)}{\Delta t \cdot 2} \left[\pi (r_w + \Delta r_j / 2)^2 - \pi r_w^2 \right] \\
& \dots \dots \dots (3.70)
\end{aligned}$$

At any pressure node (1,1; i=2, ... NRB) lying across the blind pipe the boundary condition is derived from the water balance as follows (refer Fig. 3.8-2)

$$\begin{aligned}
S_2 + S_3 + S_1 &= \frac{S_s}{\gamma} \frac{\partial p}{\partial t} \frac{(\Delta z_{i-1} + \Delta z_i)}{2} \left[\pi (r_w + \Delta r_j / 2)^2 - \pi r_w^2 \right] \\
& \frac{k_{r_{ij}}}{\mu_{ij}} \left[\frac{(p_{i,j+1,k+1}^{(\ell-1)} - p_{i,j,k+1}^{(\ell)})}{\Delta r_j} \right] \left[2\pi (r_w + \Delta r_j / 2) \frac{\Delta z_{i-1} + \Delta z_i}{2} \right] + \\
& \left\{ \frac{k_{z_{ij}}}{\mu_{ij}} \left[\frac{(p_{i+1,j,k+1}^{(\ell)} - p_{i,j,k+1}^{(\ell)})}{\Delta z_i} \right] - \gamma_{ij} \right\} + \\
& \frac{k_{z_{i-1,j}}}{\mu_{i-1,j}} \left[\frac{(p_{i-1,j,k+1}^{(\ell)} - p_{i,j,k+1}^{(\ell)})}{\Delta z_{i-1}} \right] + \gamma_{ij} \left] \left[\pi (r_w + \Delta r_j / 2)^2 - \pi r_w^2 \right] \right. \\
& = \frac{S_{s_{ij}}}{\gamma_{ij}} \frac{(p_{i,j,k+1}^{(\ell)} - p_{i,j,k}^{(\ell)}) (\Delta z_{i-1} + \Delta z_i)}{\Delta t \cdot 2} \left[\pi (r_w + \Delta r_j / 2)^2 - \pi r_w^2 \right] \\
& \dots \dots \dots (3.71)
\end{aligned}$$

At pressure node (1,1) the boundary condition is derived from the water balance as follows (refer Fig. 3.8-1)

$$\begin{aligned}
S_1 - S_2 &= \frac{S_s}{\gamma} \frac{\partial p}{\partial t} \frac{\Delta z_i}{2} [\pi(r_w + \Delta r_j/2)^2 - \pi r_w^2] \\
\frac{k_{r_{ij}}}{\mu_{ij}} & \left[\frac{(p_{i,j+1,k+1}^{(\ell)} - p_{i,j,k+1}^{(\ell)})}{\Delta r_j} \right] [2\pi(r_w + \Delta r_j/2)] \frac{\Delta z_i}{2} - \\
\frac{k_{z_{ij}}}{\mu_{ij}} & \left[\frac{(p_{i,j,k+1}^{(\ell)} - p_{i+1,j,k+1}^{(\ell-1)})}{\Delta z_i} \right] + \gamma_{ij} [\pi(r_w + \Delta r_j/2)^2 - \pi r_w^2] + \\
&= \frac{S_{s_{ij}}}{\gamma_{ij}} \frac{(p_{i,j,k+1}^{(\ell)} - p_{i,j,k}^{(\ell)})}{\Delta t} \frac{\Delta z_i}{2} [\pi(r_w + \Delta r_j/2)^2 - \pi r_w^2] \dots (3.72)
\end{aligned}$$

For known boundary conditions; p_{ijk} (from the preceding time step or initial conditions); and $p_{i,j-1,k+1}^{(\ell-1)}$, and $p_{i,j+1,k+1}^{(\ell-1)}$ (from the preceding iteration; $p_{i,j-1,k+1}^{(0)} = p_{i,j-1,k}^{(0)}$, $p_{i,j,k+1}^{(0)} = p_{i,j,k}^{(0)}$, $p_{i,j+1,k+1}^{(0)} = p_{i,j+1,k}^{(0)}$) equation (3.65) is solved for $[p_{i,j,k+1}^{(\ell)}, i=1, NR]$ successively for each pressure column by Thomas' algorithm.

3.3.5.1.7 Convergence Criteria

The differences of the $p_{i,j,k+1}^{(\ell)}$ values obtained in two successive iterations for all the pressure nodes are summed up. This sum is then compared with a prestipulated convergence factor (say ϵ). The iterations are continued until this sum attains a value less than ϵ i.e.,

$$\sum_j \sum_i | p_{i,j,k+1}^{(\ell)} - p_{i,j,k+1}^{(\ell-1)} | < \epsilon \quad (3.73)$$

$$p_{i,j,k+1}^* = p_{i,j,k+1}^{(\ell)}$$

Where $p_{i,j,k+1}^*$ is the finally converged total pressure at the pressure node (i,j) at discrete time t_{k+1} .

3.3.5.1.8 Computation of Nodal Velocities

After the simulation of nodal pressures at different discrete times, the corresponding vertical (V) and radial (U) seepage velocities are estimated in accordance with the following equations

$$V = \frac{k_z}{\phi\mu} \left[\frac{\partial p}{\partial z} + \gamma \right] \quad \dots (3.74)$$

$$U = \frac{k_r}{\phi\mu} \left[\frac{\partial p}{\partial r} + \gamma \frac{\partial z}{\partial r} \right] \quad \dots (3.75)$$

Replacing the spatial derivatives by the finite differences, the velocities at the discretized space-time points are estimated as follows

$$V_{i,j,k} = \frac{k_{z_{ij}}}{2\phi\mu_{ij}} \left[\frac{(p_{i+1,j,k}^* - p_{i,j,k}^*)}{\Delta z_i} + \frac{(p_{i,j,k}^* - p_{i-1,j,k}^*)}{\Delta z_{i-1}} - \frac{\gamma_{i+1,j}}{2} - \gamma_{ij} - \frac{\gamma_{i-1,j}}{2} \right] \quad \dots (3.76)$$

$$U_{i,j,k} = - \frac{k_{r_{ij}}}{2\phi\mu_{ij}} \left[\frac{(p_{i,j,k}^* - p_{i,j+1,k}^*)}{\Delta r_j} + \frac{(p_{i,j,k}^* - p_{i,j-1,k}^*)}{\Delta r_{j-1}} \right] \quad \dots (3.77)$$

Where V_{ijk} and U_{ijk} are respectively the vertical and radial velocities at pressure nodal point (i, j) at discrete time t_k ; $p_{i+1,j,k}^*$, $p_{i,j,k}^*$, $p_{i-1,j,k}^*$, $p_{i,j+1,k}^*$ and $p_{i,j-1,k}^*$ are the finally converged total pressures at pressure nodes (i+1, j), (i, j), (i-1, j), (i, j+1) and (i, j-1) respectively at discrete time t_k ; ϕ is the porosity of aquifer; $\gamma_{i+1,j}$, γ_{ij} and $\gamma_{i-1,j,k}$ are the specific weights at pressure nodes (i+1, j), (i, j) and (i-1, j) respectively at discrete time t_k ; μ_{ij} is the dynamic viscosity at pressure node (i, j) at discrete time t_k ; Δz_i is the grid

spacing from (i^{th}) to $(i+1)^{th}$ pressure rows, Δz_{i-1} is the grid spacing from $(i-1)^{th}$ to $(i)^{th}$ pressure rows, Δr_j is the grid spacing from $(j)^{th}$ to $(j+1)^{th}$ pressure columns, Δr_{j-1} is the grid spacing from $(j-1)^{th}$ to $(j)^{th}$ pressure columns; and $k_{z_{i,j}}$ and $k_{r_{i,j}}$ are intrinsic permeabilities in the z and r directions at pressure node (i,j) respectively.

3.3.5.1.9 Computation of Moving Point Velocities

The velocity of a moving point is interpolated from the computed seepage velocities at the four surrounding pressure nodal points. For any moving point (say m^{th}) having coordinates (R,Z) , these surrounding pressure nodal points $(i,j ; i-1,j ; i,j+1 ; i-1,j+1)$ (refer Fig. 3.9) satisfy the following inequalities

$$XF_j \leq R < XF_{j+1} \quad , \quad ZF_i \leq Z < ZF_{i-1}$$

Where XF_j is the radial coordinate of pressure nodal point (i,j) , XF_{j+1} is the radial coordinate of pressure nodal point $(i,j+1)$; ZF_i is the vertical coordinate of pressure nodal point (i,j) , ZF_{i-1} is the vertical coordinate of pressure nodal point $(i-1,j)$; R is the radial coordinate of m^{th} moving point at the k^{th} time; and Z is the vertical coordinate of m^{th} moving point at the k^{th} time. Thus the radial $[U(R,Z)]$ and vertical $[V(R,Z)]$ velocities of m^{th} moving point at the k^{th} time can be written as follows (Fig.3.9).

$$U(R,Z) = UA(i) + (UA(i) - UA(i-1))(Z - ZF_i)/\Delta Z_{i-1} \quad (3.78)$$

$$V(R,Z) = VA(i) + (VA(i) - VA(i-1))(Z - ZF_i)/\Delta Z_{i-1} \quad (3.79)$$

Where $UA(i-1) = \bar{U}_{i-1,j} + (\bar{U}_{i-1,j+1} - \bar{U}_{i-1,j})(R - XF_j)/\Delta r_j$,

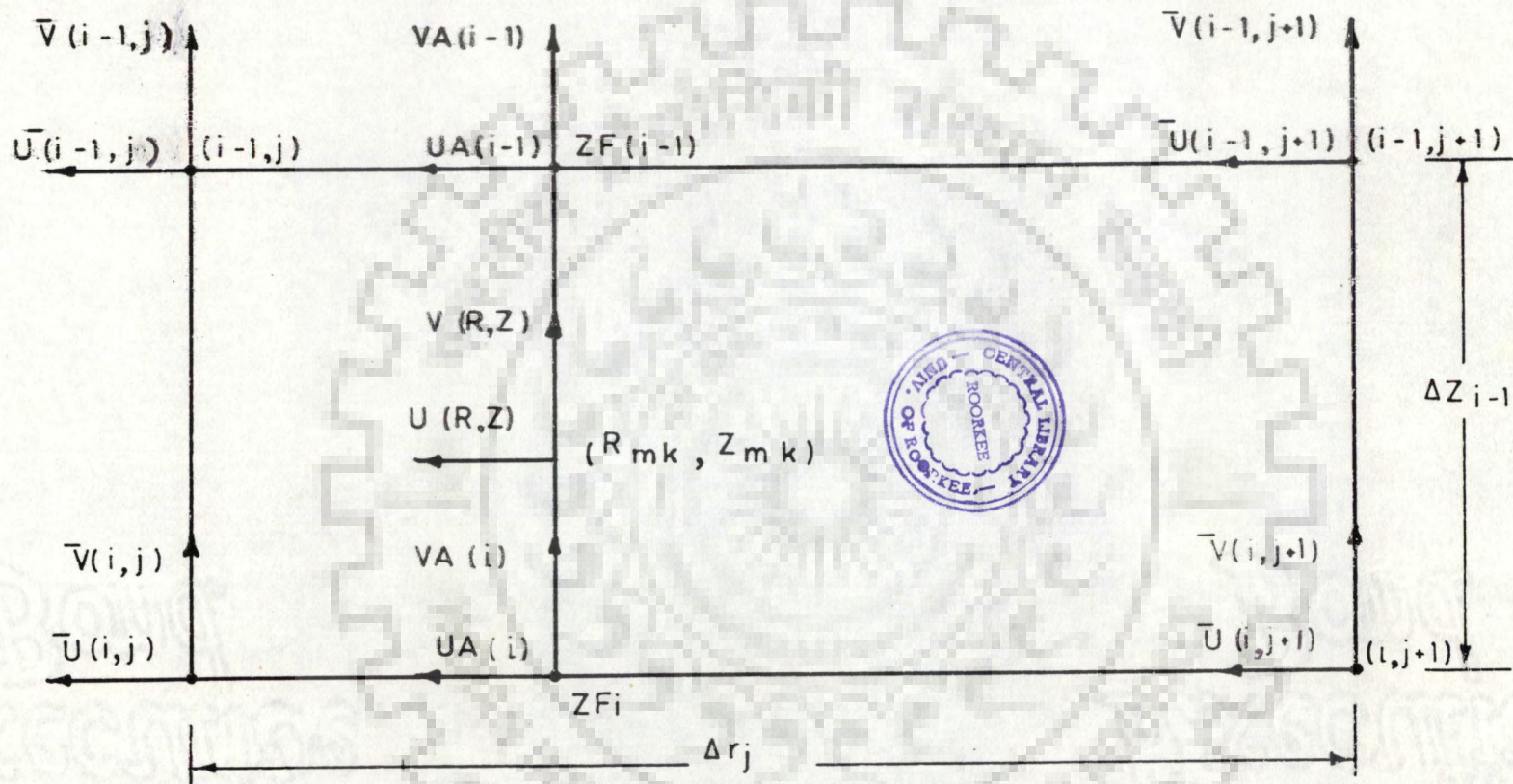


Fig (3.9) Interpolation to Calculate Velocities of Moving Points

$$\bar{U}_{i-1,j} = 0.5 (U_{i-1,j,k} + U_{i-1,j,k+1}),$$

$$\bar{U}_{i-1,j+1} = 0.5 (U_{i-1,j+1,k} + U_{i-1,j+1,k+1}),$$

$$VA(i-1) = \bar{V}_{i-1,j} + (\bar{V}_{i-1,j+1} - \bar{V}_{i-1,j})(R - XF_j)/\Delta r_j,$$

$$\bar{V}_{i-1,j} = 0.5 (V_{i-1,j,k} + V_{i-1,j,k+1}),$$

$$\bar{V}_{i-1,j+1} = 0.5 (V_{i-1,j+1,k} + V_{i-1,j+1,k+1}),$$

$$UA(i) = \bar{U}_{i,j} + (\bar{U}_{i,j+1} - \bar{U}_{i,j})(R - XF_j)/\Delta r_j,$$

$$\bar{U}_{i,j} = 0.5 (U_{i,j,k} + U_{i,j,k+1}),$$

$$\bar{U}_{i,j+1} = 0.5 (U_{i,j+1,k} + U_{i,j+1,k+1}),$$

$$VA(i) = \bar{V}_{i,j} + (\bar{V}_{i,j+1} - \bar{V}_{i,j})(R - XF_j)/\Delta r_j,$$

$$\bar{V}_{i,j+1} = 0.5 (V_{i,j,k} + V_{i,j,k+1}),$$

$$\bar{V}_{i,j} = 0.5 (V_{i,j+1,k} + V_{i,j+1,k+1}),$$

At latter times, the time step (Δt_k) for pressure simulation assumes a very large value in accordance with Rushton and Chan criteria. However, increasing Δt_s (the time step for saltwater simulation) to the same extent will cause considerable errors since the position of a moving point and hence its velocity may change considerably during the span of

Δt_k at latter times. This problem is resolved by subdividing the pressure time steps into ξ number of time steps while simulating the saltwater transport at latter times.

Thus,

$$\xi = 1 \quad \text{if } \Delta t_k \leq \Delta t_s^m \quad \dots (3.80)$$

$$\xi = \text{Integer} \left(\frac{\Delta t_k}{\Delta t_s^m} + 1 \right) \quad \text{if } \Delta t_k > \Delta t_s^m \quad \dots (3.81)$$

$$\Delta t_s^{(k)} = \Delta t_k / \xi \quad \dots (3.82)$$

Where Δt_s^m is the maximum desirable time step for simulation of saltwater transport. This subdivision of the pressure time steps into one or more number of the saltwater transport time steps is illustrated in Fig. (3.10). (The Fig. has been drawn to illustrate a situation in which $\Delta t_2 < \Delta t_s^m$ & $\Delta t_3 > \Delta t_s^m$)

Thus if $R_{m, \ell}^{(k)}$ and $Z_{m, \ell}^{(k)}$ represents r and z coordinates of m^{th} moving point at the beginning of the ℓ^{th} saltwater transport simulation time step during k^{th} pressure time step, it's coordinates at the beginning of $(\ell+1)^{\text{th}}$ saltwater transport simulation time step are given by the following equations

$$R_{m, \ell+1}^{(k)} = R_{m, \ell}^{(k)} - \Delta t_s^{(k)} \hat{U}_{m, \ell}^{(k)} \quad \dots (3.83)$$

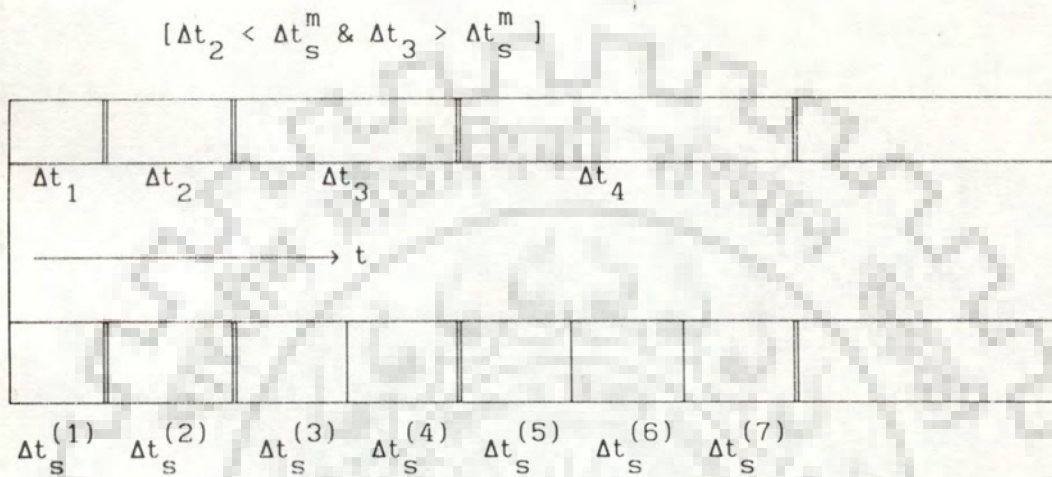
$$Z_{m, \ell+1}^{(k)} = Z_{m, \ell}^{(k)} + \Delta t_s^{(k)} \hat{V}_{m, \ell}^{(k)} \quad \dots (3.84)$$

Where

$$\hat{U}_{m, \ell}^{(k)} = U(R_{m, \ell}^{(k)}, Z_{m, \ell}^{(k)}, t_k) \quad \dots (3.85)$$

$$\hat{V}_{m, \ell}^{(k)} = V (R_{m, \ell}^{(k)}, Z_{m, \ell}^{(k)}, t_k) \quad \dots (3.86)$$

$$\Delta t_s^k = \Delta t_k / \xi \quad \dots (3.87)$$



3.3.6 TOTAL SALTWATER LIFTED INTO SUSPENSION

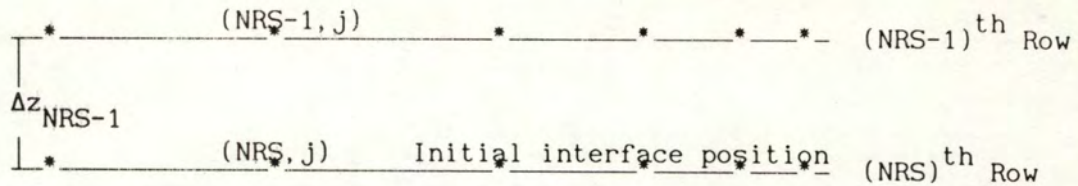
The total volume of saltwater lifted into suspension during a pressure time step is computed as follows:

1. Saltwater lifted (V_c) due to convection is estimated as follows,

$$V_c = J_s \text{ Vol} \quad \dots (3.88)$$

Where J_s is the number of take off points lifted into suspension (i.e., taken off) during the time step.

2. The Volume of saltwater (V_d) lifted due to diffusion is estimated as follows



$$V_d = \sum_{j=1}^{NCS} \frac{C_{NRS, j, k} - C_{NRS-1, j, k}^*}{\Delta z_{NRS-1}} D_{z_{NRS-1, j}} AR \Delta t_k \quad (3.89)$$

$$C_{NRS, j, k} = 1.0 \quad (3.90)$$

$$AR = Vol/d \quad (3.91)$$

Where $D_{z_{NRS-1, j}}$ is diffusive coefficient at nodes $(NRS-1, j)$ in vertical direction; $C_{NRS, j, k}$ and $C_{NRS-1, j, k}^*$ are saltwater concentrations at nodes (NRS, j) and $(NRS-1, j)$ respectively; NCS is the number of saltwater columns (i.e., the take off points); and AR is the area (in plan) assigned to each take off point.

The total volume of saltwater (V_t) lifted in the time step Δt_k is estimated as follows

$$V_t = V_c + V_d \quad \dots (3.92)$$

3.3.7 ENTRY OF SALTWATER IN THE PUMPED WELL

A moving point (say m^{th}) is assumed to have entered into the well when the following conditions are satisfied (Fig.3.2a)

$$R_{m, k+1} \leq r_w \quad \dots (3.93)$$

and

$$(B+D) \leq Z_{m, k+1} \leq (B+D+L_s) \quad \dots (3.94)$$

The cumulative volume of saltwater (VS_k) entered in the pumped water till any discrete time t_k is estimated as follows:

$$VS_k = \sum_{m \in J_G} VL_m \quad \dots\dots\dots (3.95)$$

Where J_G , a subset of the moving points, comprises of all the moving points satisfying the inequalities (equations 3.93 and 3.94) till t_k .

The saltwater concentration (CP_k) in the pumped water at the discrete time t_k , will be as follows:

$$CP_k = \frac{1}{Q} \left. \frac{dVS}{dt} \right|_{t=t_k} \quad \dots\dots\dots (3.96)$$

The derivative of VS with respect to t can be estimated numerically (refer 5.2.4) or graphically (refer 4.2.3.3) employing the model generated values of VS_k at various discrete times.

3.3.8 SETTLEMENT OF SALTWATER INTERFACE (After closure of pumpage)

The closure of the pumpage (at $t = t^*$) is incorporated in the solution by assigning $Q = 0.0$ in equations (3.55) and (3.70) (boundary condition at the screen nodal points). This causes a reversal of the vertical velocities. The downwards velocities cause movement of the moving points from suspension towards the initial position of the interface. The m^{th} moving point is assumed to have settled down when the following condition is satisfied (Fig.3.2a)

$$Z_{m, k+1} < B \quad \dots\dots\dots (3.97)$$

The cumulative volume of the saltwater (VSL_k) settled down till any discrete time t_k ($t_k > t^*$) is estimated as follows:

$$VSL_k = \sum_{m \in J_7} VL_m \quad \dots\dots(3.98)$$

Where J_7 , a subset of the moving points, comprises of all such moving points whose Z coordinates have reached or fallen below D during the period t^* to t_k .

3.4 COMPUTER CODE

The computer code, for performing the calculations of distributed model, has been written in FORTRAN IV. The programme consists of three subroutines and a main programme. Role of the main programme and each subroutine is described briefly in the following paragraphs.

MAIN PROGRAM

The following tasks are performed ,

- 1) Reading of all the input data. The details of the READ statements are as follows.
 - i) NR : number of pressure rows , NC : number of pressure columns , NCS : number of saltwater columns , NRW : number of rows upto the well bottom , NRS : number of rows upto saltwater freshwater interface, KOUNT : number of predecided iterations for pressure , IX = 0:read initial data, IX=1: read data from $m_2.dat$ (out put renamed as data), NT1:serial number of first time step,and DTS: maximum value of time step for saltwater simulation.
 - ii) QQ : constant discharge rate, RW: radius of well, PHI: aquifer

- porosity, TSTR: thickness of strip, IQ = 0: constant discharge, IQ = 1: constant head, IC=0: well has a full screen, IC=1: well has a partial screen, and NRB: number of rows upto bottom of blind pipe.
- iii) STL: desired convergence of pressure, TPQ : pumpage time , KOUNT1: number of predecided iterations for diffusive transport, and STLS: desired convergence of diffusive transport.
- iv) DAA: radial dispersivity of the aquifer, and DBB: vertical dispersivity of the aquifer.
- v) AKRU: initial value of radial intrinsic permeability, AKZU: initial value of vertical intrinsic permeability, SST: initial value of specific storage, GACC: relative density of freshwater at 4^oc, VISF: dynamic viscosity of freshwater, HIN: piezometric head, GFW: specific weight of freshwater , GSW: specific weight of saltwater, and HCD: constant head.
- vi) NT2: serial number of last time step
- vii) (DT(I), I = 1, NT2): time steps
- viii) (DR(J), J = 1, NC - 1) : radial grid spacing for pressure simulation
- ix) (DZ(I), I = 1, NR-1): vertical grid spacing
- x) (DRS(J), J=1, NCS-1): radial grid spacing for saltwater simulation.
- xi) (XL(I), I =1, NCS) : Radial coordinate of the upstream face of the jth take off point.
- xii) (XU(I), I = 1, NCS) : Radial coordinate of the dawnstream face of the jth take off point.
- xiii) VOL: (Volume of take off point)/porosity of aquifer.
- xiv) (XS(I), I = 1, NCS): radial coordinate for take off points.

If IX = 1, the details of READ statement are as follows [the output file (m3.out) renamed as input file (m2.dat)].

- i) TM : cumulative time.
 - ii) NTP : number of moving points
 - iii) (X(I), I = 1, NTP) : radial coordinate of moving points.
 - iv) (Y(I), I = 1, NTP) : Vertical distance of moving points above datum.
 - v) (YL(J), J = 1, NCS + 1) : Vertical distance of take off points above datum.
 - vi) (IN(J), J = 1, NCS + 1) : Index number of the moving points.
 - vii) (VLL(J), J = 1, NTP) : volume of the moving points .
 - viii) P(I,J) : Pressure distribution.
 - ix) (VL(J), J = 1, NCS + 1) : volume of take of points.
 - x) VSP : Cumulative saltwater lifted into suspension, CSP : Cumulative saltwater volume entered into pumped well, VSD : Cumulative saltwater volume settlement below the interface, VLAQM : saltwater concentration in pumped well, and VED: Cumulative saltwater lifted into suspension due to diffusion.
 - xi) GM (I,J) : specific weight distribution.
 - xii) VIS (I,J) : dynamic viscosity distribution.
 - xiii) SS(I,J) : specific storage distribution.
 - xiv) U(I,J) : radial velocity distribution.
 - xv) V(I,J) : vertical velocity distribution
 - xvi) VLA (I,J) : saltwater concentration distribution.
- 2) Some preliminary calculations are made, such as the radial and vertical distance.
 - 3) Computations of pressure distribution
 - 4) Computations of velocity distribution
 - 5) Calling subroutine MOVE to compute the coordinates of the take off and moving points.

- 6) Computation of nodal convective concentration, nodal viscosity , nodal specific storage, and nodal specific weight.
- 7) Calling subroutine DIFF to compute the total nodal concentration due to convective and diffusive transport.
- 8) Integrating the convective and diffusive transport.
- 9) Computation of saltwater settlement down after closure of the pumping.
- 10) Printing the computed results.

The subroutines called BST, MOVE and DIFF.

BST: In this subroutine, the matrix generated by the finite difference approximation is solved using the Thomas algorithm (Remson, et al., 1971).

MOVE: In this subroutine, during each time step, the moving point velocities are calculated by using a 3-way interpolation between nodal velocities, estimation of new position of the moving points, creating new take off points, the saltwater lifted into suspension, saltwater volume entering into the well, the saltwater settlement down after closure of the pumping and removes the moving points which enter the well or settle below the initial position of the interface after closure of the pumping.

DIFF: This subroutine solves a finite difference approximation of the mass transport equation (eqn.3.14) using IADIE scheme.

In annexure B listing of the computer code and programmes have been presented.

CHAPTER-IV

MODEL VALIDATION

The numerical model described in the preceding chapter has been validated by comparing its results with an available analytical solution as well as with a reported set of field data. The details of the two comparisons are as follows;

4.1 COMPARISON WITH AN ANALYTICAL SOLUTION

Bear and Dagan (Schmorak and Mercado, 1969) presented the following expression describing the upconing of the interface, below a partially penetrating well, in an anisotropic aquifer of infinite thickness.

$$Z(r, t) = \frac{Q}{2\pi(\Delta\gamma/\gamma)K_z D} \left[\frac{1}{(1 + R^2)^{1/2}} - \frac{1}{[(1+T)^2 + R^2]^{1/2}} \right] \quad \dots (4.1)$$

$$R = \frac{r}{D} \left(\frac{K_z}{K_x} \right)^{1/2}$$

$$T = \left(\frac{\Delta\gamma}{\gamma} \right) \frac{tK_z}{2\phi D}$$

Where $Z [=Z(r, t)]$ is the rise of interface above its initial position at a radial distance r from the centre of the well at a time t ; Q is the time invariant discharge; $\Delta\gamma$ is the specific weight difference between saltwater and freshwater; γ is the specific weight of freshwater; K_x and K_z are respectively the horizontal and the vertical hydraulic conductivities; D is the vertical distance between the initial position of the interface and the bottom of the well; and ϕ is the aquifer porosity.

The solution is based upon the following assumptions: (refer Fig. 4.1) i) Water is assumed to be abstracted from a point sink i.e. $(L_s/A) \rightarrow 0$ (L_s : screen length, and A: initial thickness of freshwater layer); ii) the aquifer is assumed to be of infinite thickness i.e., B/D , A/D , L_p/D , and H/D are assumed to be tending to infinity (H : the aquifer thickness, L_p : length of well and B: initial thickness of saltwater layer); iii) aquifer and water are assumed to be non-deformable i.e. S_s (specific storage) = 0.0; iv) only convective transport is accounted for i.e. D_r (radial diffusion coefficient) = 0.0, D_z (vertical diffusion coefficient) = 0.0 and v) $Z(0,t) \leq 0.25 D$ (i.e., the solution is valid for small upconing).

The numerical model was implicitly validated by comparing its response with the analytical solution under identical geometric/hydraulic conditions. The adopted conditions are r_w (radius of well) = 0.15 ms; γ_f (specific weight of fresh water) = 1000 kg/m^3 ; γ_s (specific weight of saltwater) = 1030 kg/m^3 ; $S_s = 0.0$ (refer assumption iii); $D_r = 0.0$ (refer assumption iv) $D_z = 0.0$ (refer assumption iv); $\phi = 0.30$; k_r (the horizontal intrinsic permeability) = $1.1 \times 10^{-11} \text{ m}^2$; k_z (the vertical intrinsic permeability) = $0.55 \times 10^{-11} \text{ m}^2$; $D = 1.0 \text{ ms}$; μ_f (the dynamic viscosity of fresh water) = $1.7 \times 10^{-6} \text{ kg. min/m}^3$; and $Q = 0.002 \text{ m}^3/\text{min}$. The model was operated for various values of L_s and H . The model computed upconed positions of the interface along with the corresponding analytical solution are presented in Figures (4.2) to (4.4).

4.1.1 Results.

Figs (4.2a) and (4.2b) indicate the influence of screen length on upconing in an aquifer of very large vertical extent (refer assumption ii). The adopted dimensions are $B = 20\text{ms}$, $D = 1.0\text{ms}$, $A = 60 \text{ ms}$

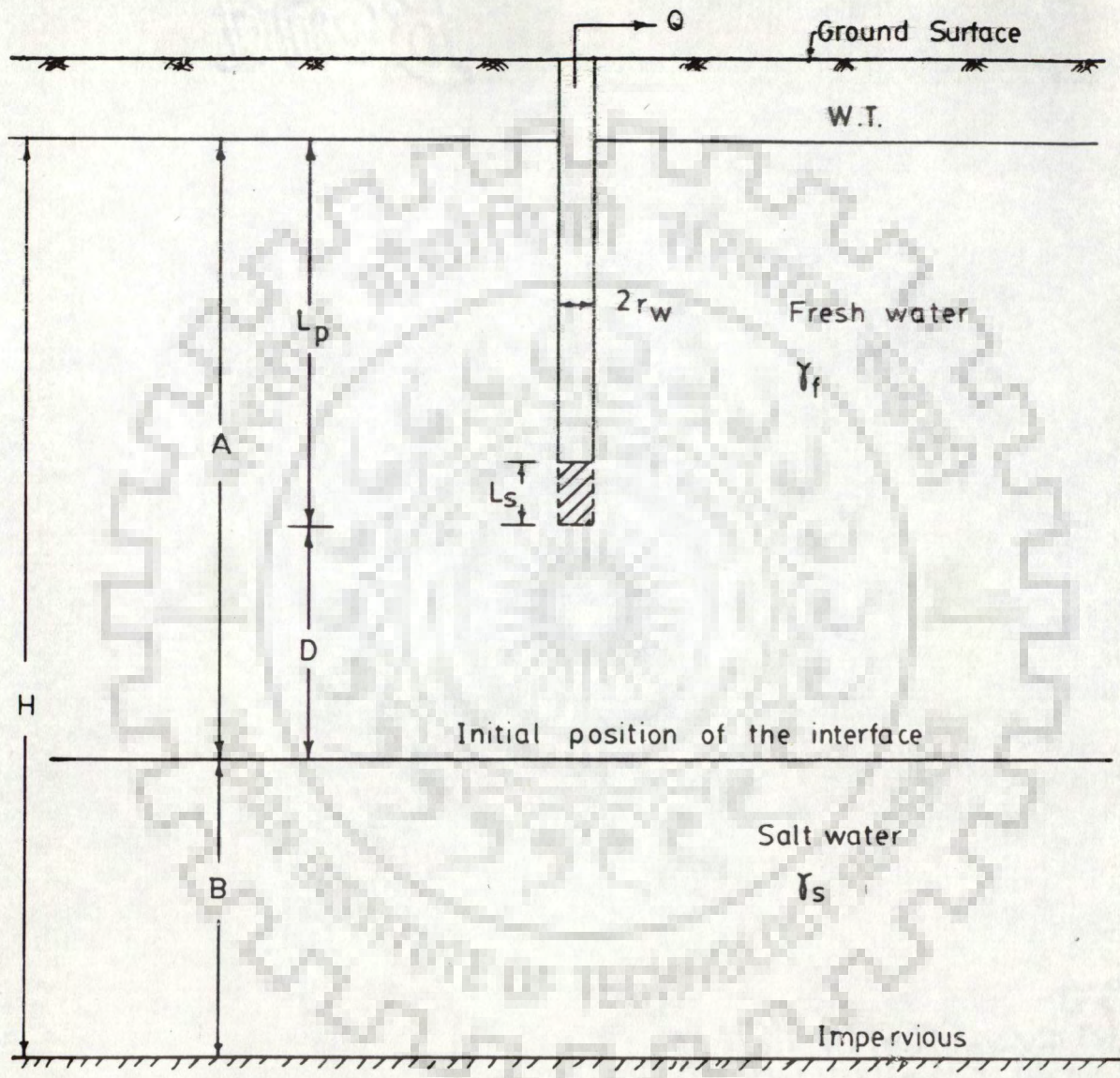


Fig.(4.1) A Pumping Well

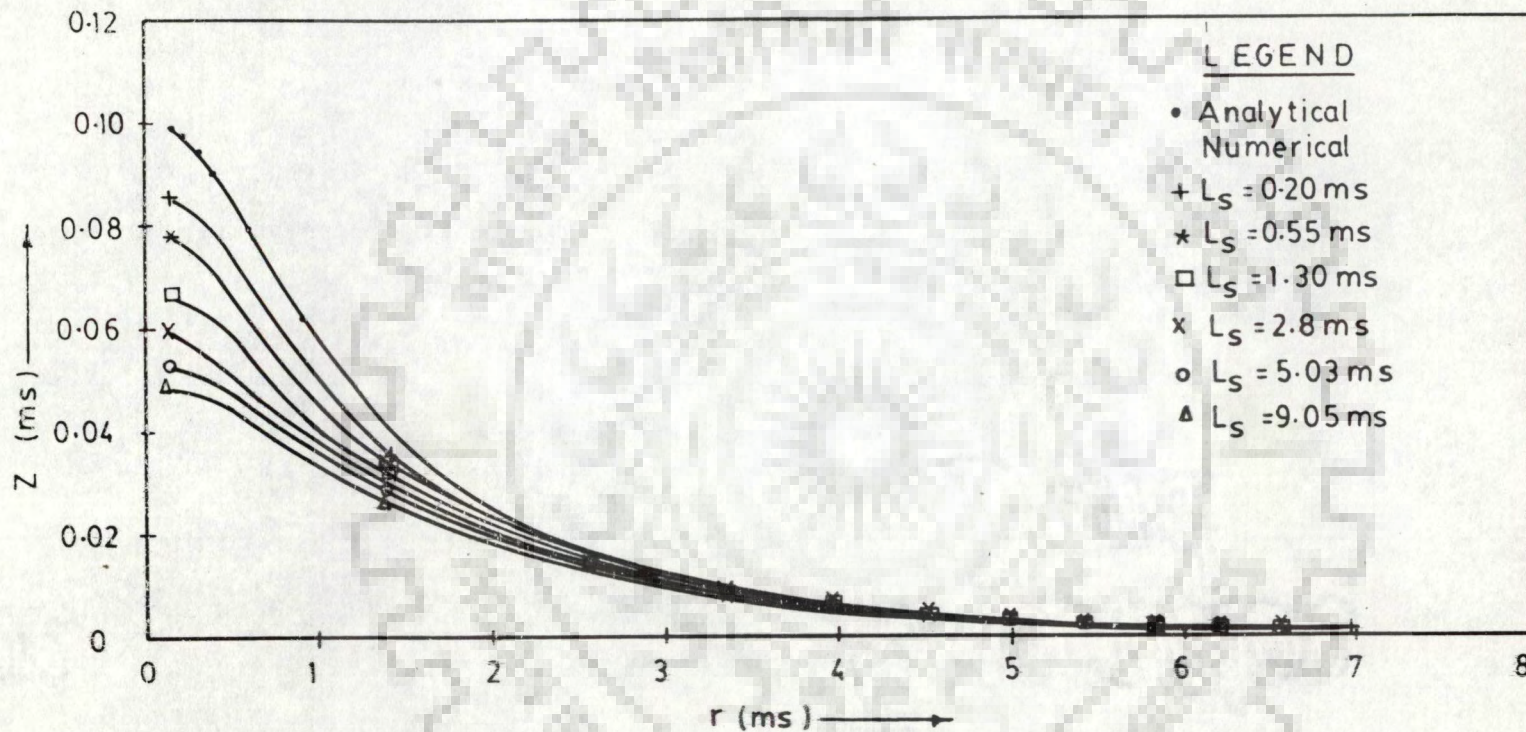


Fig (4.2a) Influence of Screen Length on Upconing.

(Time = 405 min ; $Q = 0.002 \text{ m}^3/\text{min.}$)

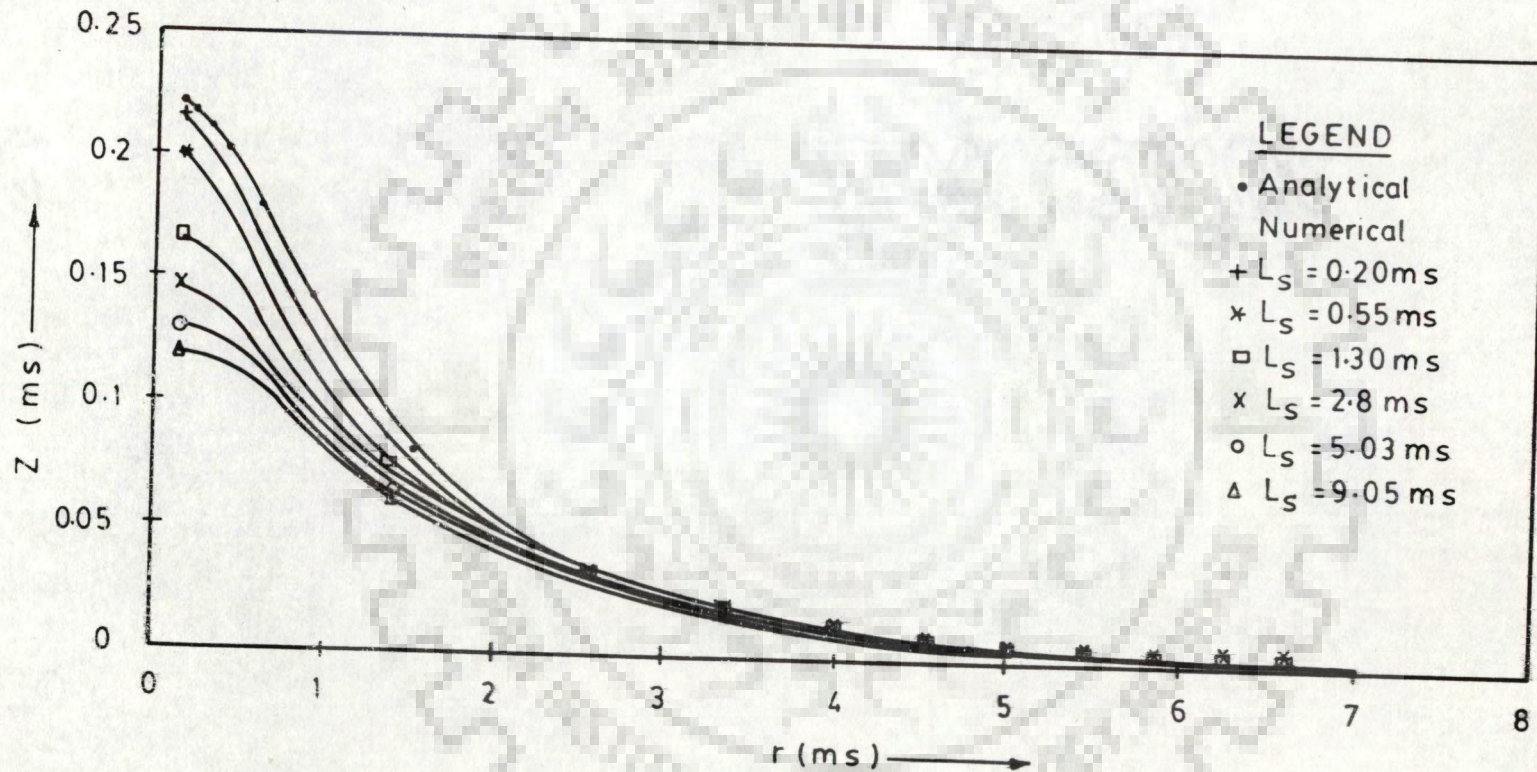


Fig (4.2 b) Influence of Screen Length on Upconing
 (Time = 973 min, $Q = 0.002 \text{ m}^3/\text{min}$)

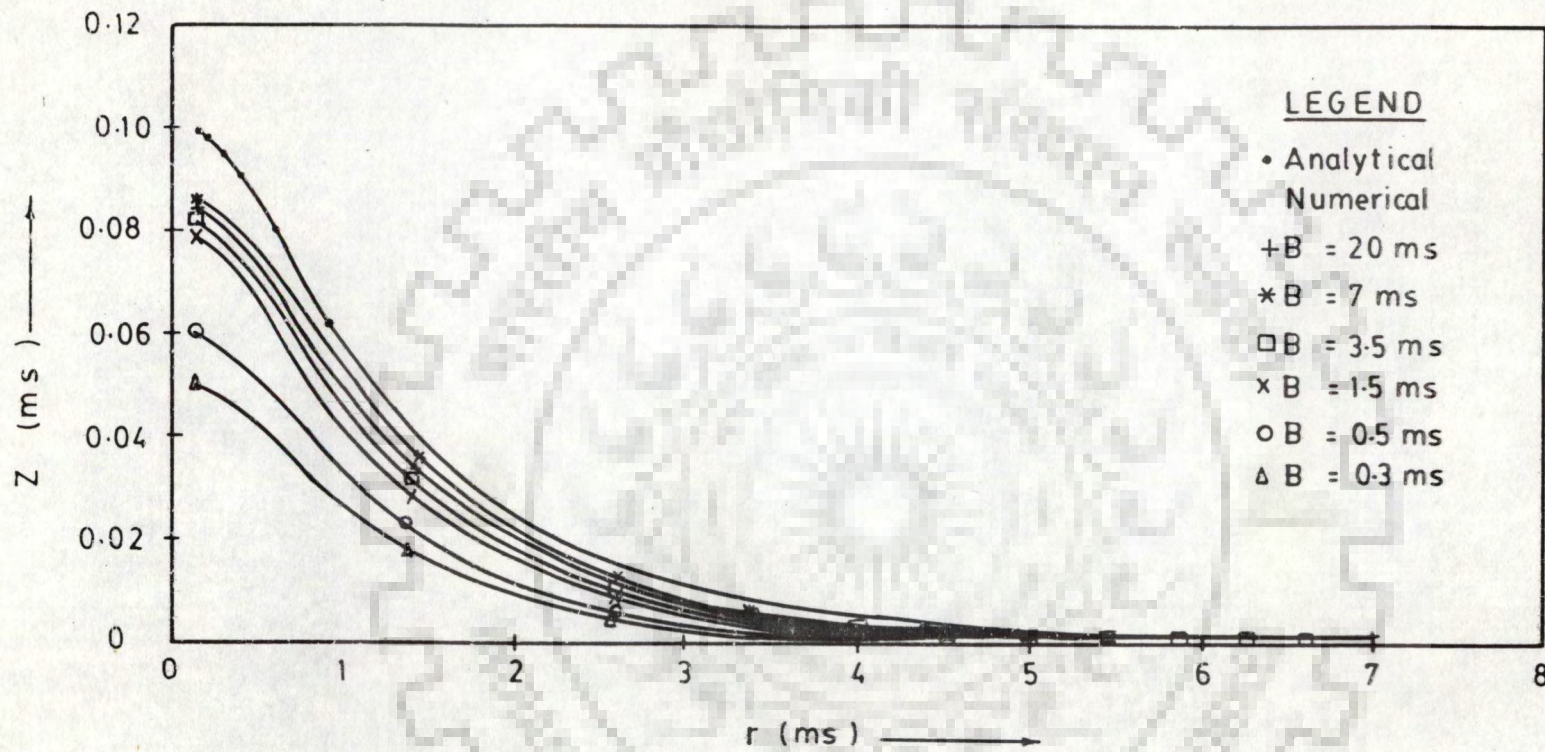


Fig. (4.3a) Influence of Salt Water Layer Thickness on Uponing

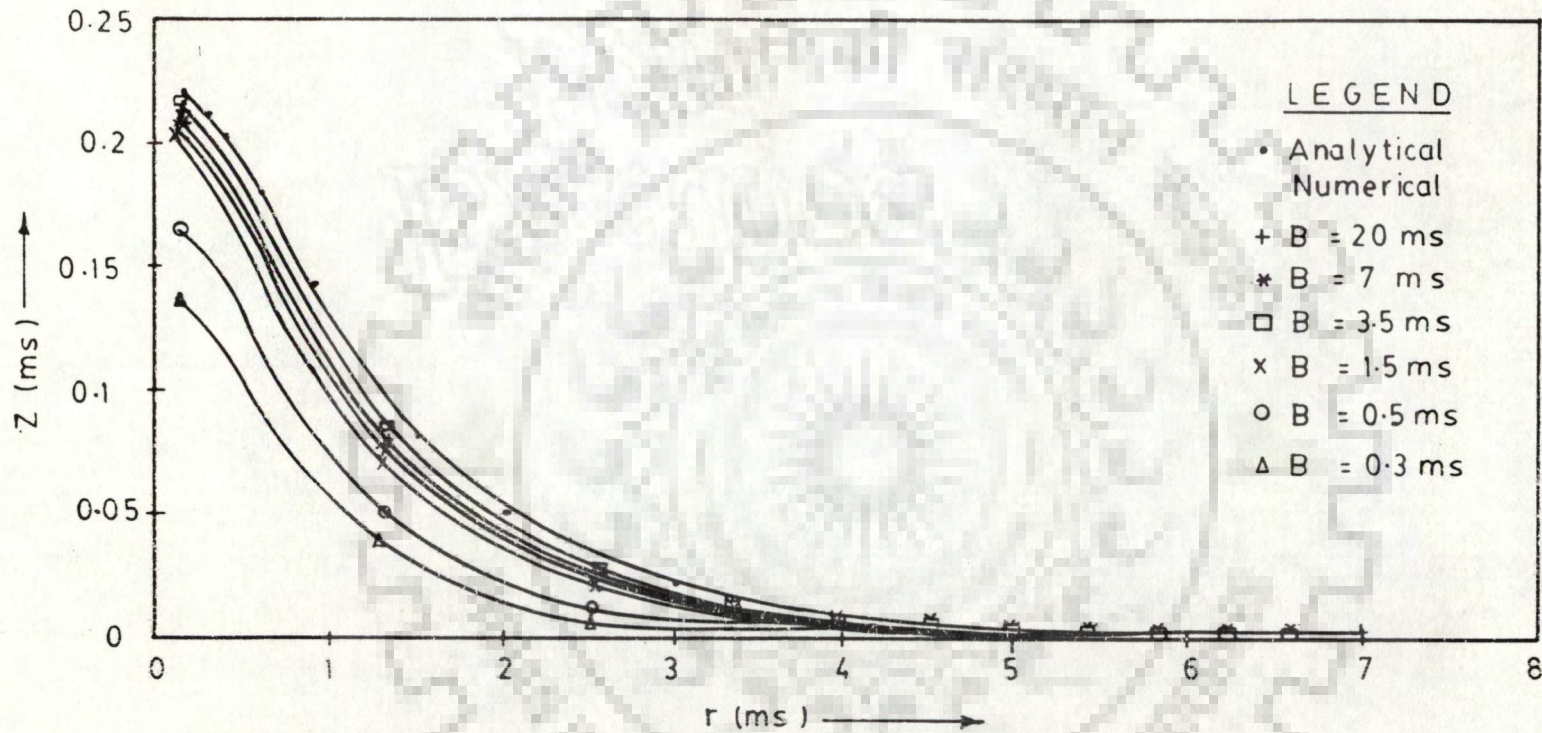


Fig. (4.3b) Influence of Salt Water Layer Thickness on Upconing
 (Time = 973 min, $Q = 0.002 \text{ m}^3/\text{min}$)

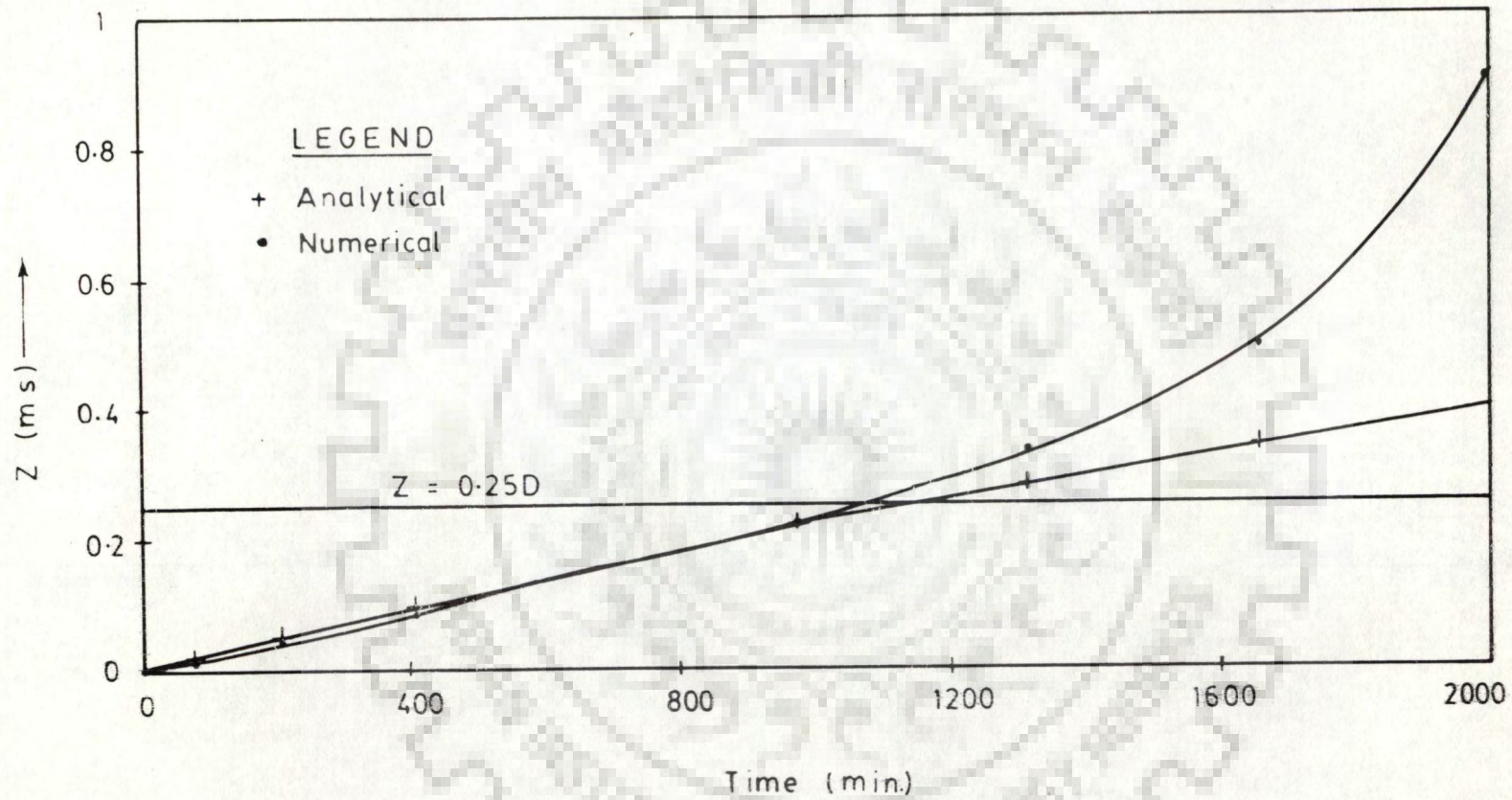


Fig. (4.4) Influence of Z/D on Upconing
 ($Q=0.002 \text{ m}^3/\text{min.}$)

; $L_p = 39$ ms, $H=80$ ms. and $L_s = 0.20, 0.55, 1.30, 2.80, 5.03,$ and 9.05 ms. The upconing is restricted to $0.25D$ (refer assumption V). These Figures reveal that the model computed interface converges to the analytical solution as L_s gets smaller and smaller.

Similarly, Figs. (4.3a) and (4.3b) indicate the influence of initial saltwater layer thickness on upconing in an aquifer of very large vertical extent (refer assumption ii). The adopted dimensions are $D=1.0$ ms, $A=60$ ms, $L_p = 39$ ms, $L_s = 0.20$ ms, $B=20, 7, 3.5, 1.5, 0.5$ and 0.3 ms, $H=80, 67, 63.5, 61.5, 60.5$ and 60.3 ms. The upconing is restricted to $0.25D$ (refer assumption v). These Figures reveal that the model computed interface converges to the analytical solution as B gets larger and larger.

Similarly, Fig. (4.4) indicates the influence of Z/D on upconing in an aquifer of very large vertical extent (refer assumption ii). The adopted dimensions are $B=20$ ms, $D=1.0$ ms, $A=60$ ms, $L_p=39$ ms, $L_s = 0.20$ ms and $H=80$ ms. This Figure reveals that for an aquifer of very large vertical extent and $Z \leq 0.25D$, the computed interface matches well with the analytical solution. However, at $Z > 0.25D$ (i.e., Z/D exceeding the range of validity of analytical solution), the model solution departs significantly from the analytical solution.

4.2 COMPARISON WITH FIELD DATA

The model results have been compared with the field data reported by Schmorak and Mercado (1969).

4.2.1 Experimental Setup

Schmorak and Mercado (1969) carried out field investigations on wells in Ashqelon region in the coastal plane of Isreal. In this area, the first impermeable clay layer is at about 70 meters below MSL

(mean sea level). The aquifer is reported to be unconfined. In the first test (termed as test A), water was pumped from a 16" diameter well for 65 days at a rate of $575 \text{ m}^3/\text{day}$. In the other test (termed as test B), water was pumped from a 16" diameter well for 84 days at a rate of $350 \text{ m}^3/\text{day}$. The pumped water and samples taken at different depths from the 2" diameter observation wells, at different times, were analyzed for saltwater concentration. The saltwater concentrations provided the position of the interface at different times. The location of the pumping and the observation wells are shown in Fig (4.5).

The durations of pumpage (64 and 84 days) during the two tests were much longer than the usual duration of the first and second segments of the time-drawdown curve of an unconfined aquifer (Kruseman and De Ridder, 1983). Thus the time-drawdown curves of both the tests would lie predominantly in the third segment and steady state. The drawdowns during the third segment and steady state are governed by the confined aquifer equations (with the storage coefficient replaced by the specific yield) provided the drawdown is small in comparison to the saturated thickness and the Dupuit Forchheimer's assumptions are satisfied. Therefore, the model though developed for confined aquifer, was employed to simulate the saltwater transport in the aquifer under study [Dupuit Forchheimer's assumptions were assumed to hold good and the drawdowns were assumed to be quite small in comparison to the saturated thickness (69.5 ms)].

4.2.2 Reported Parameters

The values of parameters reported by Schmorak and Mercado (1969) are as follows. K_x (horizontal permeability) = 16.5 m/day ; K_z (Vertical permeability) = 10.2 to 22.7 m/day (adopted K_z for model operation = 16.5 m/day); S_s (Phreatic storage coefficient per unit depth)

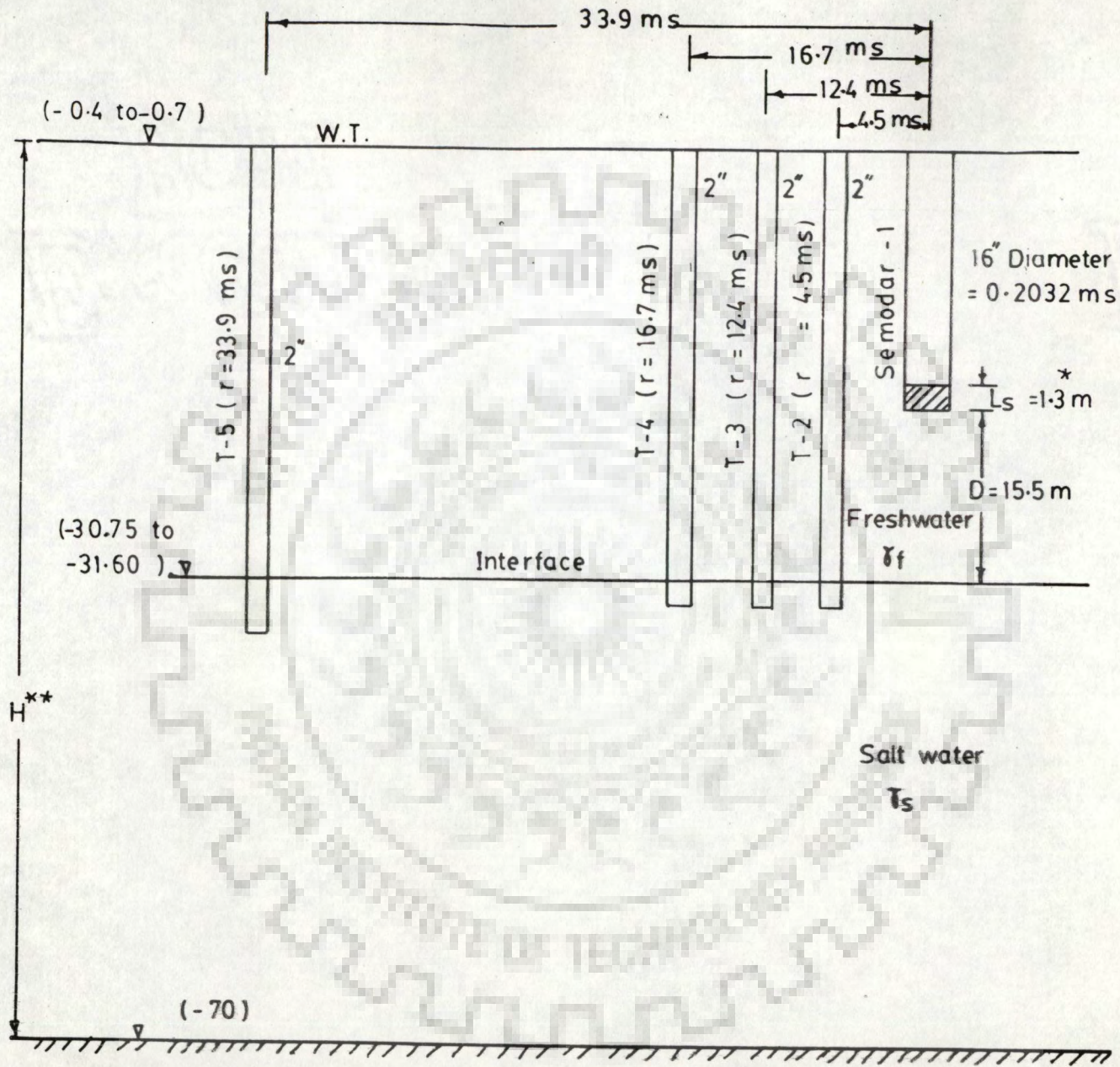


Fig.(45) Layout of Pumping and Observation Well

- * Measured from the sketch presented by Schmorak and Mercado (1969)
- ** $H = 69.3$ to 69.6 ms (H adopted for model 69.5 m.s.)

= 0.0004 to 0.0009 (adopted S_g for model operation = 0.0004); α (Dispersivity) = 0.1 to 0.8 ms [adopted α_L (horizontal dispersivity) for model operation = 0.5 ms and adopted α_T (Vertical dispersivity) for model operation = 0.5ms]; ϕ (porosity) = 0.33; COSW (salt concentration into saltwater) = 22000 ppm; and COGW (salt concentration into the aquifer's freshwater) = 145 ppm.

The values of intrinsic permeabilities (k_r and k_z) are estimated as follows

$$k_r = \frac{K_x \mu_f}{\gamma_f} = \frac{16.5 \times 1.7 \times 10^{-6}}{(24 \times 60) \times 1000} = 1.9479 \times 10^{-11} \text{ m}^2 \quad \dots (4.2)$$

$$k_z = \frac{K_z \mu_f}{\gamma_f} = \frac{16.5 \times 1.7 \times 10^{-6}}{(24 \times 60) \times 1000} = 1.9479 \times 10^{-11} \text{ m}^2 \quad \dots (4.3)$$

4.2.3 Comparison with Model Results

4.2.3.1 Model Operation

The model was operated for the reported conditions of the tests A and B. The parameters were assigned as discussed in the preceding paragraph.

4.2.3.1.1 Pressure Simulation

Radial Spacing: A no - drawdown boundary was assumed to exist at a radial distance (r) of 2032 ms. The radius of the pumped well is 20.32 cm(8"). Thus, the space domain in radial direction extends from $r=0.2032$ ms to 2032 ms. This domain has been discretized by 25 pressure columns spaced in accordance with Rushton and Chan's (1976) Criteria (refer 3.3.5.1.4, Chap. III). The adopted radial spacings are given in Table (4.1).

Vertical Spacing: In the vertical direction, an impervious layer is known to exist at a depth of 69.3 to 69.7 ms below water table (adopted

depth for model operation = 69.5 ms). Thus, the space domain in vertical direction extends from $Z=0$ (first impervious layer) to 69.5 ms (water table). This domain has been discretized by 26 pressure rows. Low vertical spacings are assigned close to the interface. The adopted vertical spacings are given in Table (4.2).

Time Domain: The time domain extending from $t=0$ (beginning of the pumpage) to $t=145$ days (the time of last observation) was discretized by 265 discrete times. The times till the closure of pumpage were chosen in accordance with Rushton and Chan's (1976) Criteria. During the subsequent recovery stage a constant time step was used. The range of time steps are given in Table (4.3).

4.2.3.1.2 Simulation of Saltwater Transport

Radial Spacing A 'no-upconing' and 'zero saltwater concentration' boundary has been assumed to occur at a distance of 35.78 ms from the center of the pumped well. Thus, the space domain in radial direction extends from $r=0.2032$ ms to 35.78 ms. This domain has been discretized by 29 columns spaced in accordance with volume of take off point's criteria (refer 3.3.3.1.1.2, Chap. III). The adopted radial spacings are given in Table (4.4).

Time Domain: The time steps for saltwater transport simulation were generated in accordance with equations 3.80 to 3.82 (Chap. III), assigning the maximum permissible time step for the saltwater transport simulation (Δt_S^m) as 300 minutes. Thus, each pressure time step was subdivided into one or more (ξ) number of equal saltwater transport time steps of duration equal to or less than 300 minutes.

4.2.3.2 Upconed Interface Positions

The model-computed positions of moving points at $t = 2.93$ and 8 days are plotted in Fig (4.6) and (4.7). The corresponding positions

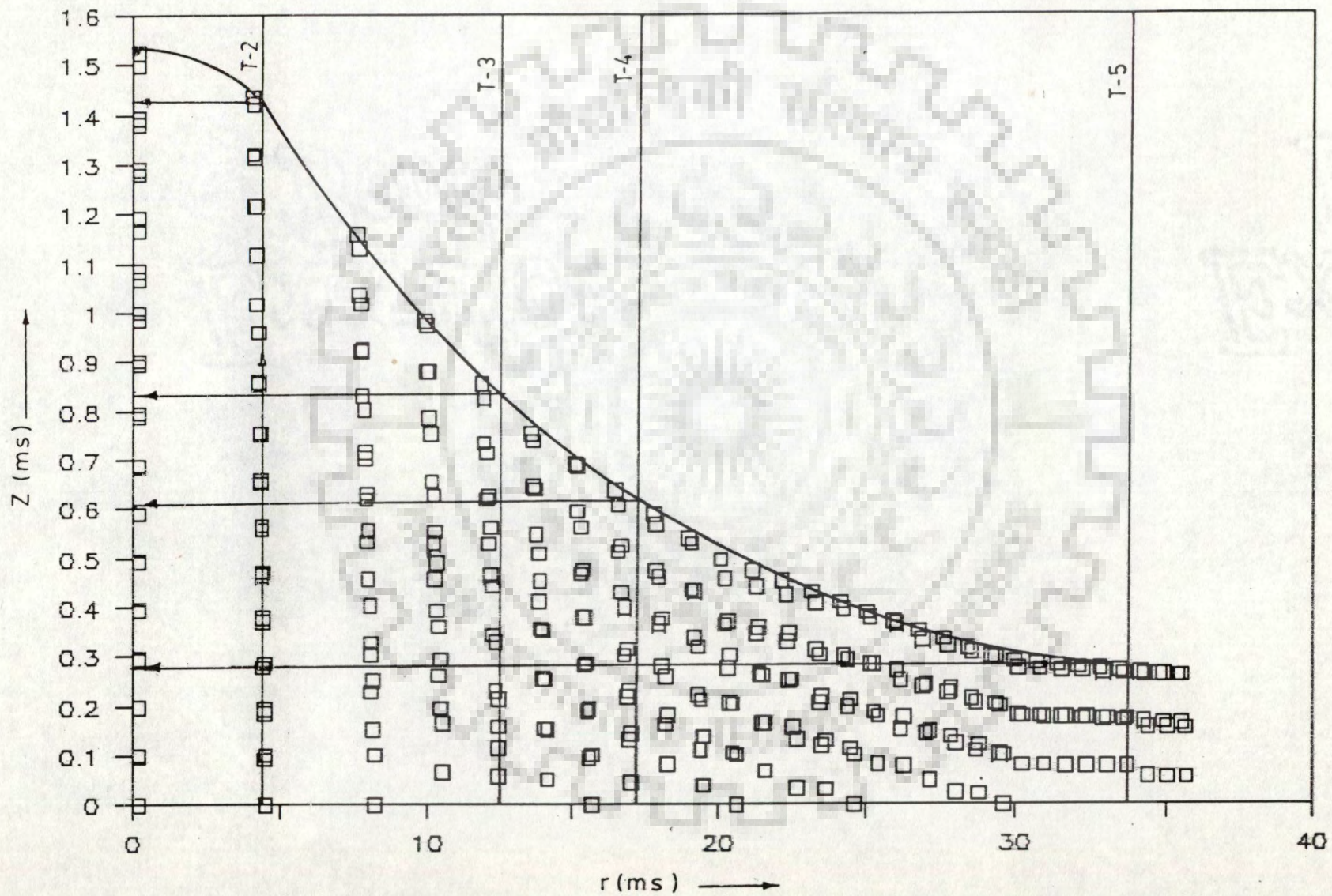


Fig (4.6) Position of Moving Points (Test A, Time=2.93 days)

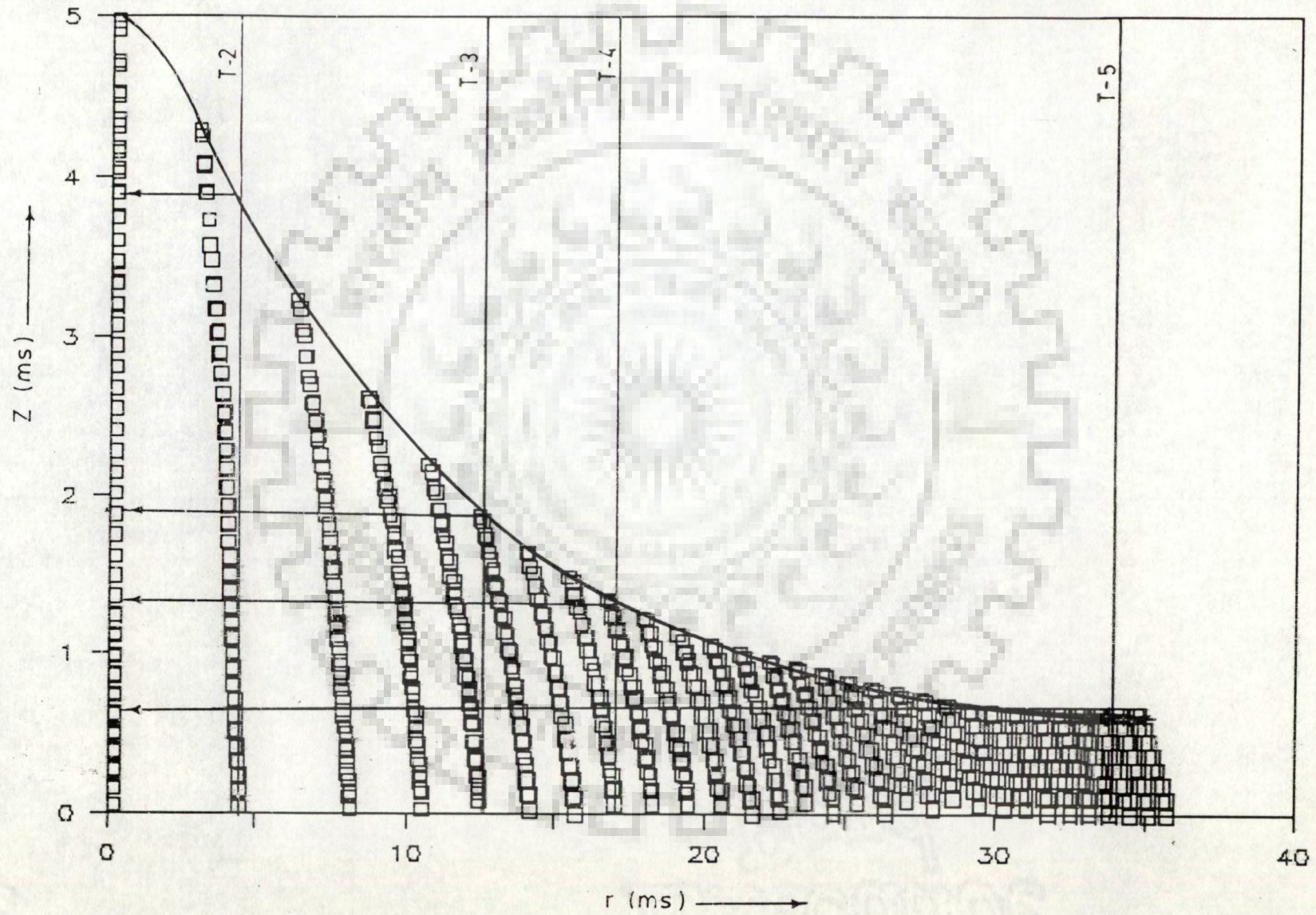


Fig (4.7) Position of Moving Points (Test A, Time = 8 days)

of the interface were obtained by drawing upper envelopes on these moving points. The elevations of the upconed interface at the locations of the observation wells were measured from these envelopes. These elevations were compared with the corresponding observed elevations (Figs. 4.8 to 4.15).

Figs. (4.8) to (4.10) reveal that, the upconing (Z) at $r=4.5$ (tests A and B) and at $r = 12.4$ ms (test A), well exceeded the range of validity of the analytical solution (0.25D). This has caused a significant departure of the analytical solution from the observed data.

Table (4.1) Radial Spacing for Pressure Simulation

S.N. of columns	Radial spacing ms	Cumulative distance ms	S.N. of columns	Radial spacing ms	Cumulative distance ms
1-2	0.10	0.30	14-15	13.95	43.78
2-3	0.14	0.44	15-16	20.48	64.26
3-4	0.20	0.64	16-17	30.06	94.32
4-5	0.30	0.94	17-18	44.12	138.44
5-6	0.45	1.39	18-19	64.76	203.20
6-7	0.64	2.03	19-20	95.10	298.30
7-8	0.95	2.98	20-21	139.50	437.80
8-9	1.40	4.38	21-22	204.80	642.60
9-10	2.01	6.39	22-23	300.60	943.20
10-11	3.01	9.40	23-24	441.20	1384.40
11-12	4.41	13.81	24-25	647.60	2032.00
12-13	6.51	20.32			
13-14	9.51	29.83			

Table (4.2) Vertical Spacing

S.N. of rows	Vertical spacing ms	Cumulative distance ms	S.N. of rows	Vertical spacing ms	Cumulative distance ms
1-2	6.15	6.15	14-15	1.50	26.61
2-3	5.00	11.15	15-16	0.75	27.36
3-4	3.00	14.15	16-17	0.75	28.11
4-5	1.30	15.45	17-18	0.75	28.86
5-6	1.30	16.75	18-19	0.75	29.61
6-7	1.18	17.93	19-20	0.75	30.36
7-8	1.18	19.11	20-21	0.75	31.11
8-9	1.00	20.11	21-22	1.00	32.11
9-10	1.00	21.11	22-23	2.89	35.00
10-11	1.00	22.11	23-24	8.00	43.00
11-12	1.00	23.11	24-25	12.00	55.00
12-13	1.00	24.11	25-26	14.50	69.50
13-14	1.00	25.11			

Table (4.3) Time Steps For Pressure Simulation

Range	S.N. of steps	Range	S.N. of steps
$0 < \Delta t \leq 10^{-4}$	1-35	$1 < \Delta t \leq 10$	202-208
$10^{-4} < \Delta t \leq 10^{-3}$	36-106	$10 < \Delta t \leq 100$	209-215
$10^{-3} < \Delta t \leq 10^{-2}$	107-158	$100 < \Delta t \leq 1000$	216-222
$10^{-2} < \Delta t \leq 10^{-1}$	159-199	$1000 < \Delta t \leq 10000$	223-265
$10^{-1} < \Delta t \leq 1$	200-201		

Table (4.4) Radial Spacing for Saltwater Simulation

S. N. of columns	Radial spacing ms	Cumulative distance ms	S. N. of columns	Radial spacing ms	Cumulative distance ms
Well-1	4.47	4.47	15-16	0.87	26.40
1-2	3.70	8.17	16-17	0.84	27.24
2-3	2.41	10.58	17-18	0.81	28.05
3-4	1.95	12.53	18-19	0.79	28.84
4-5	1.68	14.21	19-20	0.77	29.61
5-6	1.50	15.71	20-21	0.75	30.36
6-7	1.37	17.08	21-22	0.73	31.09
7-8	1.27	18.35	22-23	0.71	31.80
8-9	1.19	19.54	23-24	0.70	32.50
9-10	1.12	20.66	24-25	0.68	33.18
10-11	1.06	21.72	25-26	0.67	33.85
11-12	1.01	22.73	26-27	0.66	34.51
12-13	0.97	23.70	27-28	0.64	35.15
13-14	0.93	24.63	28-29	0.63	35.78
14-15	0.90	25.53			

However, the model has reproduced the upconing reasonably well, uniformly at all values of Z/D . The reproduction of settlement, is also fairly good for the test A at $r=4.5$ ms (Fig. 4.8) and at $r=12.4$ ms (Fig. 4.10). However, for the test B at $r=4.5$ ms (Fig. 4.9) the model computed settlement of the interface varies significantly from the observed data.

Figs. (4.11) to (4.15) reveal that, the upconing at $r = 12.4$ ms (test B); $r = 16.7$ ms (test A and B) and at $r = 33.9$ ms (test A and B), falls below or marginally exceeds $0.25D$. The model results and the

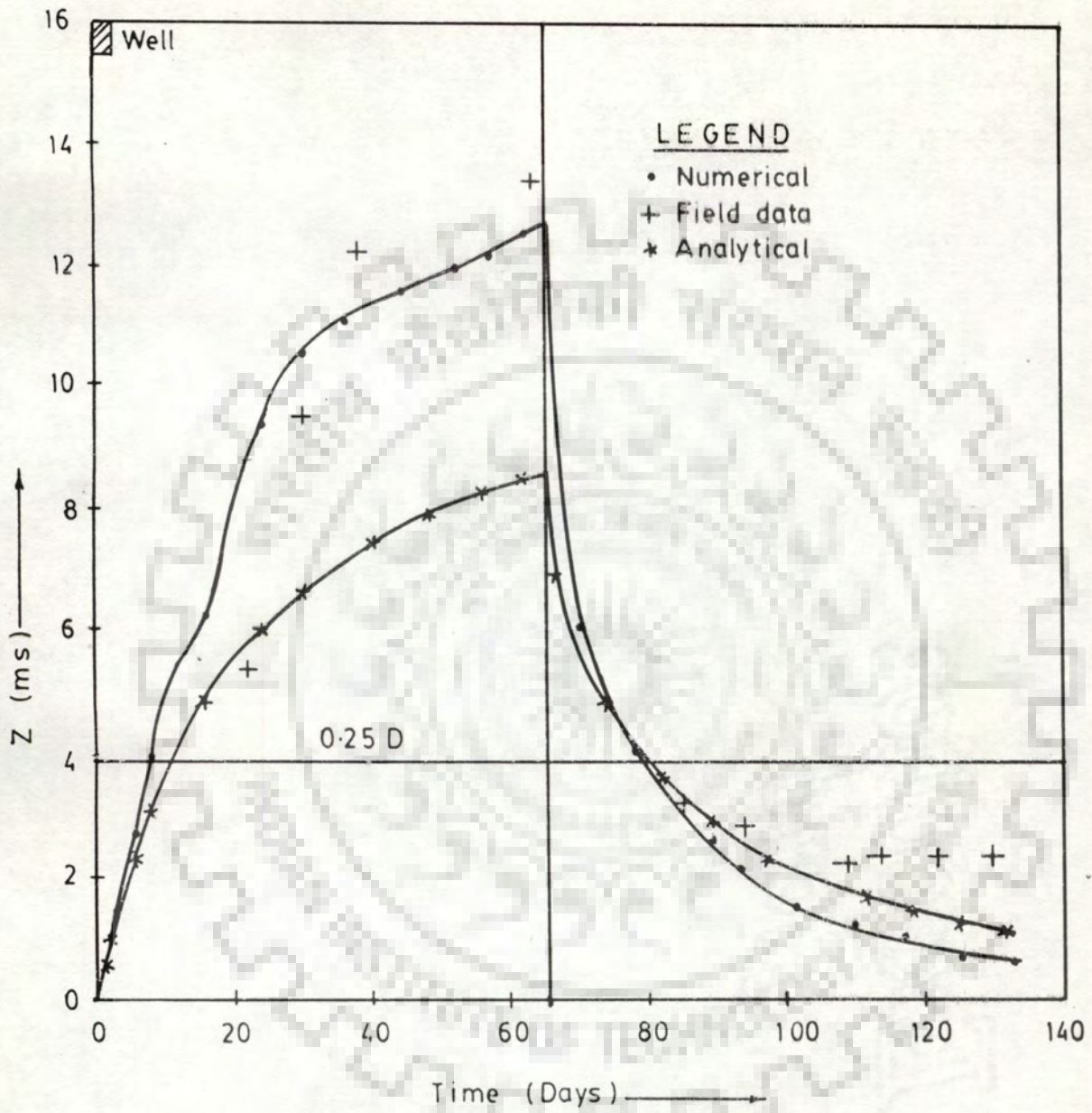


Fig (4.8) Upconing and Settlement Vs Time
(Test A, $r = 4.5$ ms)

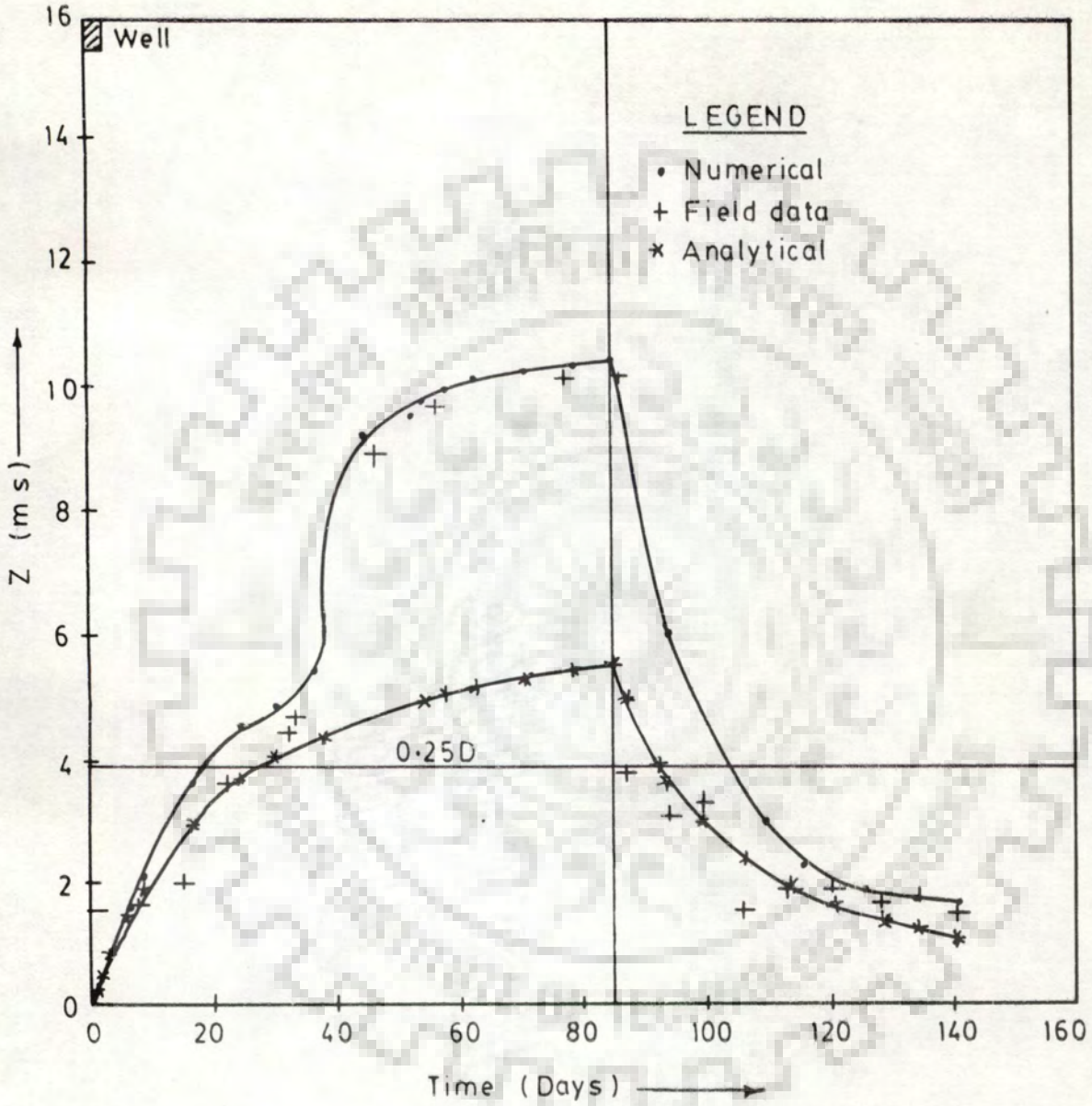


Fig. (4.9) Upconing and Settlement Vs Time
(Test - B , $r = 4.5 \text{ ms}$)

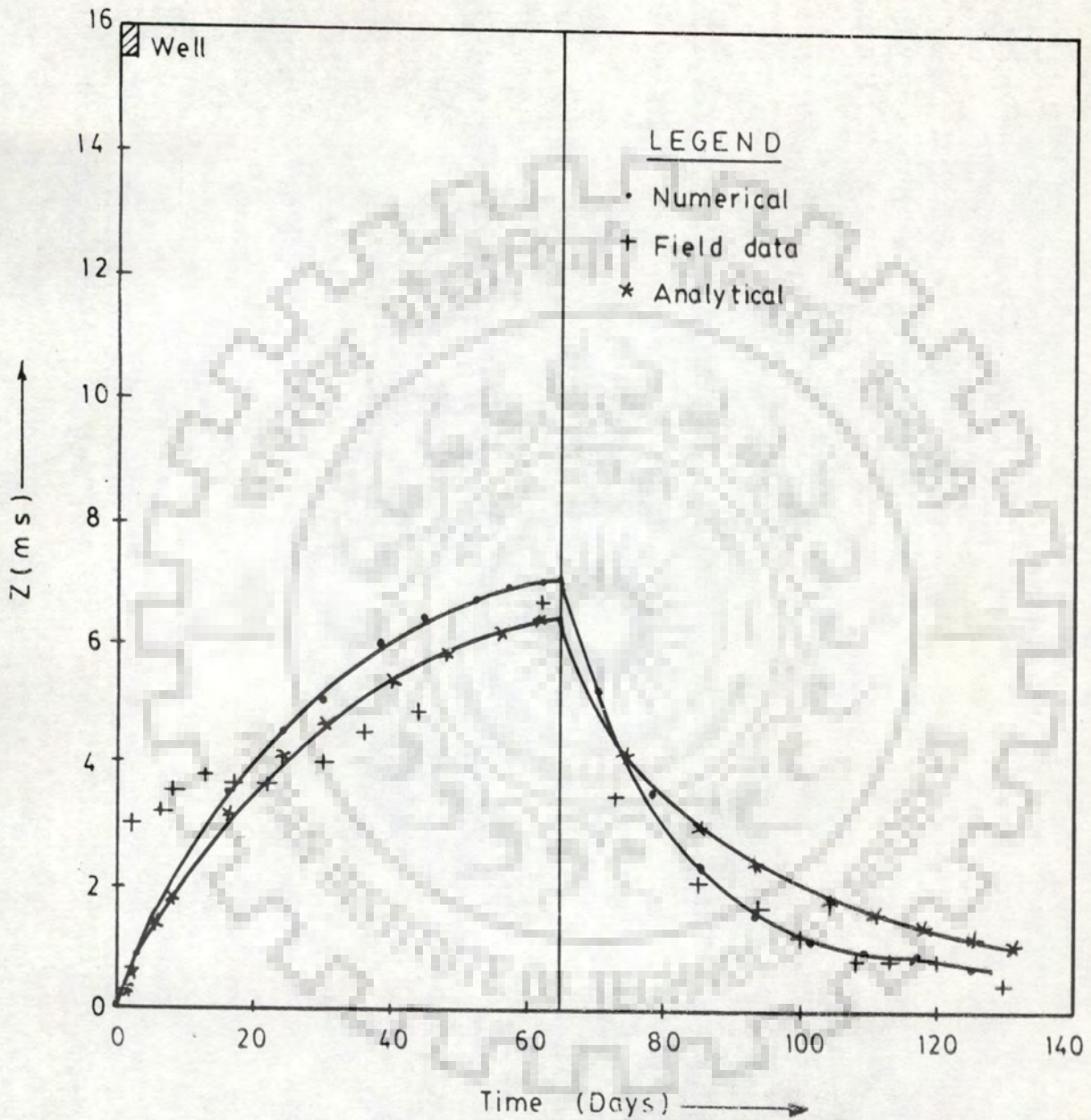


Fig. (4.10) Upconing and Settlement Vs Time
(Test - A , $r = 12.4 \text{ ms}$)

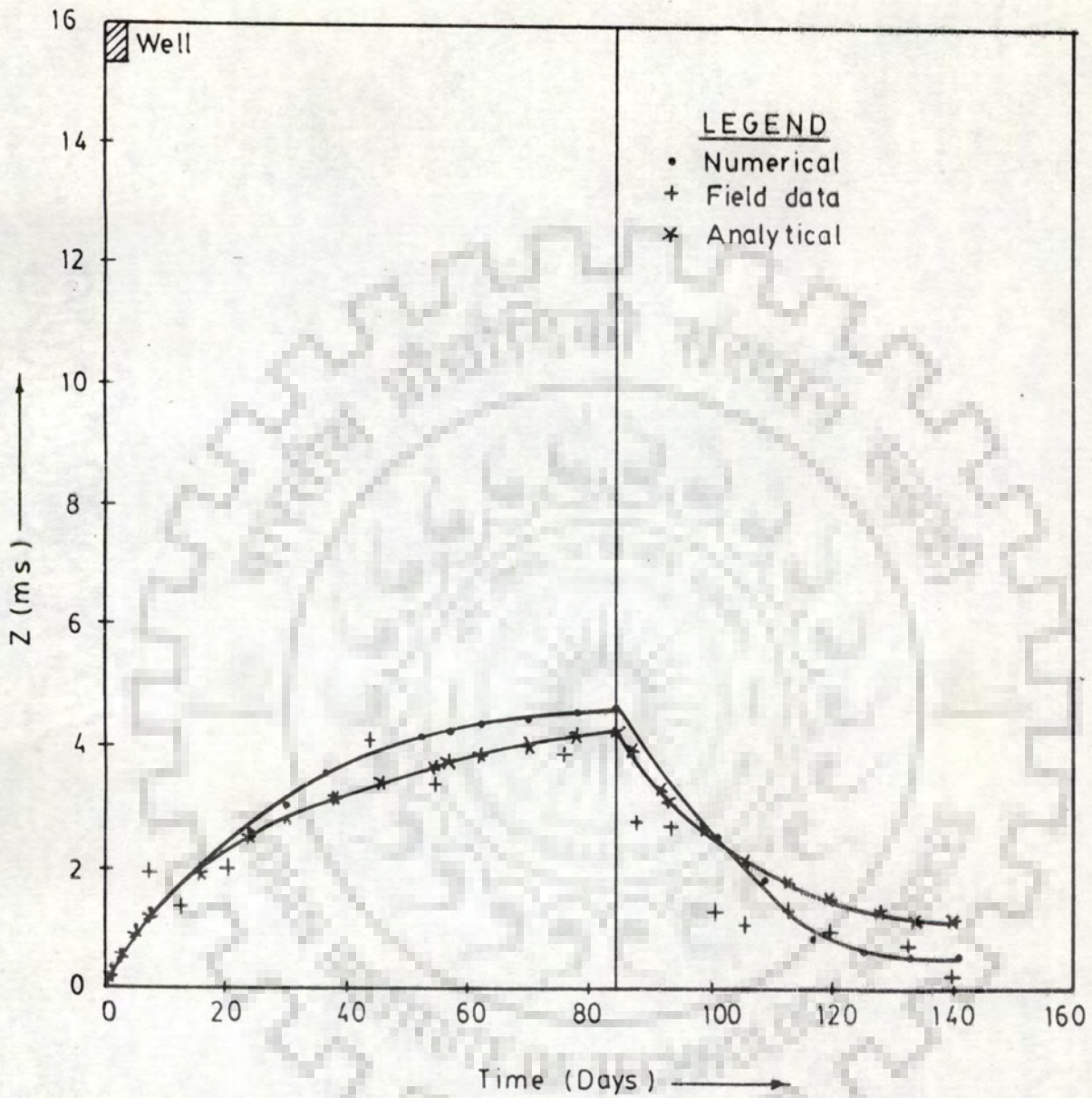


Fig (4.11) Upconing and Settlement Vs Time
(Test B , $r = 12.4$ m.s.)

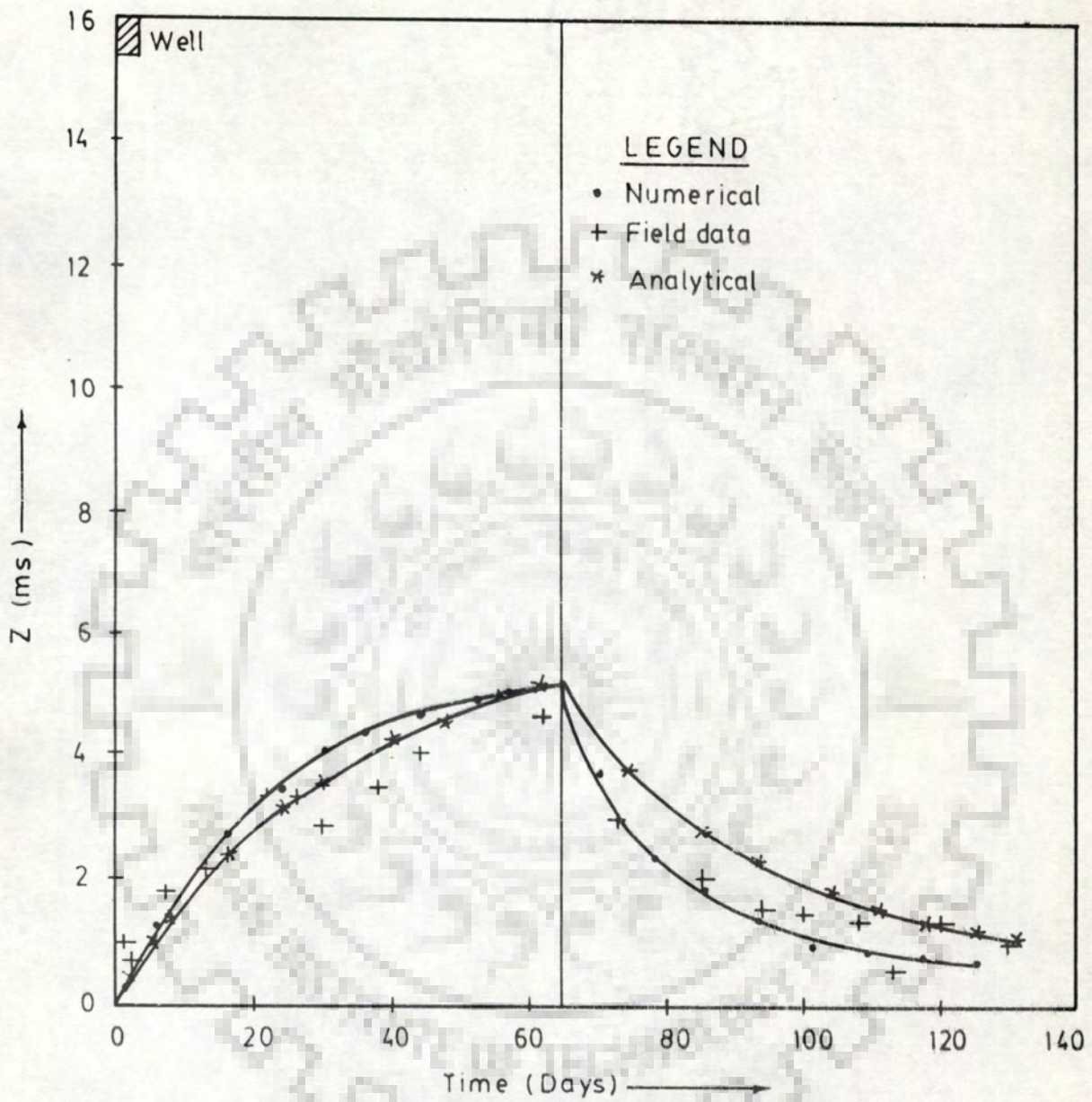


Fig (4.12) Upconing and Settlement Vs Time
(Test - A , $r = 16.7$ m.s.)

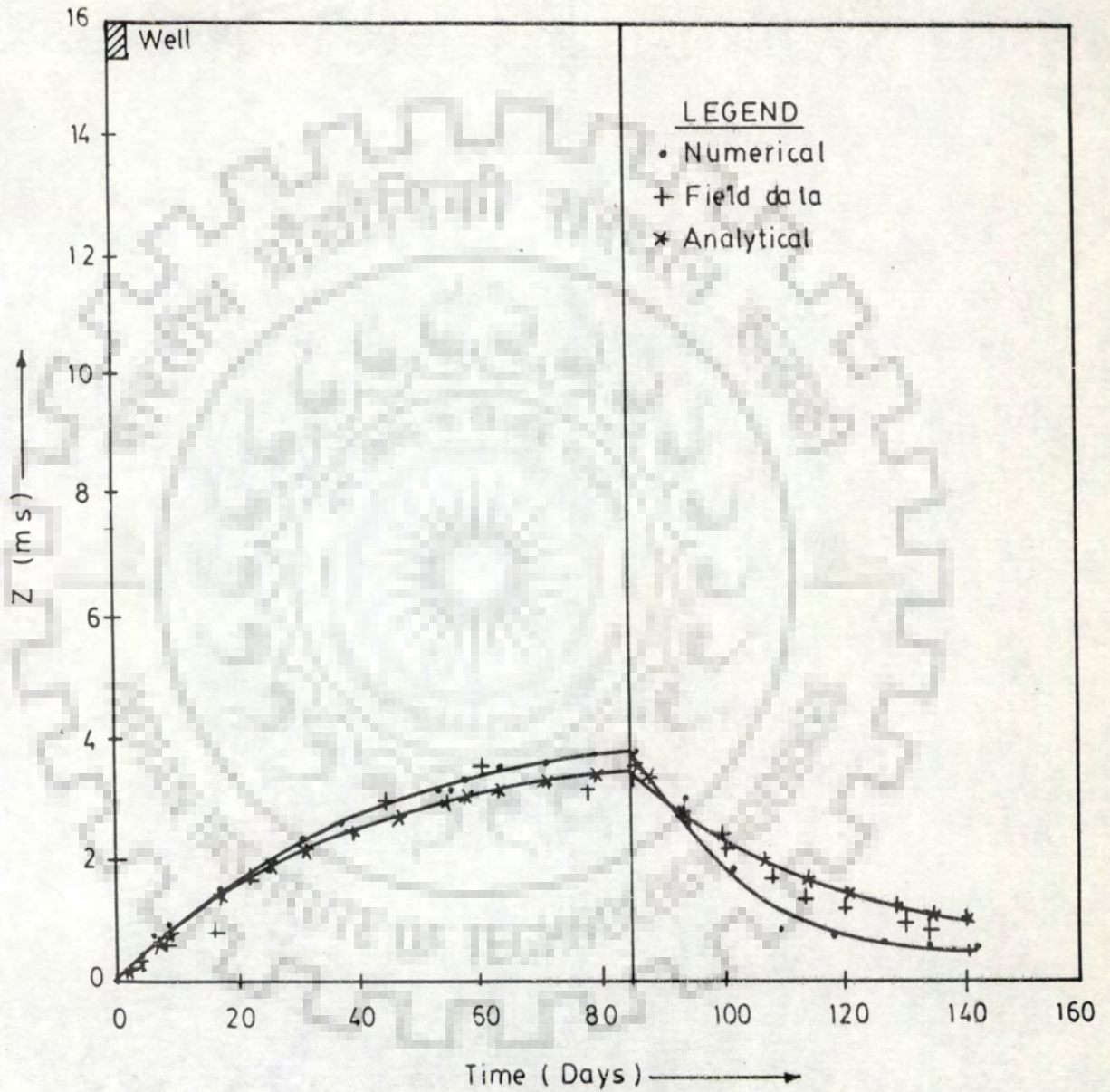


Fig (4.13) Upconing and Settlement Vs Time
 (Test B , $r = 16.7$ ms)

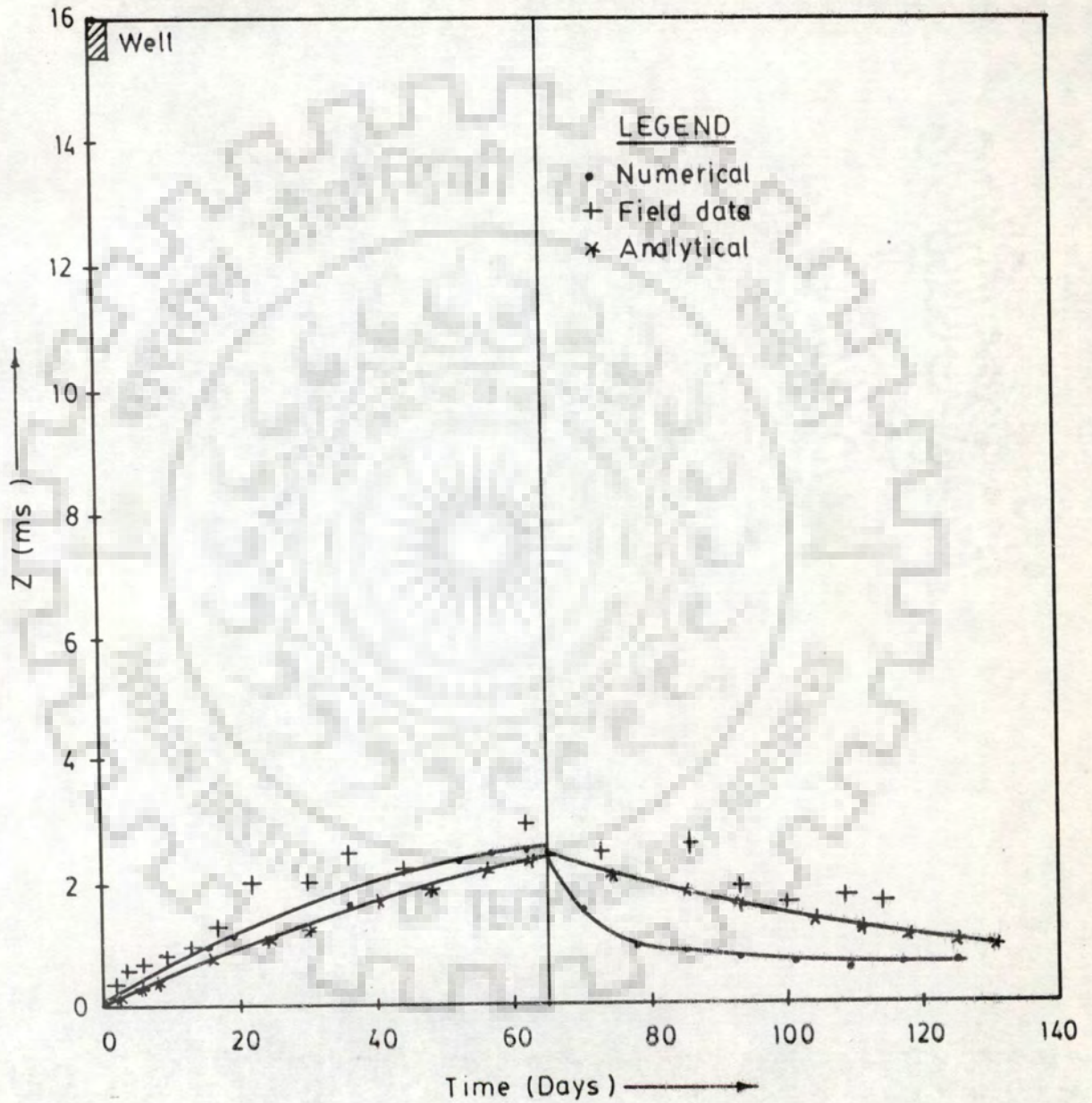


Fig.(4.14) Upconing and Settlement Vs Time
(Test A , $r = 33.9$ ms)

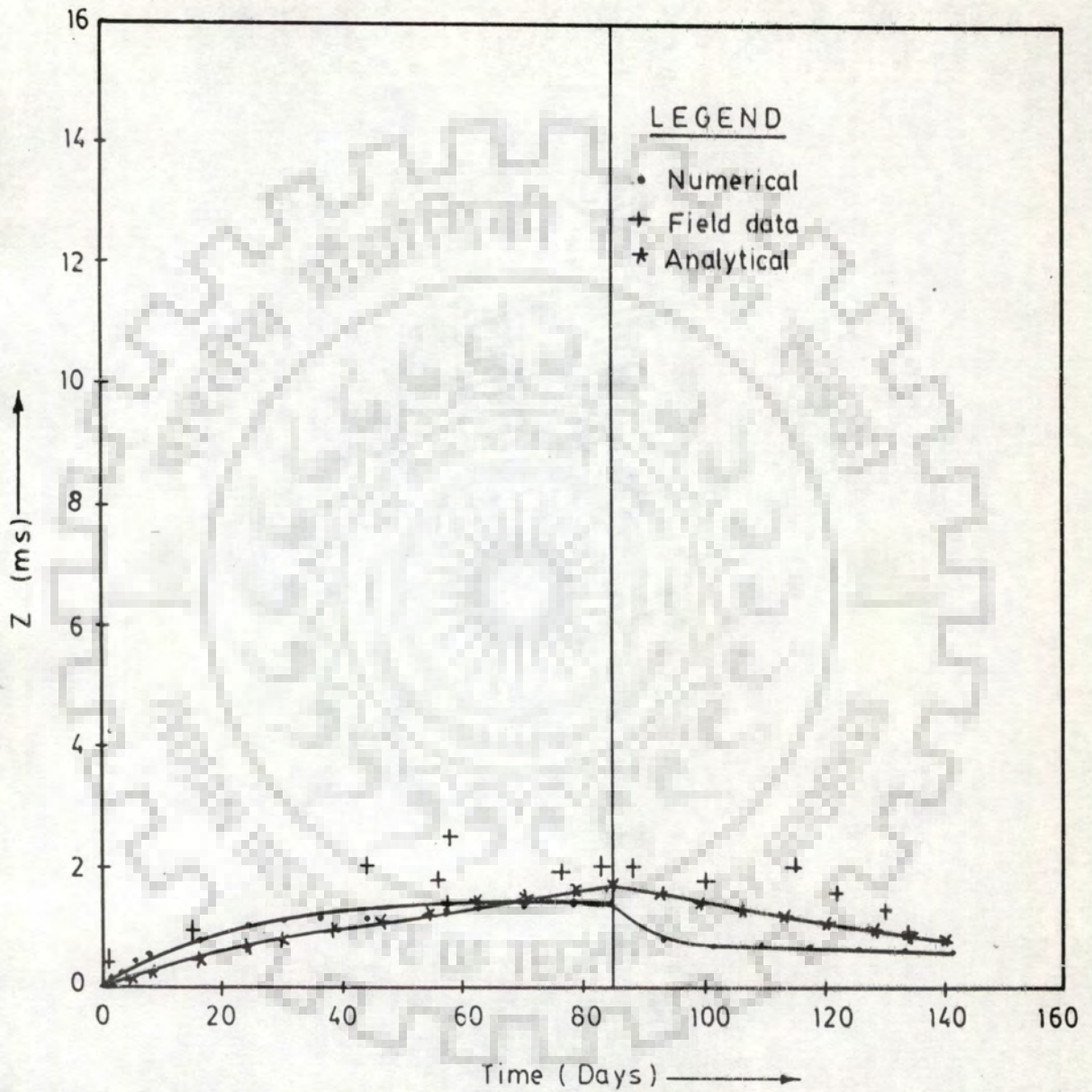


Fig.(4.15) Upconing and Settlement Vs Time
(Test B , $r = 33.9$ m.s.)

analytical solution , in these cases, are in a good agreement with the observed data. In case of test A, the reproduction of the settlement at $r=16.7$ ms is fairly good (Fig. 4.12) while the reproduction at $r=33.9$ ms is poor (Fig. 4.14). In case of test B, the reproduction of the settlement at $r=12.4$ ms and 16.7 ms are fairly good (Fig. 4.11 and 4.13) while the reproduction at $r=33.9$ ms is poor (Fig. 4.15).

Figs. (4.16) to (4.20) show the interface position at $t = 8$; 30 and 62 days (test A) ; and $t = 16$ and 57 days (test B). These Figs reveal that, in both tests, the model results are in a reasonably good agreement with observed data.

4.2.3.3 Saltwater Concentration in Pumped Water

The time-variant saltwater concentration (CP_k) in pumped water at a discrete time t_k , is obtained from the model results as follows

$$CP_k = \frac{1}{Q} \left. \frac{dVS}{dt} \right|_{t=t_k} \dots \dots (4.4)$$

Where VS is the cumulative saltwater volume entered into the pumped well till the discrete time t_k . The variation of model computed cumulative saltwater volume entry into the pumped well (VS) vs. time are plotted in Figs. (4.21) and (4.22) for test A and B. The values of $\frac{dVS}{dt}$ (i.e., gradients of the curves) at the pressure discrete times were obtained graphically (i.e., by drawing tangents to the curves) from these Figs. These fractional concentrations were subsequently converted to PPM employing the curve shown in Fig. (4.23). The computed and observed concentrations for the two tests are plotted in Figs (4.24) and (4.25). These Figs. reveal that, in case of test A, the model results match reasonably well with the observed data. However, there is some departure in case of test B.

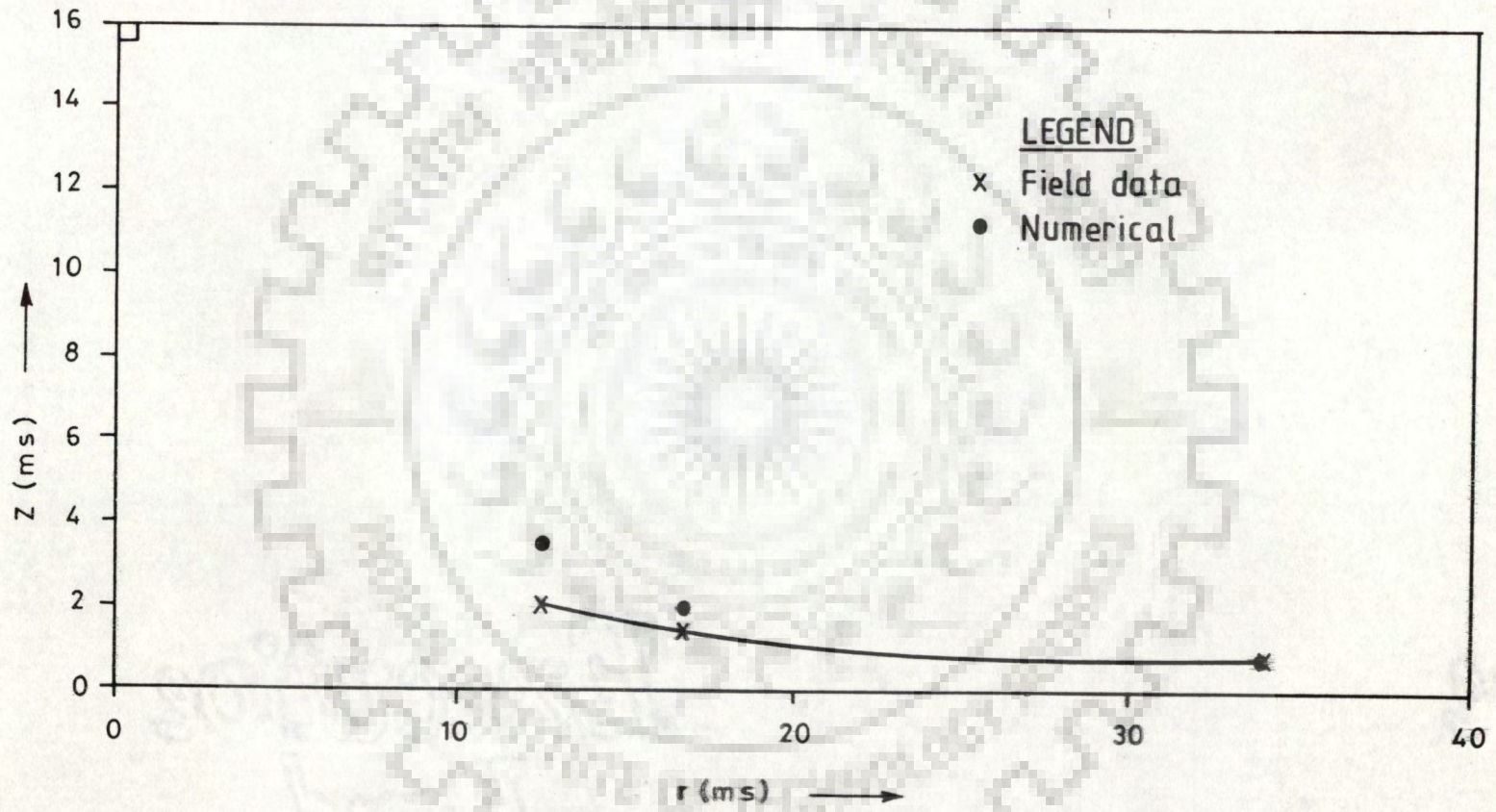


Fig.(4.16) Position of the Interface (Test A , Time 8 days)

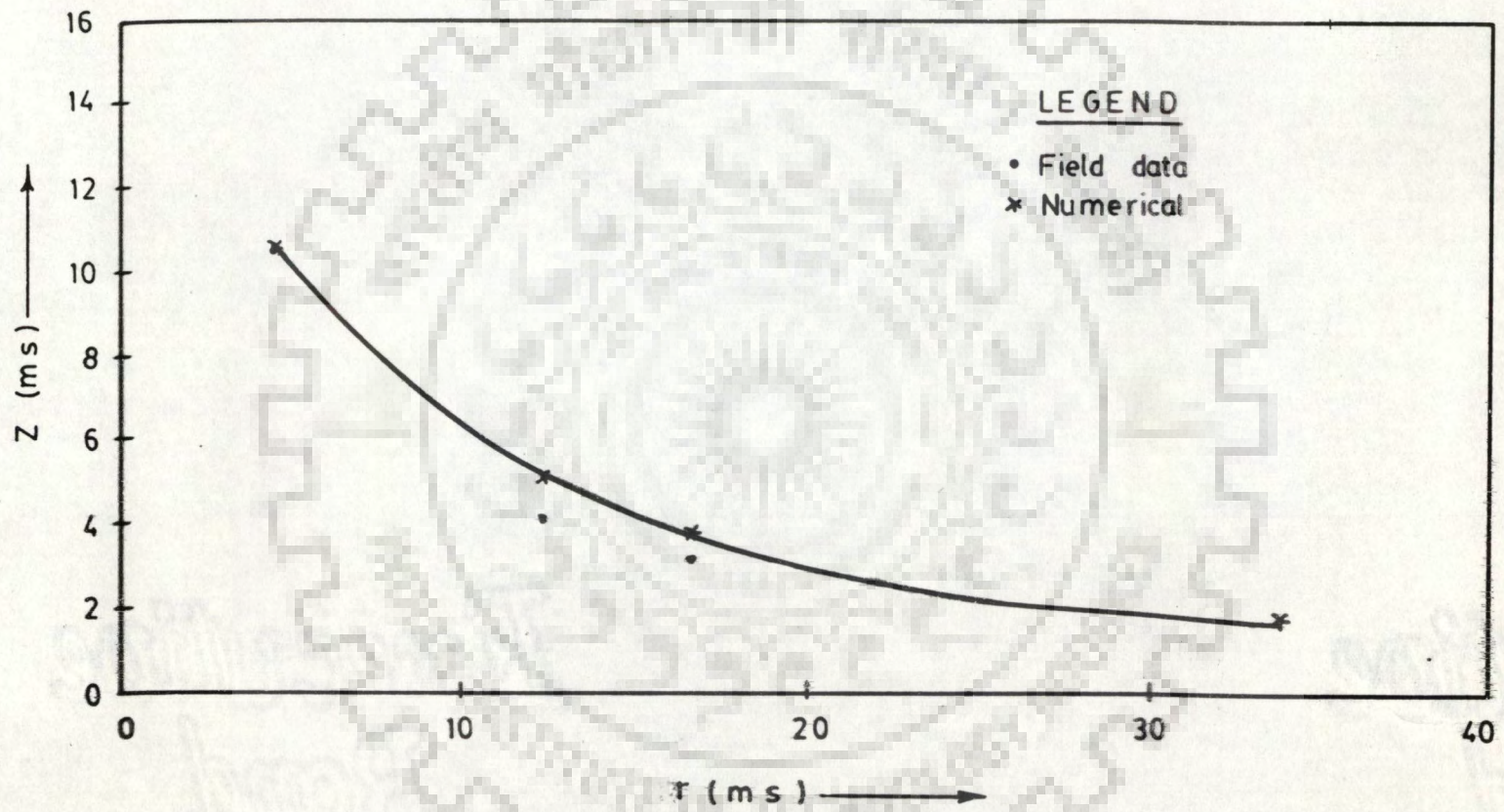
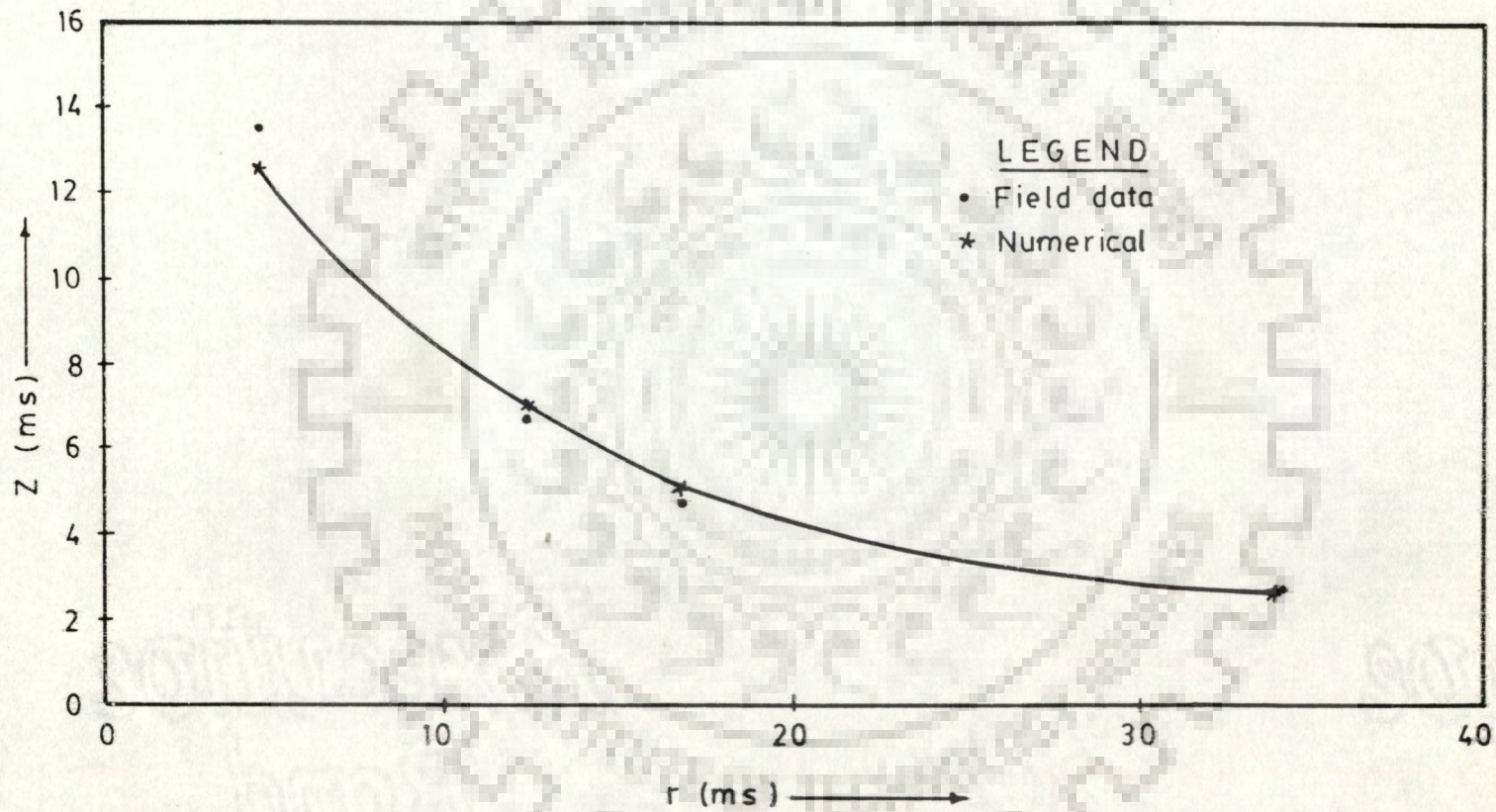


Fig. (4.17) Position of the Interface
(Test A , Time =30 days)



Fig(4.18) Position of the Interface
(Test A , Time=62 days)

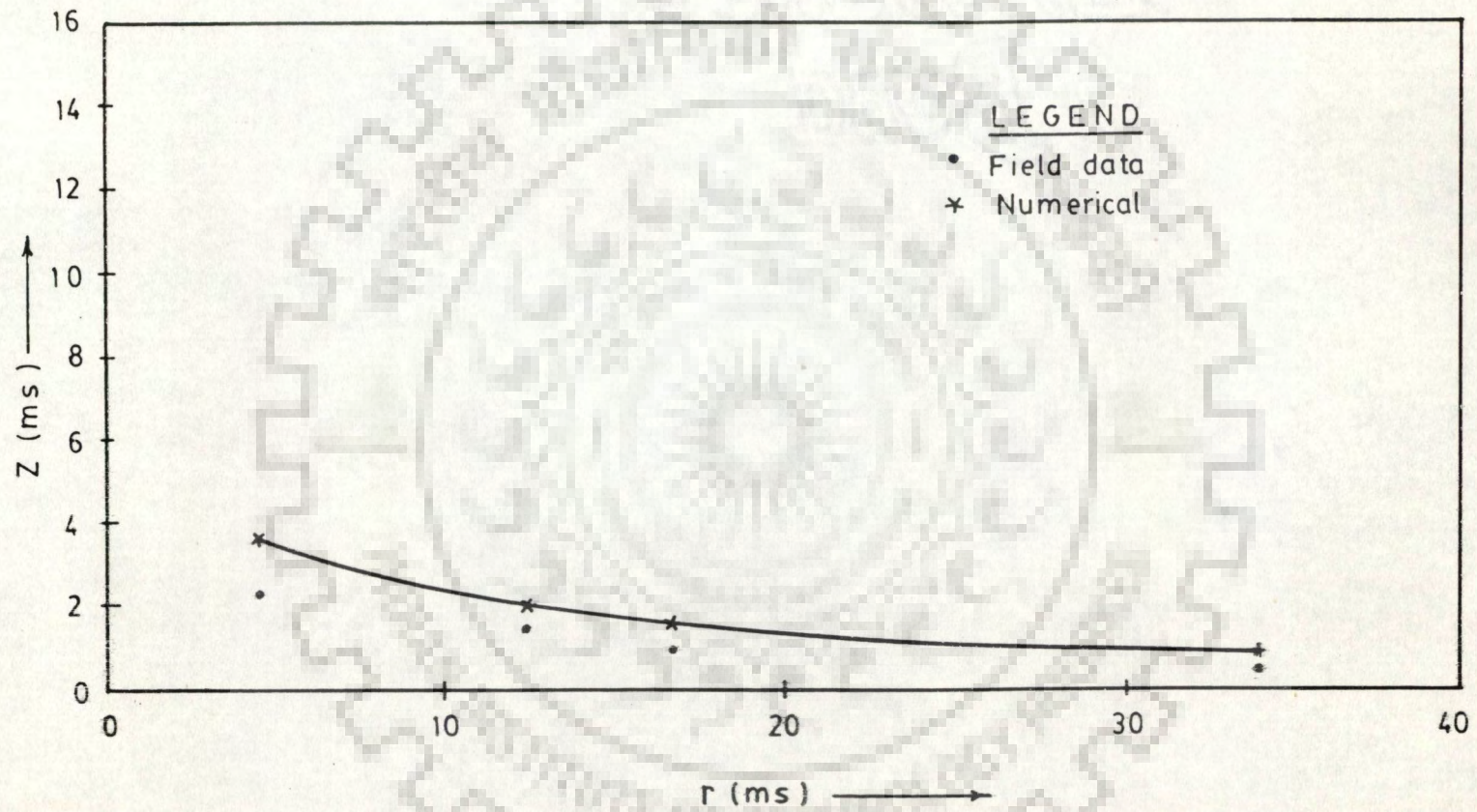


Fig (4.19) Position of the Interface
(Test B , Time =16 days)

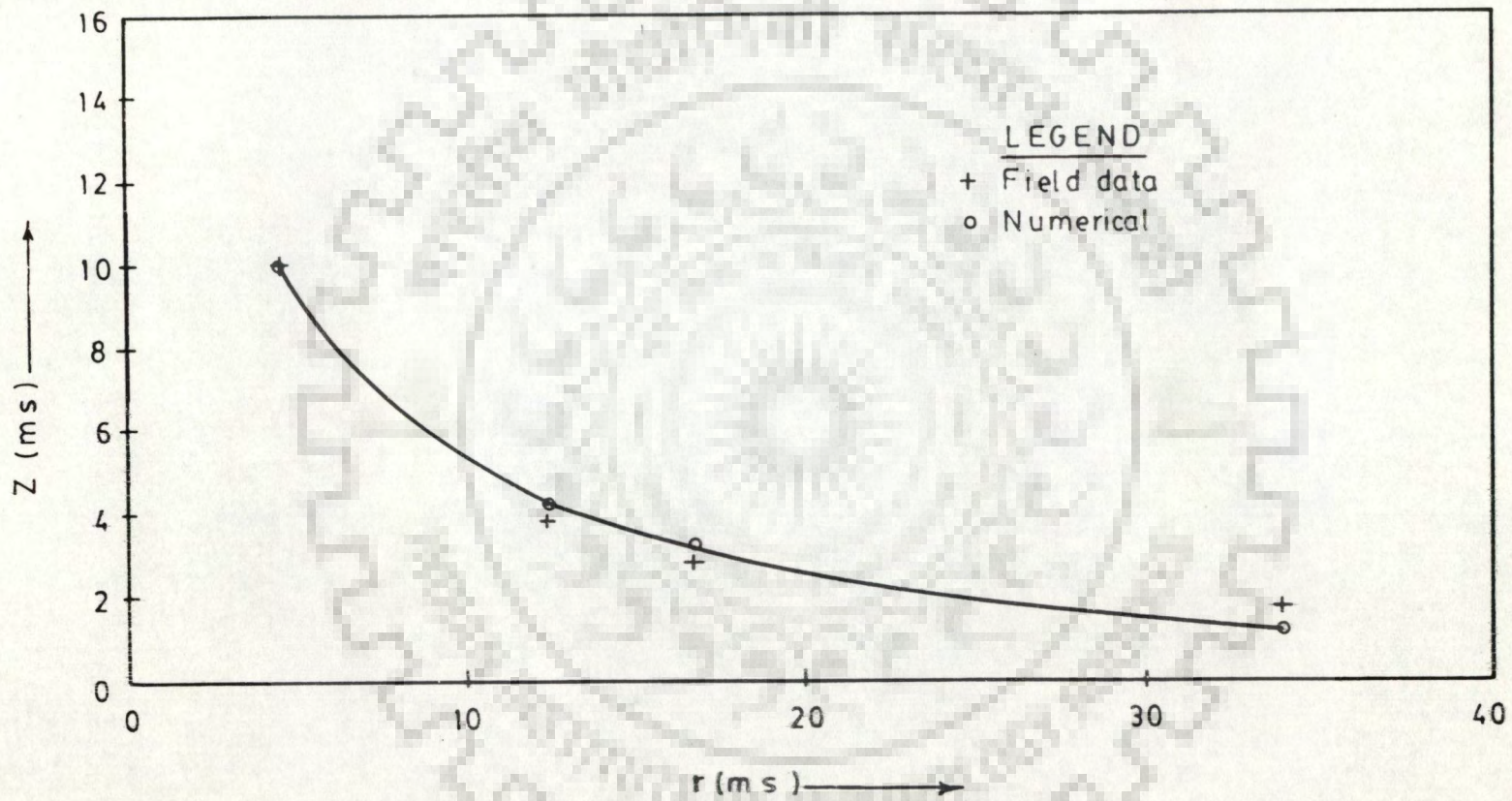


Fig. (4.20) Position of the Interface

(Test B , Time= 57 days)

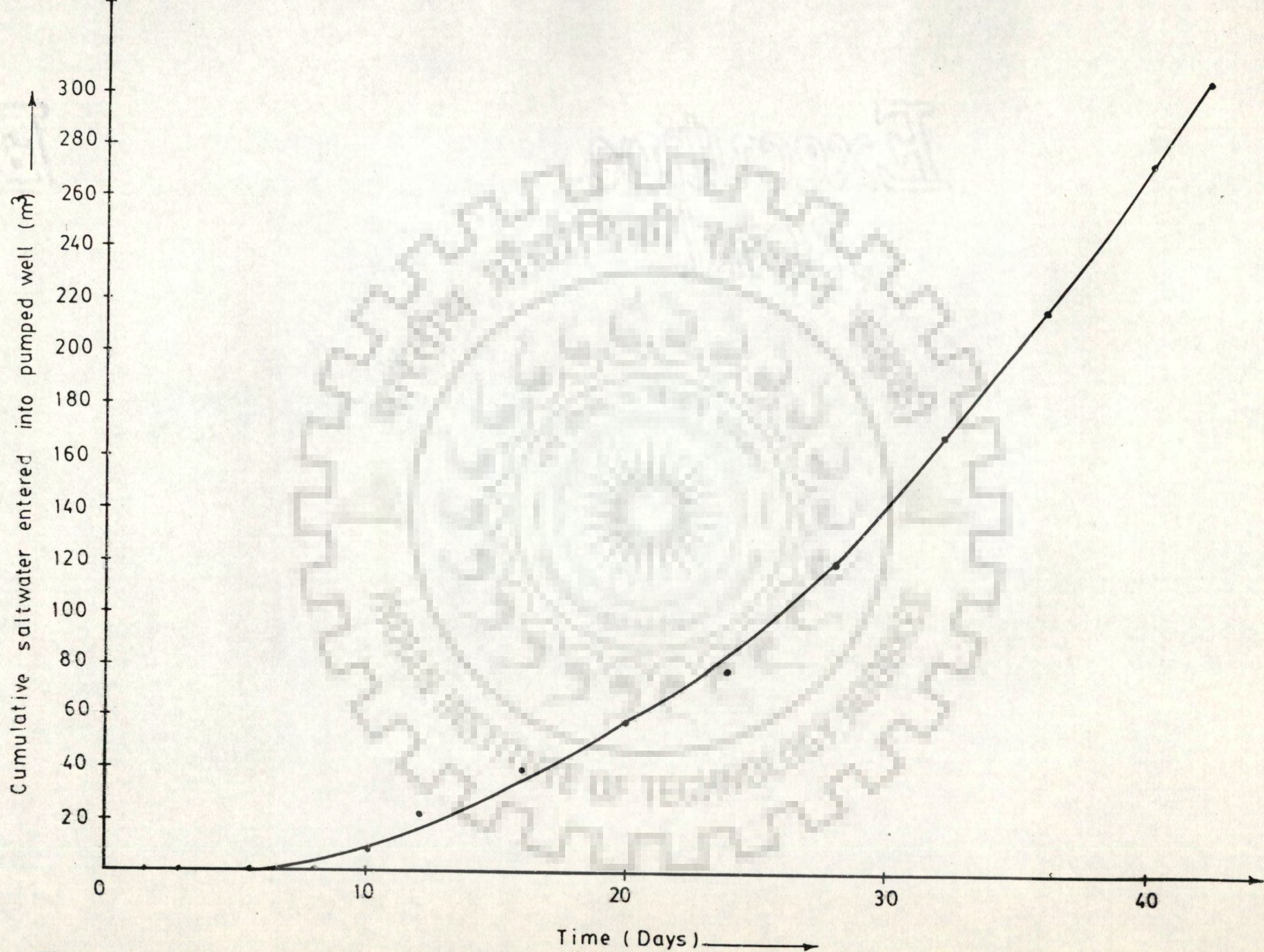


Fig (4.21) Time Variation of Cumulative Saltwater Entered into a Pumping Well (Test A)

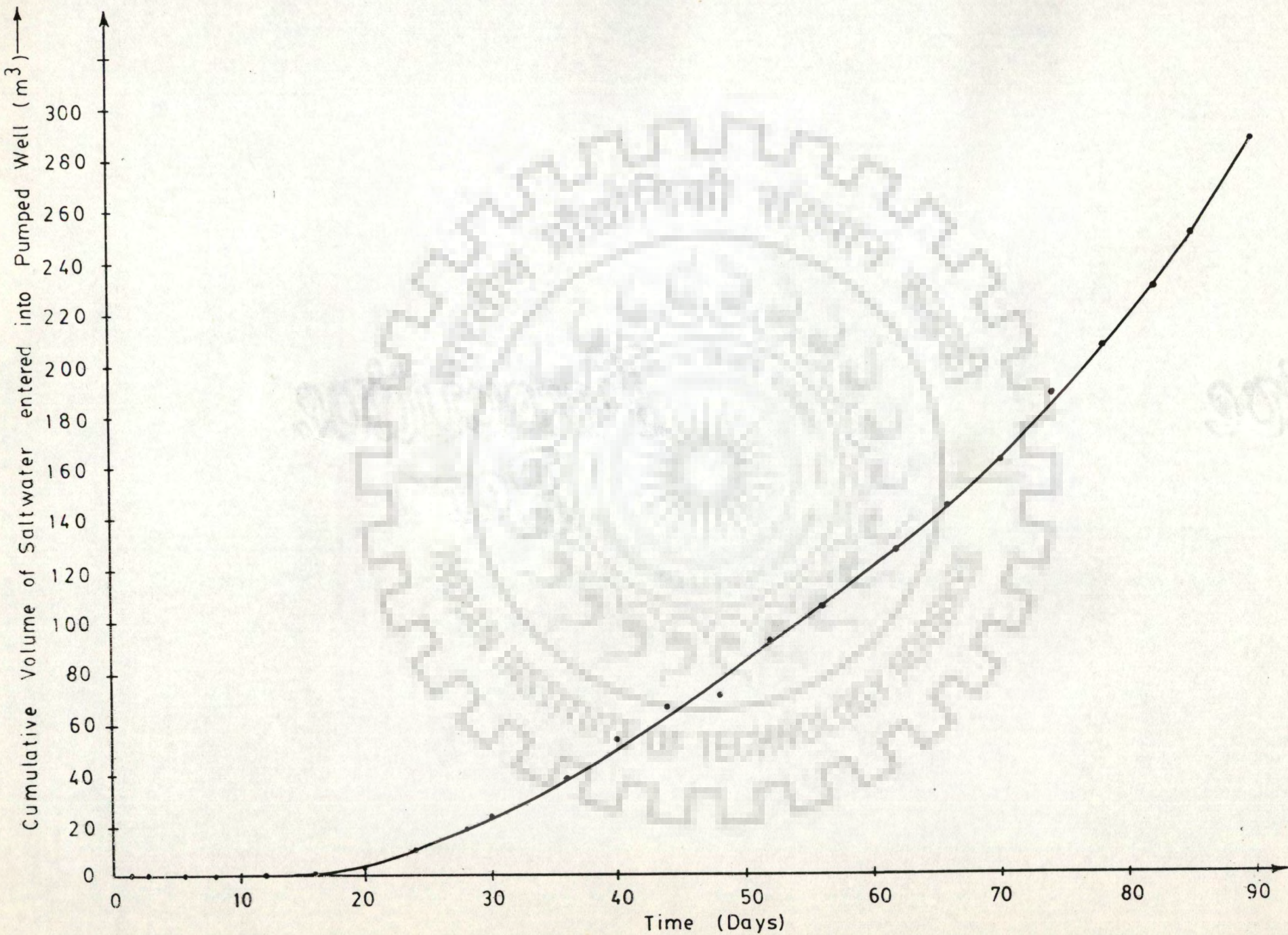


Fig (4.22) Time Variation of Cumulative Saltwater Entered into Pumping Well (Test-B)

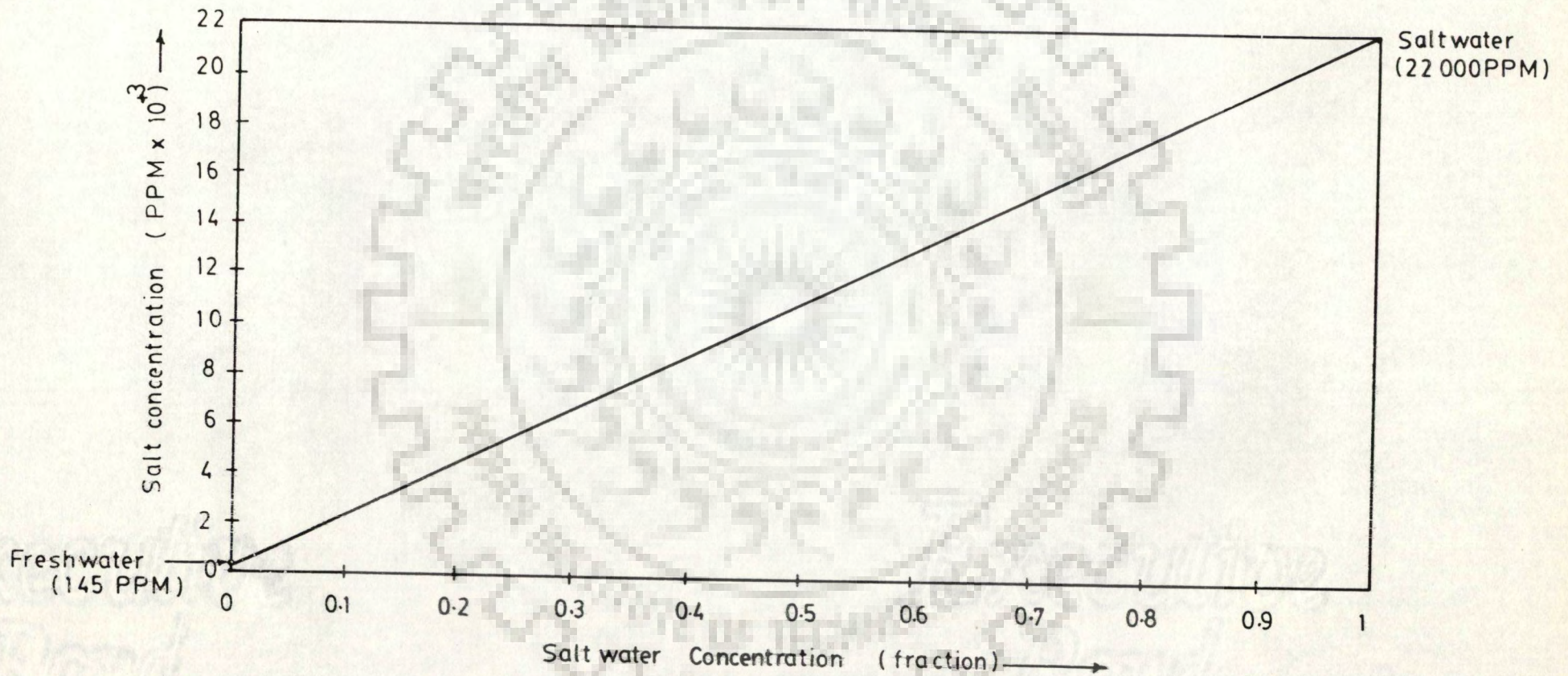


Fig (4.23) Relation Between Saltwater Concentration and Salt Concentration

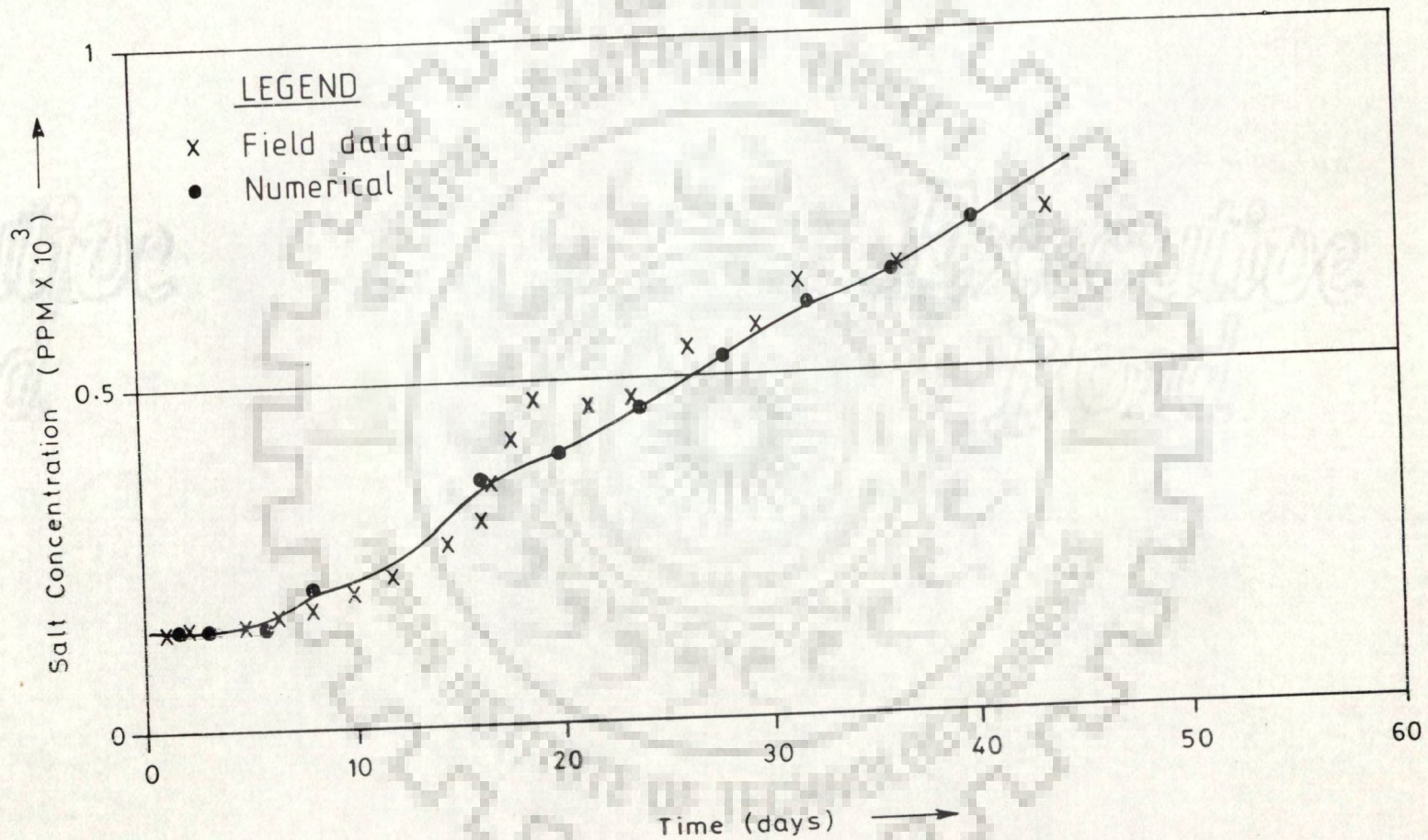


Fig.(4.24) Saltwater Concentration in Pumped water Vs Time (Test A)

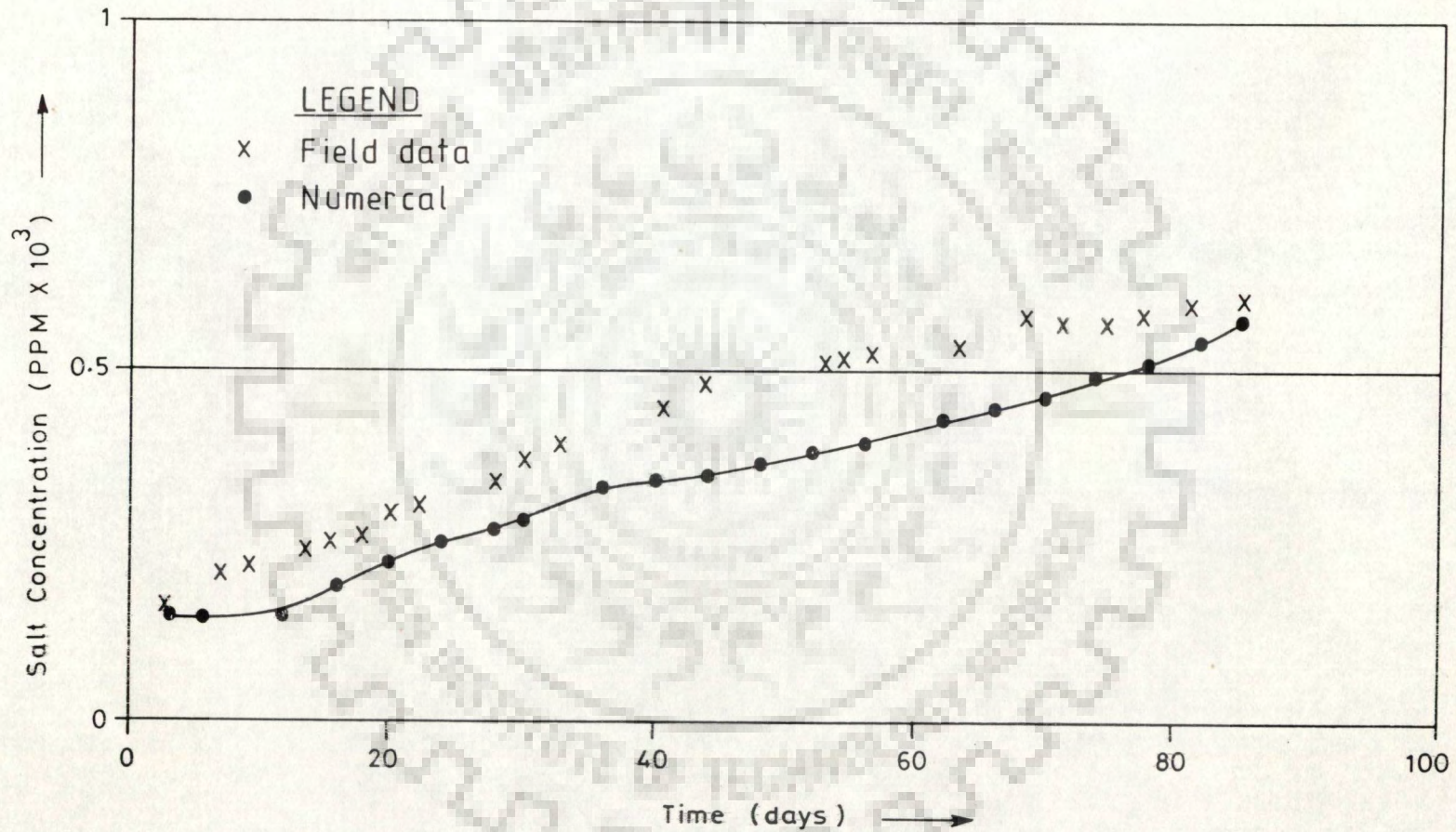


Fig.(4-25) Saltwater Concentration in Pumped Water Vs Time (Test B)

CHAPTER V
MODEL OPERATION

5.1 INFLUENCE OF THE VARIATION OF FLUID PROPERTIES ON THE SOLUTION.

The time and space variation of saltwater concentration, leads to time and space variation of specific weight (γ) and dynamic viscosity (μ). The model was operated to illustrate the influence of such variations on the computed upconing.

The values of γ and μ were computed explicitly at each node at each discrete time, in accordance with the following equations [refer equations 3.45, and 3.46b (Chap. III)].

$$\begin{aligned}\gamma_{ijk} &= 1000 \left[1 + C_{i,j,k-1} \left(\frac{1030}{1000} - 1 \right) \right] \\ &= 1000 + 0.03 C_{i,j,k-1}\end{aligned}\quad \dots (5.1)$$

$$\mu_{ijk} = 1.7 \times 10^{-6} (1 + 0.02825614 C_{i,j,k-1}) \quad \dots (5.2)$$

The time - variant upconing below a well of 0.15 ms radius, as a consequence of pumping at a rate of $0.0001 \text{ m}^3/\text{min}$, was computed three times - firstly accounting for the variation of γ and μ ;secondly accounting for variation of γ only; and finally ignoring such variations. The results are shown in Figs. (5.1a) and (5.1b). The Figs. reveal that, the variation of specific weight due to space and time variation of saltwater concentration needs to be accounted for in the computation of pressure distribution. A lack of such an accounting leads

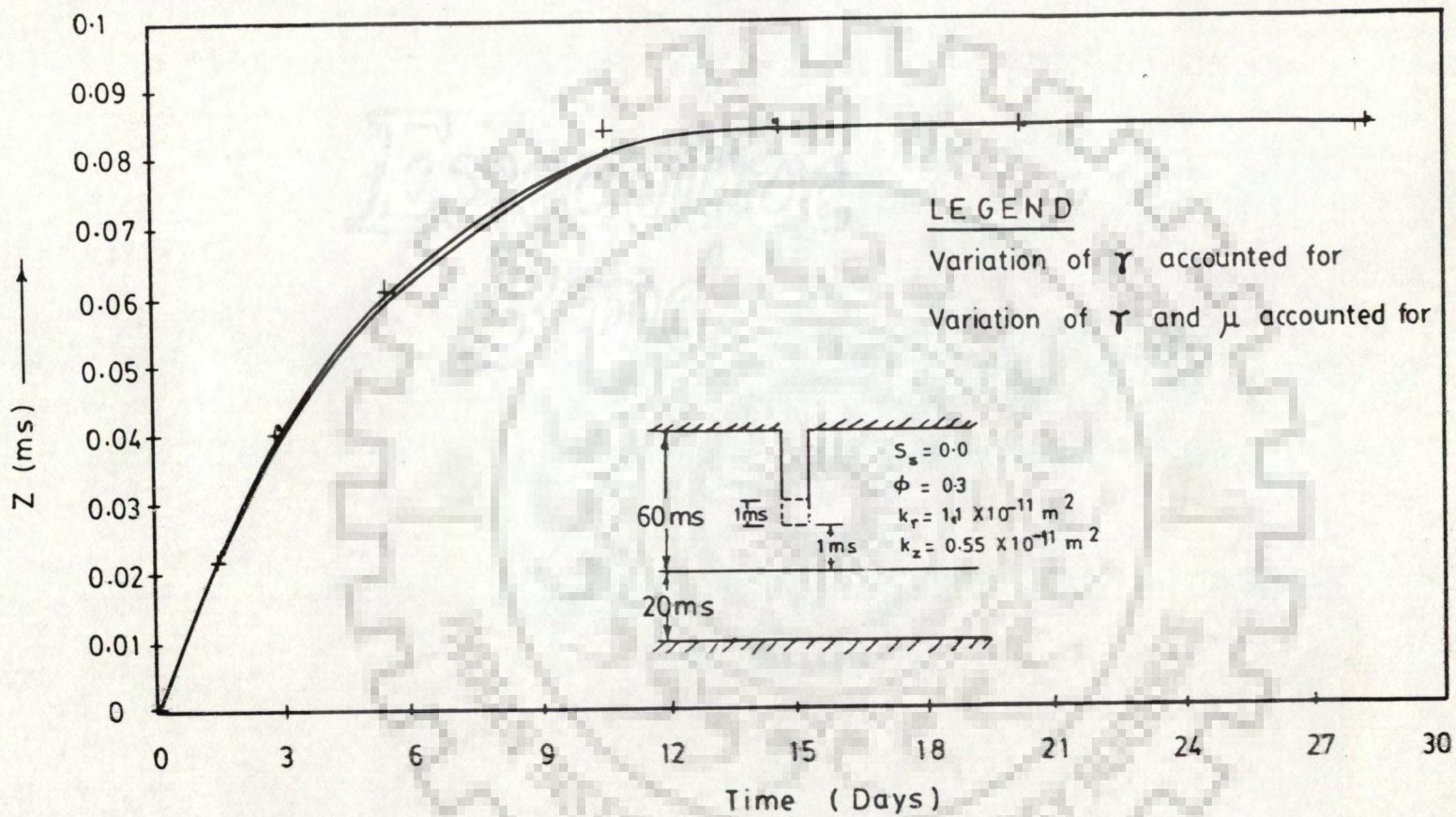


Fig (5.1a) Influence of Fluid Properties on Upcoming

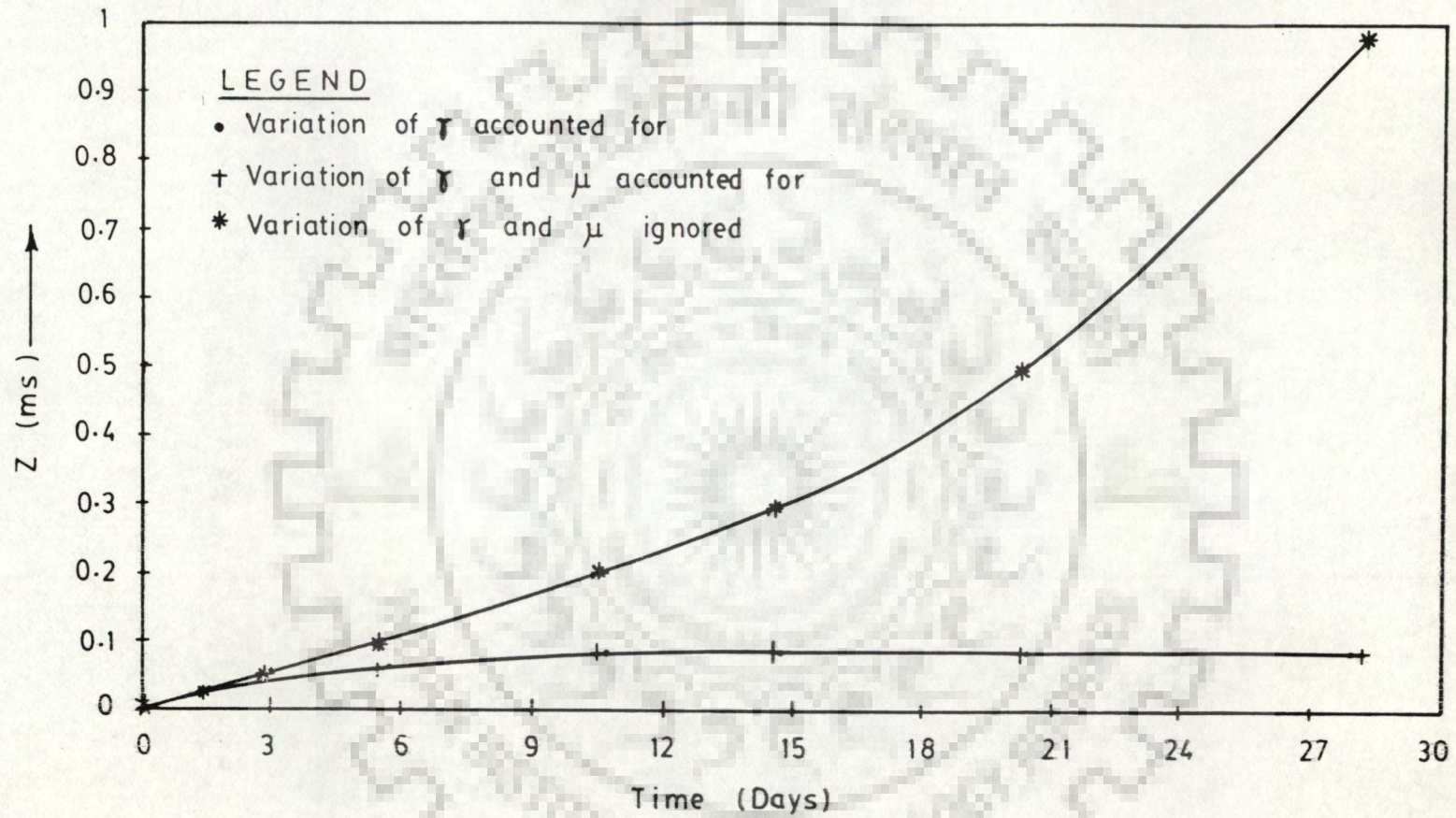


Fig. (5-1 b) Influence of Fluid Properties

to gross over - estimation of the upconing. On the other hand, the effect of dynamic viscosity changes is negligibly small (Fig.5.1a).

5.2 WELL DESIGN

5.2.1 Model Capability

The existing analytical solutions permit design of wells in coastal aquifers - only if the interface is to be kept much below the point of abstraction of water (i.e., $Z/D \leq 0.25$) and if many other restrictive assumptions [e.g., aquifer of infinitely large thickness, screen length tending to zero etc.(refer 4.1 Chap. IV)] are satisfied. On the other hand, the model is capable of yielding the well design without making these assumptions. Thus, the design is valid even for large upconing below a well of large screen length in a shallow aquifer. The design can include, among others, estimation of the permissible discharge and/or duration of pumping for restricting the saltwater concentration in the pumped water to a stipulated permissible limit. Further, the recovery 'rest period' between two successive spells of pumpage can also be estimated.

5.2.2 Design Parameters

A possible application of the proposed model in design of wells in coastal aquifers is illustrated for a hypothetical aquifer (refer Fig. 5.2). The permissible discharge, from a well tapping top 8 ms of the freshwater zone is estimated by the model. It is presumed that the well will be operated continuously for eight hours followed by sixteen hours of rest period. The model is operated to determine the permissible discharge meeting the following requirements.

i) The drawdown (SW), at the end of 8 hours of pumpage, does not

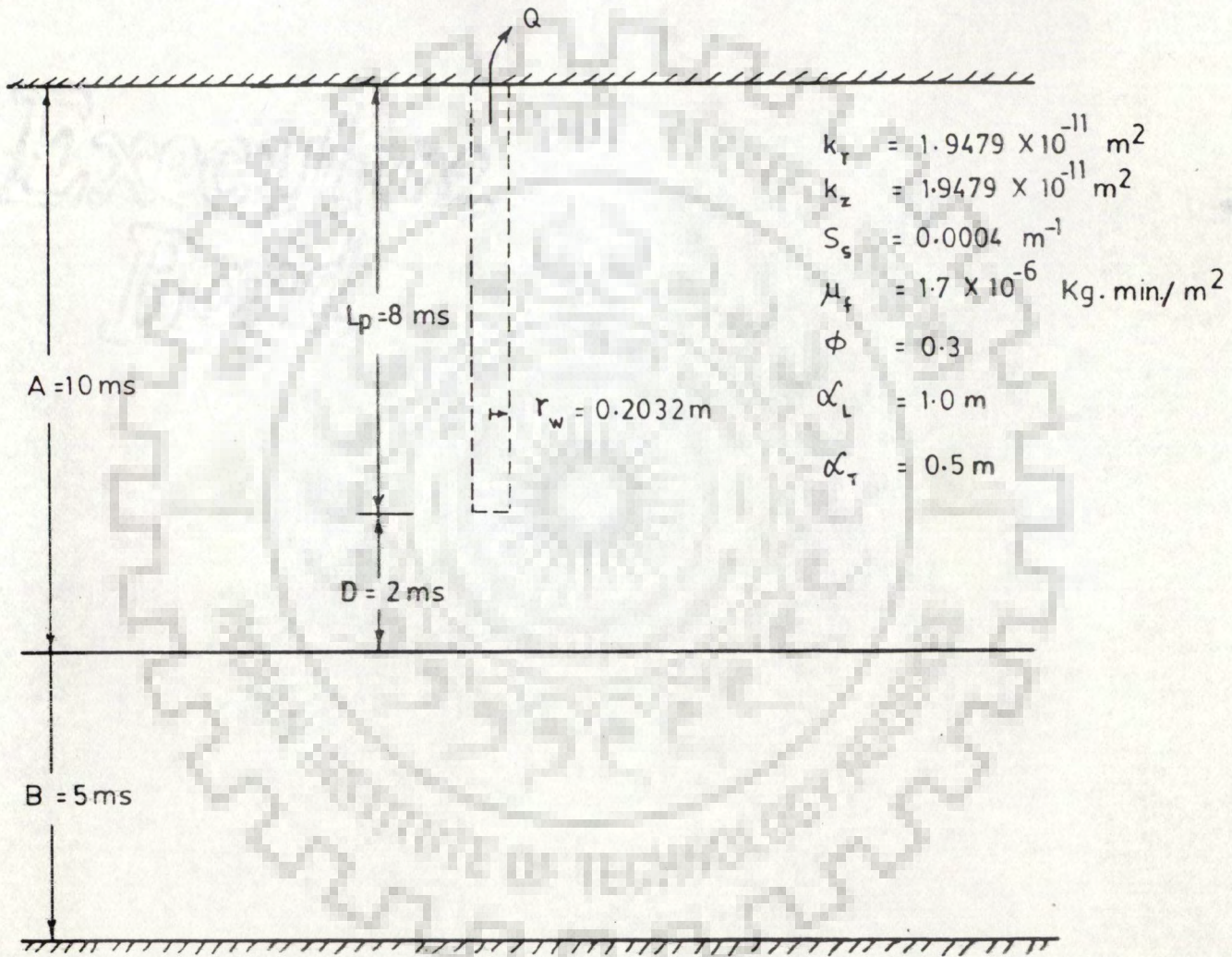


Fig. (5.2) Design of Discharge

exceed 16 ms;

ii) The saltwater concentration (CP) in the pumped water, at the end of 8 hours of pumpage, does not exceed 2%; and

iii) At least 90% of the saltwater lifted up from the interface, during 8 hours pumping, settles down in the following 16 hours of rest period.

5.2.3 Model Operation

5.2.3.1 Presssure Simulation

Radial Spacing: A 'no-drawdown boundary' was assumed to exist at a radial distance (r) of 298.3 ms. The radius of the pumped well is assumed to be 20.32 cm (8"). Thus, the space domain in radial direction extends from $r = 0.2032$ ms to 298.3 ms. This domain has been discretized by 20 pressure columns spaced in accordance with Rushton and Chan (1976) criteria (refer 3.3.5.1.4, Chap. III). The adopted radial spacings are given in table (5.1).

Vertical Spacing: In the vertical direction, the thickness of the confined aquifer was assumed to be 15 ms. Thus, the space domain in the vertical direction extends from $Z = 0$ (lower impervious layer) to 15 ms (upper impervious layer). This domain has been discretized by 17 rows. Low vertical spacing are assigned close to the interface. The adopted vertical spacing are given in table (5.2).

Time Domain: The time domain extending from $t = 0$ (beginning of the pumpage period) to $t = 24$ hours (end of rest period) has been discretized by 235 discrete times. The times till the closure of pumpage were chosen in accordance with Rushton and Chan (1976) criteria. During the subsequent recovery stage a constant time step (60 min.) was used. The range of time steps are given in table (5.3).

5.2.3.2 Simulation of Saltwater Transport

Radial Spacing: A 'no upconing' and 'zero salt water concentration' boundary has been assumed to occur at a distance of 11.60 ms from the center of the pumped well. Thus, the space domain in the radial direction extends from $r = 0.2032$ ms to 11.60 ms. This domain has been discretized by 19 columns spaced in accordance with the volume of take off point's criteria (refer 3.3.3.1.1.2, Chap. III). The adopted radial spacings are given in table (5.4).

Time Domain: The time steps for saltwater transport simulation were generated in accordance with equations 3.80 to 3.82(Chap. III), assigning the maximum permissible time step for the saltwater transport simulation (Δt_s^m) as 60 minutes. Thus, each pressure time step was subdivided into one or more (ξ) number of equal saltwater transport time steps of duration equal to or less than 60 minutes.

5.2.4 Model Results

The model was operated to estimate the drawdown and saltwater concentration in the pumped water at the end of 8 hours pumping. Subsequent to this pumping spell, the discharge is assigned a zero value and the model was operated for another sixteen hours. The convective saltwater settlement during this rest period was estimated. Thus, the convective saltwater settlement (η) during rest period, expressed as a fraction of the saltwater lifted during the pumping was computed as follows

$$\eta = \frac{VSL(24)}{V_c(8) - VS(8)} \quad \dots (5.3)$$

Where VSL(24) is the cumulative volume of saltwater settlement (to the

initial position of interface) at a time of 24 hours since the beginning of the pumpage (or at the end of 16 hours of rest period); $V_c(8)$ is the cumulative saltwater volume lifted during the pumping period due to convection; and $VS(8)$ is the cumulative saltwater entry into pumped water during the pumping period.

The time-variant saltwater concentration (CP_k) in pumped water at a discrete time t_k was obtained numerically from the model results as follows

$$CP_k = \frac{1}{Q} \frac{\Delta VS}{\Delta t} \quad (3.6)$$

$$= \frac{1}{Q} \frac{VS(8) - VS(6)}{8 - 6} \quad (3.7)$$

Where $V(6)$ is the cumulative saltwater volume entering into the pumped water during the pumping period 6 hours.

The average drawdown, corresponding to freshwater, in the well screen (SW_k), at discrete time t_k was estimated as follows

$$SW_k = \frac{\sum_{i=NRB}^{NRW} (p_{i,NC,k} - p_{i,1,k})}{(NRW - NRB - 1) \gamma_f} \quad (3.8)$$

The results are plotted in Figs (5.3) to (5.5). Fig.(5.3) indicates the influence of discharge on saltwater concentration in the pumped water .Fig. (5.4) indicates the influence of discharge on drawdown in the well . Fig. (5.5) indicates the influence of discharge on the percentage of saltwater settlement below initial position of the interface after the closure of pumpage.

Table (5.1) Radial Spacing for Pressure Simulation

S.No. of columns	Radial spacing ms	Cumulative distance ms	S.No. of columns	Radial spacing ms	Cumulative distance ms
1-2	0.10	0.30	11-12	4.41	13.81
2-3	0.14	0.44	12-13	6.51	20.32
3-4	0.20	0.64	13-14	9.51	29.83
4-5	0.30	0.94	14-15	13.95	43.78
5-6	0.45	1.39	15-16	20.48	64.26
6-7	0.64	2.03	16-17	30.06	94.32
7-8	0.95	2.98	17-18	44.12	138.44
8-9	1.40	4.38	18-19	64.76	203.20
9-10	2.01	6.39	19-20	95.10	298.30
10-11	3.01	9.40			

Table (5.2) Vertical Spacing

S.No. of rows	Vertical spacing ms	Cumulative distance ms	S.No. of rows	Vertical spacing ms	Cumulative distance ms
1-2	1.4	1.4	9-10	0.6	8.9
2-3	1.3	2.7	10-11	0.5	9.4
3-4	1.2	3.9	11-12	0.4	9.8
4-5	1.1	5.0	12-13	0.4	10.2
5-6	1.0	6.0	13-14	0.7	10.9
6-7	0.9	6.9	14-15	1.0	11.9
7-8	0.8	7.7	15-16	1.4	13.3
8-9	0.6	8.3	16-17	1.7	15.0

Table (5.3) Time Steps For Pressure Simulation

Range	S.No. of steps	Range	S.No. of steps
$0 < \Delta t \leq 10^{-4}$	1-35	$10^{-1} < \Delta t \leq 1$	200-201
$10^{-4} < \Delta t \leq 10^{-3}$	36-106	$1 < \Delta t \leq 10$	202-208
$10^{-3} < \Delta t \leq 10^{-2}$	107-158	$10 < \Delta t \leq 100$	209-235
$10^{-2} < \Delta t \leq 10^{-1}$	159-199		

Table (5.4) Radial Spacing for Saltwater Simulation

S.No. of Columns	Radial spacing ms	Cumulative distance ms	S.No. of columns	Radial spacing ms	Cumulative distance ms
Well-1	1.81	1.81	10-11	0.43	8.73
1-2	1.48	3.29	11-12	0.41	9.14
2-3	0.96	4.25	12-13	0.39	9.53
3-4	0.78	5.03	13-14	0.37	9.90
4-5	0.68	5.71	14-15	0.36	10.26
5-6	0.60	6.31	15-16	0.35	10.61
6-7	0.55	6.86	16-17	0.34	10.95
7-8	0.51	7.37	17-18	0.33	11.28
8-9	0.48	7.85	18-19	0.32	11.60
9-10	0.45	8.30			

From curve (5.3), the value of discharge (Q_1) corresponding to the permissible value of saltwater concentration in the pumped well (CP = 2%) is $11.3 \text{ m}^3/\text{hr}$.

From curve (5.4), the value of discharge (Q_2) corresponding to the permissible value of drawdown in the pumped well (SW = 16ms) is $84 \text{ m}^3/\text{hr}$.

From curve (5.5), the value of discharge (Q_3)

corresponding to the percentage of saltwater settlement below the initial position of the interface after the closure of the pumpage ($\eta=90\%$) is $7\text{m}^3/\text{hr}$.

The value of permissible discharge (Q_d), which takes into account the permissible values of CP; η and SW, is thus, $7\text{m}^3/\text{hr}$ (minimum of Q_1 , Q_2 and Q_3).



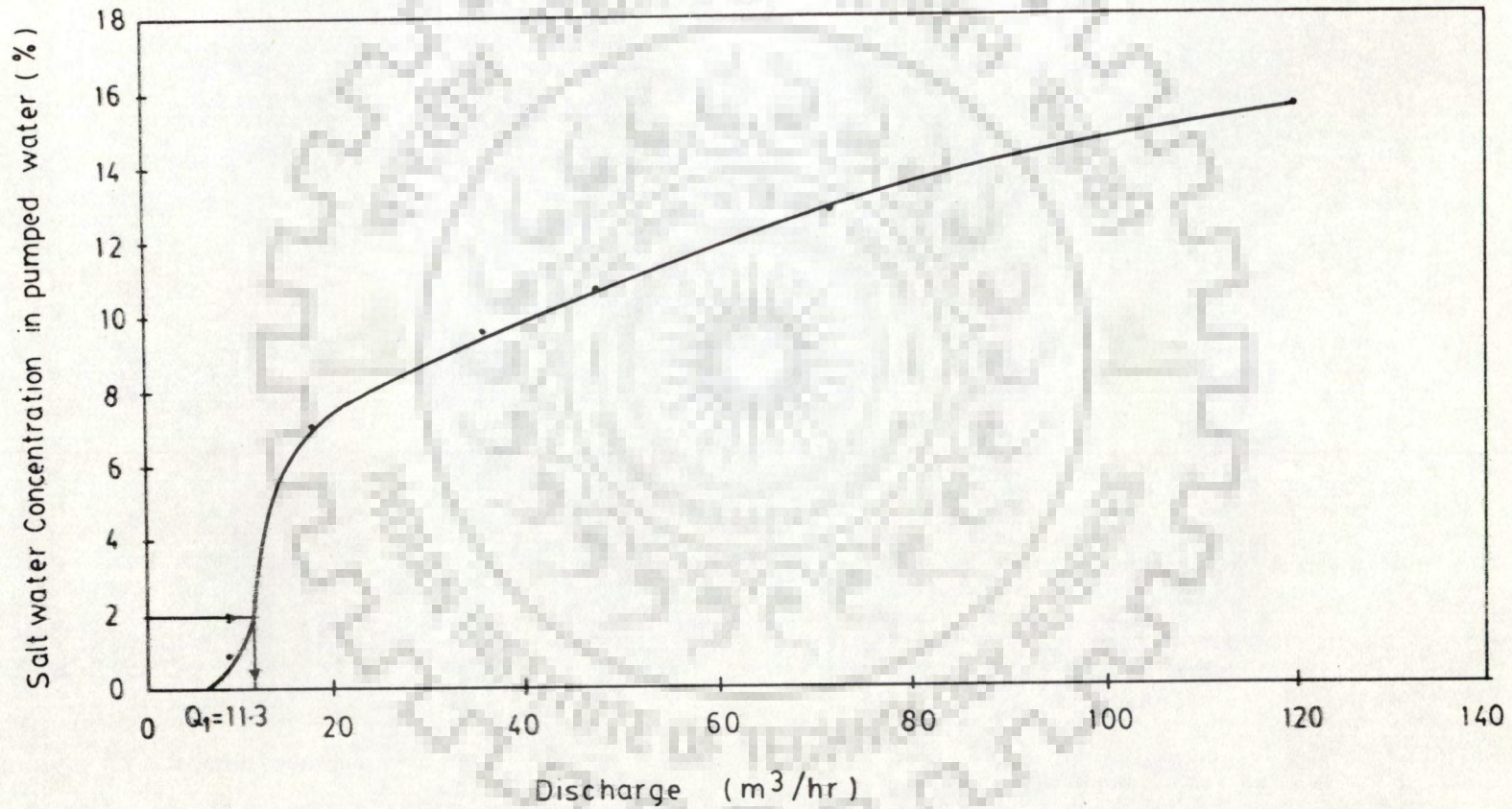


Fig (5.3) Salt water Concentration in Pumped Water Vs Discharge

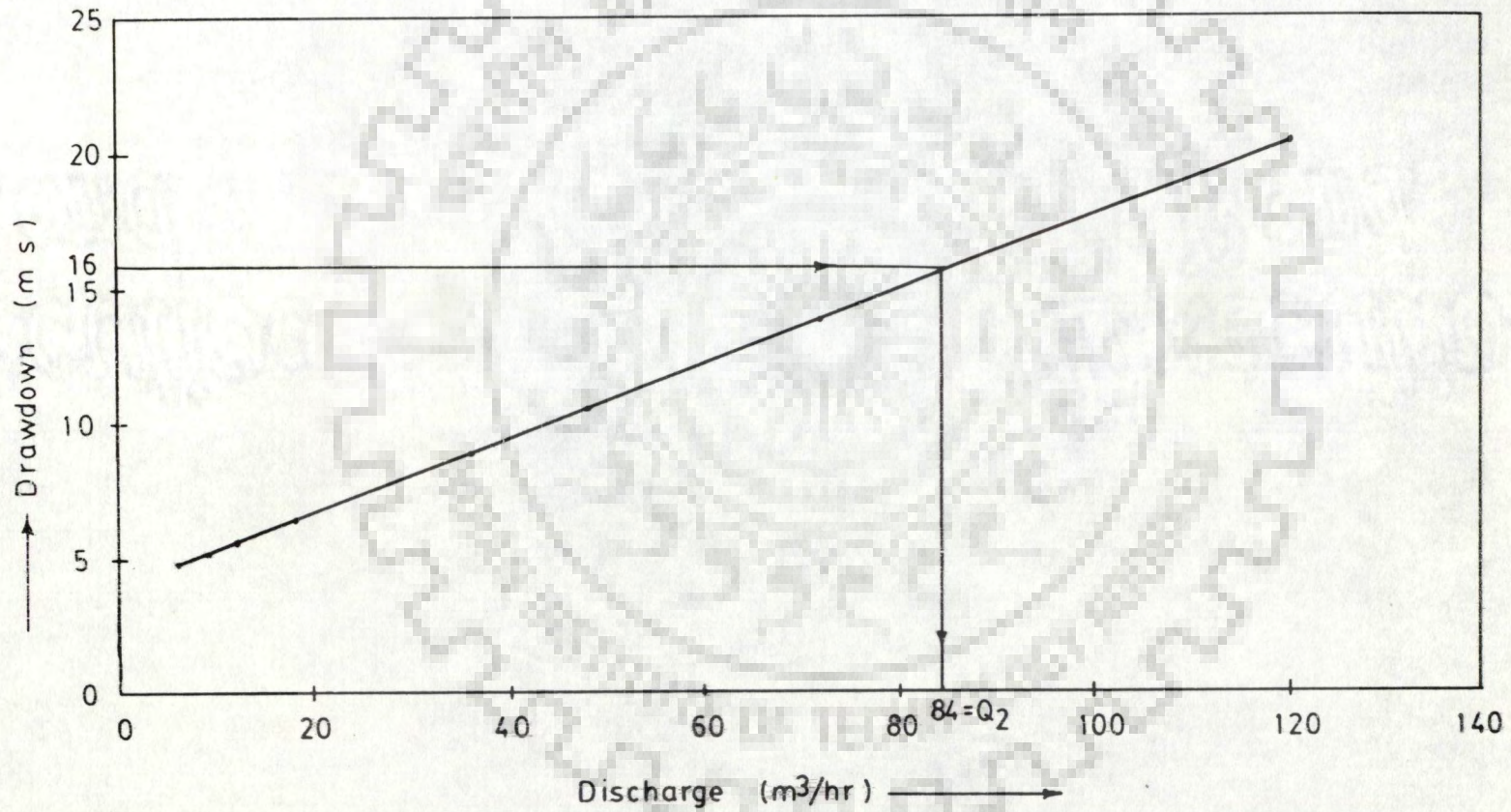


Fig. (5.4) Drawdown in Pumped Well Vs Discharge

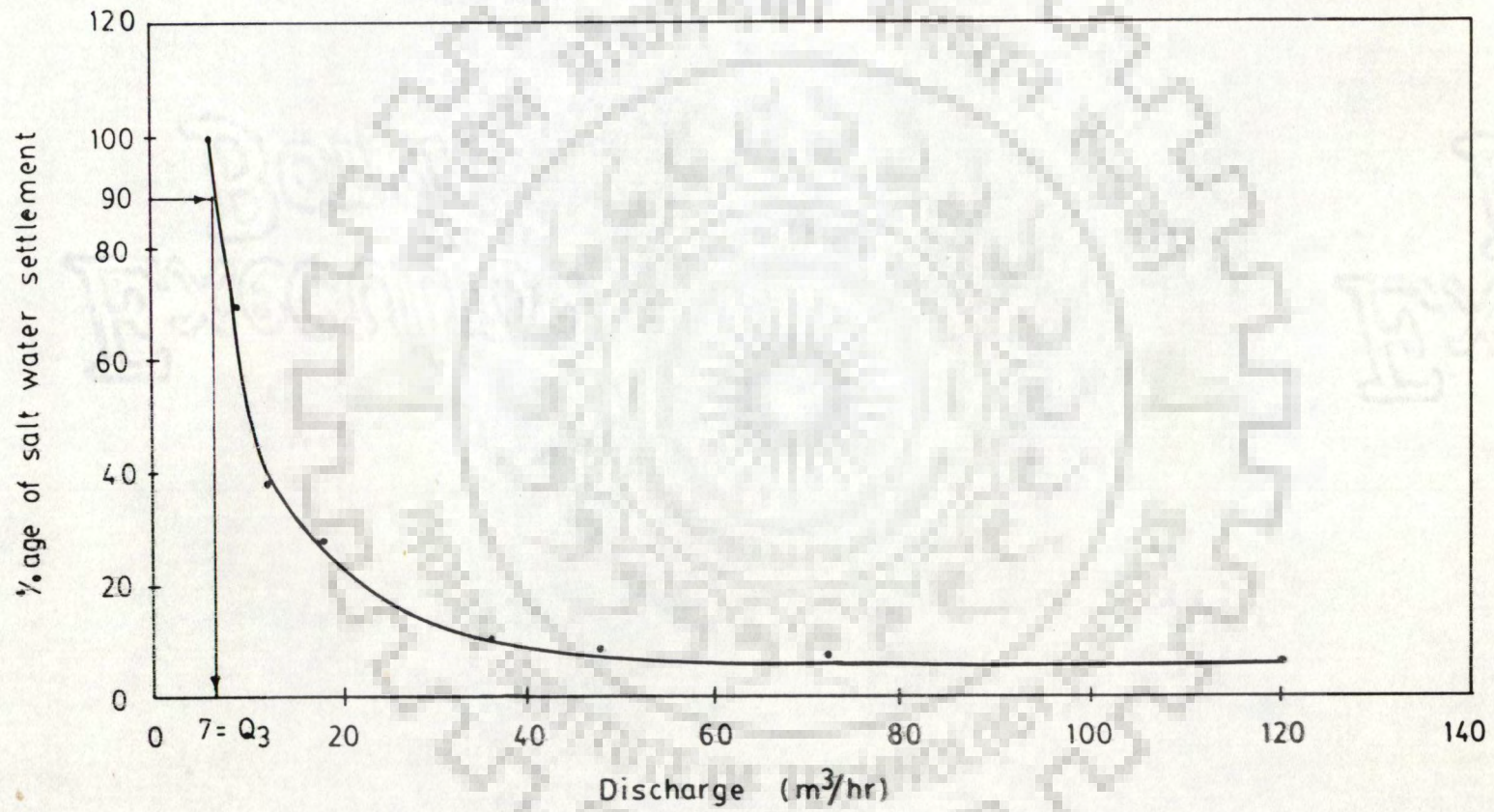


Fig. (5.5) Salt water Settlement Vs Discharge

CHAPTER VI

CONCLUSION

A numerical model has been developed for simulation of saltwater transport induced by pumpage from a well tapping only the upper fresh water zone and underlain by saltwater. The model accounts for both convective and diffusive transports. The convective transport is computed by the method of characteristics, and the diffusive transport by finite differences. The velocity distribution, necessary for the estimation of convective transport, is arrived at by calculating the pressure distribution employing finite differences. While calculating the pressure distribution, the variation of the specific weight and dynamic viscosity of the fluid (due to time and space variation of saltwater concentration) is accounted for. The prominent conclusions of the study are as follows.

- 1) The model, based on a numerical solution, eliminates many of the restrictive assumptions involved in the available analytical solutions. The analytical solutions permit estimation of only the convective upconing below a point sink/horizontal drain (and not a well) in an incompressible aquifer (i.e., specific storage = 0) provided the upconing does not exceed a threshold fraction of the initial cushion (initial cushion: the vertical distance between the initial position of the interface and the bottom of the well). The threshold fraction varies between 0.25 to 0.5.
- 2) The model is capable of simulating the upwards saltwater transport and its entry into the well during the pumping; and its

settlement subsequent to the closure of pumping. Thus, the model can be employed to determine the permissible discharge and pumping schedules for wells underlain by saltwater.

- 3) The model results as well as the analytical solution of Bear and Dagan (Schmorak and Mercado, 1969) have been compared with field data, from Ashqelon region-Isreal, reported by Schmorak and Mercado (1969). They conducted two sets of experiments termed as test A (average pumping rate = $575 \text{ m}^3/\text{day}$ and pumping period = 65 days) and test B (average pumping rate = $350 \text{ m}^3/\text{day}$ and pumping period = 84 days). Water was pumped from a 40.64 cm diameter and 16.1 ms deep well. Screen was provided in the bottom 1.3 meters of the well. The saltwater occurred in the bottom 37.9 ms of the total saturated thickness of 69.5 ms. This provided an initial cushion of 15.5 m . Samples were taken at different depths from 4 observation wells , each having a diameter of 20.32 cm and located at distance of 4.5, 12.4, 16.7 and 33.9 ms from the pumped well.

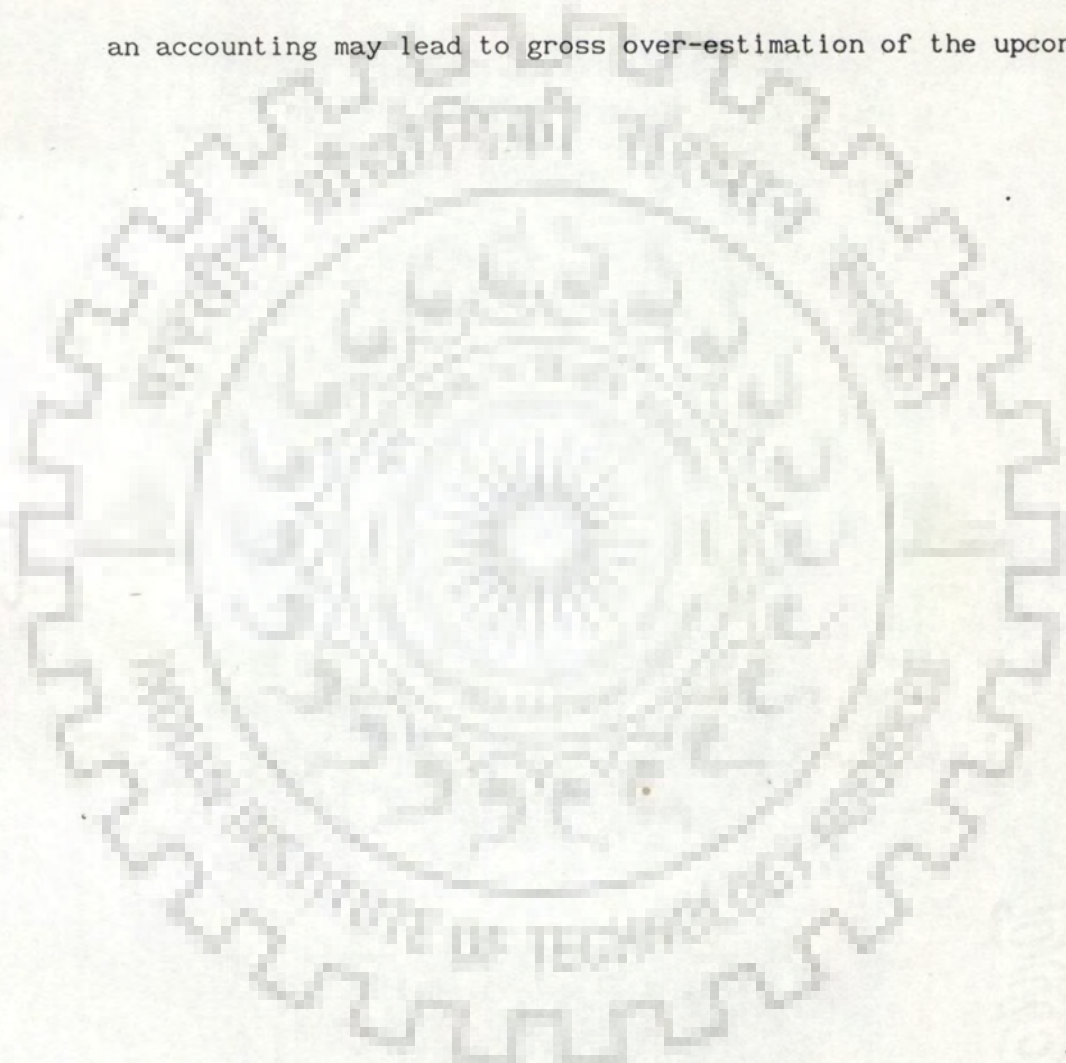
The comparison reveals that

- i) Analytical solution of Bear and Dagan (Schmorak and Mercado, 1969) tends to under estimate the upconing in case it exceeds twenty five percent of the initial cushion. However, the proposed model permits estimation of the upconing quite well even beyond this limit.
- ii) The proposed model permits estimation of the time - variant position of the interface quite well.
- iii) The model permits estimation of the time-variant saltwater concentration in the pumped water. The model results match fairly well with the field data.

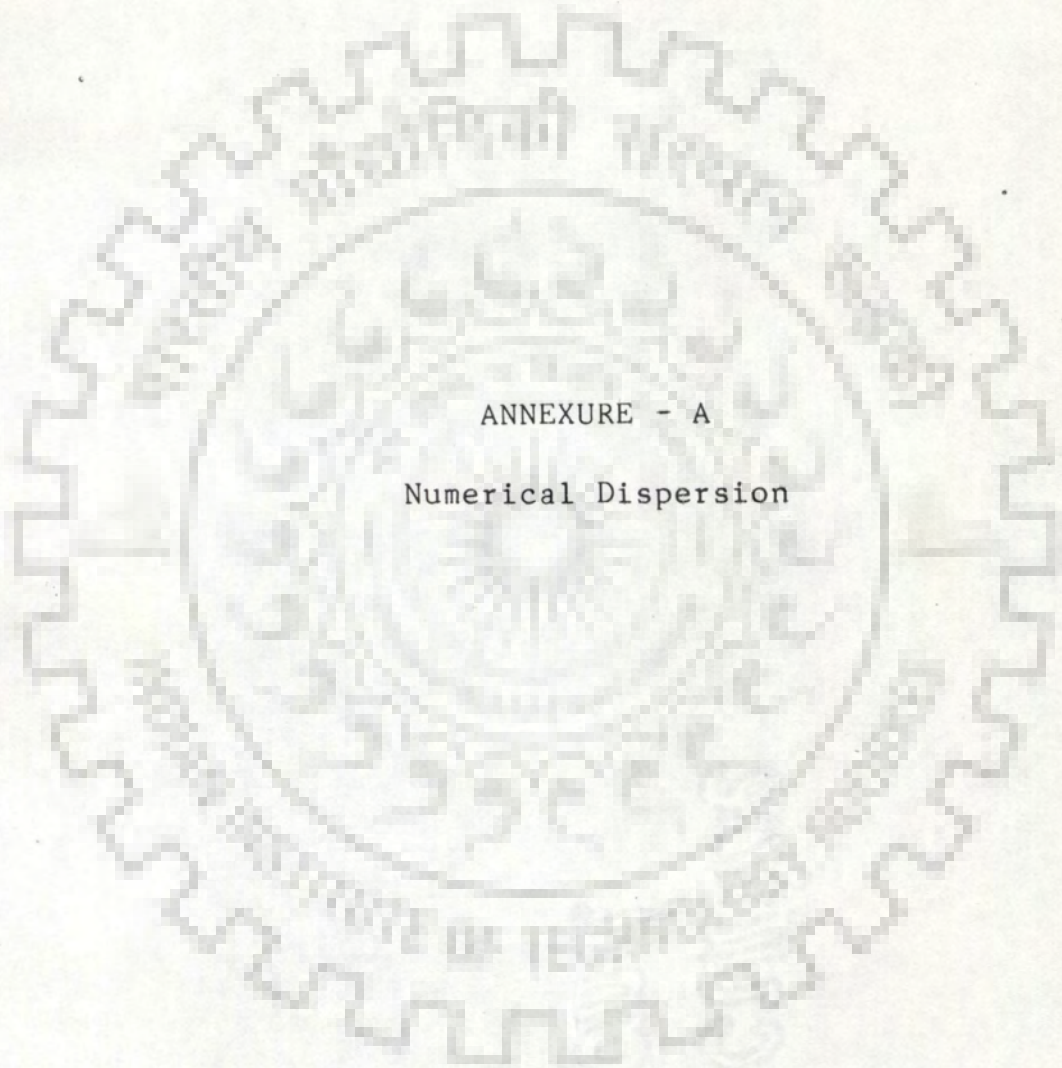
- 4) The upconed position of the interface , as computed by the proposed model, was found to converge to the analytical solution of Bear and Dagan (Schmorak and Mercado, 1969) as the ideal conditions (assumed in the analytical solution) are approached. However, under non-ideal conditions , the numerical solution varies significantly from the analytical solution. The details are as follows
- i) The analytical solution is based upon the assumption of screen length tending to zero (point sink). The study has revealed that an indiscriminate use of this solution ,even for wells having substantial screen lengths ,leads to an over estimation of the upconing. For example, the analytical solution is found to over estimate the upconing at 405 min. by as much as 51%, when the screen length is 15% of the initial freshwater thickness.
 - ii) The analytical solution is based upon the assumption of large depth of saltwater thickness (in comparison with the initial cushion). The study has revealed that an indiscriminate use of this solution ,even for shallow saltwater depths, leads to an over estimation of the upconing. For example, the analytical solution is found to over estimate the upconing at 405 min. by as much as 49.38%, when the initial saltwater thickness is 30% of the initial cushion.
 - iii) The analytical solution is based upon the assumption of the upconing not exceeding twenty five percent of the initial cushion. The study has revealed that an indiscriminate use of this solution, even for large upconing, leads to under estimation of the upconing. For example, the analytical

solution is found to under estimate the upconing at 405 min. by as much as 129%, when the upconing is 90% of the initial cushion.

- 5) The variation of the fluid properties, due to time and space variation of saltwater concentration, needs to be accounted for in the computation of pressure / velocity distribution. A lack of such an accounting may lead to gross over-estimation of the upconing.



APR 19 2014



ANNEXURE - A

Numerical Dispersion

APR 19 2014

NUMERICAL DISPERSION

The numerical dispersion occurs in equation (A-1) due to the approximation of the first order derivatives ($\frac{\partial C}{\partial r}$ or $\frac{\partial C}{\partial z}$ or $\frac{\partial C}{\partial t}$) by neglecting the term proportional to the second order derivative.

$$\frac{D_r}{r} \frac{\partial}{\partial r} \left(r \frac{\partial C}{\partial r} \right) + D_z \frac{\partial^2 C}{\partial z^2} - \frac{q_r}{\phi} \frac{\partial C}{\partial r} - \frac{q_z}{\phi} \frac{\partial C}{\partial z} = \frac{\partial C}{\partial t} \quad \dots (A-1)$$

For $\frac{\partial C}{\partial z}$ the numerical dispersion can be estimated as follows

$$\left(\frac{\partial C}{\partial z} \right)_i = \frac{C_i - C_{i-1}}{\Delta z} \quad \text{backward difference} \quad \dots (A-2)$$

Substituting equation (A-2) into equation (A-1),

$$\frac{D_r}{r} \frac{\partial}{\partial r} \left(r \frac{\partial C}{\partial r} \right) + D_z \frac{\partial^2 C}{\partial z^2} - \frac{q_r}{\phi} \frac{\partial C}{\partial r} - \frac{q_z}{\phi} \left(\frac{C_i - C_{i-1}}{\Delta z} \right) = \frac{\partial C}{\partial t} \quad (A-3)$$

Taylor's series about z in the positive direction can be written as

$$C(z - \Delta z) = C(z) - \Delta z \frac{dC}{dz} + \frac{(\Delta z)^2}{2!} \frac{d^2 C}{dz^2} - \frac{(\Delta z)^3}{3!} \frac{d^3 C}{dz^3} + \dots$$

$$\frac{dC}{dz} = \frac{C(z) - C(z - \Delta z)}{\Delta z} + \frac{\Delta z}{2!} \frac{d^2 C}{dz^2} \quad \left| \begin{array}{l} \dots \\ \text{truncate} \end{array} \right.$$

$$\frac{C(z) - C(z - \Delta z)}{\Delta z} = \frac{dC}{dz} - \frac{\Delta z}{2!} \frac{d^2 C}{dz^2} \quad (A-4)$$

Substituting equation (A-4) into equation (A-3)

$$\frac{D_r}{r} \frac{\partial}{\partial r} \left(r \frac{\partial C}{\partial r} \right) + D_z \frac{\partial^2 C}{\partial z^2} - \frac{q_r}{\phi} \frac{\partial C}{\partial r} - \frac{q_z}{\phi} \left(\frac{\partial C}{\partial z} - \frac{\Delta z}{2} \frac{\partial^2 C}{\partial z^2} \right) = \frac{\partial C}{\partial t}$$

$$\frac{D_r}{r} \frac{\partial}{\partial r} \left(r \frac{\partial C}{\partial r} \right) + \frac{\partial^2 C}{\partial z^2} \left(D_z + \frac{q_z \Delta z}{2} \right) - \frac{q_r}{\phi} \frac{\partial C}{\partial r} - \frac{q_z}{\phi} \frac{\partial C}{\partial z} = \frac{\partial C}{\partial t} \quad (A-5)$$

By comparing equation (A-5) with equation (A-1), equation (A-5) increases dispersion by $\left(\frac{q_z \Delta z}{2\phi} \right)$. This quantity is called **numerical dispersion**.

Similarly in radial direction, the numerical dispersion is $\left(-\frac{D_r \Delta r}{2r} + \frac{q_r \Delta r}{2\phi} \right)$.

For $\frac{\partial C}{\partial t}$, the numerical dispersion can be estimated as follows

$$\frac{\partial C}{\partial t} = \frac{C^{k+1} - C^k}{\Delta t} = \frac{D_r}{r} \frac{\partial}{\partial r} \left(r \frac{\partial C}{\partial r} \right) + D_z \frac{\partial^2 C}{\partial z^2} - \frac{q_r}{\phi} \frac{\partial C}{\partial r} - \frac{q_z}{\phi} \frac{\partial C}{\partial z} \quad \dots (A-6)$$

$$C^{k+1} = C^k + \left(\frac{\partial C}{\partial t} \right)_k \Delta t + \left(\frac{\partial^2 C}{\partial t^2} \right)_k \frac{\Delta t^2}{2!} + \dots \quad \dots (A-7)$$

$$\frac{C^{k+1} - C^k}{\Delta t} = \frac{\partial C}{\partial t} + \left(\frac{\partial^2 C}{\partial t^2} \right) \frac{\Delta t}{2} \quad \dots (A-8)$$

Obtain $\frac{\partial^2 C}{\partial t^2}$ in terms of $\frac{\partial^2 C}{\partial z^2}$ from equation (A-1).

Take $\frac{\partial}{\partial t}$ of equation (A-6)

$$\frac{\partial^2 C}{\partial t^2} = - \frac{q_z}{\phi} \frac{\partial}{\partial t} \left(\frac{\partial C}{\partial z} \right) \quad \dots (A-9)$$

Take $\frac{\partial}{\partial z}$ of equation (A-6)

$$\frac{\partial}{\partial z} \left(\frac{\partial C}{\partial t} \right) = - \frac{q_z}{\phi} \frac{\partial^2 C}{\partial z^2} \quad \dots (A-10)$$

Multiply (A-10) by $-\frac{q_z}{\phi}$

$$-\frac{q_z}{\phi} \frac{\partial}{\partial t} \left(\frac{\partial C}{\partial z} \right) = + \frac{q_z^2}{\phi^2} \frac{\partial^2 C}{\partial z^2} \dots\dots\dots (A-11)$$

From equations (A-9) and (A-11)

$$\frac{\partial^2 C}{\partial t^2} = \frac{q_z^2}{\phi^2} \frac{\partial^2 C}{\partial z^2} \dots\dots\dots (A-12)$$

Substituting equation (A-12) into equation (A-8),

$$\frac{C^{k+1} - C^k}{\Delta t} = \frac{\partial C}{\partial t} + \frac{q_z^2}{\phi^2} \left(\frac{\partial^2 C}{\partial z^2} \right) \frac{\Delta t}{2} \dots\dots\dots (A-13)$$

Substituting equation (A-13) into equation (A-6)

$$\frac{\partial C}{\partial t} = \frac{D_r}{r} \frac{\partial}{\partial r} \left(r \frac{\partial C}{\partial r} \right) + \left(D_z - \frac{q_z^2}{\phi^2} \frac{\Delta t}{2} \right) \frac{\partial^2 C}{\partial z^2} - \frac{q_r}{\phi} \frac{\partial C}{\partial r} - \frac{q_z}{\phi} \frac{\partial C}{\partial z} \dots\dots\dots (A-14)$$

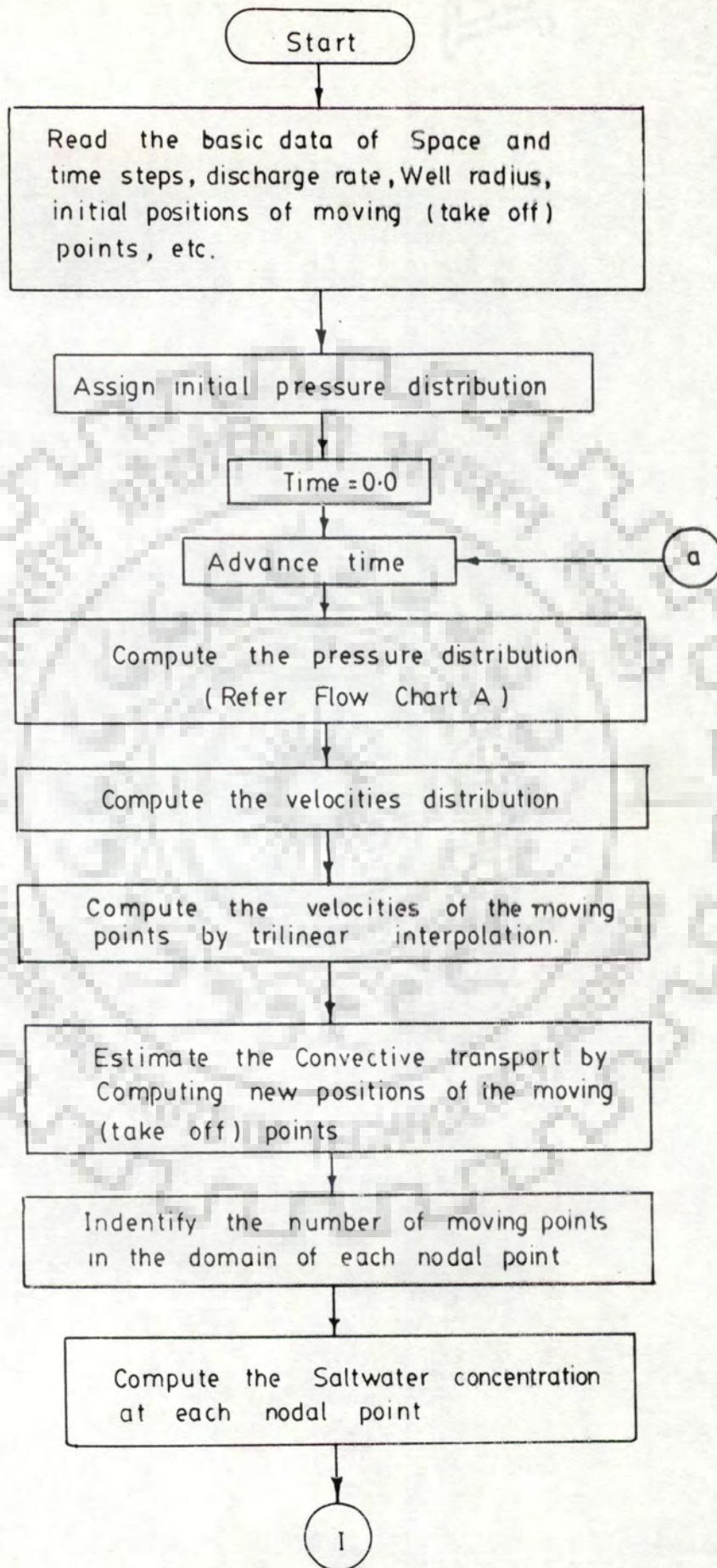
Comparing equation (A-14) with equation (A-6), the numerical dispersion

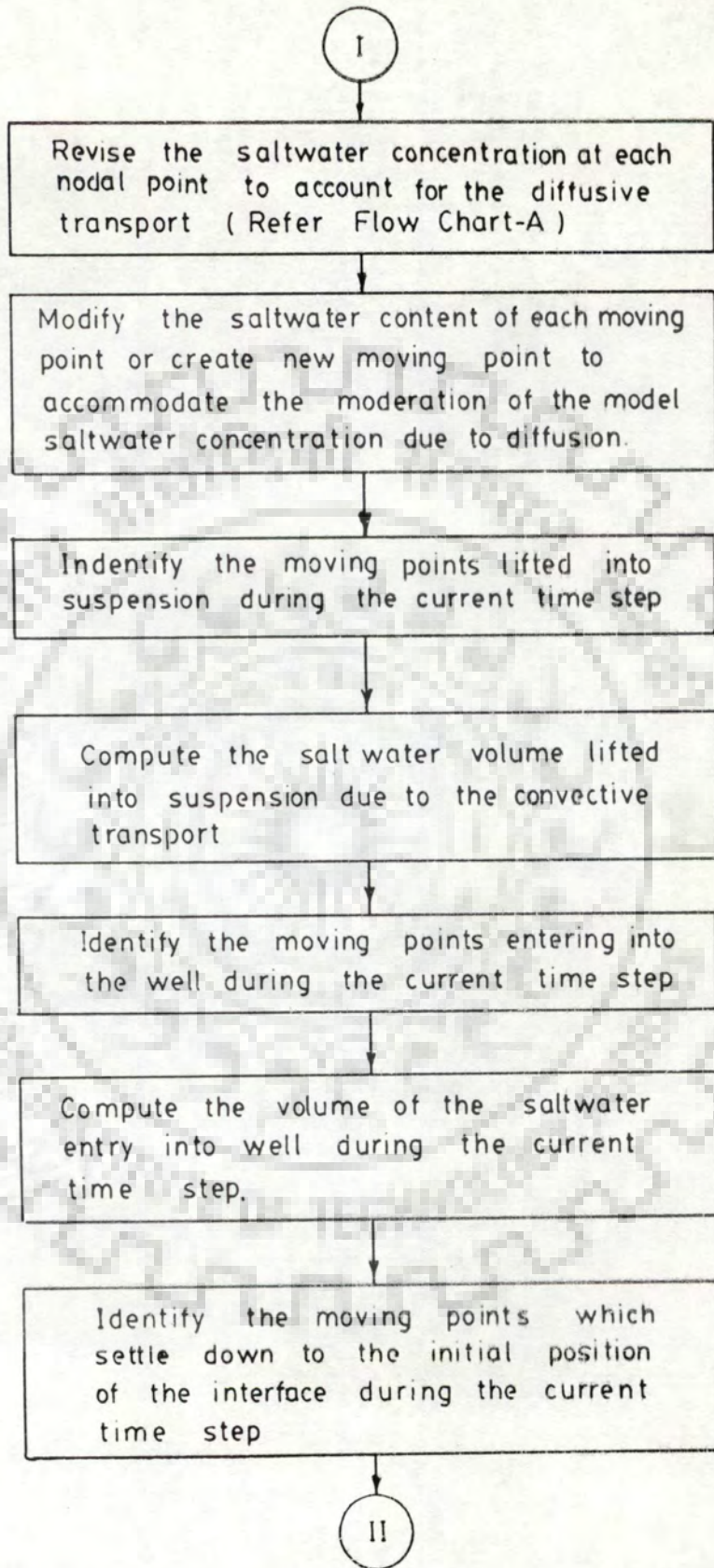
is $\left(-\frac{q_z^2 \Delta t}{2 \phi^2} \right)$.



ANNEXURE - B

Computer Code





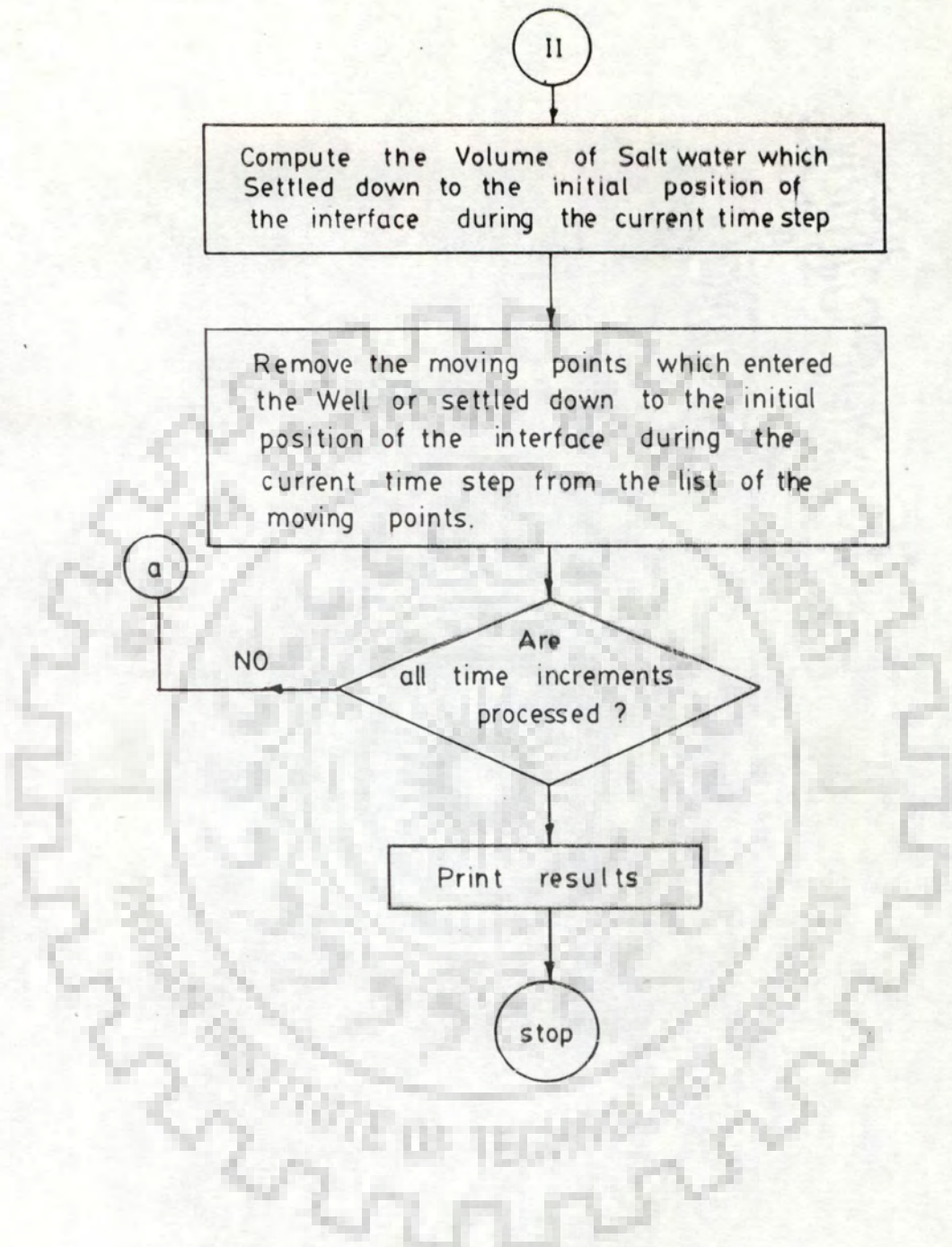
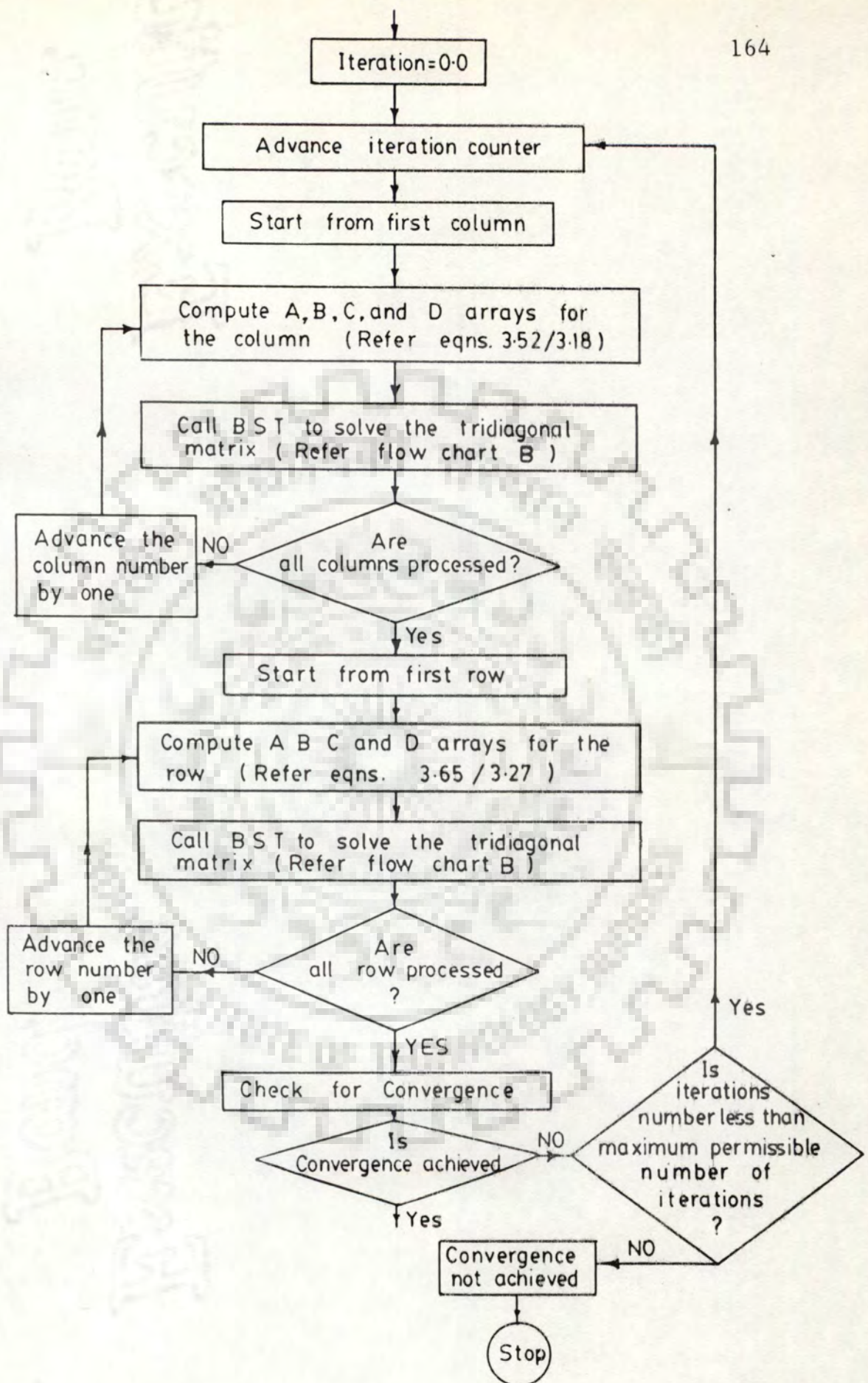
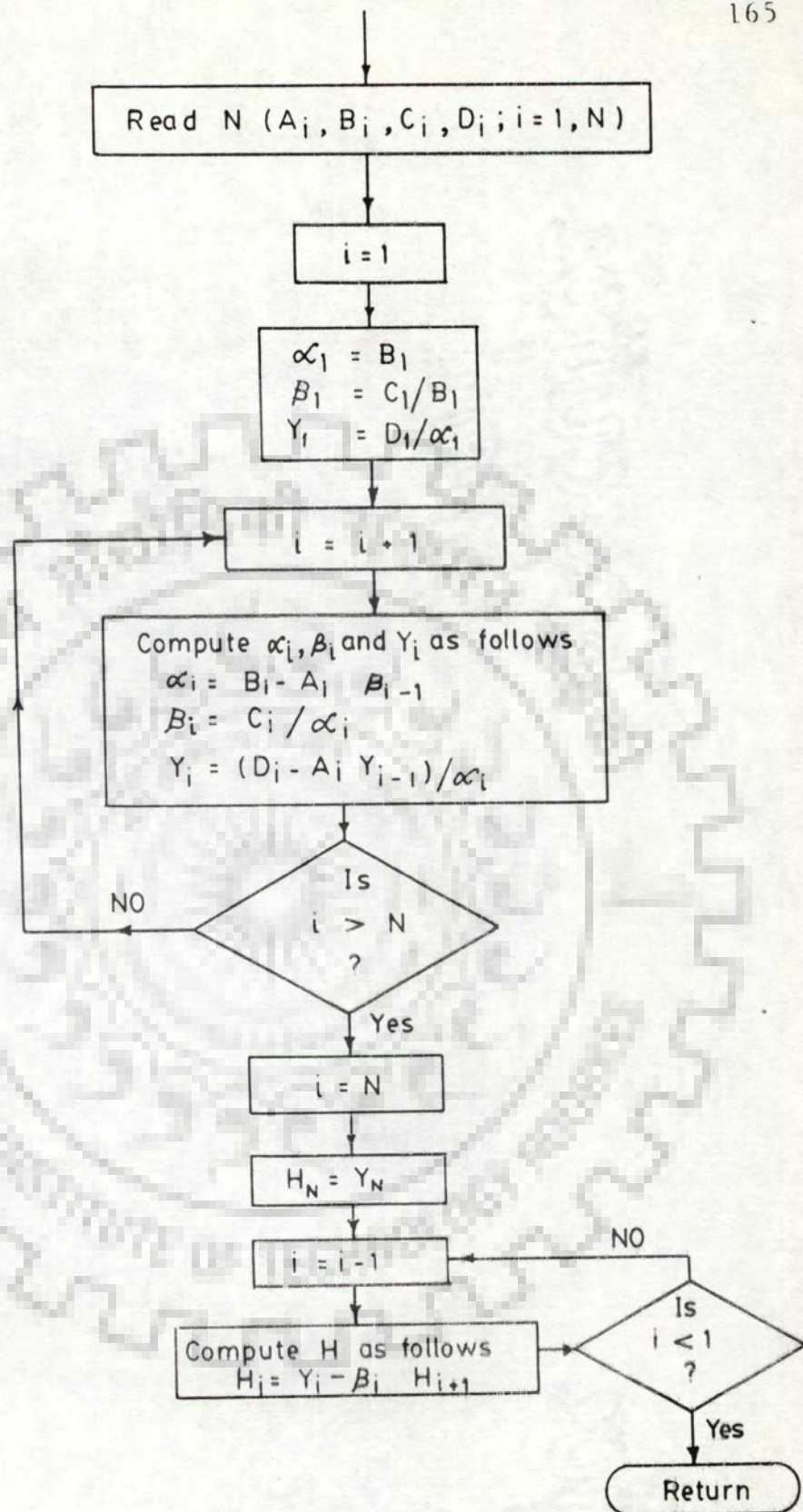


Fig. (B-1) General Flow Chart for Simulation of Salt Water Movement.



Fig(B-2) General flow Chart -A

To Compute Pressure Distribution / Diffusive Transport



Fig(B-3) General Flow Chart (B) to Solve the Tridiagonal Matrix : Subroutine BST

\$LARGE

```

C      PROGRAM M.FOR<DISSERTATION WORK BY M-E-E-SHALABY>
C*****
C      SIMULATIN PROGRAMME FOR SALTWATER TRANSPORT
C-----
C      DEFINITION OF VARIABLES
C-----
C      P(I,J)-----PRESSURE AT NODE(I,J)
C      NR-----NO. OF ROWS
C      NC-----NO. OF COLUMNS
C      NT1-----INITIAL TIME STEP
C      NT2-----FINAL TIME STEP
C      XS(J)-----RADIAL COORDINATES OF (J)TH TAKE OFF POINT
C      XF(J)-----RADIAL COORDINATES OF NOD (I,J)
C      YF(I)-----VERTICAL COORDINATES OF NODE (I,J)
C      IX-----IX=0: READ INITIAL DATA
C              IX=1: READ DATA FROM M2.DAT
C      IQ-----IQ=0: CONSTANT DISCHARGE
C              IQ=1: CONSTANT HEAD
C      IC-----IC=0: WELL HAVE FULL SCREEN
C              IC=1 WELL HAVE PARTIAL SCREEN
C      IN(J)-----INDEX NUMBER OF THE MOVING POINTS
C      NRW-----NO. OF ROWS UP TO THE WELL BOTTOM
C      NRB-----NO. OF ROWS UP TO THE BOTTOM OF BLIND PIPE
C      NRS-----NO. ROWS UP TO SALTWATER-FRESHWATER THE INTERFACE
C      VLL(J)-----VOLUME OF THE (K) MOVING POINT
C      VSP-----CUMULATIVE SALTWATER VOLUME LIFTED INTO SUSPENSION
C      TM-----CUMULATIVE TIME
C      VOL-----VOLUME OF TAKE OFF POINT/POROSITY OF AQUIFER
C      VL(J)-----VOLUME OF (J) TAKE OFF POINT
C      VIS(I,J)---DYNAMIC VISCOSITY AT PRESSURE NODE (I,J)
C      VISF-----DYNAMIC VISCOSITY OF FRESH WATER
C      SM-----SUM OF THE MODULI OF CHANGE IN PRESSURE IN THE
C              CURRENT ITERATION
C      KOUNT-----MAXIMUM PERMISSIBLE NUMBER OF ITERATIONS FOR
C              PRSSURE SIMULATION
C      KOUNT1-----MAXIMUM PERMISSIBLE NUMBER OF ITERATIONS FOR
C              SALTWATER SIMULATION
C      STL-----DESIRED CONVERGENCE OF PRESSURE SIMULATION
C      STLS-----DESIRED CONVERGENCE OF SALTWATER SIMULATION
C      X(K)-----RADIAL COORDINATE OF K(TH) MOVING POINT
C      Y(K)-----VERTICAL COORDINATE OF K(TH) MOVING POINT ABOVE DATUME
C      QQ-----CONSTANT DISCHARGE RATE(CUM/MIN)
C      UM(K)-----REDIAL VELOCITY OF K(TH) MOVING POINT
C      VM(K)-----VERTICAL VELOCITY OF K(TH) MOVING POINT
C      NTP-----NUMBER OF MOVING POINTS
C      YL(J)-----VERTICAL TRANSPORT OF (J)TH TAKE OFF POINT
C      CSP-----CUMULATIVE SALTWATER ENTRY INTO PUMPED WELL
C      VSD-----CUMULATIVE SALTWATER SETTLEMENT DOWN BELOW INTERFACE
C      RW-----RADIUS OF WELL(M)
C      DT(IPD)----TIME STEP FOR PRESSURE SIMULATION
C      IE-----NUMBER OF POINTS EXITING FROM INTERFACE
C      ITO-----NUMBER OF MOVING POINTS ENTERING INTO THE PUMED WELL
C      NCS-----NUMBER OF COLUMNS FOR SALTWATER SIMULATION
C      IS-----NUMBER OF STEPS
C      PPM(I,J)---PRESSURE AT PERVIOUS TIME STEP AT PRESSURE NODE (I,J)
C      DZ(I)-----VERTICAL GRID SPACING BETWEEN NODE (I,J) AND
C              NODE(I+1,J)
C      PHI-----POROSITY OF THE AQUIFER
C      DR(J)-----RADIAL GRID SPACING BETWEEN PRESSURE NODE (I,J) AND
C              PRESSURE NODE(I,J+1) FOR PRESSURE SIMULATION

```

```

C      DRS(J)-----RADIAL GRID SPACING BETWEEN NODE (I,J) AND
C      NODE(I,J+1) FOR SALTWATER SIMULATION
C      NNA(I,J)---NUMBER OF MOVING POINTS IN THE DOMAIN OF NODE(I,J)
C      VLX-----VOLUME OF WATER IN THE DOMAIN OF NODE(I,J)
C      GM(I,J)----SPECIFIC WEIGHT AT PRESSURE NODE (I,J)
C      AKR(I,J)---REDIAL INTRINSIC PERMEABILITY
C      AKZ(I,J)---VERTICAL INTRINSIC PERMEABILITY
C      SS(I,J)----SPECIFIC STORAGE
C      A,B,C,D----COEFFCIENTS IN WATER BALANCE EQUATION
C      DAA-----RADIAL DISPERSIVITY OF AQUIFER
C      DBB-----VERTICAL DISPERSIVITY OF AQUIFER
C      SUMP-----DRAWDOWN AT THE WELL
C      DTS-----MAXIMUM VALUE OF TIME STEP FOR SIMULATION SALTWATER
C      AKRU-----INITIAL VALUE OF RADIAL INTRINSIC PERMEABILITY
C      AKRZ-----INITIAL VALUE OF VRTICAL INTRINSIC PERMEABILITY
C      SST-----INITIAL VALUE OF SPECIFIC STORAGE
C      GACC-----RELATIVE DENSITY OF FRESHWATER AT 4 C
C      HIN-----PIEZOMETRIC HEAD
C      GFW-----SPECIFIC WEIGHT OF FRESHWATER
C      GSW-----SPECIFIC WEIGHT OF SALTWATER
C      HCD-----CONSTANT HEAD
C      XL(I)-----UPSTREAM RADIAL DISTANCE FOR (I)TH TAKE OFF POINT
C      XU(I)-----DOWNSTREAM RADIAL DISTANCE FOR (I)TH TAKE OFF POINT
C      U(I,J)-----RADIAL VELOCITY AT PRESSUR NODE (I,J)
C      V(I,J)-----VERTICAL VELOCITY AT PRESSURE NODE (I,J)
C      VLA(I,J)---SALTWATER CONCENTRATION AT NODE (I,J)
C      VLAQM-----SALTWATER CONCENTRATION AT PUMPED WELL
C      VED-----CUMULATIVE SALTWATER LIFTED INTO SUSPENSION DUE
C      TO DIFFUSION
C      USS(I,J)---RADIAL VELOCITY AT NODE (I,J)
C      VSS(I,J)---VERTICAL VELOCITY AT NODE (I,J)
C      TPQ-----PUMPAGE TIME
C*****
C      DIMENSION DR(30),SS(30,30),AKR(30,30),AKZ(30,30),Z(30)
C      DIMENSION HH(30),P(30,30),DT(270),VLA(30,30),DST(30,30)
C      DIMENSION A(30),B(30),C(30),D(30),USS(30,30),VSS(30,30)
C      DIMENSION PPM(30,30),PP(30,30),INA(5000),VSI(270),VEDF(270)
C      DIMENSION X(5000),Y(5000),VL(30),XF(30),YF(30),DZ(30)
C      DIMENSION U(30,30),V(30,30),YL(30),IN(30),CS(270),XU(30)
C      DIMENSION NLF(270),VSL(270),VLL(5000),TME(270),XS(30),XL(30)
C      DIMENSION GM(30,30),VIS(30,30),PIN(30),RR(30),SY(30,30)
C      DIMENSION YUP(5000),DRS(30),VLF(30),VV(30,30),UU(30,30)
C      DIMENSION VLI(30,30),VLAP(30,30),VLII(30,30),VLAFL(30,30)
C*****
C      OPEN(UNIT=1,FILE='M1.DAT')
C      OPEN(UNIT=2,FILE='M2.DAT')
C      OPEN(UNIT=3,FILE='M4.DAT')
C      OPEN(UNIT=4,FILE='M5.DAT')
C      OPEN(UNIT=5,FILE='M6.DAT')
C      OPEN(UNIT=6,FILE='M8.DAT')
C      OPEN(UNIT=7,FILE='M3.OUT',STATUS='NEW')
C      OPEN(UNIT=8,FILE='M7.OUT',STATUS='NEW')
C*****
C      READ(1,*)NR,NC,NCS,NRW,NRS,KOUNT,IX,NT1,DTS
C      READ(1,*)QQ,RW,PHI,TSTR,IQ,IC,NRB
C      READ(1,*)STL,TPQ,KOUNT1,STLS
C      READ(1,*)DAA,DBB

```

```

READ(1,*)AKRU,AKZU,SST,GACC,VISF,HIN,GFW,GSW,HCD
READ(3,*)NT2
READ(3,*)(DT(I),I=1,NT2)
READ(4,*)(DR(J),J=1,NC-1)
READ(5,*)(DZ(I),I=1,NR-1)
READ(6,*)(DRS(J),J=1,NCS-1)
READ(6,*)(XL(I),I=1,NCS)
READ(6,*)(XU(I),I=1,NCS)
READ(6,*)VOL
READ(6,*)(XS(I),I=1,NCS)
C*****
Z(NR)=0.0
DO 1053 I=1,NR-1
J=NR-I
1053 Z(J)=Z(J+1)+DZ(J)
CONTINUE
RR(1)=RW
DO 503 J=2,NC
503 RR(J)=RR(J-1)+DR(J-1)
CONTINUE
DS=Z(NRW)-Z(NRS)-0.5*DZ(NRW)
DSC=DS-0.5*DZ(NRS-1)
IF(IC.EQ.1)ALS=Z(NRB)-Z(NRW)-0.5*DZ(NRB)+0.5*DZ(NRW)
IF(IC.EQ.0)ALS=Z(1)-Z(NRW)+0.5*DZ(NRW)
DSA=DS+ALS
XF(1)=RW
DO 2500 J=2,NC
2500 XF(J)=XF(J-1)+DR(J-1)
CONTINUE
YF(1)=0.0
DO 2510 I=2,NRS
2510 YF(I)=YF(I-1)+DZ(NRS-I+1)
CONTINUE
DO 196 I=1,NRS
DO 197 J=1,NCS
IF(I.EQ.1)GO TO 198
VLA(I,J)=0.0
GO TO 197
198 VLA(I,J)=1.0
197 CONTINUE
196 CONTINUE
IF(IX.EQ.1)GO TO 920
NTP=NCS+1
DO 2550 J=1,NCS
2550 X(J)=XS(J)
Y(J)=0.5*DZ(NRS-1)
YL(J)=0.0
IN(J)=J
JJ=J
NCSJ=NCS
VL(J)=VOL
VLL(J)=VL(J)*PHI
VSP=0.0
CSP=0.0
VSD=0.0
VED=0.0
VLAQ=0.0
CONTINUE
X(NCS+1)=RW
Y(NCS+1)=0.5*DZ(NRS-1)
YL(NCS+1)=0.0
VLL(NCS+1)=0.0

```

```

IN(NCS+1)=NCS+1
VL(NCS+1)=0.0
DO 1 I=1,NRS-1
DO 2 J=1,NC
GM(I,J)=GFW*GACC
VIS(I,J)=VISF
SS(I,J)=SST
2 CONTINUE
1 CONTINUE
DO 5 I=NRS,NR
DO 6 J=1,NC
GM(I,J)=GSW*GACC
VIS(I,J)=VISF*(1.0+0.02825614)
SS(I,J)=SST*GSW/(GFW*GACC)
6 CONTINUE
5 CONTINUE
C*****INITIAL CONDITIONS*****
DO 10 I=1,NRS-1
DO 10 J=1,NC
P(I,J)=(HIN-Z(I))*GM(I,J)
10 CONTINUE
DO 11 I=NRS,NR
DO 11 J=1,NC
P(I,J)=(HIN-(Z(NRS)-Z(NR)))*GFW*GACC+(Z(NRS)-Z(I))*GM(I,
1J)+0.5*DZ(NRS-1)*(GSW-GFW)
11 CONTINUE
C*****START OF SIMULATION*****
TM=0.0
GO TO 925
920 READ(2,*)TM
READ(2,167)NTP
READ(2,168)(X(I),I=1,NTP)
READ(2,168)(Y(I),I=1,NTP)
READ(2,168)(YL(J),J=1,NCS+1)
READ(2,167)(IN(J),J=1,NCS+1)
READ(2,170)(VLL(J),J=1,NTP)
DO 145 I=1,NR
READ(2,161)(P(I,J),J=1,NC)
145 CONTINUE
READ(2,170)(VL(J),J=1,NCS+1)
READ(2,*)VSP,CSP,VSD,VLAQM,VED
DO 1442 I=1,NR
READ(2,160)(GM(I,J),J=1,NC)
1442 CONTINUE
DO 1452 I=1,NR
READ(2,160)(VIS(I,J),J=1,NC)
1452 CONTINUE
DO 25 I=1,NR
READ(2,160)(SS(I,J),J=1,NC-1)
25 CONTINUE
DO 1015 I=1,NRS
READ(2,182)(U(I,J),J=1,NC)
1015 CONTINUE
DO 2015 I=1,NRS
READ(2,182)(V(I,J),J=1,NC)
2015 CONTINUE
DO 383 I=1,NRS
READ(2,173)(VLA(I,J),J=1,NCS)
383 CONTINUE
925 CONTINUE

```

```

DO 930 I=1,NR
DO 935 J=1,NC
PP(I,J)=P(I,J)
935 CONTINUE
PIN(I)=P(I,NC)
930 CONTINUE
DO 3 I=1,NR
DO 4 J=1,NC
AKR(I,J)=AKRU
AKZ(I,J)=AKZU
SY(I,J)=SYT
4 CONTINUE
3 CONTINUE
DO 205 IPD=NT1,NT2
IF(TM.GE.TPQ) GO TO 2055
Q=QQ
GO TO 2060
2055 Q=0.0
2060 CONTINUE
TM=TM+DT(IPD)
TME(IPD)=TM
TMI=DT(IPD)
C*****SIMULATION OF PRESSURE*****
DO 1000 IT=1,KOUNT
DO 100 JA=1,NC-1
J=NC-JA
DO 110 IA=1,NR
I=NR+1-IA
R=RW
IF(J.EQ.1) GO TO 776
DO 600 JJ=1,J-1
R=R+DR(JJ)
600 CONTINUE
776 GM11=GM(I,J+1)-GM(I,J)
GM1=GM(I,J)-GM(I,J-1)
GM2=GM(I-1,J)-GM(I,J)
GM22=GM(I,J)-GM(I+1,J)
GM3=(GM(I,J)+GM(I+1,J))/2.0
GM4=(GM(I,J)+GM(I-1,J))/2.0
VIS11=VIS(I,J+1)-VIS(I,J)
VIS1=VIS(I,J)-VIS(I,J-1)
VIS2=VIS(I-1,J)-VIS(I,J)
VIS22=VIS(I,J)-VIS(I+1,J)
VIS7=(VIS(I,J)+VIS(I+1,J))/2.0
VIS8=(VIS(I,J)+VIS(I,J-1))/2.0
VIS3=VIS(I,J)
VIS4=VIS(I,J)
VIS5=(VIS(I,J)+VIS(I,J+1))/2.0
VIS6=(VIS(I,J)+VIS(I-1,J))/2.0
Z3=(Z(I)+Z(I+1))/2.0
AKR12=AKR(I,J+1)-AKR(I,J)
AKR11=AKR(I,J)-AKR(I,J-1)
AKR5=(AKR(I,J)+AKR(I,J-1))/2.0
AKR4=(AKR(I,J)+AKR(I,J+1))/2.0
AKR3=AKR(I,J)
DR1=DR(J)+DR(J-1)
DZ1=(DZ(I)+DZ(I-1))/2.0
AKZ2=AKZ(I-1,J)-AKZ(I,J)
AKZ22=AKZ(I,J)-AKZ(I+1,J)
AKZ4=(AKZ(I,J)+AKZ(I+1,J))/2.0
AKZ3=AKZ(I,J)
AKZ6=(AKZ(I,J)+AKZ(I-1,J))/2.0

```

```

IF(J.GT.1) GO TO 400
IF(I.LE.NRW) GO TO 993
IF(I.LT.NR) GO TO 888
A(I)=AKZ6*DR(1)*(RW+DR(1)/4.0)/(VIS6*DZ(I-1)*DZ(I-1))
B90=-A(I)-AKR4*(RW+DR(1)/2.0)/(VIS5*DR(1))
B91=-SS(I,J)*DR(1)*(RW+DR(1)/4.0)/(2.0*GM(I,J)*DT(IPD))
B(I)=B90+B91
C(I)=0.0
DD1=-P(I,J+1)*AKR4*(RW+DR(1)/2.0)/(VIS5*DR(1))
DD2=-PP(I,J)*SS(I,J)*(DR(1)*(RW+DR(1)/4.0)/2.0)
DD3=DD2/(GM(I,J)*DT(IPD))
DD4=-GM4*A(I)*DZ(I-1)
D(I)=DD1+DD3+DD4
GO TO 115
993 IF(IQ.EQ.0) GO TO 995
A(I)=0.0
B(I)=1.0/GM(I,1)
C(I)=0.0
D(I)=HIN-HCD-Z(I)
GO TO 115
995 A13=3.1416*DR(1)*(RW+DR(1)/4.0)
D200=-Q/(FLOAT(NRW)-0.5)
IF(IC.EQ.1.AND.I.LE.NRB) D200=0.0
IF(IC.EQ.1.AND.I.GT.NRB) D200=-Q/(FLOAT(NRW)-FLOAT(NRB)+
10.5*DZ(NRW)-0.5*DZ(NRB))
IF(I.EQ.1) GO TO 712
AA12=AKZ(I,1)/(VIS(I,1)*DZ(I))
A12=AKZ(I,1)/(VIS(I,1)*DZ(I-1))
D201=P(I,J+1)
AC1=SS(I,J)*DZ1/(GM(I,J)*DT(IPD))
D202=6.2832*(RW+DR(1)/2.0)*DZ1*AKR4/(VIS5*DR(1))
B(I)=-A13*(A12+AA12)-D202-AC1*A13
A(I)=+A12*A13
C(I)=AA12*A13
D203=-GM3+GM4
D(I)=-D200-(D201*D202)-A(I)*D203*DZ(I-1)-PP(I,J)*AC1*A13
GO TO 115
712 AC1=SS(I,J)*DZ(I)/(GM(I,J)*DT(IPD))
AA12=AKZ4/(VIS7*DZ(I))
D202=6.2832*(RW+DR(1)/2.0)*DZ(I)*AKR4/(VIS5*DR(1))
B(I)=-2.0*AA12*A13-D202-AC1*A13
D201=P(I,J+1)
A(I)=0.0
C(I)=2.0*AA12*A13
D204=-GM3
D(I)=-D200-(D201*D202)-C(I)*D204*DZ(I)-PP(I,J)*AC1*A13
GO TO 115
888 AA1=AKZ6/(VIS6*DZ1*DZ(I-1))
AA2=DR(1)*(RW+DR(1)/4.0)
A(I)=AA1*AA2
B92=2.0*AKR4*(RW+DR(1)/2.0)/(VIS5*DR(1))
B93=AKZ4/(VIS7*DZ1*DZ(I))
B94=SS(I,J)/(GM(I,J)*DT(IPD))
B(I)=-B92-AA2*(B93+AA1+B94)
C(I)=B93*AA2
DD6=-(-GM3*B93*DZ(I)+GM4*AA1*DZ(I-1))*AA2
D(I)=-P(I,J+1)*B92-PP(I,J)*B94*AA2+DD6
GO TO 115
400 IF(I.GT.1.AND.I.LT.NR) GO TO 350
IF(I.EQ.1) GO TO 361
AA3=AKZ6/(VIS6*DZ(I-1)*DZ(I-1))
AA4=R*(DR(J)+DR(J-1))+DR(J)*DR(J)-DR(J-1)*DR(J-1)/4.0

```



```

A(I)=AA3*AA4
B113=AKR4*(R+DR(J)/2.0)/(VIS5*DR(J))
B114=AKR5*(R-DR(J-1)/2.0)/(VIS8*DR(J-1))
B115=SS(I,J)/(2.0*GM(I,J)*DT(IPD))
B(I)=-B113-B114+AA4*(-AA3-B115)
C(I)=0.0
D(I)=-P(I,J+1)*B113-P(I,J-1)*B114-PP(I,J)*B115*AA4
D(I)=D(I)-GM4*AA3*DZ(I-1)*AA4
GO TO 115
361 A(I)=0.0
B104=-AKR4*(R+DR(J)/2.0)/(VIS5*DR(J))
B105=-AKR5*(R-DR(J-1)/2.0)/(VIS8*DR(J-1))
B106=-AKZ4/(VIS7*DZ(I)*DZ(I))
B107=R*(DR(J)+DR(J-1))+(DR(J)*DR(J)-DR(J-1)*DR(J-1))/4.0
C(I)=-B106*B107
B108=-SS(I,J)/(2.0*GM(I,J)*DT(IPD))
B(I)=B104+B105+B107*(B106+B108)
D(I)=P(I,J+1)*B104+P(I,J-1)*B105+PP(I,J)*B108*B107
D(I)=D(I)+B106*DZ(I)*(-GM3)*B107
GO TO 115
350 A4=AKZ3/(2.0*DZ(I-1)*DZ(I-1)*VIS3)
A44=AKZ3/(2.0*VIS3)
A5=(2.0*DZ(I-1)/DZ1+AKZ2/AKZ3-VIS2/VIS3)
A(I)=A4*A5
C1=A4*DZ(I-1)*DZ(I-1)/(DZ(I)*DZ(I))
C2=(2.0*DZ(I)/DZ1-AKZ22/AKZ3+VIS22/VIS3)
C(I)=C1*C2
B2=-SS(I,J)/(GM(I,J)*DT(IPD))
DAR=ALOG(RR(J+1))-ALOG(RR(J))
D43=AKR3/(2.0*DAR*DAR*RR(J)*RR(J)*VIS4)
D44=-4.0+(AKR11-AKR12)/AKR3+(VIS1-VIS11)/VIS4
D301=D43*D44
B(I)=-C(I)-A(I)+B2+D301
D46=-2.0*(P(I,J+1)+P(I,J-1))
D47=-P(I,J+1)*AKR12/AKR3+P(I,J-1)*AKR11/AKR3
D48=P(I,J+1)*VIS11/VIS4-P(I,J-1)*VIS1/VIS4
D49=-((AKZ2/DZ(I-1)+AKZ22/DZ(I))/AKZ3+(VIS2/DZ(I-1)+VIS22
1/DZ(I))/VIS3)
D50=GM3*D49
D69=-((GM2/DZ(I-1)+GM22/DZ(I))*AKZ3)/(2.0*VIS3)
D(I)=D43*(D46+D47+D48)+A44*(D50)+PP(I,J)*B2+D69
115 CONTINUE
110 CONTINUE
CALL BST (NR,A,B,C,D,HH)
DO 120 I=1,NR
P(I,J)=HH(I)
IF(P(I,J).GT.PIN(I)) P(I,J)=PIN(I)
120 CONTINUE
100 CONTINUE
DO 70 IB=1,NR
I=NR+1-IB
DO 80 JB=1,NC
J=NC+1-JB
KK=J
R=RW
IF(KK.EQ.1) GO TO 550
DO 500 JJ=1,KK-1
R=R+DR(JJ)
500 CONTINUE
550 GM11=GM(I,J+1)-GM(I,J)
GM1=GM(I,J)-GM(I,J-1)
GM2=GM(I-1,J)-GM(I,J)

```

```

GM22=GM(I,J)-GM(I+1,J)
GM3=(GM(I,J)+GM(I+1,J))/2.0
GM4=(GM(I,J)+GM(I-1,J))/2.0
GM5=GM(I,J)
VIS11=VIS(I,J+1)-VIS(I,J)
VIS1=VIS(I,J)-VIS(I,J-1)
VIS2=VIS(I-1,J)-VIS(I,J)
VIS22=VIS(I,J)-VIS(I+1,J)
VIS7=(VIS(I,J)+VIS(I+1,J))/2.0
VIS8=(VIS(I,J)+VIS(I,J-1))/2.0
VIS3=VIS(I,J)
VIS4=VIS(I,J)
VIS6=(VIS(I,J)+VIS(I-1,J))/2.0
VIS5=(VIS(I,J)+VIS(I,J+1))/2.0
AKR12=AKR(I,J+1)-AKR(I,J)
AKR11=AKR(I,J)-AKR(I,J-1)
AKR5=(AKR(I,J)+AKR(I,J-1))/2.0
AKR3=AKR(I,J)
AKR4=(AKR(I,J)+AKR(I,J+1))/2.0
AKZ2=AKZ(I-1,J)-AKZ(I,J)
AKZ22=AKZ(I,J)-AKZ(I+1,J)
AKZ4=(AKZ(I,J)+AKZ(I+1,J))/2.0
AKZ3=AKZ(I,J)
AKZ6=(AKZ(I,J)+AKZ(I-1,J))/2.0
Z3=(Z(I)+Z(I+1))/2.0
DR1=DR(J)+DR(J-1)
DZ1=(DZ(I)+DZ(I-1))/2.0
IF(J.GT.1.AND.J.LT.NC) GO TO 250
IF(J.EQ.NC) GO TO 223
IF(I.GT.NRW) GO TO 337
IF(IQ.EQ.0) GO TO 41
A(J)=0.0
B(J)=1.0/GM(I,1)
C(J)=0.0
D(J)=HIN-HCD-Z(I)
GO TO 85
41 A(J)=0.0
DX9=Q/(FLOAT(NRW)-0.5)
IF(IC.EQ.1.AND.I.LE.NRB) DX9=0.0
IF(IC.EQ.1.AND.I.GT.NRB) DX9=Q/(FLOAT(NRW)-FLOAT(NRB))+0.
15*DZ(NRW)-0.5*DZ(NRB))
IF(I.EQ.1) GO TO 711
DX5=AKZ(I,1)/VIS(I,1)
B(J)=-6.2832*(RW+DR(1)/2.)*DZ1*AKR4/(VIS5*DR(1))
C(J)=-B(J)
DX2=-3.1416*DR(1)*(RW+DR(1)/4.0)*(1.0/DZ(I)+1.0/DZ(I-1))
AB=SS(I,J)*DZ1/(GM(I,J)*DT(IPD))
B(J)=B(J)+DX2*DX5+AB*DX2/(1.0/DZ(I)+1.0/DZ(I-1))
DX4=(P(I+1,1)/DZ(I)+P(I-1,1)/DZ(I-1)+(-GM3+GM4))
DX4=DX4/(1.0/DZ(I)+1.0/DZ(I-1))
DX8=DX2*DX5*DX4
D(J)=DX8+DX9+PP(I,J)*AB*DX2/(1.0/DZ(I)+1.0/DZ(I-1))
GO TO 85
711 B(J)=-6.2832*(RW+DR(1)/2.)*DZ(I)*AKR4/(VIS5*DR(1))
DX5=AKZ4/VIS7
C(J)=-B(J)
DX2=-3.1416*DR(1)*(RW+DR(1)/4.0)/DZ(I)
AB=SS(I,J)*DZ(I)/(GM(I,J)*DT(IPD))
B(J)=B(J)+2.0*DX2*DX5+AB*DX2*DZ(I)
DX12=P(I+1,1)-GM3*DZ(I)
DX10=2.0*DX2*DX5*DX12
D(J)=DX10+DX9+PP(I,J)*AB*DX2*DZ(I)

```

```

GO TO 85
337 IF(I.EQ.NR) GO TO 705
A(J)=0.0
B99=-2.0*AKR4*(RW+DR(1)/2.0)/(VIS5*DR(1))
B100=AKZ4/(VIS7*DZ1*DZ(I))
B101=AKZ6/(VIS6*DZ1*DZ(I-1))
B102=DR(1)*(RW+DR(1)/4.0)
B103=SS(I,J)/(GM(I,J)*DT(IPD))
B(J)=B99-B102*(B100+B101+B103)
C(J)=-B99
DD17=P(I+1,J)-GM3*DZ(I)
DD18=-P(I-1,J)-GM4*DZ(I-1)
D(J)=-B102*(DD17*B100-DD18*B101+PP(I,J)*B103)
GO TO 85
705 A(J)=0.0
B95=-AKR4*(RW+DR(1)/2.0)/(VIS5*DR(1))
B96=-AKZ6/(VIS6*DZ(I-1)*DZ(I-1))
B97=DR(1)*(RW+DR(1)/4.0)
B98=-SS(I,J)/(2.0*GM(I,J)*DT(IPD))
B(J)=B95+B97*(B96+B98)
C(J)=-B95
D(J)=(P(I-1,J)+GM4*DZ(I-1))*B96*B97+PP(I,J)*B98*B97
GO TO 85
223 A(J)=0.0
B(J)=+1.0
C(J)=0.0
D(J)=PIN(I)
GO TO 85
250 IF(I.EQ.1) GO TO 701
IF(I.EQ.NR) GO TO 702
D14=AKZ3/(2.0*VIS3)
D15=-(1./DZ1)*(1.0/DZ(I)+1.0/DZ(I-1))
D15=D15-AKZ2/(AKZ3*DZ(I-1)*DZ(I-1))
D15=D15+VIS2/(VIS3*DZ(I-1)*DZ(I-1))
D16=(1./DZ1)*(1./DZ(I)+1./DZ(I-1))
D16=D16-AKZ22/(AKZ3*DZ(I-1)*DZ(I-1))
D16=D16+VIS22/(VIS3*DZ(I-1)*DZ(I-1))
D115=D15+(1./DZ1)*(1./DZ(I)+1./DZ(I-1))-2.0/(DZ1*DZ(I-1))
D116=D16-(1./DZ1)*(1./DZ(I)+1./DZ(I-1))+2.0/(DZ1*DZ(I))
D17=(P(I-1,J)*D115-P(I+1,J)*D116)
D20=(AKZ2/DZ(I-1)+AKZ22/DZ(I))*(GM5/AKZ3)
D21=(VIS2/DZ(I-1)+VIS22/DZ(I))*(GM5/VIS3)
D22=(SS(I,J)*PP(I,J))/(GM(I,J)*DT(IPD))
D66=-((GM2/DZ(I-1)+GM22/DZ(I))*AKZ3)/(2.0*VIS3)
D(J)=D14*(D17-D20+D21)-D22+D66
DAR=ALOG(RR(J+1))-ALOG(RR(J))
AD1=AKR3/(2.0*RR(J)*RR(J)*VIS4)
AD2=(2.0-AKR11/AKR3+VIS1/VIS4)
A(J)=AD1*AD2/(DAR*DAR)
AD3=(-2.0-AKR12/AKR3+VIS11/VIS4)
B(J)=AD1*(AD3/(DAR*DAR)-AD2/(DAR*DAR))
B(J)=B(J)-(SS(I,J)/(GM(I,J)*DT(IPD)))
B(J)=B(J)+D14*(D15-D16)
C(J)=AD1*(-AD3)/(DAR*DAR)
GO TO 85
701 A(J)=AKR5*(R-DR(J-1)/2.0)/(VIS8*DR(J-1))
B109=AKR4*(R+DR(J)/2.0)/(VIS5*DR(J))
B110=AKZ4/(VIS7*DZ(I)*DZ(I))
B112=R*(DR(J)+DR(J-1))+DR(J)*DR(J)-DR(J-1)*DR(J-1)/4.0
C(J)=B109
B111=SS(I,J)/(2.0*GM(I,J)*DT(IPD))
B(J)=-B109-A(J)-B112*(B110+B111)

```

```

D(J)=B112*((-P(I+1,J)-(-GM3)*DZ(I))*B110-PP(I,J)*B111)
GO TO 85
702 A(J)=AKR5*(R-DR(J-1)/2.0)/(VIS8*DR(J-1))
      B116=AKR4*(R+DR(J)/2.0)/(VIS5*DR(J))
      B117=AKZ6/(VIS6*DZ(I-1)*DZ(I-1))
      B118=SS(I,J)/(2.0*GM(I,J)*DT(IPD))
      B119=R*(DR(J)+DR(J-1))+(DR(J)*DR(J)-DR(J-1)*DR(J-1))/4.0
      B(J)=-B116-A(J)-B119*(B117+B118)
      C(J)=B116
      D(J)=B119*((-P(I-1,J)+(-GM4)*DZ(I-1))*B117-PP(I,J)*B118)
85 CONTINUE
80 CONTINUE
      CALL BST (NC,A,B,C,D,HH)
      DO 90 J=1,NC
      P(I,J)=HH(J)
      IF(P(I,J).GT.PIN(I)) P(I,J)=PIN(I)
90 CONTINUE
70 CONTINUE
      IF(IT.EQ.1)GO TO 1050
      SM=0.0
      DO 1010 I=1,NR
      DO 1020 J=1,NC
      SM=SM+ABS(P(I,J)-PPM(I,J))
1020 CONTINUE
1010 CONTINUE
      IF(SM.LT.STL) GO TO 20
1050 DO 1030 I=1,NR
      DO 1040 J=1,NC
      PPM(I,J)=P(I,J)
1040 CONTINUE
1030 CONTINUE
      SMP=SM
1000 CONTINUE
      GO TO 144
20 CONTINUE
C*****CALCULATION OF VELOCITIES*****
DO 2520 I=1,NRS
  II=NRS-I+1
  DO 2530 J=1,NC
    VV(II,J)=V(II,J)
    UU(II,J)=U(II,J)
    AKZ4=(AKZ(I,J)+AKZ(I+1,J))/2.0
    VIS7=(VIS(I,J)+VIS(I+1,J))/2.0
    DV2=(P(I+1,J)-P(I,J))/DZ(I)
    IF(I.EQ.1) GO TO 2526
    DV1=AKZ(I,J)/(2.0*VIS(I,J))
    DV3=(P(I,J)-P(I-1,J))/DZ(I-1)
    DV4=-GM(I+1,J)/2.0-GM(I,J)-GM(I-1,J)/2.0
    V(II,J)=DV1*(DV2+DV3+DV4)
    GO TO 2527
2526 DV5=-GM(I+1,J)+GM(I,J))/2.0
      DV1=AKZ4/(2.0*VIS7)
      V(II,J)=2.0*DV1*(DV2+DV5)
2527 V(II,J)=V(II,J)/PHI
2802 IF(J.EQ.NC) GO TO 2528
      DU2=(P(I,J)-P(I,J+1))/DR(J)
      IF(J.EQ.1)GO TO 2540
      VD2=(AKR(I,J)+AKR(I,J-1))/(VIS(I,J)+VIS(I,J-1))
      VV2=VD2*(P(I,J-1)-P(I,J))/DR(J-1)
      VD1=(AKR(I,J)+AKR(I,J+1))/(VIS(I,J)+VIS(I,J+1))
      VV1=VD1*(P(I,J)-P(I,J+1))/DR(J)
      DRV=DR(J-1)/(DR(J)+DR(J-1))

```

```

U(II,J)=VV2+(VV1-VV2)*DRV
GO TO 2535
2540 AKR4=(AKR(I,J)+AKR(I,J+1))/2.0
VIS5=(VIS(I,J)+VIS(I,J+1))/2.0
DU1=AKR4/(2.0*VIS5)
U(II,J)=2.0*DU1*DU2
GO TO 2535
2528 DU4=(P(I,J-1)-P(I,J))/DR(J-1)
AKR5=(AKR(I,J)+AKR(I,J-1))/2.0
VIS4=(VIS(I,J)+VIS(I,J-1))/2.0
DU1=AKR5/(2.0*VIS4)
U(II,J)=2.0*DU1*DU4
2535 U(II,J)=U(II,J)/PHI
IF(IPD.EQ.1.OR.Q.EQ.0.0) UU(II,J)=U(II,J)
IF(IPD.EQ.1.OR.Q.EQ.0.0) VV(II,J)=V(II,J)
2530 CONTINUE
2520 CONTINUE
DO 315 I=1,NRS
DO 317 L=1,NCS
DO 316 J=2,NC
IF(XS(L).GE.XF(J-1).AND.XS(L).LT.XF(J))GO TO 318
GO TO 316
318 XCC=(XS(L)-XF(J-1))/(XF(J)-XF(J-1))
VSS(I,L)=V(I,J-1)+(V(I,J)-V(I,J-1))*XCC
USS(I,L)=U(I,J-1)+(U(I,J)-U(I,J-1))*XCC
GO TO 317
316 CONTINUE
317 CONTINUE
315 CONTINUE
182 FORMAT(2X,12E10.3)
DP=DT(IPD)
CALL MOVE(NTP,X,Y,VL,NRS,YF,U,V,DP,IN,DZ,YL,VE,VQ,DS,
1RW,VLL,XS,DTS,TSTR,PHI,VV,UU,DSA,NCS,TM,TPQ,XF,NC,VS)
IF(NTP.LT.9000)GO TO 147
1416 FORMAT(10X,' NTP EXCEEDS')
GO TO 144
147 CONTINUE
DO 310 I=1,NR
DO 320 J=1,NC
PP(I,J)=P(I,J)
320 CONTINUE
310 CONTINUE
DO 32 I=1,NRS
IF(I.GT.1)GO TO 135
DO 136 J=1,NCS
VLA(I,J)=1.0
VLI(I,J)=VLA(I,J)
136 CONTINUE
GO TO 32
135 CONTINUE
DO 33 J=1,NCS
IF(I.EQ.1) GO TO 1620
YYL=YF(I-1)+0.5*DZ(NRS-I+1)
GO TO 1630
1620 YYL=YF(I)
1630 CONTINUE
IF(I.EQ.NRS) GO TO 1815
YYU=YF(I)+0.5*DZ(NRS-I)
GO TO 1820
1815 YYU=YF(I)
1820 CONTINUE
VLI(I,J)=VLA(I,J)

```

```

VLA(I,J)=0.0
DO 34 K=1,NTP
IF(J.EQ.NCS.AND.X(K).EQ.XU(J)) GO TO 334
IF(X(K).LT.XL(J).OR.X(K).GE.XU(J)) GO TO 34
334 IF(Y(K).LT.YYL.OR.Y(K).GE.YYU) GO TO 34
VLA(I,J) =VLA(I,J)+VLL(K)
34 CONTINUE
VLX=VL(J)*(0.5*(DZ(NRS-I+1)+DZ(NRS-I)))*PHI/TSTR
VLA(I,J) =VLA(I,J)/VLX
VLII(I,J)=VLA(I,J)
33 CONTINUE
32 CONTINUE
DP=DT(IPD)
IF(TM.LE.TPQ) VLAQ=VQ/(Q*DP)
IF(TM.GT.TPQ) VLAQ=VLAQM
CALL DIFF(ITT,KOUNT1,NCS,NRS,VLA,STLS,DRS,DAA,DBB,DZ,
1DP,VLI,RW,NRB,NRW,USS,VSS,DTS,XS,VLAQ,XU)
DO 35 I=1,NRS
DO 36 J=1,NCS
DST(I,J)=(VLA(I,J)-VLII(I,J))/DT(IPD)
36 CONTINUE
35 CONTINUE
49 CONTINUE
DO 103 I=2,NRS
DO 104 J=1,NC
IF(XF(J).GT.XS(NCS)) GO TO 107
DO 105 L=2,NCS
IF(XF(J).GE.XS(L-1).AND.XF(J).LT.XS(L)) GO TO 106
GO TO 105
106 XC=(XF(J)-XS(L-1))/(XS(L)-XS(L-1))
VLAF(I,J)=VLA(I,L-1)+(VLA(I,L)-VLA(I,L-1))*XC
GO TO 104
105 CONTINUE
XC=(XF(J)-XS(1))/(XS(2)-XS(1))
VLAF(I,J)=VLA(I,1)+(VLA(I,2)-VLA(I,1))*XC
GO TO 108
107 VLAF(I,J)=0.0
108 CONTINUE
104 CONTINUE
103 CONTINUE
DO 7 I=NRS,NR
DO 8 J=1,NC
GM(I,J)=GSW*GACC
VIS(I,J)=VISF*(1.0+0.02825614)
8 CONTINUE
7 CONTINUE
DO 14 I=NRW,NRS-1
II=NRS-I+1
DO 15 J=1,NC
GM(I,J)=((GSW-GFW)*VLAF(II,J)+GFW)*GACC
VIS(I,J)=VISF*(1.0+0.02825614*VLAF(II,J))
IF(GM(I,J).GT.(GSW*GACC)) GM(I,J)=GSW*GACC
IF(VIS(I,J).GT.(VISF*1.02825614)) VIS(I,J)=VISF*1.02825614
15 CONTINUE
14 CONTINUE
DO 16 I=1,NR
DO 17 J=1,NC-1
SS(I,J)=SST*GM(I,J)/(GFW*GACC)
17 CONTINUE
16 CONTINUE
DO 1354 I=2,NRS
DO 1355 J=1,NCS

```

```

NMP=0
DO 341 K=1,NTP
IF(I.EQ.1) GO TO 1621
YYL=YF(I-1)+0.5*DZ(NRS-I+1)
GO TO 1631
1621 YYL=YF(I)
1631 CONTINUE
IF(I.EQ.NRS) GO TO 1816
YYU=YF(I)+0.5*DZ(NRS-I)
GO TO 1821
1816 YYU=YF(I)
1821 CONTINUE
IF(J.EQ.NCS.AND.X(K).EQ.XU(J)) GO TO 342
IF(X(K).LT.XL(J).OR.X(K).GE.XU(J)) GO TO 341
342 IF(Y(K).LT.YYL.OR.Y(K).GE.YYU) GO TO 341
NMP=NMP+1
INA(NMP)=K
341 CONTINUE
IF(DST(I,J).EQ.0.0) GO TO 1355
IF(NMP.GT.0)GO TO 138
NTP=NTP+1
X(NTP)=XS(J)
Y(NTP)=YF(I)
VLL(NTP)=DST(I,J)*DT(IPD)*VL(J)*(0.5*(DZ(NRS-I+1)+DZ(NR
1S-I)))*PHI/TSTR
NMP=NMP+1
INA(NMP)=NTP
GO TO 1355
138 CONTINUE
VLX=VL(J)*(0.5*(DZ(NRS-I+1)+DZ(NRS-I)))*PHI/TSTR
CSV=DST(I,J)*DT(IPD)*VLX
SUM=0.0
DO 1357 KK=1,NMP
K=INA(KK)
SUM=SUM+VLL(K)
1357 CONTINUE
DO 1356 KK=1,NMP
K=INA(KK)
IF(SUM.EQ.0.0)GO TO 1356
VLL(K)=VLL(K)+CSV*VLL(K)/SUM
1356 CONTINUE
1355 CONTINUE
1354 CONTINUE
VEI=0.0
DO 1095 J=1,NCS
DB=ABS(DBB*VSS(2,J))
RATE=(1.0-VLA(2,J))*DB/DZ(NRS-1)
AREA=3.1415*(XU(J)**2-XL(J)**2)*PHI
VEI=VEI+AREA*RATE*DT(IPD)
1095 CONTINUE
VE=VE+VEI
VED=VED+VEI
VEDF(IPD)=VED
VSP=VSP+VE
CSP=CSP+VQ
VSL(IPD)=VSP
VSD=VSD+VS
VSI(IPD)=VSD
CS(IPD)=CSP
NLF(IPD)=NTP
205 CONTINUE
GO TO 149

```

```

144     CONTINUE
146     FORMAT(5X, 'CONVERGENCE NOT ACHIEVED', I5, 5X, E16.7)
      NT2=IPD-1
149     CONTINUE
      DO 39 I=1, NTP
      YUP(I)=Y(I)-0.5*DZ(NRS-1)
39      CONTINUE
      SUMP=0.0
      DO 1234 I=1, NRW
1234     SUMP=SUMP+(P(I, NC)-P(I, 1))/1000
      CONTINUE
      SUMP=SUMP/FLOAT(NRW)
      WRITE(8, 150)
      WRITE(8, 164) (TME(IPD), IPD=NT1, NT2)
      WRITE(8, 175)
      WRITE(8, 164) (CS(I), I=NT1, NT2)
      WRITE(8, 176)
      WRITE(8, 164) (VSL(I), I=NT1, NT2)
      WRITE(8, 1011)
      WRITE(8, 164) (VSI(I), I=NT1, NT2)
      WRITE(8, 1012)
      WRITE(8, 164) (VEDF(I), I=NT1, NT2)
      WRITE(8, 177)
      WRITE(8, 167) (NLF(I), I=NT1, NT2)
      WRITE(8, 178)
      WRITE(8, 164) (X(I), I=1, NTP)
      WRITE(8, 179)
      WRITE(8, 164) (YUP(I), I=1, NTP)
      WRITE(8, 190)
      DO 380 I=1, NRS
380     WRITE(8, 173) (VLA(I, J), J=1, NCS)
      CONTINUE
      WRITE(8, 191)
      WRITE(8, *) SUMP
      WRITE(7, *) TM
      WRITE(7, 167) NTP
      WRITE(7, 168) (X(I), I=1, NTP)
      WRITE(7, 168) (Y(I), I=1, NTP)
      WRITE(7, 168) (YL(J), J=1, NCS+1)
      WRITE(7, 167) (IN(J), J=1, NCS+1)
      WRITE(7, 170) (VLL(J), J=1, NTP)
      DO 143 I=1, NR
143     WRITE(7, 161) (PP(I, J), J=1, NC)
      CONTINUE
      WRITE(7, 170) (VL(J), J=1, NCS+1)
      WRITE(7, *) VSP, CSP, VSD, VLAQ, VED
      DO 1441 I=1, NR
1441     WRITE(7, 160) (GM(I, J), J=1, NC)
      CONTINUE
      DO 1451 I=1, NR
1451     WRITE(7, 160) (VIS(I, J), J=1, NC)
      CONTINUE
      DO 26 I=1, NR
26      WRITE(7, 160) (SS(I, J), J=1, NC-1)
      CONTINUE
      DO 1025 I=1, NRS
1025     WRITE(7, 182) (U(I, J), J=1, NC)
      CONTINUE
      DO 2025 I=1, NRS
2025     WRITE(7, 182) (V(I, J), J=1, NC)
      CONTINUE
      DO 382 I=1, NRS

```



```

WRITE (7,173) (VLA(I,J),J=1,NCS)
382 CONTINUE
175 FORMAT(/5X,'CUMULATIVE SALT WATER ENTRY INTO WELL'//)
176 FORMAT(/5X,'CUMULATIVE SALT WATER LIFTING INTO SUSPENSION'//)
1011 FORMAT(/5X,'CUMULATIVE SALT WATER ENTRY BELOW INTERFACE'//)
1012 FORMAT(/5X,'CUMULATIVE SALT WATER LIFTING INTO SUSP. (DIFF)'//)
177 FORMAT(/5X,' NUMBER OF POINTS LIFTED'//)
178 FORMAT(/5X,' X-COORDINATES'//)
179 FORMAT(/5X,' Y-COORDINATES'//)
180 FORMAT(/5X,' HORIZONTAL VELOCITIES'//)
181 FORMAT(/5X,' VERTICAL VELOCITIES'//)
190 FORMAT(/5X,'CONCENTRATION OF SALT WATER'//)
191 FORMAT(/5X,'PRESSURE'//)
192 FORMAT(/5X,'VISCOSITY'//)
193 FORMAT(/5X,'SPECIFIC WEIGHT'//)
165 FORMAT(5X,12E11.4)
166 FORMAT(5X,12E12.5)
167 FORMAT(5X,16I7)
168 FORMAT(5X,11E10.4)
164 FORMAT(5X,10E10.4)
169 FORMAT(5X,8E10.3)
170 FORMAT(5X,6E16.7)
171 FORMAT(5X,6E16.7)
150 FORMAT(5X,'CUMULATIVE TIME')
161 FORMAT(5X,6E16.7)
160 FORMAT(5X,6E16.7)
162 FORMAT(1H0)
172 FORMAT(5X,12E12.5)
173 FORMAT(5X,10E12.5)
CLOSE(UNIT=1)
CLOSE(UNIT=2)
CLOSE(UNIT=3)
CLOSE(UNIT=4)
CLOSE(UNIT=5)
CLOSE(UNIT=6)
CLOSE(UNIT=7)
CLOSE(UNIT=8)
STOP
END

```

```

C*****
C*****SUBROUTINE TO SOLVE TRIDIAGONAL MATRIX*****

```

```

SUBROUTINE BST(N,A,B,C,D,H)
DIMENSION A(30),B(30),C(30),D(30),AL(30),BT(30),Y(30)
DIMENSION H(30)
AL(1)=B(1)
BT(1)=C(1)/B(1)
DO 100 I=2,N
AL(I)=B(I)-A(I)*BT(I-1)
BT(I)=C(I)/AL(I)
100 CONTINUE
Y(1)=D(1)/AL(1)
DO 120 I=2,N
Y(I)=(D(I)-A(I)*Y(I-1))/AL(I)
120 CONTINUE
H(N)=Y(N)
DO 300 I=2,N
II=N-I+1
H(II)=Y(II)-BT(II)*H(II+1)
300 CONTINUE
RETURN
END

```

```

C*****

```

```

SUBROUTINE MOVE(NTP,X,Y,VL,NRS,YF,U,V,DT,IN,DZ,YL,VE,
1VQ,DS,RW,VLL,XS,DTS,TSTR,PHI,VV,UU,DSA,NCS,TM,TPQ,XF,NC,VS)
DIMENSION X(5000),Y(5000),VL(30),UM(5000),VM(5000),VLL(5000)
DIMENSION YF(30),U(30,30),V(30,30),YL(30),IN(30),XS(30)
DIMENSION TEMP(5000),DZ(30),UU(30,30),VV(30,30),XF(30)
DIMENSION UA(30,30),VA(30,30),YM(5000)
IE=0.0
VE=0.0
ITQ=0
ITS=0
VS=0.0
VQ=0.0
IF(DTS.GE.DT) GO TO 250
NSTP=DT/DTS+1
DTSM=DT/FLOAT(NSTP)
DTSA=DTSM
GO TO 260
250 NSTP=1
DTSM=DT
DTSA=DTSM
260 DO 1000 IST=1,NSTP
IF(IST.LT.NSTP) GO TO 1500
DTSM=DT-(FLOAT(IST)-1.0)*DTSA
GO TO 1550
1500 DTSM=DTSA
1550 CONTINUE
WRITE(*,*)IST,NSTP
DO 100 K=1,NTP
IF(Y(K).EQ.1.0E+28)GO TO 700
DO 200 J=1,NC
IF(X(K).LT.XF(J).OR.X(K).GE.XF(J+1))GO TO 200
DO 300 I=1,NRS
IF(Y(K).LT.YF(I).OR.Y(K).GE.YF(I+1))GO TO 300
AA=(X(K)-XF(J))/(XF(J+1)-XF(J))
BB=(Y(K)-YF(I))/(YF(I+1)-YF(I))
UA(I,J)=(UU(I,J)+U(I,J))/2.0
UA(I,J+1)=(UU(I,J+1)+U(I,J+1))/2.0
UA(I+1,J)=(UU(I+1,J)+U(I+1,J))/2.0
UA(I+1,J+1)=(UU(I+1,J+1)+U(I+1,J+1))/2.0
CC=UA(I,J)+(UA(I,J+1)-UA(I,J))*AA
DD=UA(I+1,J)+(UA(I+1,J+1)-UA(I+1,J))*AA
UM(K)=CC+(DD-CC)*BB
VA(I,J)=(VV(I,J)+V(I,J))/2.0
VA(I,J+1)=(VV(I,J+1)+V(I,J+1))/2.0
VA(I+1,J)=(VV(I+1,J)+V(I+1,J))/2.0
VA(I+1,J+1)=(VV(I+1,J+1)+V(I+1,J+1))/2.0
CC=VA(I,J)+(VA(I,J+1)-VA(I,J))*AA
DD=VA(I+1,J)+(VA(I+1,J+1)-VA(I+1,J))*AA
VM(K)=CC+(DD-CC)*BB
GO TO 100
300 CONTINUE
200 CONTINUE
700 CONTINUE
UM(K)=0.0
VM(K)=0.0
100 CONTINUE
DO 400 I=1,NTP
YM(I)=Y(I)
X(I)=X(I)+UM(I)*DTSM
Y(I)=Y(I)+VM(I)*DTSM
IF(X(I).LT.RW) X(I)=RW
IF(Y(I).LT.YM(I).AND.TM.LE.TPQ) Y(I)=YM(I)

```

```

CONTINUE
NTT=NTP
IF(TM.GT.TPQ) GO TO 501
DO 500 J=1,NCS+1
K=IN(J)
AA=VM(K)*DTSM
YL(J)=YL(J)+AA
IF(YL(J).LT.TSTR)GO TO 500
ETP=YL(J)/TSTR
NMP=IFIX(ETP)
YL(J)=(ETP-FLOAT(NMP))*TSTR
IN(J)=NTP+NMP+1
DO 510 K=NTP+1,NTP+NMP
KK=K-NTP
Y(K)=FLOAT(KK)*TSTR+0.5*DZ(NRS-1)
XS(NCS+1)=RW
X(K)=XS(J)
VLL(K)=VL(J)*PHI
510 CONTINUE
X(IN(J))=XS(J)
Y(IN(J))=0.5*DZ(NRS-1)
NTP=NTP+NMP+1
IE=IE+NMP
VE=VE+VL(J)*PHI*FLOAT(NMP)
500 CONTINUE
501 CONTINUE
IF(Q.EQ.0.0) GO TO 1024
DO 1023 I=1,NTP
IF(X(I).LE.RW) X(I)=1.01*RW
1023 CONTINUE
1024 CONTINUE
DO 600 I=1,NTT
IF(X(I).GT.RW.OR.Y(I).LT.DS)GO TO 600
IF(Y(I).GT.DSA) GO TO 600
ITQ=ITQ+1
Y(I)=1.0E+28
VQ=VQ+VLL(I)
600 CONTINUE
DO 10 I=1,NTT
IF(Y(I)-0.5*DZ(NRS-1))20,10,10
20 ITS=ITS+1
VS=VS+VLL(I)
Y(I)=1.0E+28
10 CONTINUE
DO 3055 I=1,NTT
IF(I.GT.NTP) GO TO 3066
IF(Y(I).NE.1.0E+28) GO TO 3055
DO 605 II=I,NTP-1
TEMP(II)=X(II+1)
605 CONTINUE
DO 606 II=I,NTP-1
X(II)=TEMP(II)
606 CONTINUE
DO 607 II=I,NTP-1
TEMP(II)=Y(II+1)
607 CONTINUE
DO 608 II=I,NTP-1
Y(II)=TEMP(II)
608 CONTINUE
DO 609 II=I,NTP-1
TEMP(II)=VLL(II+1)
609 CONTINUE

```

```

DO 604 II=I,NTP-1
VLL(II)=TEMP(II)
604 CONTINUE
DO 1111 J=1,NCS
K=IN(J)
IF(K.GE.I) IN(J)=IN(J)-1
1111 CONTINUE
NTP=NTP-1
3055 CONTINUE
3066 CONTINUE
1000 CONTINUE
DTSM=DTSA
RETURN
END

```

```

C-----
SUBROUTINE DIFF(ITT,KOUNT1,NCS,NRS,VLA,STLS,DRS,DAA,DBB,
1DZ,DT,VLJ,RW,NRB,NRW,USS,VSS,DTS,XS,VLAQ,XU)
DIMENSION VLA(30,30),XS(30),QD(30,30),DRS(30),DZ(30)
DIMENSION USS(30,30),VSS(30,30),VLJ(30,30)
DIMENSION A(30),B(30),C(30),D(30),HH(30)
DIMENSION VLAP(30,30),VLAC(30,30),XU(30)
DO 75 I=1,NRS
DO 76 J=1,NCS
VLAC(I,J)=VLA(I,J)
QD(I,J)=(VLAC(I,J)-VLJ(I,J))/DT
76 CONTINUE
75 CONTINUE
IF(DTS.GE.DT) GO TO 250
NSTP=DT/DTS+1
DTSM=DT/FLOAT(NSTP)
DTSA=DTSM
GO TO 260
250 NSTP=1
DTSM=DT
DTSA=DTSM
260 DO 2000 IST=1,NSTP
IF(IST.LT.NSTP)GO TO 500
DTSM=DT-(FLOAT(IST)-1.0)*DTSA
GO TO 550
500 DTSM=DTSA
550 CONTINUE
DO 1000 ITT=1,KOUNT1
DO 100 J=1,NCS
DO 110 I=1,NRS
DA=ABS(DAA*USS(I,J))
DB=ABS(DBB*VSS(I,J))
IF(J.EQ.1.OR.J.EQ.NCS) GO TO 5
IF(I.EQ.1.OR.I.EQ.NRS) GO TO 6
R1=2.0*DB/(DZ(NRS-I)+DZ(NRS-I+1))
A(I)=R1/DZ(NRS-I+1)
R2=DA/(XS(J)*(DRS(J-1)+DRS(J)))
R4=(XS(J)+XS(J-1))/DRS(J-1)
R3=(XS(J+1)+XS(J))/DRS(J)
R5=-2.0*DB/(DZ(NRS-I)*DZ(NRS-I+1))-1.0/DTSM
B(I)=R2*(-R3-R4)+R5
C(I)=R1/DZ(NRS-I)
R6=R2*(VLA(I,J+1)*R3+VLA(I,J-1)*R4)
D(I)=-R6-QD(I,J)-VLJ(I,J)/DTSM
GO TO 115
5 IF(J.EQ.1) GO TO 7
A(I)=0.0
B(I)=1.0

```

```

C(I)=0.0
D(I)=0.0
GO TO 115
6 IF(I.EQ.NRS) GO TO 8
A(I)=0.0
B(I)=1.0
C(I)=0.0
D(I)=1.0
GO TO 115
7 IF(I.EQ.1) GO TO 6
IF(I.EQ.NRS) GO TO 9
R1=0.5*(DZ(NRS-I+1)+DZ(NRS-I))
A(I)=DB/(DZ(NRS-I+1)*R1)
R2=XU(1)/(XU(1)**2-RW**2)
B(I)=-2.*DA*R2/DRS(J)-2.*DB/(DZ(NRS-I+1)*DZ(NRS-I))-1./DTSM
C(I)=DB/(R1*DZ(NRS-I))
D(I)=-2.*DA*R2*VLA(I,J+1)/DRS(J)-QD(I,J)-VLI(I,J)/DTSM
IF(I.GE.(NRS-NRB+1).OR.I.LT.(NRS-NRW+1)) GO TO 115
CC=-2.*DA*RW/((XS(J)-RW)*(XU(J)**2-RW**2))
B(I)=B(I)+CC
D(I)=D(I)+CC*VLAQ
GO TO 115
9 A(I)=2.0*DB/(DZ(NRS-I+1)*DZ(NRS-I+1))
R1=XU(1)/(XU(1)**2-RW**2)
B(I)=-2.0*DA*R1/DRS(J)-A(I)-1.0/DTSM
C(I)=0.0
R2=-2.0*DA*R1*VLA(I,J+1)/DRS(J)
D(I)=R2-QD(I,J)-VLI(I,J)/DTSM
GO TO 115
8 A(I)=2.0*DB/(DZ(NRS-I+1)*DZ(NRS-I+1))
R1=XU(J-1)
R2=XU(J)
R3=(XU(J)**2-XU(J-1)**2)
B(I)=-2.*DA*(R1/DRS(J-1)+R2/DRS(J))/R3-A(I)-1./DTSM
C(I)=0.0
R4=-2.*DA*(R1*VLA(I,J-1)/DRS(J-1)+R2*VLA(I,J)/DRS(J))/R3
D(I)=R4-QD(I,J)-VLI(I,J)/DTSM
115 CONTINUE
110 CONTINUE
CALL BST(NRS,A,B,C,D,HH)
DO 120 I=1,NRS
VLA(I,J)=HH(I)
120 CONTINUE
100 CONTINUE
DO 70 I=1,NRS
DO 80 J=1,NCS
DA=ABS(DAA*USS(I,J))
DB=ABS(DBB*VSS(I,J))
IF(J.EQ.1.OR.J.EQ.NCS) GO TO 11
IF(I.EQ.1.OR.I.EQ.NRS) GO TO 12
R7=DA/(XS(J)*(DRS(J-1)+DRS(J)))
A(J)=R7*(XS(J)+XS(J-1))/DRS(J-1)
R8=(XS(J+1)+XS(J))/DRS(J)
R9=2.0*DB/(DZ(NRS-I)+DZ(NRS-I+1))
R10=-R7*(XS(J)+XS(J+1))/DRS(J)-A(J)
B(J)=R10+R9*(-1.0/DZ(NRS-I)-1.0/DZ(NRS-I+1))-1.0/DTSM
C(J)=R7*R8
R11=VLA(I+1,J)/DZ(NRS-I)+VLA(I-1,J)/DZ(NRS-I+1)
D(J)=-R9*R11-QD(I,J)-VLI(I,J)/DTSM
GO TO 85
11 IF(J.EQ.1) GO TO 13
A(J)=0.0

```

```

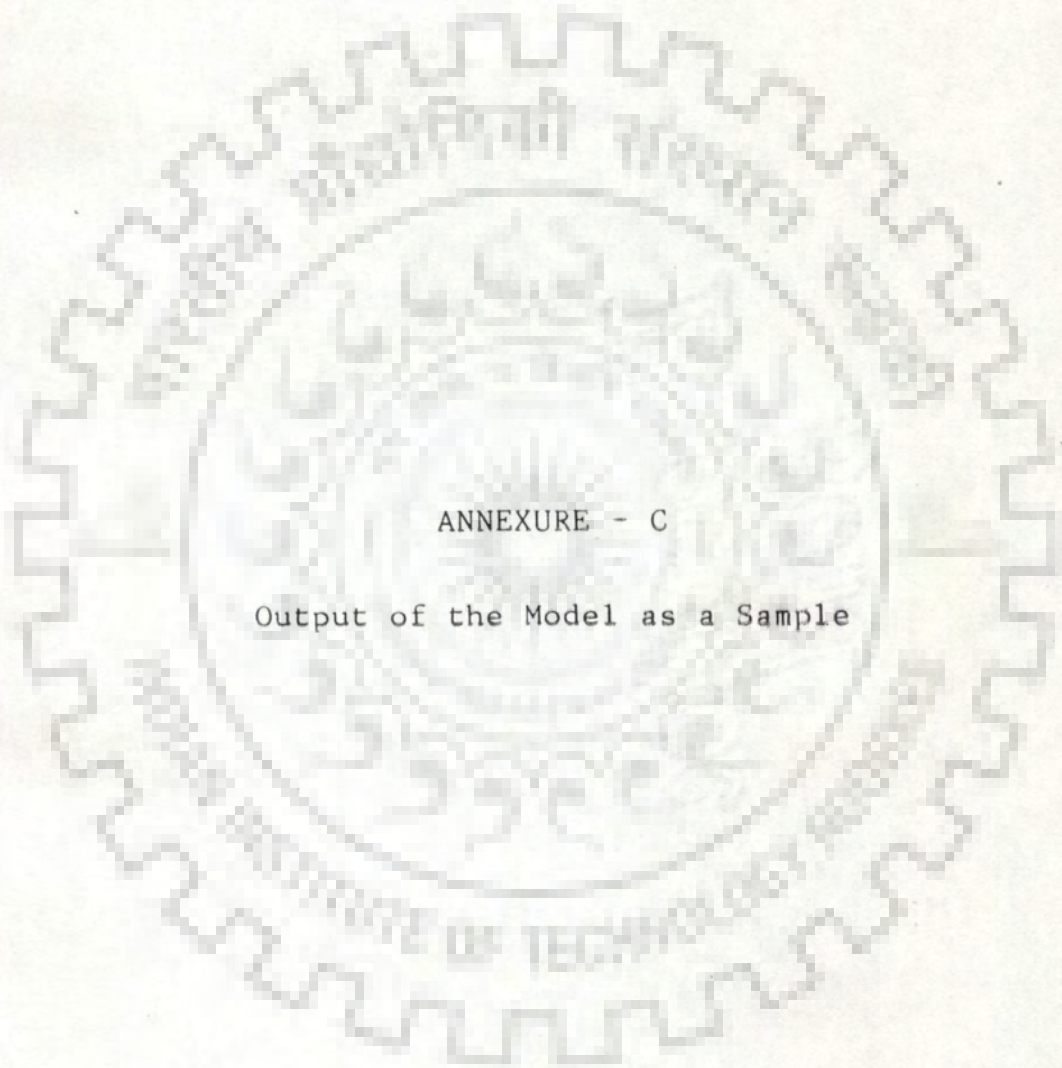
B(J)=1.0
C(J)=0.0
D(J)=0.0
GO TO 85
12 IF(I.EQ.NRS) GO TO 14
A(J)=0.0
B(J)=1.0
C(J)=0.0
D(J)=1.0
GO TO 85
13 IF(I.EQ.1) GO TO 12
IF(I.EQ.NRS) GO TO 16
A(J)=0.0
R1=0.5*(DZ(NRS-I+1)+DZ(NRS-I))
R2=XU(1)/(XU(1)**2-RW**2)
R4=(1.0/DZ(NRS-I+1)+1.0/DZ(NRS-I))
B(J)=-2.*DA*R2/DRS(J)-2.*DB/(DZ(NRS-I+1)*DZ(NRS-I))-1
1./DTSM
C(J)=2.*DA*R2/DRS(J)
R3=-DB*(VLA(I-1,J)/DZ(NRS-I+1)+VLA(I+1,J)/DZ(NRS-I))
D(J)=R3/R1-QD(I,J)-VLI(I,J)/DTSM
IF(I.GE.(NRS-NRB+1).OR.I.LT.(NRS-NRW+1)) GO TO 85
CC=-2.*DA*RW/((XS(J)-RW)*(XU(J)**2-RW**2))
B(J)=B(J)+CC
D(J)=D(J)+CC*VLAQ
GO TO 85
16 A(J)=0.0
R1=2.0*XU(1)/(XU(1)**2-RW**2)
R2=2.0*DB/(DZ(NRS-I+1)*DZ(NRS-I+1))
C(J)=DA*R1/DRS(J)
B(J)=-C(J)-R2-1.0/DTSM
D(J)=-R2*VLA(I-1,J)-QD(I,J)-VLI(I,J)/DTSM
GO TO 85
14 R1=XU(J-1)
R2=XU(J)
R3=(XU(J)**2-XU(J-1)**2)
A(J)=2.0*DA*R1/(R3*DRS(J-1))
R4=2.0*DB/(DZ(NRS-I+1)*DZ(NRS-I+1))
C(J)=2.0*DA*R2/(R3*DRS(J))
B(J)=-A(J)-C(J)-R4-1.0/DTSM
D(J)=-R4*VLA(I-1,J)-QD(I,J)-VLI(I,J)/DTSM
85 CONTINUE
80 CONTINUE
CALL BST(NCS,A,B,C,D,HH)
DO 90 J=1,NCS
VLA(I,J)=HH(J)
90 CONTINUE
70 CONTINUE
IF(ITT.EQ.1) GO TO 1050
SMS=0.0
DO 1010 I=1,NRS
DO 1020 J=1,NCS
SMS=SMS+ABS(VLA(I,J)-VLAP(I,J))
1020 CONTINUE
1010 CONTINUE
IF(SMS.LT.STLS) GO TO 20
1050 DO 1030 I=1,NRS
DO 1040 J=1,NCS
VLAP(I,J)=VLA(I,J)
1040 CONTINUE
1030 CONTINUE
SMPS=SMS

```

```
1000 CONTINUE
WRITE(26,145)
WRITE(*,145)
145  FORMAT(5X,'CONVERGENCSE NOT ACHIEVED VLA',I5,5X,E16.7)
20   CONTINUE
DO 71 I=1,NRS
DO 72 J=1,NCS
VLI(I,J)=VLA(I,J)
72  CONTINUE
71  CONTINUE
2000 CONTINUE
DTSM=DTSA
RETURN
END
```

186





ANNEXURE - C

Output of the Model as a Sample

CUMULATIVE TIME

.3037E+04 .4220E+04

CUMULATIVE SALT WATER ENTRY INTO WELL

.0000E+00 .0000E+00

CUMULATIVE SALT WATER LIFTING INTO SUSPENSION

.1325E+04 .1818E+04

NUMBER OF POINTS LIFTED

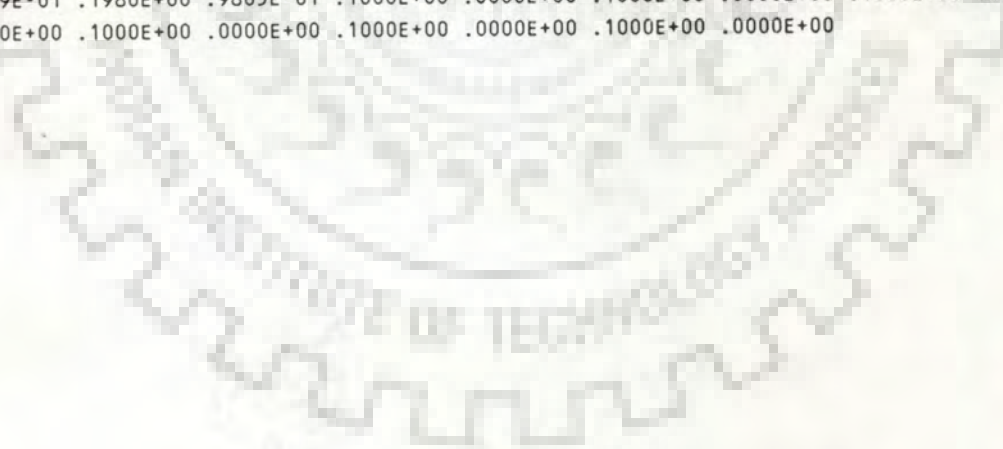
239 317

X-COORDINATES

.4026E+01	.7553E+01	.9923E+01	.1187E+02	.1355E+02	.1509E+02	.1647E+02	.1777E+02	.1896E+02	.2011E+02
.2118E+02	.2219E+02	.2319E+02	.2413E+02	.2505E+02	.2592E+02	.2676E+02	.2761E+02	.2840E+02	.2918E+02
.2995E+02	.3069E+02	.3141E+02	.3211E+02	.3281E+02	.3349E+02	.3415E+02	.3480E+02	.3544E+02	.2071E+00
.4057E+01	.4069E+01	.2067E+00	.2072E+00	.7612E+01	.7625E+01	.9974E+01	.9992E+01	.4096E+01	.4108E+01
.1196E+02	.1196E+02	.1363E+02	.1364E+02	.1516E+02	.1516E+02	.2067E+00	.2070E+00	.7679E+01	.7692E+01
.1004E+02	.1005E+02	.1658E+02	.1659E+02	.1786E+02	.1788E+02	.1906E+02	.1906E+02	.2067E+00	.2069E+00
.4171E+01	.4160E+01	.4182E+01	.7732E+01	.7743E+01	.1204E+02	.1206E+02	.1372E+02	.1374E+02	.2024E+02
.2024E+02	.2131E+02	.2131E+02	.2233E+02	.2234E+02	.2331E+02	.2332E+02	.2425E+02	.2425E+02	.2516E+02
.2516E+02	.2604E+02	.2604E+02	.2065E+00	.2067E+00	.1014E+02	.1015E+02	.1528E+02	.1528E+02	.1666E+02
.1666E+02	.2690E+02	.2691E+02	.2772E+02	.2773E+02	.2853E+02	.2853E+02	.2930E+02	.2930E+02	.2065E+00
.2065E+00	.4227E+01	.4236E+01	.7805E+01	.7814E+01	.1211E+02	.1213E+02	.1797E+02	.1797E+02	.1916E+02
.1917E+02	.3008E+02	.3008E+02	.3081E+02	.3081E+02	.3154E+02	.3154E+02	.3224E+02	.3224E+02	.3293E+02
.3293E+02	.3360E+02	.3360E+02	.3426E+02	.3427E+02	.3492E+02	.3492E+02	.3555E+02	.3555E+02	.2064E+00
.2064E+00	.4263E+01	.4271E+01	.7852E+01	.7860E+01	.1022E+02	.1023E+02	.1217E+02	.1217E+02	.1384E+02
.1385E+02	.1535E+02	.1537E+02	.2033E+02	.2034E+02	.2140E+02	.2141E+02	.2242E+02	.2242E+02	.2062E+00
.2061E+00	.4299E+01	.4304E+01	.7898E+01	.7904E+01	.1028E+02	.1028E+02	.1389E+02	.1390E+02	.1678E+02
.1679E+02	.1806E+02	.1807E+02	.2344E+02	.2344E+02	.2438E+02	.2438E+02	.2527E+02	.2528E+02	.2059E+00
.2058E+00	.4328E+01	.4331E+01	.7940E+01	.7945E+01	.1032E+02	.1033E+02	.1226E+02	.1227E+02	.1545E+02
.1545E+02	.1929E+02	.1929E+02	.2041E+02	.2042E+02	.2618E+02	.2618E+02	.2702E+02	.2702E+02	.2784E+02
.2784E+02	.2057E+00	.2053E+00	.4356E+01	.4358E+01	.1398E+02	.1399E+02	.1687E+02	.1687E+02	.2152E+02
.2152E+02	.2253E+02	.2254E+02	.2866E+02	.2867E+02	.2944E+02	.2944E+02	.2052E+00	.2047E+00	.4383E+01
.4384E+01	.8021E+01	.8024E+01	.1041E+02	.1041E+02	.1235E+02	.1235E+02	.1553E+02	.1554E+02	.1818E+02
.1818E+02	.2354E+02	.2354E+02	.2447E+02	.2448E+02	.3022E+02	.3022E+02	.3095E+02	.3095E+02	.3167E+02
.3167E+02	.3237E+02	.3237E+02	.3305E+02	.3306E+02	.3373E+02	.3373E+02	.2046E+00	.2042E+00	.4406E+01
.4407E+01	.8059E+01	.8061E+01	.1045E+02	.1045E+02	.1407E+02	.1407E+02	.1695E+02	.1695E+02	.1941E+02
.1941E+02	.2053E+02	.2053E+02	.2541E+02	.2541E+02	.2628E+02	.2628E+02	.3441E+02	.3441E+02	.3506E+02
.3506E+02	.3569E+02	.3570E+02	.2041E+00	.2038E+00	.4428E+01	.4429E+01	.8096E+01	.8097E+01	.1244E+02
.1244E+02	.1562E+02	.1562E+02	.1826E+02	.1826E+02	.2163E+02	.2163E+02	.2715E+02	.2715E+02	.2037E+00
.2035E+00	.4451E+01	.4451E+01	.1054E+02	.1054E+02	.1248E+02	.1248E+02	.1416E+02	.1416E+02	.1704E+02
.1704E+02	.1949E+02	.1949E+02	.2268E+02	.2268E+02	.2365E+02	.2365E+02	.2800E+02	.2800E+02	.2879E+02
.2879E+02	.2034E+00	.2033E+00	.4473E+01	.4473E+01	.8169E+01	.8169E+01	.1571E+02	.1571E+02	.2065E+02
.2065E+02	.2462E+02	.2462E+02	.2959E+02	.2959E+02	.2032E+00	.2032E+00			

Y-COORDINATES

.1436E+01	.1159E+01	.9822E+00	.8551E+00	.7512E+00	.6903E+00	.6362E+00	.5857E+00	.5387E+00	.4955E+00
.4720E+00	.4500E+00	.4285E+00	.4082E+00	.3885E+00	.3696E+00	.3515E+00	.3333E+00	.3160E+00	.2994E+00
.2883E+00	.2846E+00	.2809E+00	.2773E+00	.2739E+00	.2704E+00	.2671E+00	.2638E+00	.2604E+00	.1524E+01
.1421E+01	.1320E+01	.1497E+01	.1393E+01	.1130E+01	.1035E+01	.9723E+00	.8795E+00	.1315E+01	.1215E+01
.8246E+00	.7325E+00	.7362E+00	.6448E+00	.6852E+00	.5937E+00	.1381E+01	.1280E+01	.1017E+01	.9201E+00
.8782E+00	.7841E+00	.6047E+00	.5115E+00	.5651E+00	.4710E+00	.5275E+00	.4334E+00	.1290E+01	.1191E+01
.1116E+01	.1216E+01	.1016E+01	.9253E+00	.8284E+00	.7126E+00	.6184E+00	.6390E+00	.5452E+00	.4562E+00
.3618E+00	.4393E+00	.3448E+00	.4231E+00	.3285E+00	.4075E+00	.3131E+00	.3927E+00	.2983E+00	.3784E+00
.2839E+00	.3645E+00	.2700E+00	.1167E+01	.1068E+01	.7503E+00	.6548E+00	.5602E+00	.4653E+00	.5239E+00
.4289E+00	.3327E+00	.2379E+00	.3206E+00	.2257E+00	.3087E+00	.2139E+00	.2972E+00	.2024E+00	.1084E+01
.9844E+00	.9592E+00	.8587E+00	.8007E+00	.7032E+00	.6228E+00	.5271E+00	.4595E+00	.3643E+00	.4304E+00
.3354E+00	.2752E+00	.1800E+00	.2732E+00	.1779E+00	.2712E+00	.1759E+00	.2693E+00	.1739E+00	.2674E+00
.1719E+00	.2655E+00	.1700E+00	.2637E+00	.1681E+00	.2618E+00	.1662E+00	.2601E+00	.1644E+00	.1000E+01
.9011E+00	.8547E+00	.7544E+00	.7156E+00	.6177E+00	.6260E+00	.5293E+00	.5601E+00	.4637E+00	.5059E+00
.4101E+00	.4738E+00	.3779E+00	.3699E+00	.2744E+00	.3569E+00	.2613E+00	.3444E+00	.2489E+00	.8936E+00
.7941E+00	.7506E+00	.6504E+00	.6304E+00	.5323E+00	.5532E+00	.4559E+00	.4509E+00	.3546E+00	.3983E+00
.3021E+00	.3751E+00	.2789E+00	.3018E+00	.2057E+00	.2918E+00	.1957E+00	.2822E+00	.1861E+00	.7866E+00
.6869E+00	.6570E+00	.5568E+00	.5543E+00	.4559E+00	.4883E+00	.3907E+00	.4403E+00	.3432E+00	.3777E+00
.2810E+00	.3178E+00	.2212E+00	.3018E+00	.2053E+00	.2486E+00	.1520E+00	.2409E+00	.1442E+00	.2333E+00
.1367E+00	.6883E+00	.5886E+00	.5635E+00	.4634E+00	.3515E+00	.2542E+00	.3141E+00	.2169E+00	.2607E+00
.1636E+00	.2528E+00	.1558E+00	.2054E+00	.1082E+00	.1994E+00	.1022E+00	.5900E+00	.4902E+00	.4701E+00
.3700E+00	.4020E+00	.3032E+00	.3583E+00	.2601E+00	.3269E+00	.2290E+00	.2860E+00	.1883E+00	.2587E+00
.1611E+00	.2169E+00	.1193E+00	.2111E+00	.1135E+00	.1776E+00	.7992E-01	.1768E+00	.7909E-01	.1761E+00
.7828E-01	.1753E+00	.7749E-01	.1746E+00	.7672E-01	.1738E+00	.7596E-01	.4916E+00	.3919E+00	.3774E+00
.2773E+00	.3266E+00	.2275E+00	.2939E+00	.1953E+00	.2514E+00	.1532E+00	.2291E+00	.1309E+00	.2100E+00
.1118E+00	.2022E+00	.1040E+00	.1793E+00	.8104E-01	.1752E+00	.7695E-01	.1550E+00	.5655E-01	.1545E+00
.5600E-01	.1539E+00	.5545E-01	.3938E+00	.2940E+00	.2848E+00	.1848E+00	.2511E+00	.1517E+00	.2137E+00
.1148E+00	.1933E+00	.9451E-01	.1796E+00	.8082E-01	.1649E+00	.6615E-01	.1476E+00	.4876E-01	.2959E+00
.1960E+00	.1923E+00	.9232E-01	.1648E+00	.6523E-01	.1569E+00	.5746E-01	.1507E+00	.5125E-01	.1432E+00
.4378E-01	.1368E+00	.3739E-01	.1309E+00	.3154E-01	.1294E+00	.3001E-01	.1225E+00	.2314E-01	.1213E+00
.2189E-01	.1980E+00	.9805E-01	.1000E+00	.0000E+00	.1000E+00	.0000E+00	.1000E+00	.0000E+00	.1000E+00
.0000E+00	.1000E+00	.0000E+00	.1000E+00	.0000E+00	.1000E+00	.0000E+00	.0000E+00	.0000E+00	.1000E+00



CUMULATIVE TIME

.2880E+05 .3456E+05

CUMULATIVE SALT WATER ENTRY INTO WELL

.9303E+02 .1861E+03

CUMULATIVE SALT WATER LIFTING INTO SUSPENSION

.1044E+05 .1194E+05

NUMBER OF POINTS LIFTED

1546 1698

X-COORDINATES

.2668E+01	.6644E+01	.9020E+01	.1100E+02	.1281E+02	.1456E+02	.1610E+02	.1742E+02	.1859E+02	.1974E+02
.2079E+02	.2179E+02	.2274E+02	.2361E+02	.2450E+02	.2531E+02	.2611E+02	.2689E+02	.2763E+02	.2836E+02
.2905E+02	.2977E+02	.3047E+02	.3114E+02	.3182E+02	.3249E+02	.3173E+01	.3871E+01	.6840E+01	.7244E+01
.9137E+01	.9424E+01	.1122E+02	.1145E+02	.1299E+02	.1323E+02	.1471E+02	.1488E+02	.4160E+01	.4792E+01
.7375E+01	.7752E+01	.1632E+02	.1646E+02	.1761E+02	.1775E+02	.1879E+02	.1891E+02	.1989E+02	.2001E+02
.2093E+02	.2103E+02	.2193E+02	.2202E+02	.2286E+02	.2294E+02	.9662E+01	.9948E+01	.1151E+02	.1174E+02
.2377E+02	.2385E+02	.2462E+02	.2469E+02	.2545E+02	.2551E+02	.2624E+02	.2630E+02	.4852E+01	.5438E+01
.1338E+02	.1360E+02	.1503E+02	.1521E+02	.2703E+02	.2709E+02	.2775E+02	.2782E+02	.2849E+02	.2856E+02
.2919E+02	.2925E+02	.2989E+02	.2996E+02	.3059E+02	.3064E+02	.3127E+02	.3133E+02	.3194E+02	.3200E+02
.3260E+02	.3265E+02	.4316E+00	.2181E+01	.5315E+01	.5819E+01	.8022E+01	.8370E+01	.1001E+02	.1030E+02
.1656E+02	.1673E+02	.1783E+02	.1798E+02	.1898E+02	.1911E+02	.2026E+01	.2938E+01	.8282E+01	.8618E+01
.1195E+02	.1221E+02	.1369E+02	.1391E+02	.2015E+02	.2027E+02	.2117E+02	.2128E+02	.2213E+02	.2222E+02
.2734E+01	.3506E+01	.6076E+01	.6516E+01	.1040E+02	.1064E+02	.1539E+02	.1555E+02	.1677E+02	.1693E+02
.2309E+02	.2317E+02	.2396E+02	.2404E+02	.2480E+02	.2486E+02	.8730E+01	.9058E+01	.1226E+02	.1250E+02
.1810E+02	.1822E+02	.1922E+02	.1935E+02	.2565E+02	.2572E+02	.2644E+02	.2650E+02	.3830E+01	.4439E+01
.6698E+01	.7068E+01	.1072E+02	.1097E+02	.1410E+02	.1429E+02	.2036E+02	.2047E+02	.2135E+02	.2146E+02
.2723E+02	.2730E+02	.2796E+02	.2803E+02	.2868E+02	.2874E+02	.2938E+02	.2944E+02	.3008E+02	.3015E+02
.3078E+02	.3083E+02	.5313E+00	.4290E+01	.4851E+01	.9158E+01	.9438E+01	.1257E+02	.1279E+02	.1571E+02
.1588E+02	.1705E+02	.1719E+02	.2236E+02	.2244E+02	.2326E+02	.2332E+02	.3147E+02	.3154E+02	.3215E+02
.3221E+02	.3280E+02	.3287E+02	.1778E+01	.7244E+01	.7590E+01	.1104E+02	.1129E+02	.1437E+02	.1454E+02
.1834E+02	.1846E+02	.2417E+02	.2423E+02	.5112E+01	.5555E+01	.7484E+01	.7834E+01	.9559E+01	.9815E+01
.1288E+02	.1308E+02	.1594E+02	.1608E+02	.1953E+02	.1965E+02	.2057E+02	.2066E+02	.2505E+02	.2510E+02
.2583E+02	.2590E+02	.2361E+01	.3041E+01	.1137E+02	.1158E+02	.1733E+02	.1745E+02	.2161E+02	.2170E+02
.2665E+02	.2672E+02	.2967E+01	.3536E+01	.5779E+01	.6140E+01	.8005E+01	.8317E+01	.9926E+01	.1015E+02
.1474E+02	.1491E+02	.1859E+02	.1871E+02	.2260E+02	.2267E+02	.2347E+02	.2354E+02	.2745E+02	.2751E+02
.2818E+02	.2824E+02	.2888E+02	.2895E+02	.2958E+02	.2964E+02	.3029E+02	.3033E+02	.3473E+01	.3959E+01
.6081E+01	.6424E+01	.1169E+02	.1191E+02	.1331E+02	.1351E+02	.1625E+02	.1638E+02	.1977E+02	.1987E+02
.2437E+02	.2444E+02	.3102E+02	.3106E+02	.3168E+02	.3175E+02	.3234E+02	.3240E+02	.3299E+02	.3304E+02
.3906E+01	.4327E+01	.6356E+01	.6683E+01	.8490E+01	.8756E+01	.1027E+02	.1049E+02	.1499E+02	.1515E+02
.1760E+02	.1772E+02	.2086E+02	.2094E+02	.2180E+02	.2189E+02	.2524E+02	.2531E+02	.8705E+01	.8942E+01
.1200E+02	.1221E+02	.1361E+02	.1379E+02	.1646E+02	.1658E+02	.1884E+02	.1895E+02	.2277E+02	.2286E+02
.2608E+02	.2614E+02	.4613E+01	.4911E+01	.6875E+01	.7151E+01	.1059E+02	.1080E+02	.1523E+02	.1538E+02
.1999E+02	.2010E+02	.2370E+02	.2377E+02	.2689E+02	.2696E+02	.2763E+02	.2769E+02	.4868E+01	.5131E+01
.7094E+01	.7345E+01	.9064E+01	.9259E+01	.1230E+02	.1248E+02	.1387E+02	.1404E+02	.1787E+02	.1798E+02
.2105E+02	.2115E+02	.2459E+02	.2464E+02	.2841E+02	.2847E+02	.2911E+02	.2918E+02	.2981E+02	.2987E+02
.3050E+02	.3056E+02	.5093E+01	.5334E+01	.1087E+02	.1105E+02	.1673E+02	.1684E+02	.1908E+02	.1917E+02
.2205E+02	.2212E+02	.2545E+02	.2551E+02	.3122E+02	.3128E+02	.3190E+02	.3194E+02	.3255E+02	.3261E+02
.3319E+02	.3325E+02	.7470E+01	.7680E+01	.9352E+01	.9525E+01	.1099E+02	.1118E+02	.1254E+02	.1272E+02

.1409E+02	.1425E+02	.1552E+02	.1564E+02	.2020E+02	.2029E+02	.2301E+02	.2307E+02	.2628E+02	.2633E+02
.5491E+01	.5687E+01	.7637E+01	.7826E+01	.9481E+01	.9640E+01	.1810E+02	.1820E+02	.2123E+02	.2131E+02
.2390E+02	.2398E+02	.5663E+01	.5841E+01	.1126E+02	.1141E+02	.1570E+02	.1582E+02	.1697E+02	.1709E+02
.1930E+02	.1939E+02	.2223E+02	.2230E+02	.2479E+02	.2485E+02	.2712E+02	.2719E+02	.2787E+02	.2793E+02
.9379E+00	.5824E+01	.5978E+01	.7922E+01	.8068E+01	.9729E+01	.9882E+01	.1290E+02	.1305E+02	.1442E+02
.1454E+02	.2040E+02	.2047E+02	.2863E+02	.2869E+02	.2935E+02	.2940E+02	.3005E+02	.3010E+02	.3072E+02
.3079E+02	.9376E+00	.1338E+01	.1149E+02	.1162E+02	.1833E+02	.1841E+02	.2322E+02	.2328E+02	.2569E+02
.2574E+02	.3144E+02	.3151E+02	.3211E+02	.3216E+02	.3276E+02	.3281E+02	.3340E+02	.3344E+02	.1355E+01
.1657E+01	.6089E+01	.6200E+01	.8161E+01	.8284E+01	.9957E+01	.1009E+02	.1312E+02	.1326E+02	.1460E+02
.1473E+02	.1595E+02	.1606E+02	.1721E+02	.1731E+02	.1950E+02	.1959E+02	.2147E+02	.2155E+02	.2412E+02
.2418E+02	.2652E+02	.2656E+02	.6197E+01	.6288E+01	.8268E+01	.8375E+01	.1167E+02	.1180E+02	.2245E+02
.2251E+02	.2500E+02	.2504E+02	.2732E+02	.2737E+02	.1941E+01	.2149E+01	.1015E+02	.1026E+02	.1332E+02
.1344E+02	.1477E+02	.1487E+02	.1610E+02	.1620E+02	.1736E+02	.1745E+02	.1855E+02	.1861E+02	.2063E+02
.2071E+02	.2338E+02	.2343E+02	.2811E+02	.2816E+02	.2168E+01	.2347E+01	.6372E+01	.6435E+01	.8448E+01
.8536E+01	.1969E+02	.1976E+02	.2164E+02	.2171E+02	.2589E+02	.2593E+02	.2887E+02	.2892E+02	.2957E+02
.2964E+02	.3028E+02	.3033E+02	.3096E+02	.3101E+02	.3163E+02	.3168E+02	.2369E+01	.2521E+01	.6444E+01
.6494E+01	.1032E+02	.1042E+02	.1196E+02	.1206E+02	.1349E+02	.1360E+02	.1867E+02	.1873E+02	.2260E+02
.2266E+02	.2433E+02	.2437E+02	.2671E+02	.2676E+02	.3233E+02	.3239E+02	.3298E+02	.3302E+02	.3361E+02
.3367E+02	.2541E+01	.2674E+01	.6507E+01	.6544E+01	.8616E+01	.8685E+01	.1500E+02	.1509E+02	.1633E+02
.1641E+02	.1757E+02	.1764E+02	.2080E+02	.2086E+02	.2519E+02	.2523E+02	.2695E+01	.2807E+01	.8687E+01
.8746E+01	.1048E+02	.1056E+02	.1212E+02	.1221E+02	.1366E+02	.1375E+02	.1987E+02	.1993E+02	.2181E+02
.2186E+02	.2358E+02	.2363E+02	.2756E+02	.2761E+02	.2829E+01	.2923E+01	.6605E+01	.6622E+01	.1055E+02
.1062E+02	.1515E+02	.1522E+02	.1647E+02	.1654E+02	.1769E+02	.1775E+02	.1885E+02	.1892E+02	.2608E+02
.2613E+02	.2835E+02	.2840E+02	.2906E+02	.2911E+02	.2943E+01	.3021E+01	.6645E+01	.6656E+01	.8812E+01
.8852E+01	.1227E+02	.1235E+02	.2096E+02	.2101E+02	.2281E+02	.2286E+02	.2452E+02	.2456E+02	.2981E+02
.2987E+02	.3051E+02	.3056E+02	.3118E+02	.3123E+02	.3186E+02	.3190E+02	.1385E+02	.1391E+02	.2001E+02
.2007E+02	.3253E+02	.3258E+02	.3317E+02	.3321E+02	.3381E+02	.3386E+02	.3073E+01	.3131E+01	.6688E+01
.6691E+01	.8884E+01	.8918E+01	.1071E+02	.1077E+02	.1237E+02	.1243E+02	.1531E+02	.1536E+02	.1661E+02
.1666E+02	.2197E+02	.2201E+02	.2374E+02	.2379E+02	.2539E+02	.2544E+02	.2697E+02	.2701E+02	.3142E+01
.3190E+01	.1787E+02	.1792E+02	.1903E+02	.1908E+02	.3202E+01	.3244E+01	.6731E+01	.6725E+01	.8964E+01
.8990E+01	.1081E+02	.1086E+02	.1401E+02	.1407E+02	.2111E+02	.2116E+02	.2295E+02	.2299E+02	.2466E+02
.2470E+02	.2627E+02	.2631E+02	.2780E+02	.2784E+02	.1253E+02	.1258E+02	.1545E+02	.1550E+02	.1674E+02
.1680E+02	.2018E+02	.2021E+02	.2856E+02	.2862E+02	.3309E+01	.3340E+01	.6764E+01	.6750E+01	.9036E+01
.9056E+01	.1090E+02	.1094E+02	.1411E+02	.1416E+02	.1800E+02	.1804E+02	.1915E+02	.1919E+02	.2213E+02
.2216E+02	.2932E+02	.2937E+02	.3003E+02	.3007E+02	.3072E+02	.3077E+02	.3140E+02	.3145E+02	.3207E+02
.3211E+02	.3272E+02	.3277E+02	.3356E+01	.3380E+01	.6777E+01	.6759E+01	.1263E+02	.1267E+02	.1554E+02
.1559E+02	.2123E+02	.2126E+02	.2393E+02	.2397E+02	.2559E+02	.2563E+02	.2716E+02	.2720E+02	.3340E+02
.3345E+02	.3403E+02	.3407E+02	.2032E+00	.3397E+01	.3415E+01	.9102E+01	.9115E+01	.1099E+02	.1101E+02
.1688E+02	.1691E+02	.2310E+02	.2313E+02	.2032E+00	.2032E+00	.6798E+01	.6779E+01	.1271E+02	.1276E+02
.1424E+02	.1428E+02	.1812E+02	.1816E+02	.2032E+02	.2036E+02	.2484E+02	.2488E+02	.2032E+00	.2032E+00
.3465E+01	.3472E+01	.9161E+01	.9167E+01	.1106E+02	.1108E+02	.1567E+02	.1570E+02	.1931E+02	.1934E+02
.2227E+02	.2230E+02	.2649E+02	.2653E+02	.2802E+02	.2806E+02	.2032E+00	.2032E+00	.3492E+01	.3492E+01
.6819E+01	.6801E+01	.9191E+01	.9192E+01	.1433E+02	.1436E+02	.1700E+02	.1702E+02	.2137E+02	.2140E+02
.2408E+02	.2411E+02	.2879E+02	.2883E+02	.2032E+00	.2032E+00	.3513E+01	.3509E+01	.6830E+01	.6812E+01
.1113E+02	.1115E+02	.1284E+02	.1286E+02	.2577E+02	.2581E+02	.2954E+02	.2959E+02	.3025E+02	.3029E+02
.3095E+02	.3099E+02	.3163E+02	.3167E+02	.3229E+02	.3233E+02	.3295E+02	.3299E+02	.3358E+02	.3362E+02
.3422E+02	.3425E+02	.2032E+00	.2032E+00	.9232E+01	.9241E+01	.1578E+02	.1581E+02	.1827E+02	.1831E+02
.1942E+02	.1945E+02	.2046E+02	.2049E+02	.2327E+02	.2331E+02	.2738E+02	.2742E+02	.2032E+00	.2032E+00
.3544E+01	.3530E+01	.6854E+01	.6836E+01	.1120E+02	.1121E+02	.1291E+02	.1293E+02	.1444E+02	.1446E+02
.1710E+02	.1713E+02	.2241E+02	.2244E+02	.2503E+02	.2506E+02	.2032E+00	.2032E+00	.3554E+01	.3535E+01
.9282E+01	.9281E+01	.1585E+02	.1588E+02	.2151E+02	.2154E+02	.2668E+02	.2670E+02	.2032E+00	.2032E+00
.3559E+01	.3536E+01	.6878E+01	.6863E+01	.1126E+02	.1127E+02	.1298E+02	.1300E+02	.1451E+02	.1453E+02
.1839E+02	.1840E+02	.2057E+02	.2059E+02	.2425E+02	.2429E+02	.2824E+02	.2827E+02	.2032E+00	.2032E+00
.6892E+01	.6876E+01	.9331E+01	.9330E+01	.1721E+02	.1723E+02	.1956E+02	.1958E+02	.2341E+02	.2345E+02
.2595E+02	.2598E+02	.2032E+00	.2032E+00	.3559E+01	.3528E+01	.1133E+02	.1133E+02	.1304E+02	.1306E+02

.1595E+02	.1598E+02	.2255E+02	.2257E+02	.2756E+02	.2758E+02	.2905E+02	.2908E+02	.2977E+02	.2979E+02
.3047E+02	.3051E+02	.3117E+02	.3120E+02	.3184E+02	.3188E+02	.3251E+02	.3254E+02	.3316E+02	.3319E+02
.3380E+02	.3384E+02	.3443E+02	.3446E+02	.2032E+00	.2032E+00	.3554E+01	.3520E+01	.6920E+01	.6906E+01
.9381E+01	.9379E+01	.1461E+02	.1462E+02	.1848E+02	.1850E+02	.2164E+02	.2166E+02	.2520E+02	.2522E+02
.2032E+00	.2032E+00	.3547E+01	.3512E+01	.2069E+02	.2071E+02	.2439E+02	.2441E+02	.6951E+01	.6942E+01
.9430E+01	.9428E+01	.1141E+02	.1142E+02	.1314E+02	.1314E+02	.1467E+02	.1468E+02	.1605E+02	.1606E+02
.1733E+02	.1735E+02	.1968E+02	.1969E+02	.2687E+02	.2691E+02	.2032E+00	.2032E+00	.3531E+01	.3496E+01
.2357E+02	.2359E+02	.2611E+02	.2614E+02	.2844E+02	.2847E+02	.3523E+01	.3487E+01	.6987E+01	.6980E+01
.9469E+01	.9467E+01	.1146E+02	.1146E+02	.1320E+02	.1320E+02	.1860E+02	.1861E+02	.2270E+02	.2271E+02
.2921E+02	.2923E+02	.2993E+02	.2995E+02	.3063E+02	.3067E+02	.3133E+02	.3136E+02	.3201E+02	.3204E+02
.3268E+02	.3270E+02	.3332E+02	.3336E+02	.3397E+02	.3399E+02	.3459E+02	.3463E+02	.2032E+00	.2032E+00
.7006E+01	.7000E+01	.1475E+02	.1476E+02	.1613E+02	.1614E+02	.1742E+02	.1743E+02	.2178E+02	.2179E+02
.2535E+02	.2537E+02	.2774E+02	.2776E+02	.3505E+01	.3469E+01	.9518E+01	.9516E+01	.1151E+02	.1152E+02
.1978E+02	.1979E+02	.2083E+02	.2084E+02	.2454E+02	.2456E+02	.3496E+01	.3459E+01	.7046E+01	.7044E+01
.1328E+02	.1329E+02	.2369E+02	.2370E+02	.2703E+02	.2705E+02	.2037E+00	.2044E+00	.3485E+01	.3452E+01
.9568E+01	.9567E+01	.1157E+02	.1157E+02	.1483E+02	.1483E+02	.1522E+02	.1623E+02	.1750E+02	.1751E+02
.1870E+02	.1871E+02	.2281E+02	.2282E+02	.7091E+01	.7091E+01	.1333E+02	.1334E+02	.2189E+02	.2190E+02
.2629E+02	.2631E+02	.2863E+02	.2864E+02	.3216E+02	.3220E+02	.3283E+02	.3286E+02	.3349E+02	.3351E+02
.3413E+02	.3415E+02	.3476E+02	.3478E+02	.3474E+01	.3449E+01	.9619E+01	.9620E+01	.1989E+02	.1990E+02
.2093E+02	.2094E+02	.2550E+02	.2551E+02	.2939E+02	.2941E+02	.3011E+02	.3014E+02	.3083E+02	.3085E+02
.3152E+02	.3154E+02	.3474E+01	.3453E+01	.7139E+01	.7142E+01	.1164E+02	.1165E+02	.1491E+02	.1492E+02
.1630E+02	.1630E+02	.2468E+02	.2470E+02	.2792E+02	.2795E+02	.2071E+00	.2078E+00	.3476E+01	.3459E+01
.9661E+01	.9664E+01	.1341E+02	.1342E+02	.1760E+02	.1761E+02	.1381E+02	.1882E+02	.2383E+02	.2385E+02
.2718E+02	.2719E+02	.7189E+01	.7194E+01	.1170E+02	.1170E+02	.1497E+02	.1497E+02	.2294E+02	.2295E+02
.3492E+01	.3484E+01	.7216E+01	.7221E+01	.9716E+01	.9720E+01	.1347E+02	.1347E+02	.1637E+02	.1638E+02
.1999E+02	.1999E+02	.2103E+02	.2104E+02	.2202E+02	.2203E+02	.2644E+02	.2645E+02	.2877E+02	.2878E+02
.3365E+02	.3367E+02	.3428E+02	.3430E+02	.3491E+02	.3494E+02	.3506E+01	.3501E+01	.1175E+02	.1176E+02
.1768E+02	.1768E+02	.1889E+02	.1889E+02	.2564E+02	.2565E+02	.3098E+02	.3099E+02	.3167E+02	.3169E+02
.3236E+02	.3238E+02	.3302E+02	.3304E+02	.2090E+00	.2090E+00	.7268E+01	.7275E+01	.9772E+01	.9777E+01
.1504E+02	.1504E+02	.2482E+02	.2483E+02	.2808E+02	.2809E+02	.2958E+02	.2959E+02	.3030E+02	.3032E+02
.3541E+01	.3542E+01	.1181E+02	.1181E+02	.1354E+02	.1354E+02	.2396E+02	.2397E+02	.3562E+01	.3565E+01
.7324E+01	.7331E+01	.9821E+01	.9827E+01	.1647E+02	.1647E+02	.2112E+02	.2113E+02	.2212E+02	.2212E+02
.2307E+02	.2308E+02	.2734E+02	.2735E+02	.1510E+02	.1511E+02	.1777E+02	.1777E+02	.1897E+02	.1897E+02
.2010E+02	.2010E+02	.2657E+02	.2658E+02	.3443E+02	.3444E+02	.3506E+02	.3507E+02	.3609E+01	.3618E+01
.7379E+01	.7387E+01	.1188E+02	.1188E+02	.1361E+02	.1361E+02	.2576E+02	.2577E+02	.2893E+02	.2894E+02
.3249E+02	.3250E+02	.3316E+02	.3317E+02	.3381E+02	.3383E+02	.2066E+00	.2057E+00	.3636E+01	.3647E+01
.9899E+01	.9905E+01	.1653E+02	.1653E+02	.2493E+02	.2494E+02	.3042E+02	.3044E+02	.3114E+02	.3115E+02
.3183E+02	.3184E+02	.7435E+01	.7444E+01	.1517E+02	.1517E+02	.2407E+02	.2408E+02	.2822E+02	.2823E+02
.2972E+02	.2973E+02	.3695E+01	.3709E+01	.9951E+01	.9956E+01	.1195E+02	.1195E+02	.1367E+02	.1368E+02
.1785E+02	.1785E+02	.2018E+02	.2018E+02	.2122E+02	.2122E+02	.2222E+02	.2222E+02	.2317E+02	.2318E+02
.2746E+02	.2747E+02	.2039E+00	.2033E+00	.3726E+01	.3740E+01	.7492E+01	.7501E+01	.1907E+02	.1907E+02
.3519E+02	.3520E+02	.1200E+02	.1200E+02	.1661E+02	.1662E+02	.2670E+02	.2671E+02	.3394E+02	.3395E+02
.3458E+02	.3460E+02	.3788E+01	.3801E+01	.7549E+01	.7557E+01	.1003E+02	.1003E+02	.1374E+02	.1374E+02
.1525E+02	.1526E+02	.1791E+02	.1791E+02	.2590E+02	.2590E+02	.2907E+02	.2908E+02	.3196E+02	.3197E+02
.3264E+02	.3265E+02	.3331E+02	.3332E+02	.3818E+01	.3832E+01	.2418E+02	.2418E+02	.2506E+02	.2507E+02
.3057E+02	.3058E+02	.3129E+02	.3130E+02	.1008E+02	.1008E+02	.1207E+02	.1207E+02	.1378E+02	.1379E+02
.1668E+02	.1668E+02	.1915E+02	.1915E+02	.2027E+02	.2027E+02	.2132E+02	.2132E+02	.2232E+02	.2232E+02
.2328E+02	.2328E+02	.2836E+02	.2837E+02	.2987E+02	.2988E+02	.3879E+01	.3892E+01	.7633E+01	.7641E+01
.1532E+02	.1532E+02	.2760E+02	.2761E+02	.2032E+00	.2032E+00	.3909E+01	.3921E+01	.1799E+02	.1799E+02
.2682E+02	.2682E+02	.3471E+02	.3472E+02	.3534E+02	.3535E+02	.7689E+01	.7696E+01	.1016E+02	.1016E+02
.1214E+02	.1214E+02	.1385E+02	.1385E+02	.1674E+02	.1674E+02	.2601E+02	.2601E+02	.3343E+02	.3344E+02
.3409E+02	.3410E+02	.3968E+01	.3980E+01	.1538E+02	.1538E+02	.1922E+02	.1922E+02	.2034E+02	.2034E+02
.2428E+02	.2428E+02	.2517E+02	.2517E+02	.3211E+02	.3211E+02	.3279E+02	.3280E+02	.3998E+01	.4009E+01
.7744E+01	.7751E+01	.1021E+02	.1021E+02	.1219E+02	.1219E+02	.2141E+02	.2141E+02	.2242E+02	.2242E+02
.2338E+02	.2338E+02	.2924E+02	.2925E+02	.3072E+02	.3073E+02	.3143E+02	.3144E+02	.2032E+00	.2032E+00

.1391E+02	.1391E+02	.1807E+02	.1807E+02	.2850E+02	.2850E+02	.3001E+02	.3002E+02	.4059E+01	.4069E+01
.7797E+01	.7803E+01	.1544E+02	.1544E+02	.1681E+02	.1681E+02	.2773E+02	.2774E+02	.3546E+02	.3547E+02
.4089E+01	.4098E+01	.1027E+02	.1028E+02	.1225E+02	.1225E+02	.2694E+02	.2695E+02	.3420E+02	.3421E+02
.3485E+02	.3486E+02	.1397E+02	.1397E+02	.1931E+02	.1931E+02	.2043E+02	.2043E+02	.2613E+02	.2613E+02
.3357E+02	.3357E+02	.2032E+00	.2032E+00	.4148E+01	.4156E+01	.7875E+01	.7881E+01	.1814E+02	.1814E+02
.2150E+02	.2150E+02	.2251E+02	.2251E+02	.2347E+02	.2347E+02	.2440E+02	.2440E+02	.2529E+02	.2529E+02
.3292E+02	.3292E+02	.1034E+02	.1034E+02	.1551E+02	.1551E+02	.1688E+02	.1689E+02	.3226E+02	.3226E+02
.4206E+01	.4213E+01	.7926E+01	.7931E+01	.1233E+02	.1233E+02	.2938E+02	.2939E+02	.3158E+02	.3158E+02
.4234E+01	.4240E+01	.1404E+02	.1404E+02	.1938E+02	.1938E+02	.3088E+02	.3089E+02	.3559E+02	.3559E+02
.1041E+02	.1041E+02	.1557E+02	.1557E+02	.1821E+02	.1821E+02	.2051E+02	.2051E+02	.2866E+02	.2866E+02
.3017E+02	.3018E+02	.3433E+02	.3433E+02	.3497E+02	.3498E+02	.4290E+01	.4295E+01	.8002E+01	.8005E+01
.1239E+02	.1239E+02	.1696E+02	.1696E+02	.2159E+02	.2159E+02	.2708E+02	.2708E+02	.2789E+02	.2789E+02
.3369E+02	.3370E+02	.2032E+00	.2032E+00	.1410E+02	.1410E+02	.2261E+02	.2261E+02	.2358E+02	.2358E+02
.2451E+02	.2451E+02	.2540E+02	.2540E+02	.2626E+02	.2626E+02	.3304E+02	.3304E+02	.4344E+01	.4348E+01
.8051E+01	.8053E+01	.1047E+02	.1047E+02	.4371E+01	.4374E+01	.1245E+02	.1245E+02	.1564E+02	.1564E+02
.1701E+02	.1701E+02	.1946E+02	.1946E+02	.3240E+02	.3240E+02	.3569E+02	.3569E+02	.1415E+02	.1415E+02
.1829E+02	.1829E+02	.2060E+02	.2060E+02	.3172E+02	.3172E+02	.3507E+02	.3508E+02	.2032E+00	.2032E+00
.4423E+01	.4424E+01	.8123E+01	.8123E+01	.1054E+02	.1054E+02	.2167E+02	.2167E+02	.2955E+02	.2955E+02
.3103E+02	.3103E+02	.1251E+02	.1251E+02	.1569E+02	.1569E+02	.2270E+02	.2270E+02	.2880E+02	.2880E+02
.3447E+02	.3447E+02	.4473E+01	.4473E+01	.8169E+01	.8169E+01	.1421E+02	.1421E+02	.1708E+02	.1708E+02
.1953E+02	.1953E+02	.2369E+02	.2369E+02	.2462E+02	.2462E+02	.2551E+02	.2551E+02	.2638E+02	.2638E+02
.2721E+02	.2721E+02	.2803E+02	.2803E+02	.3034E+02	.3034E+02	.3383E+02	.3383E+02		

Y-COORDINATES

.1065E+02	.7083E+01	.5752E+01	.4902E+01	.4370E+01	.3849E+01	.3382E+01	.3036E+01	.2783E+01	.2567E+01
.2355E+01	.2152E+01	.1970E+01	.1809E+01	.1657E+01	.1526E+01	.1411E+01	.1311E+01	.1234E+01	.1176E+01
.1140E+01	.1127E+01	.1128E+01	.1129E+01	.1129E+01	.1130E+01	.9933E+01	.9031E+01	.6957E+01	.6628E+01
.5695E+01	.5466E+01	.4801E+01	.4651E+01	.4312E+01	.4180E+01	.3797E+01	.3678E+01	.8740E+01	.8113E+01
.6544E+01	.6221E+01	.3296E+01	.3192E+01	.2971E+01	.2877E+01	.2731E+01	.2645E+01	.2525E+01	.2441E+01
.2317E+01	.2238E+01	.2122E+01	.2049E+01	.1945E+01	.1879E+01	.5330E+01	.5105E+01	.4645E+01	.4507E+01
.1774E+01	.1710E+01	.1632E+01	.1574E+01	.1504E+01	.1455E+01	.1394E+01	.1349E+01	.8075E+01	.7558E+01
.4132E+01	.3995E+01	.3635E+01	.3510E+01	.1290E+01	.1249E+01	.1218E+01	.1180E+01	.1165E+01	.1129E+01
.1133E+01	.1102E+01	.1126E+01	.1097E+01	.1127E+01	.1100E+01	.1128E+01	.1103E+01	.1129E+01	.1106E+01
.1130E+01	.1108E+01	.1498E+02	.1092E+02	.7677E+01	.7246E+01	.6022E+01	.5721E+01	.5091E+01	.4877E+01
.3173E+01	.3066E+01	.2869E+01	.2771E+01	.2643E+01	.2556E+01	.1124E+02	.9640E+01	.5817E+01	.5522E+01
.4430E+01	.4294E+01	.3980E+01	.3838E+01	.2407E+01	.2321E+01	.2207E+01	.2126E+01	.2027E+01	.1952E+01
.9969E+01	.8867E+01	.7068E+01	.6694E+01	.4844E+01	.4673E+01	.3448E+01	.3330E+01	.3076E+01	.2969E+01
.1840E+01	.1772E+01	.1694E+01	.1631E+01	.1562E+01	.1506E+01	.5463E+01	.5178E+01	.4291E+01	.4158E+01
.2747E+01	.2653E+01	.2540E+01	.2449E+01	.1432E+01	.1379E+01	.1331E+01	.1284E+01	.8502E+01	.7855E+01
.6567E+01	.6231E+01	.4652E+01	.4496E+01	.3765E+01	.3630E+01	.2312E+01	.2224E+01	.2123E+01	.2041E+01
.1234E+01	.1191E+01	.1169E+01	.1128E+01	.1123E+01	.1086E+01	.1099E+01	.1065E+01	.1098E+01	.1068E+01
.1102E+01	.1073E+01	.1460E+02	.8018E+01	.7479E+01	.5128E+01	.4880E+01	.4152E+01	.4017E+01	.3279E+01
.3159E+01	.2936E+01	.2832E+01	.1923E+01	.1849E+01	.1770E+01	.1703E+01	.1100E+01	.1072E+01	.1103E+01
.1077E+01	.1106E+01	.1080E+01	.1102E+02	.6110E+01	.5786E+01	.4481E+01	.4341E+01	.3625E+01	.3491E+01
.2631E+01	.2535E+01	.1614E+01	.1552E+01	.7274E+01	.6868E+01	.5901E+01	.5569E+01	.4839E+01	.4640E+01
.4004E+01	.3866E+01	.3163E+01	.3050E+01	.2400E+01	.2308E+01	.2213E+01	.2126E+01	.1475E+01	.1419E+01
.1373E+01	.1319E+01	.9824E+01	.8692E+01	.4326E+01	.4198E+01	.2798E+01	.2698E+01	.2005E+01	.1924E+01
.1267E+01	.1219E+01	.8816E+01	.8023E+01	.6693E+01	.6350E+01	.5446E+01	.5118E+01	.4606E+01	.4449E+01
.3415E+01	.3285E+01	.2513E+01	.2416E+01	.1819E+01	.1744E+01	.1680E+01	.1609E+01	.1176E+01	.1131E+01
.1117E+01	.1075E+01	.1080E+01	.1040E+01	.1065E+01	.1029E+01	.1070E+01	.1036E+01	.8118E+01	.7524E+01
.6426E+01	.6094E+01	.4172E+01	.4031E+01	.3773E+01	.3625E+01	.2999E+01	.2887E+01	.2291E+01	.2200E+01
.1531E+01	.1469E+01	.1069E+01	.1037E+01	.1074E+01	.1043E+01	.1079E+01	.1050E+01	.1082E+01	.1055E+01
.7599E+01	.7133E+01	.6176E+01	.5851E+01	.4974E+01	.4703E+01	.4413E+01	.4277E+01	.3278E+01	.3149E+01
.2660E+01	.2557E+01	.2077E+01	.1991E+01	.1915E+01	.1831E+01	.1403E+01	.1345E+01	.4775E+01	.4553E+01

.4008E+01	.3861E+01	.3605E+01	.3457E+01	.2888E+01	.2778E+01	.2394E+01	.2296E+01	.1739E+01	.1662E+01
.1293E+01	.1240E+01	.6856E+01	.6528E+01	.5688E+01	.5382E+01	.4251E+01	.4119E+01	.3144E+01	.3019E+01
.2182E+01	.2087E+01	.1584E+01	.1513E+01	.1197E+01	.1147E+01	.1126E+01	.1080E+01	.6593E+01	.6293E+01
.5473E+01	.5172E+01	.4494E+01	.4339E+01	.3843E+01	.3693E+01	.3448E+01	.3303E+01	.2525E+01	.2422E+01
.1979E+01	.1888E+01	.1449E+01	.1387E+01	.1062E+01	.1018E+01	.1034E+01	.9917E+00	.1029E+01	.9909E+00
.1037E+01	.1001E+01	.6354E+01	.6071E+01	.4104E+01	.3965E+01	.2739E+01	.2627E+01	.2278E+01	.2181E+01
.1797E+01	.1715E+01	.1333E+01	.1275E+01	.1038E+01	.1003E+01	.1044E+01	.1012E+01	.1050E+01	.1019E+01
.1056E+01	.1027E+01	.5062E+01	.4799E+01	.4310E+01	.4191E+01	.4029E+01	.3884E+01	.3683E+01	.3529E+01
.3303E+01	.3162E+01	.2969E+01	.2849E+01	.2077E+01	.1982E+01	.1635E+01	.1560E+01	.1232E+01	.1179E+01
.5917E+01	.5663E+01	.4875E+01	.4643E+01	.4238E+01	.4119E+01	.2397E+01	.2294E+01	.1884E+01	.1797E+01
.1495E+01	.1425E+01	.5717E+01	.5470E+01	.3868E+01	.3717E+01	.2857E+01	.2737E+01	.2594E+01	.2483E+01
.2167E+01	.2069E+01	.1712E+01	.1630E+01	.1371E+01	.1309E+01	.1130E+01	.1077E+01	.1065E+01	.1016E+01
.1202E+02	.5521E+01	.5287E+01	.4569E+01	.4393E+01	.4092E+01	.3962E+01	.3437E+01	.3286E+01	.3093E+01
.2962E+01	.1972E+01	.1879E+01	.1010E+01	.9629E+00	.9890E+00	.9449E+00	.9933E+00	.9527E+00	.1003E+01
.9641E+00	.1203E+02	.1057E+02	.3700E+01	.3541E+01	.2270E+01	.2168E+01	.1537E+01	.1462E+01	.1249E+01
.1190E+01	.1005E+01	.9678E+00	.1014E+01	.9779E+00	.1021E+01	.9873E+00	.1028E+01	.9956E+00	.1054E+02
.9630E+01	.5163E+01	.4951E+01	.4337E+01	.4199E+01	.3938E+01	.3798E+01	.3282E+01	.3136E+01	.2964E+01
.2834E+01	.2692E+01	.2574E+01	.2448E+01	.2338E+01	.2054E+01	.1953E+01	.1757E+01	.1669E+01	.1408E+01
.1338E+01	.1157E+01	.1102E+01	.4999E+01	.4804E+01	.4243E+01	.4111E+01	.3539E+01	.3378E+01	.1599E+01
.1518E+01	.1294E+01	.1232E+01	.1075E+01	.1021E+01	.8925E+01	.8417E+01	.3779E+01	.3633E+01	.3136E+01
.2996E+01	.2841E+01	.2716E+01	.2584E+01	.2466E+01	.2350E+01	.2241E+01	.2136E+01	.2032E+01	.1829E+01
.1733E+01	.1461E+01	.1386E+01	.1003E+01	.9519E+00	.8398E+01	.7980E+01	.4707E+01	.4543E+01	.4069E+01
.3935E+01	.1935E+01	.1834E+01	.1662E+01	.1572E+01	.1180E+01	.1121E+01	.9554E+00	.9061E+00	.9445E+00
.8978E+00	.9555E+00	.9112E+00	.9666E+00	.9247E+00	.9771E+00	.9366E+00	.7958E+01	.7611E+01	.4580E+01
.4428E+01	.3613E+01	.3458E+01	.3294E+01	.3144E+01	.2999E+01	.2863E+01	.2047E+01	.1943E+01	.1513E+01
.1432E+01	.1318E+01	.1251E+01	.1095E+01	.1038E+01	.9795E+00	.9400E+00	.9883E+00	.9507E+00	.9965E+00
.9602E+00	.7594E+01	.7295E+01	.4462E+01	.4323E+01	.3890E+01	.3752E+01	.2663E+01	.2541E+01	.2422E+01
.2308E+01	.2204E+01	.2096E+01	.1720E+01	.1624E+01	.1218E+01	.1155E+01	.7280E+01	.7022E+01	.3800E+01
.3658E+01	.3438E+01	.3288E+01	.3142E+01	.2997E+01	.2864E+01	.2733E+01	.1815E+01	.1712E+01	.1563E+01
.1475E+01	.1361E+01	.1287E+01	.1004E+01	.9493E+00	.7007E+01	.6781E+01	.4256E+01	.4131E+01	.3354E+01
.3206E+01	.2546E+01	.2425E+01	.2317E+01	.2203E+01	.2108E+01	.1999E+01	.1914E+01	.1808E+01	.1112E+01
.1050E+01	.9406E+00	.8865E+00	.9111E+00	.8595E+00	.6772E+01	.6571E+01	.4161E+01	.4036E+01	.3614E+01
.3467E+01	.2995E+01	.2857E+01	.1612E+01	.1517E+01	.1401E+01	.1321E+01	.1233E+01	.1164E+01	.8995E+00
.8506E+00	.9137E+00	.8666E+00	.9269E+00	.8809E+00	.9387E+00	.8943E+00	.2702E+01	.2576E+01	.1714E+01
.1611E+01	.9456E+00	.9028E+00	.9554E+00	.9147E+00	.9653E+00	.9254E+00	.6495E+01	.6321E+01	.4035E+01
.3911E+01	.3481E+01	.3336E+01	.3153E+01	.3013E+01	.2892E+01	.2759E+01	.2411E+01	.2294E+01	.2197E+01
.2083E+01	.1460E+01	.1373E+01	.1281E+01	.1206E+01	.1136E+01	.1070E+01	.1013E+01	.9524E+00	.6340E+01
.6177E+01	.1961E+01	.1851E+01	.1780E+01	.1672E+01	.6196E+01	.6037E+01	.3878E+01	.3754E+01	.3317E+01
.3178E+01	.3012E+01	.2878E+01	.2539E+01	.2417E+01	.1512E+01	.1417E+01	.1324E+01	.1243E+01	.1172E+01
.1100E+01	.1045E+01	.9801E+00	.9348E+00	.8762E+00	.2706E+01	.2580E+01	.2270E+01	.2154E+01	.2071E+01
.1960E+01	.1593E+01	.1490E+01	.8804E+00	.8224E+00	.5917E+01	.5765E+01	.3721E+01	.3597E+01	.3160E+01
.3026E+01	.2876E+01	.2747E+01	.2432E+01	.2314E+01	.1848E+01	.1740E+01	.1679E+01	.1572E+01	.1365E+01
.1278E+01	.8484E+00	.7926E+00	.8564E+00	.8031E+00	.8715E+00	.8196E+00	.8848E+00	.8351E+00	.8974E+00
.8494E+00	.9091E+00	.8628E+00	.5783E+01	.5634E+01	.3643E+01	.3517E+01	.2589E+01	.2466E+01	.2177E+01
.2063E+01	.1431E+01	.1338E+01	.1189E+01	.1111E+01	.1060E+01	.9906E+00	.9493E+00	.8864E+00	.9129E+00
.8671E+00	.9230E+00	.8789E+00	.1409E+02	.5652E+01	.5507E+01	.3008E+01	.2880E+01	.2745E+01	.2622E+01
.1947E+01	.1837E+01	.1240E+01	.1159E+01	.1422E+02	.1208E+02	.3485E+01	.3360E+01	.2474E+01	.2355E+01
.2279E+01	.2164E+01	.1738E+01	.1629E+01	.1473E+01	.1372E+01	.1087E+01	.1014E+01	.1214E+02	.1098E+02
.5398E+01	.5259E+01	.2864E+01	.2739E+01	.2620E+01	.2499E+01	.2042E+01	.1929E+01	.1547E+01	.1441E+01
.1272E+01	.1185E+01	.9607E+00	.8926E+00	.8652E+00	.8028E+00	.1102E+02	.1022E+02	.5276E+01	.5139E+01
.3328E+01	.3206E+01	.2793E+01	.2670E+01	.2180E+01	.2066E+01	.1826E+01	.1717E+01	.1327E+01	.1234E+01
.1113E+01	.1034E+01	.8155E+00	.7546E+00	.1026E+02	.9650E+01	.5155E+01	.5022E+01	.3251E+01	.3131E+01
.2497E+01	.2379E+01	.2308E+01	.2193E+01	.9823E+00	.9100E+00	.7919E+00	.7319E+00	.8058E+00	.7480E+00
.8213E+00	.7650E+00	.8357E+00	.7811E+00	.8492E+00	.7961E+00	.8618E+00	.8102E+00	.8735E+00	.8234E+00
.8846E+00	.8360E+00	.9674E+01	.9181E+01	.2656E+01	.2534E+01	.1909E+01	.1799E+01	.1592E+01	.1485E+01

.1449E+01	.1344E+01	.1356E+01	.1256E+01	.1137E+01	.1053E+01	.8721E+00	.8051E+00	.9204E+01	.8786E+01
.4922E+01	.4793E+01	.3100E+01	.2982E+01	.2378E+01	.2261E+01	.2202E+01	.2088E+01	.2033E+01	.1923E+01
.1707E+01	.1598E+01	.1180E+01	.1091E+01	.1002E+01	.9249E+00	.8804E+01	.8445E+01	.4809E+01	.4680E+01
.2521E+01	.2404E+01	.1822E+01	.1712E+01	.1224E+01	.1130E+01	.8888E+00	.8183E+00	.8460E+01	.8138E+01
.4697E+01	.4570E+01	.2952E+01	.2837E+01	.2260E+01	.2147E+01	.2097E+01	.1986E+01	.1938E+01	.1830E+01
.1485E+01	.1379E+01	.1270E+01	.1171E+01	.1018E+01	.9371E+00	.7928E+00	.7268E+00	.8152E+01	.7862E+01
.2879E+01	.2766E+01	.2391E+01	.2275E+01	.1589E+01	.1482E+01	.1321E+01	.1217E+01	.1053E+01	.9670E+00
.9033E+00	.8282E+00	.7875E+01	.7614E+01	.4477E+01	.4351E+01	.2146E+01	.2034E+01	.1995E+01	.1886E+01
.1693E+01	.1586E+01	.1087E+01	.9974E+00	.8056E+00	.7357E+00	.7376E+00	.6720E+00	.7340E+00	.6696E+00
.7507E+00	.6880E+00	.7666E+00	.7053E+00	.7815E+00	.7215E+00	.7957E+00	.7370E+00	.8088E+00	.7517E+00
.8213E+00	.7657E+00	.8330E+00	.7787E+00	.7625E+01	.7388E+01	.4372E+01	.4246E+01	.2737E+01	.2625E+01
.2266E+01	.2152E+01	.1804E+01	.1696E+01	.1384E+01	.1278E+01	.1125E+01	.1030E+01	.9152E+00	.8363E+00
.7393E+01	.7173E+01	.4266E+01	.4140E+01	.1164E+01	.1064E+01	.9436E+00	.8610E+00	.2601E+01	.2489E+01
.2147E+01	.2035E+01	.1991E+01	.1882E+01	.1860E+01	.1753E+01	.1721E+01	.1615E+01	.1580E+01	.1474E+01
.1447E+01	.1342E+01	.1207E+01	.1104E+01	.8015E+00	.7268E+00	.6975E+01	.6781E+01	.4055E+01	.3928E+01
.9532E+00	.8662E+00	.8245E+00	.7466E+00	.7172E+00	.6463E+00	.3948E+01	.3820E+01	.2464E+01	.2353E+01
.2032E+01	.1921E+01	.1890E+01	.1783E+01	.1772E+01	.1667E+01	.1262E+01	.1158E+01	.9814E+00	.8904E+00
.6776E+00	.6080E+00	.6809E+00	.6124E+00	.6979E+00	.6307E+00	.7142E+00	.6481E+00	.7296E+00	.6645E+00
.7441E+00	.6803E+00	.7577E+00	.6954E+00	.7707E+00	.7096E+00	.7831E+00	.7233E+00	.6607E+01	.6433E+01
.2396E+01	.2285E+01	.1599E+01	.1495E+01	.1469E+01	.1365E+01	.1347E+01	.1244E+01	.1010E+01	.9151E+00
.8306E+00	.7492E+00	.7230E+00	.6490E+00	.3735E+01	.3604E+01	.1917E+01	.1809E+01	.1791E+01	.1685E+01
.1099E+01	.9961E+00	.1040E+01	.9400E+00	.8525E+00	.7677E+00	.3628E+01	.3496E+01	.2261E+01	.2151E+01
.1642E+01	.1538E+01	.8747E+00	.7864E+00	.7266E+00	.6491E+00	.6105E+01	.5938E+01	.3520E+01	.3389E+01
.1805E+01	.1698E+01	.1694E+01	.1589E+01	.1480E+01	.1377E+01	.1360E+01	.1257E+01	.1249E+01	.1145E+01
.1143E+01	.1039E+01	.8968E+00	.8049E+00	.2128E+01	.2018E+01	.1557E+01	.1454E+01	.9191E+00	.8235E+00
.7281E+00	.6470E+00	.6370E+00	.5624E+00	.6728E+00	.6028E+00	.6876E+00	.6185E+00	.7017E+00	.6335E+00
.7152E+00	.6481E+00	.7279E+00	.6621E+00	.3305E+01	.3173E+01	.1695E+01	.1590E+01	.9923E+00	.8893E+00
.9417E+00	.8419E+00	.7443E+00	.6603E+00	.6024E+00	.5285E+00	.6122E+00	.5390E+00	.6293E+00	.5564E+00
.6455E+00	.5734E+00	.3198E+01	.3066E+01	.1995E+01	.1887E+01	.1550E+01	.1447E+01	.1362E+01	.1260E+01
.1253E+01	.1151E+01	.7603E+00	.6729E+00	.6369E+00	.5587E+00	.5457E+01	.5295E+01	.3091E+01	.2960E+01
.1588E+01	.1484E+01	.1430E+01	.1329E+01	.1119E+01	.1016E+01	.1025E+01	.9215E+00	.7755E+00	.6854E+00
.6498E+00	.5692E+00	.1864E+01	.1757E+01	.1456E+01	.1354E+01	.1284E+01	.1182E+01	.7909E+00	.6976E+00
.2879E+01	.2747E+01	.1799E+01	.1693E+01	.1481E+01	.1379E+01	.1347E+01	.1246E+01	.1147E+01	.1045E+01
.8871E+00	.7842E+00	.8441E+00	.7444E+00	.8055E+00	.7089E+00	.6456E+00	.5616E+00	.5681E+00	.4898E+00
.6404E+00	.5661E+00	.6539E+00	.5805E+00	.6669E+00	.5946E+00	.2773E+01	.2643E+01	.1363E+01	.1262E+01
.1022E+01	.9193E+00	.9371E+00	.8338E+00	.6563E+00	.5696E+00	.5673E+00	.4895E+00	.5832E+00	.5057E+00
.5986E+00	.5216E+00	.6134E+00	.5369E+00	.4821E+01	.4657E+01	.1671E+01	.1566E+01	.1377E+01	.1276E+01
.1169E+01	.1067E+01	.6663E+00	.5769E+00	.5626E+00	.4811E+00	.5242E+00	.4456E+00	.5383E+00	.4597E+00
.2574E+01	.2446E+01	.1279E+01	.1178E+01	.1229E+01	.1127E+01	.6773E+00	.5852E+00	.2480E+01	.2353E+01
.1564E+01	.1459E+01	.1294E+01	.1194E+01	.1015E+01	.9122E+00	.7518E+00	.6518E+00	.7188E+00	.6216E+00
.6879E+00	.5933E+00	.5570E+00	.4726E+00	.1068E+01	.9662E+00	.9054E+00	.8023E+00	.8310E+00	.7279E+00
.7648E+00	.6621E+00	.5648E+00	.4781E+00	.5868E+00	.5064E+00	.5996E+00	.5199E+00	.2296E+01	.2170E+01
.1457E+01	.1354E+01	.1164E+01	.1063E+01	.1121E+01	.1019E+01	.5721E+00	.4832E+00	.4853E+00	.4030E+00
.5319E+00	.4496E+00	.5459E+00	.4636E+00	.5595E+00	.4774E+00	.4038E+01	.3861E+01	.2205E+01	.2081E+01
.1170E+01	.1070E+01	.9227E+00	.8199E+00	.5788E+00	.4876E+00	.4745E+00	.3923E+00	.4893E+00	.4068E+00
.5038E+00	.4210E+00	.1353E+01	.1251E+01	.9679E+00	.8655E+00	.5849E+00	.4916E+00	.4767E+00	.3915E+00
.4471E+00	.3644E+00	.2027E+01	.1905E+01	.1087E+01	.9875E+00	.1049E+01	.9479E+00	.1013E+01	.9108E+00
.7931E+00	.6902E+00	.6724E+00	.5702E+00	.6431E+00	.5433E+00	.6160E+00	.5184E+00	.5905E+00	.4949E+00
.4811E+00	.3939E+00	.3532E+01	.3341E+01	.1940E+01	.1819E+01	.1249E+01	.1148E+01	.7036E+00	.6010E+00
.5253E+00	.4394E+00	.9721E+00	.8709E+00	.8002E+00	.6973E+00	.4687E+00	.3790E+00	.4854E+00	.3992E+00
.4976E+00	.4111E+00	.1769E+01	.1650E+01	.1147E+01	.1045E+01	.9640E+00	.8639E+00	.9040E+00	.8018E+00
.8342E+00	.7315E+00	.7095E+00	.6068E+00	.4709E+00	.3793E+00	.4012E+00	.3148E+00	.4333E+00	.3470E+00
.4458E+00	.3593E+00	.4580E+00	.3713E+00	.1685E+01	.1568E+01	.4918E+00	.3969E+00	.4724E+00	.3789E+00
.3938E+00	.3072E+00	.4064E+00	.3196E+00	.8817E+00	.7814E+00	.8569E+00	.7554E+00	.8314E+00	.7289E+00
.7087E+00	.6058E+00	.6028E+00	.5006E+00	.5583E+00	.4567E+00	.5350E+00	.4353E+00	.5132E+00	.4151E+00

.4926E+00	.3960E+00	.3876E+00	.2986E+00	.3673E+00	.2801E+00	.1521E+01	.1407E+01	.9945E+00	.8930E+00
.7342E+00	.6313E+00	.3875E+00	.2968E+00	.2470E+01	.2293E+01	.1440E+01	.1328E+01	.5988E+00	.4962E+00
.3866E+00	.2942E+00	.4177E+00	.3280E+00	.4280E+00	.3382E+00	.8934E+00	.7920E+00	.7582E+00	.6575E+00
.7416E+00	.6397E+00	.7222E+00	.6193E+00	.6176E+00	.5147E+00	.3849E+00	.2909E+00	.3808E+00	.2907E+00
.3912E+00	.3009E+00	.1283E+01	.1173E+01	.6343E+00	.5312E+00	.5031E+00	.4012E+00	.4681E+00	.3667E+00
.3977E+00	.3012E+00	.3822E+00	.2868E+00	.3443E+00	.2537E+00	.3547E+00	.2640E+00	.1206E+01	.1097E+01
.7928E+00	.6915E+00	.6758E+00	.5749E+00	.6646E+00	.5624E+00	.4275E+00	.3274E+00	.4104E+00	.3114E+00
.3942E+00	.2963E+00	.2988E+00	.2072E+00	.3082E+00	.2170E+00	.3187E+00	.2274E+00	.1853E+01	.1703E+01
.6164E+00	.5131E+00	.4913E+00	.3891E+00	.2988E+00	.2060E+00	.2865E+00	.1949E+00	.1067E+01	.9587E+00
.7095E+00	.6081E+00	.5410E+00	.4380E+00	.5021E+00	.3996E+00	.2977E+00	.2037E+00	.3464E+00	.2537E+00
.9985E+00	.8908E+00	.5740E+00	.4727E+00	.5643E+00	.4619E+00	.2954E+00	.2003E+00	.3150E+00	.2219E+00
.3229E+00	.2298E+00	.5178E+00	.4148E+00	.3878E+00	.2864E+00	.3634E+00	.2625E+00	.2918E+00	.1957E+00
.2928E+00	.1993E+00	.1365E+01	.1237E+01	.8633E+00	.7568E+00	.5852E+00	.4837E+00	.3919E+00	.2902E+00
.3306E+00	.2306E+00	.3189E+00	.2197E+00	.3078E+00	.2093E+00	.2971E+00	.1994E+00	.2870E+00	.1899E+00
.2715E+00	.1776E+00	.4719E+00	.3708E+00	.4214E+00	.3192E+00	.3932E+00	.2914E+00	.2511E+00	.1568E+00
.7306E+00	.6253E+00	.5028E+00	.4015E+00	.4304E+00	.3286E+00	.2184E+00	.1235E+00	.2317E+00	.1369E+00
.6651E+00	.5604E+00	.3873E+00	.2852E+00	.2983E+00	.1973E+00	.2133E+00	.1180E+00	.2505E+00	.1550E+00
.3700E+00	.2692E+00	.3326E+00	.2311E+00	.2935E+00	.1925E+00	.2615E+00	.1609E+00	.2006E+00	.1044E+00
.1959E+00	.1001E+00	.2252E+00	.1292E+00	.2297E+00	.1337E+00	.5359E+00	.4323E+00	.3803E+00	.2794E+00
.3306E+00	.2293E+00	.2855E+00	.1844E+00	.2342E+00	.1342E+00	.1985E+00	.1010E+00	.1933E+00	.9617E-01
.2058E+00	.1094E+00	.7393E+00	.6280E+00	.2906E+00	.1892E+00	.2094E+00	.1098E+00	.2040E+00	.1048E+00
.1988E+00	.9999E-01	.1939E+00	.9539E-01	.1891E+00	.9096E-01	.1874E+00	.9050E-01	.4088E+00	.3063E+00
.2995E+00	.1988E+00	.2684E+00	.1679E+00	.3461E+00	.2441E+00	.2314E+00	.1306E+00	.2156E+00	.1148E+00
.2056E+00	.1049E+00	.1876E+00	.8715E-01	.1562E+00	.5830E-01	.1679E+00	.6990E-01	.1948E+00	.9414E-01
.1721E+00	.7170E-01	.1603E+00	.6013E-01	.1404E+00	.4202E-01	.1494E+00	.5091E-01	.3659E+00	.2618E+00
.2221E+00	.1211E+00	.1793E+00	.7910E-01	.1672E+00	.6704E-01	.1383E+00	.3828E-01	.1240E+00	.2508E-01
.1258E+00	.2684E-01	.1327E+00	.3256E-01	.1288E+00	.2858E-01	.1182E+00	.1829E-01	.1127E+00	.1321E-01
.1160E+00	.1650E-01	.1000E+00	.0000E+00	.1000E+00	.0000E+00	.1000E+00	.0000E+00	.1000E+00	.0000E+00
.1000E+00	.0000E+00	.1000E+00	.0000E+00	.1000E+00	.0000E+00	.1000E+00	.0000E+00	.1000E+00	.0000E+00
.1000E+00	.0000E+00	.1000E+00	.0000E+00	.1000E+00	.0000E+00	.1000E+00	.0000E+00	.1000E+00	.0000E+00



CUMULATIVE TIME

.3037E+04 .4220E+04

CUMULATIVE SALT WATER ENTRY INTO WELL

.0000E+00 .0000E+00

CUMULATIVE SALT WATER LIFTING INTO SUSPENSION

.4158E+03 .6202E+03

NUMBER OF POINTS LIFTED

162 224

X-COORDINATES

.4173E+01	.7784E+01	.1018E+02	.1213E+02	.1381E+02	.1534E+02	.1672E+02	.1801E+02	.1920E+02	.2033E+02
.2140E+02	.2243E+02	.2340E+02	.2434E+02	.2525E+02	.2613E+02	.2696E+02	.2780E+02	.2860E+02	.2937E+02
.3013E+02	.3086E+02	.3159E+02	.3230E+02	.3298E+02	.3366E+02	.3432E+02	.3496E+02	.3561E+02	.2158E+00
.4202E+01	.4209E+01	.2147E+00	.2144E+00	.7834E+01	.7843E+01	.1025E+02	.1025E+02	.1220E+02	.1221E+02
.1388E+02	.1389E+02	.2136E+00	.2130E+00	.4261E+01	.4266E+01	.7889E+01	.7894E+01	.1543E+02	.1543E+02
.1681E+02	.1681E+02	.1809E+02	.1810E+02	.1928E+02	.1928E+02	.4277E+01	.4282E+01	.1030E+02	.1031E+02
.2043E+02	.2043E+02	.2149E+02	.2149E+02	.2251E+02	.2251E+02	.2348E+02	.2348E+02	.2118E+00	.2108E+00
.7931E+01	.7937E+01	.1227E+02	.1228E+02	.2444E+02	.2444E+02	.2533E+02	.2535E+02	.2621E+02	.2621E+02
.2109E+00	.2098E+00	.4318E+01	.4322E+01	.1036E+02	.1036E+02	.1399E+02	.1399E+02	.1549E+02	.1550E+02
.1687E+02	.1687E+02	.2707E+02	.2707E+02	.2789E+02	.2789E+02	.2868E+02	.2868E+02	.2946E+02	.2946E+02
.3021E+02	.3021E+02	.4342E+01	.4345E+01	.7989E+01	.7994E+01	.1234E+02	.1234E+02	.1818E+02	.1818E+02
.1936E+02	.1937E+02	.3096E+02	.3096E+02	.3168E+02	.3168E+02	.3238E+02	.3238E+02	.3306E+02	.3306E+02
.3374E+02	.3374E+02	.3440E+02	.3440E+02	.3504E+02	.3504E+02	.3569E+02	.3569E+02	.2081E+00	.2071E+00
.1404E+02	.1405E+02	.2051E+02	.2051E+02	.2157E+02	.2158E+02	.2070E+00	.2062E+00	.4381E+01	.4384E+01
.8041E+01	.8045E+01	.1044E+02	.1044E+02	.1558E+02	.1558E+02	.2261E+02	.2261E+02	.2358E+02	.2358E+02
.1241E+02	.1242E+02	.1697E+02	.1698E+02	.1825E+02	.1825E+02	.2453E+02	.2453E+02	.2543E+02	.2543E+02
.2052E+00	.2048E+00	.4419E+01	.4420E+01	.8093E+01	.8095E+01	.1050E+02	.1050E+02	.1412E+02	.1413E+02
.1946E+02	.1946E+02	.2632E+02	.2632E+02	.2716E+02	.2716E+02	.2046E+00	.2043E+00	.4437E+01	.4438E+01
.1247E+02	.1247E+02	.1566E+02	.1566E+02	.2060E+02	.2060E+02	.2799E+02	.2799E+02	.2878E+02	.2878E+02
.8144E+01	.8145E+01	.1055E+02	.1055E+02	.1705E+02	.1705E+02	.2169E+02	.2169E+02	.2270E+02	.2270E+02
.2957E+02	.2957E+02	.3032E+02	.3032E+02	.3105E+02	.3105E+02	.2036E+00	.2035E+00	.4473E+01	.4473E+01
.1421E+02	.1421E+02	.1835E+02	.1835E+02	.2369E+02	.2369E+02	.3178E+02	.3178E+02	.3248E+02	.3248E+02
.3316E+02	.3316E+02	.3383E+02	.3383E+02						

Y-COORDINATES

.8975E+00	.7375E+00	.6425E+00	.5712E+00	.5115E+00	.4719E+00	.4362E+00	.4026E+00	.3719E+00	.3451E+00
.3307E+00	.3170E+00	.3040E+00	.2915E+00	.2793E+00	.2676E+00	.2564E+00	.2453E+00	.2345E+00	.2242E+00
.2175E+00	.2135E+00	.2096E+00	.2058E+00	.2023E+00	.1985E+00	.1951E+00	.1917E+00	.1883E+00	.9505E+00
.8953E+00	.8020E+00	.9370E+00	.8460E+00	.7223E+00	.6294E+00	.6069E+00	.5128E+00	.5513E+00	.4566E+00
.5049E+00	.4103E+00	.8478E+00	.7549E+00	.7381E+00	.6429E+00	.6239E+00	.5289E+00	.4381E+00	.3433E+00
.4122E+00	.3175E+00	.3881E+00	.2934E+00	.3658E+00	.2712E+00	.6891E+00	.5933E+00	.5239E+00	.4283E+00
.3284E+00	.2336E+00	.3190E+00	.2241E+00	.3100E+00	.2150E+00	.3012E+00	.2063E+00	.7148E+00	.6203E+00
.5448E+00	.4486E+00	.4490E+00	.3533E+00	.2775E+00	.1823E+00	.2701E+00	.1749E+00	.2631E+00	.1678E+00
.6603E+00	.5655E+00	.5737E+00	.4765E+00	.4435E+00	.3472E+00	.3778E+00	.2819E+00	.3560E+00	.2601E+00
.3360E+00	.2402E+00	.2376E+00	.1418E+00	.2317E+00	.1359E+00	.2258E+00	.1300E+00	.2201E+00	.1243E+00
.2166E+00	.1209E+00	.5070E+00	.4094E+00	.4382E+00	.3413E+00	.3663E+00	.2697E+00	.2887E+00	.1924E+00
.2739E+00	.1777E+00	.1987E+00	.1027E+00	.1969E+00	.1010E+00	.1952E+00	.9935E-01	.1934E+00	.9776E-01

.1917E+00	.9618E-01	.1901E+00	.9464E-01	.1885E+00	.9314E-01	.1869E+00	.9164E-01	.5127E+00	.4167E+00
.3064E+00	.2096E+00	.2392E+00	.1425E+00	.2332E+00	.1365E+00	.4517E+00	.3551E+00	.3902E+00	.2920E+00
.3430E+00	.2452E+00	.3136E+00	.2160E+00	.2590E+00	.1617E+00	.2069E+00	.1097E+00	.2023E+00	.1051E+00
.2530E+00	.1551E+00	.2179E+00	.1202E+00	.2092E+00	.1115E+00	.1788E+00	.8108E-01	.1753E+00	.7760E-01
.3285E+00	.2307E+00	.2739E+00	.1751E+00	.2466E+00	.1481E+00	.2289E+00	.1305E+00	.2035E+00	.1052E+00
.1759E+00	.7766E-01	.1541E+00	.5580E-01	.1517E+00	.5335E-01	.2719E+00	.1735E+00	.2161E+00	.1169E+00
.1768E+00	.7787E-01	.1640E+00	.6511E-01	.1473E+00	.4849E-01	.1329E+00	.3406E-01	.1314E+00	.3252E-01
.1490E+00	.4952E-01	.1431E+00	.4366E-01	.1297E+00	.3025E-01	.1227E+00	.2327E-01	.1217E+00	.2228E-01
.1150E+00	.1554E-01	.1146E+00	.1515E-01	.1143E+00	.1493E-01	.1576E+00	.5817E-01	.1000E+00	.0000E+00
.1000E+00	.0000E+00	.1000E+00	.0000E+00	.1000E+00	.0000E+00	.1000E+00	.0000E+00	.1000E+00	.0000E+00
.1000E+00	.0000E+00	.1000E+00	.0000E+00	.1000E+00	.0000E+00	.1000E+00	.0000E+00	.1000E+00	.0000E+00



CUMULATIVE TIME

.4032E+05 .4320E+05

CUMULATIVE SALT WATER ENTRY INTO WELL

.9303E+01 .1163E+02

CUMULATIVE SALT WATER LIFTING INTO SUSPENSION

.4369E+04 .4602E+04

NUMBER OF POINTS LIFTED

1357 1418

X-COORDINATES

.3264E+01	.5535E+01	.7774E+01	.9993E+01	.1170E+02	.1341E+02	.1509E+02	.1650E+02	.1775E+02	.1893E+02
.2003E+02	.2104E+02	.2198E+02	.2288E+02	.2373E+02	.2454E+02	.2535E+02	.2614E+02	.2690E+02	.2763E+02
.2834E+02	.2906E+02	.2976E+02	.3044E+02	.3113E+02	.3181E+02	.3246E+02	.3312E+02	.3354E+01	.3705E+01
.5722E+01	.6020E+01	.7922E+01	.8233E+01	.1010E+02	.1034E+02	.3753E+01	.4057E+01	.1187E+02	.1206E+02
.1358E+02	.1377E+02	.1521E+02	.1537E+02	.1659E+02	.1670E+02	.6033E+01	.6339E+01	.1788E+02	.1797E+02
.1903E+02	.1911E+02	.2012E+02	.2020E+02	.2113E+02	.2118E+02	.4028E+01	.4319E+01	.8332E+01	.8647E+01
.2208E+02	.2215E+02	.2296E+02	.2303E+02	.2382E+02	.2387E+02	.9164E+00	.6342E+01	.6634E+01	.1052E+02
.1074E+02	.1209E+02	.1229E+02	.1380E+02	.1398E+02	.2466E+02	.2471E+02	.2544E+02	.2551E+02	.2622E+02
.2628E+02	.2699E+02	.2703E+02	.2772E+02	.2775E+02	.7409E+00	.1303E+01	.4381E+01	.4660E+01	.8672E+01
.8980E+01	.1546E+02	.1558E+02	.1678E+02	.1690E+02	.2844E+02	.2850E+02	.2915E+02	.2919E+02	.2986E+02
.2989E+02	.3052E+02	.3058E+02	.3122E+02	.3126E+02	.3189E+02	.3194E+02	.3254E+02	.3259E+02	.3321E+02
.3324E+02	.1073E+02	.1096E+02	.1805E+02	.1815E+02	.1919E+02	.1930E+02	.1446E+01	.1983E+01	.4686E+01
.4965E+01	.6811E+01	.7117E+01	.1238E+02	.1258E+02	.2032E+02	.2038E+02	.2128E+02	.2136E+02	.9118E+01
.9409E+01	.1416E+02	.1432E+02	.1564E+02	.1577E+02	.2224E+02	.2229E+02	.2311E+02	.2317E+02	.2135E+01
.2548E+01	.4998E+01	.5276E+01	.7129E+01	.7431E+01	.1105E+02	.1126E+02	.1701E+02	.1712E+02	.2398E+02
.2403E+02	.2479E+02	.2485E+02	.2417E+01	.2760E+01	.9399E+01	.9640E+01	.1267E+02	.1288E+02	.1824E+02
.1834E+02	.2561E+02	.2566E+02	.2638E+02	.2643E+02	.5310E+01	.5578E+01	.7441E+01	.7735E+01	.1439E+02
.1456E+02	.1942E+02	.1951E+02	.2046E+02	.2056E+02	.2714E+02	.2720E+02	.2786E+02	.2792E+02	.2858E+02
.2863E+02	.2852E+01	.3097E+01	.1136E+02	.1156E+02	.1590E+02	.1603E+02	.2147E+02	.2154E+02	.2929E+02
.2935E+02	.2999E+02	.3005E+02	.3068E+02	.3073E+02	.3135E+02	.3141E+02	.5623E+01	.5886E+01	.7767E+01
.8047E+01	.9781E+01	.1001E+02	.1296E+02	.1316E+02	.1722E+02	.1733E+02	.2240E+02	.2248E+02	.2327E+02
.2332E+02	.3205E+02	.3210E+02	.3270E+02	.3275E+02	.3335E+02	.3338E+02	.3182E+01	.3368E+01	.1464E+02
.1480E+02	.1845E+02	.1854E+02	.2413E+02	.2420E+02	.2032E+00	.3319E+01	.3474E+01	.5938E+01	.6185E+01
.1002E+02	.1023E+02	.1165E+02	.1183E+02	.1610E+02	.1622E+02	.1962E+02	.1971E+02	.2497E+02	.2502E+02
.2576E+02	.2582E+02	.8230E+01	.8460E+01	.1326E+02	.1345E+02	.2068E+02	.2076E+02	.2162E+02	.2168E+02
.2654E+02	.2659E+02	.2032E+00	.2032E+00	.3532E+01	.3622E+01	.6234E+01	.6450E+01	.1184E+02	.1203E+02
.1488E+02	.1502E+02	.1745E+02	.1755E+02	.2255E+02	.2260E+02	.2731E+02	.2737E+02	.2804E+02	.2809E+02
.8484E+01	.8707E+01	.1035E+02	.1053E+02	.1866E+02	.1876E+02	.2345E+02	.2349E+02	.2876E+02	.2882E+02
.2946E+02	.2952E+02	.3017E+02	.3022E+02	.3084E+02	.3091E+02	.2032E+00	.2032E+00	.3647E+01	.3696E+01
.6476E+01	.6652E+01	.1353E+02	.1371E+02	.1635E+02	.1645E+02	.1981E+02	.1989E+02	.2430E+02	.2437E+02
.3155E+02	.3159E+02	.3220E+02	.3225E+02	.3285E+02	.3289E+02	.8726E+01	.8909E+01	.1210E+02	.1227E+02
.2085E+02	.2091E+02	.2515E+02	.2520E+02	.3351E+02	.3356E+02	.2032E+00	.2032E+00	.3718E+01	.3736E+01
.6679E+01	.6814E+01	.1062E+02	.1076E+02	.1517E+02	.1529E+02	.1767E+02	.1777E+02	.2181E+02	.2188E+02
.2594E+02	.2599E+02	.8933E+01	.9086E+01	.1379E+02	.1394E+02	.1886E+02	.1894E+02	.2273E+02	.2279E+02
.2672E+02	.2678E+02	.2032E+00	.2032E+00	.3754E+01	.3744E+01	.6843E+01	.6946E+01	.1079E+02	.1092E+02
.1235E+02	.1250E+02	.1659E+02	.1668E+02	.1999E+02	.2006E+02	.2362E+02	.2368E+02	.2750E+02	.2754E+02
.3760E+01	.3736E+01	.1537E+02	.1546E+02	.1783E+02	.1791E+02	.2101E+02	.2108E+02	.2448E+02	.2452E+02
.2824E+02	.2830E+02	.2895E+02	.2900E+02	.2033E+00	.2032E+00	.9187E+01	.9291E+01	.1402E+02	.1416E+02

.2967E+02	.2972E+02	.3036E+02	.3042E+02	.3103E+02	.3110E+02	.3170E+02	.3175E+02	.3754E+01	.3714E+01
.7023E+01	.7091E+01	.1099E+02	.1111E+02	.1258E+02	.1272E+02	.1674E+02	.1683E+02	.1905E+02	.1914E+02
.2200E+02	.2205E+02	.2534E+02	.2539E+02	.3238E+02	.3244E+02	.3303E+02	.3308E+02	.3367E+02	.3371E+02
.2032E+00	.2032E+00	.9307E+01	.9397E+01	.1553E+02	.1562E+02	.2291E+02	.2297E+02	.2614E+02	.2619E+02
.2032E+00	.2032E+00	.3730E+01	.3684E+01	.7112E+01	.7158E+01	.1804E+02	.1811E+02	.2022E+02	.2028E+02
.2379E+02	.2385E+02	.1119E+02	.1130E+02	.1280E+02	.1292E+02	.1429E+02	.1438E+02	.2121E+02	.2126E+02
.2696E+02	.2701E+02	.2032E+00	.2032E+00	.3698E+01	.3647E+01	.7183E+01	.7210E+01	.9457E+01	.9523E+01
.1695E+02	.1703E+02	.1924E+02	.1931E+02	.2216E+02	.2220E+02	.2468E+02	.2474E+02	.2772E+02	.2778E+02
.1131E+02	.1140E+02	.1574E+02	.1583E+02	.2847E+02	.2851E+02	.2917E+02	.2922E+02	.2985E+02	.2992E+02
.2032E+00	.2107E+00	.3660E+01	.3606E+01	.7238E+01	.7249E+01	.9543E+01	.9599E+01	.1298E+02	.1308E+02
.1446E+02	.1454E+02	.1824E+02	.1831E+02	.2039E+02	.2043E+02	.2309E+02	.2314E+02	.2554E+02	.2559E+02
.3058E+02	.3063E+02	.3125E+02	.3131E+02	.3192E+02	.3196E+02	.3257E+02	.3262E+02	.3320E+02	.3325E+02
.3383E+02	.3389E+02	.1710E+02	.1717E+02	.2634E+02	.2640E+02	.2117E+00	.2192E+00	.3630E+01	.3578E+01
.1145E+02	.1151E+02	.2138E+02	.2142E+02	.2399E+02	.2405E+02	.7281E+01	.7281E+01	.9626E+01	.9661E+01
.1456E+02	.1465E+02	.1591E+02	.1598E+02	.1944E+02	.1949E+02	.2187E+00	.2252E+00	.3605E+01	.3554E+01
.1314E+02	.1322E+02	.2234E+02	.2239E+02	.2487E+02	.2492E+02	.2716E+02	.2722E+02	.1840E+02	.1845E+02
.2053E+02	.2057E+02	.2259E+00	.2307E+00	.7315E+01	.7311E+01	.9696E+01	.9709E+01	.1157E+02	.1162E+02
.1726E+02	.1732E+02	.2327E+02	.2332E+02	.2572E+02	.2577E+02	.2795E+02	.2800E+02	.2290E+00	.2330E+00
.3571E+01	.3526E+01	.1324E+02	.1330E+02	.1470E+02	.1476E+02	.1604E+02	.1610E+02	.2153E+02	.2157E+02
.2870E+02	.2873E+02	.2940E+02	.2944E+02	.3008E+02	.3014E+02	.3078E+02	.3083E+02	.3145E+02	.3150E+02
.3211E+02	.3217E+02	.3276E+02	.3280E+02	.3339E+02	.3344E+02	.3403E+02	.3407E+02	.1959E+02	.1963E+02
.2417E+02	.2422E+02	.2336E+00	.2366E+00	.3554E+01	.3515E+01	.7345E+01	.7341E+01	.1164E+02	.1168E+02
.2657E+02	.2662E+02	.9761E+01	.9770E+01	.1855E+02	.1858E+02	.2066E+02	.2071E+02	.2251E+02	.2256E+02
.2371E+00	.2390E+00	.1336E+02	.1340E+02	.1482E+02	.1487E+02	.1616E+02	.1622E+02	.1741E+02	.1746E+02
.2508E+02	.2511E+02	.2738E+02	.2742E+02	.2384E+00	.2394E+00	.3537E+01	.3510E+01	.7375E+01	.7367E+01
.2344E+02	.2348E+02	.9800E+01	.9799E+01	.1173E+02	.1176E+02	.1973E+02	.1978E+02	.2170E+02	.2174E+02
.2592E+02	.2596E+02	.2394E+00	.2388E+00	.3535E+01	.3514E+01	.7392E+01	.7384E+01	.1865E+02	.1869E+02
.2434E+02	.2439E+02	.2818E+02	.2822E+02	.3231E+02	.3236E+02	.3296E+02	.3301E+02	.3359E+02	.3363E+02
.3422E+02	.3426E+02	.1346E+02	.1350E+02	.1493E+02	.1497E+02	.1628E+02	.1632E+02	.1752E+02	.1756E+02
.2266E+02	.2269E+02	.2893E+02	.2897E+02	.2964E+02	.2968E+02	.3033E+02	.3037E+02	.3101E+02	.3106E+02
.3169E+02	.3173E+02	.2386E+00	.2370E+00	.3540E+01	.3527E+01	.9840E+01	.9839E+01	.1179E+02	.1181E+02
.2083E+02	.2087E+02	.2678E+02	.2681E+02	.7419E+01	.7411E+01	.2524E+02	.2528E+02	.2367E+00	.2346E+00
.1988E+02	.1991E+02	.2183E+02	.2186E+02	.2361E+02	.2366E+02	.2356E+00	.2331E+00	.3561E+01	.3556E+01
.9870E+01	.9869E+01	.1355E+02	.1358E+02	.1503E+02	.1506E+02	.1638E+02	.1640E+02	.1763E+02	.1764E+02
.1879E+02	.1882E+02	.2761E+02	.2764E+02	.7446E+01	.7438E+01	.1186E+02	.1188E+02	.2612E+02	.2615E+02
.2327E+00	.2298E+00	.3580E+01	.3582E+01	.2096E+02	.2098E+02	.2281E+02	.2285E+02	.2454E+02	.2457E+02
.3378E+02	.3383E+02	.3441E+02	.3444E+02	.2841E+02	.2844E+02	.3122E+02	.3125E+02	.3188E+02	.3191E+02
.3254E+02	.3258E+02	.3318E+02	.3322E+02	.2292E+00	.2253E+00	.7471E+01	.7464E+01	.9910E+01	.9910E+01
.1362E+02	.1365E+02	.1998E+02	.2002E+02	.2696E+02	.2700E+02	.2914E+02	.2918E+02	.2986E+02	.2990E+02
.3055E+02	.3058E+02	.3619E+01	.3625E+01	.1192E+02	.1193E+02	.1511E+02	.1513E+02	.1646E+02	.1647E+02
.1771E+02	.1774E+02	.1890E+02	.1892E+02	.2197E+02	.2200E+02	.2375E+02	.2379E+02	.2543E+02	.2545E+02
.2247E+00	.2202E+00	.2220E+00	.2177E+00	.9951E+01	.9953E+01	.2107E+02	.2109E+02	.3664E+01	.3675E+01
.7507E+01	.7502E+01	.1369E+02	.1370E+02	.2295E+02	.2297E+02	.2467E+02	.2470E+02	.2628E+02	.2632E+02
.2780E+02	.2783E+02	.2173E+00	.2148E+00	.1197E+02	.1197E+02	.1518E+02	.1519E+02	.2011E+02	.2012E+02
.3457E+02	.3462E+02	.1654E+02	.1656E+02	.1781E+02	.1782E+02	.1899E+02	.1902E+02	.2208E+02	.2211E+02
.3271E+02	.3275E+02	.3335E+02	.3340E+02	.3399E+02	.3402E+02	.2144E+00	.2118E+00	.3715E+01	.3729E+01
.7535E+01	.7535E+01	.9994E+01	.9996E+01	.2390E+02	.2391E+02	.3142E+02	.3145E+02	.3208E+02	.3213E+02
.1200E+02	.1201E+02	.1374E+02	.1374E+02	.2116E+02	.2119E+02	.2558E+02	.2561E+02	.2715E+02	.2718E+02
.2863E+02	.2865E+02	.3076E+02	.3078E+02	.2114E+00	.2087E+00	.3750E+01	.3765E+01	.1523E+02	.1523E+02
.2937E+02	.2940E+02	.3009E+02	.3012E+02	.2099E+00	.2072E+00	.7566E+01	.7569E+01	.1661E+02	.1661E+02
.1787E+02	.1789E+02	.2020E+02	.2021E+02	.2308E+02	.2309E+02	.1004E+02	.1004E+02	.1909E+02	.1910E+02
.2484E+02	.2485E+02	.2069E+00	.2050E+00	.3803E+01	.3819E+01	.1205E+02	.1205E+02	.1378E+02	.1378E+02
.2221E+02	.2222E+02	.2647E+02	.2649E+02	.2799E+02	.2802E+02	.3476E+02	.3479E+02	.7600E+01	.7605E+01
.3415E+02	.3419E+02	.2047E+00	.2036E+00	.1529E+02	.1529E+02	.2128E+02	.2128E+02	.2404E+02	.2405E+02
.3291E+02	.3294E+02	.3356E+02	.3359E+02	.3848E+01	.3863E+01	.1007E+02	.1007E+02	.1667E+02	.1668E+02

.2573E+02	.2575E+02	.3227E+02	.3231E+02	.2037E+00	.2032E+00	.1796E+02	.1797E+02	.1916E+02	.1917E+02
.2030E+02	.2030E+02	.2319E+02	.2320E+02	.3163E+02	.3165E+02	.7637E+01	.7642E+01	.1209E+02	.1209E+02
.1382E+02	.1381E+02	.2734E+02	.2736E+02	.3096E+02	.3099E+02	.2032E+00	.2032E+00	.2884E+02	.2886E+02
.3028E+02	.3030E+02	.3901E+01	.3917E+01	.1010E+02	.1010E+02	.1533E+02	.1534E+02	.2231E+02	.2231E+02
.2497E+02	.2498E+02	.2959E+02	.2960E+02	.2032E+00	.2032E+00	.1673E+02	.1674E+02	.3493E+02	.3496E+02
.7675E+01	.7681E+01	.1212E+02	.1212E+02	.1384E+02	.1384E+02	.1802E+02	.1803E+02	.2137E+02	.2137E+02
.2663E+02	.2665E+02	.3433E+02	.3436E+02	.3941E+01	.3956E+01	.1923E+02	.1924E+02	.2037E+02	.2036E+02
.2416E+02	.2417E+02	.2818E+02	.2820E+02	.3372E+02	.3375E+02	.2032E+00	.2032E+00	.1013E+02	.1015E+02
.3310E+02	.3312E+02	.1539E+02	.1538E+02	.2330E+02	.2330E+02	.2588E+02	.2589E+02	.3246E+02	.3248E+02
.2032E+00	.2032E+00	.7713E+01	.7720E+01	.1678E+02	.1678E+02	.3181E+02	.3183E+02	.3993E+01	.4008E+01
.1216E+02	.1216E+02	.1388E+02	.1388E+02	.2240E+02	.2240E+02	.2749E+02	.2751E+02	.3114E+02	.3116E+02
.2032E+00	.2032E+00	.1809E+02	.1809E+02	.2510E+02	.2510E+02	.3507E+02	.3510E+02	.1019E+02	.1019E+02
.1931E+02	.1930E+02	.2145E+02	.2145E+02	.2904E+02	.2904E+02	.3048E+02	.3049E+02	.3447E+02	.3450E+02
.2032E+00	.2032E+00	.4032E+01	.4047E+01	.7752E+01	.7759E+01	.1543E+02	.1543E+02	.2044E+02	.2043E+02
.2426E+02	.2426E+02	.2978E+02	.2979E+02	.3387E+02	.3388E+02	.1219E+02	.1220E+02	.2678E+02	.2679E+02
.1392E+02	.1392E+02	.1684E+02	.1684E+02	.3325E+02	.3327E+02	.2032E+00	.2032E+00	.1022E+02	.1022E+02
.2340E+02	.2340E+02	.2836E+02	.2836E+02	.3261E+02	.3263E+02	.4074E+01	.4087E+01	.2601E+02	.2601E+02
.7795E+01	.7801E+01	.1547E+02	.1547E+02	.1815E+02	.1815E+02	.2248E+02	.2248E+02	.3197E+02	.3198E+02
.3521E+02	.3522E+02	.2032E+00	.2032E+00	.1223E+02	.1223E+02	.3130E+02	.3130E+02	.1396E+02	.1396E+02
.1937E+02	.1936E+02	.2152E+02	.2152E+02	.2521E+02	.2521E+02	.2764E+02	.2765E+02	.3462E+02	.3463E+02
.1025E+02	.1027E+02	.1688E+02	.1688E+02	.3061E+02	.3063E+02	.3400E+02	.3401E+02	.2032E+00	.2032E+00
.4121E+01	.4132E+01	.7826E+01	.7832E+01	.2050E+02	.2050E+02	.2918E+02	.2919E+02	.3336E+02	.3337E+02
.2437E+02	.2437E+02	.2689E+02	.2689E+02	.2992E+02	.2993E+02	.1227E+02	.1227E+02	.1399E+02	.1399E+02
.1551E+02	.1551E+02	.3273E+02	.3274E+02	.2032E+00	.2032E+00	.1820E+02	.1820E+02	.3532E+02	.3533E+02
.4157E+01	.4168E+01	.1030E+02	.1030E+02	.2349E+02	.2349E+02	.2848E+02	.2849E+02	.3208E+02	.3209E+02
.7866E+01	.7872E+01	.2612E+02	.2612E+02	.3473E+02	.3474E+02	.1230E+02	.1230E+02	.1694E+02	.1694E+02
.2256E+02	.2256E+02	.3142E+02	.3143E+02	.3410E+02	.3411E+02	.1403E+02	.1403E+02	.1555E+02	.1555E+02
.1943E+02	.1943E+02	.4192E+01	.4202E+01	.2531E+02	.2531E+02	.2777E+02	.2777E+02	.3074E+02	.3075E+02
.3348E+02	.3349E+02	.1034E+02	.1034E+02	.2160E+02	.2160E+02	.2032E+00	.2032E+00	.7908E+01	.7913E+01
.2931E+02	.2932E+02	.3005E+02	.3006E+02	.3285E+02	.3286E+02	.3543E+02	.3544E+02	.1825E+02	.1825E+02
.2057E+02	.2057E+02	.2446E+02	.2446E+02	.2700E+02	.2701E+02	.4234E+01	.4242E+01	.1235E+02	.1235E+02
.3220E+02	.3221E+02	.3483E+02	.3484E+02	.1407E+02	.1407E+02	.1698E+02	.1698E+02	.2859E+02	.2860E+02
.1039E+02	.1039E+02	.1560E+02	.1560E+02	.2357E+02	.2357E+02	.3153E+02	.3154E+02	.3422E+02	.3423E+02
.7960E+01	.7964E+01	.2622E+02	.2622E+02	.4276E+01	.4283E+01	.3359E+02	.3360E+02	.1948E+02	.1947E+02
.2264E+02	.2263E+02	.2786E+02	.2786E+02	.3086E+02	.3086E+02	.3553E+02	.3554E+02	.2032E+00	.2032E+00
.1240E+02	.1240E+02	.2539E+02	.2539E+02	.3295E+02	.3296E+02	.8000E+01	.8003E+01	.2165E+02	.2165E+02
.2941E+02	.2942E+02	.3016E+02	.3016E+02	.3493E+02	.3493E+02	.4317E+01	.4322E+01	.1044E+02	.1044E+02
.1412E+02	.1412E+02	.1829E+02	.1829E+02	.3230E+02	.3231E+02	.1564E+02	.1564E+02	.1702E+02	.1702E+02
.2453E+02	.2453E+02	.2710E+02	.2710E+02	.3431E+02	.3432E+02	.2062E+02	.2062E+02	.2869E+02	.2869E+02
.3163E+02	.3163E+02	.3369E+02	.3369E+02	.4356E+01	.4359E+01	.8050E+01	.8052E+01	.1245E+02	.1245E+02
.2363E+02	.2363E+02	.2629E+02	.2630E+02	.3563E+02	.3563E+02	.2032E+00	.2032E+00	.3095E+02	.3096E+02
.3304E+02	.3305E+02	.1049E+02	.1049E+02	.1416E+02	.1416E+02	.2795E+02	.2795E+02	.3502E+02	.3503E+02
.4386E+01	.4388E+01	.1952E+02	.1952E+02	.2269E+02	.2269E+02	.2547E+02	.2547E+02	.2951E+02	.2952E+02
.3026E+02	.3026E+02	.3240E+02	.3240E+02	.3440E+02	.3441E+02	.8103E+01	.8104E+01	.1568E+02	.1568E+02
.1833E+02	.1833E+02	.1706E+02	.1706E+02	.2170E+02	.2170E+02	.2717E+02	.2718E+02	.3172E+02	.3173E+02
.3377E+02	.3378E+02	.2032E+00	.2032E+00	.4430E+01	.4431E+01	.2459E+02	.2459E+02	.3572E+02	.3572E+02
.1250E+02	.1250E+02	.2064E+02	.2064E+02	.2879E+02	.2879E+02	.1056E+02	.1056E+02	.3104E+02	.3105E+02
.3314E+02	.3314E+02	.3511E+02	.3511E+02	.4462E+01	.4462E+01	.2368E+02	.2368E+02	.2637E+02	.2637E+02
.8169E+01	.8169E+01	.2803E+02	.2803E+02	.3248E+02	.3248E+02	.3449E+02	.3449E+02		

Y-COORDINATES

.5765E+01	.4635E+01	.4233E+01	.3761E+01	.3375E+01	.2946E+01	.2538E+01	.2236E+01	.1996E+01	.1810E+01
.1675E+01	.1533E+01	.1402E+01	.1289E+01	.1196E+01	.1116E+01	.1044E+01	.9822E+00	.9279E+00	.8818E+00
.8469E+00	.8256E+00	.8261E+00	.8437E+00	.8594E+00	.8745E+00	.8876E+00	.9004E+00	.5668E+01	.5238E+01

.4537E+01	.4368E+01	.4204E+01	.4094E+01	.3733E+01	.3600E+01	.5209E+01	.4914E+01	.3317E+01	.3204E+01
.2887E+01	.2779E+01	.2506E+01	.2417E+01	.2215E+01	.2147E+01	.4375E+01	.4249E+01	.1968E+01	.1909E+01
.1792E+01	.1740E+01	.1664E+01	.1614E+01	.1521E+01	.1477E+01	.4956E+01	.4725E+01	.4071E+01	.3935E+01
.1384E+01	.1342E+01	.1277E+01	.1240E+01	.1186E+01	.1152E+01	.1012E+02	.4256E+01	.4190E+01	.3531E+01
.3393E+01	.3210E+01	.3093E+01	.2780E+01	.2678E+01	.1100E+01	.1070E+01	.1033E+01	.1004E+01	.9745E+00
.9472E+00	.9220E+00	.8968E+00	.8770E+00	.8546E+00	.1122E+02	.8233E+01	.4701E+01	.4534E+01	.3943E+01
.3796E+01	.2393E+01	.2313E+01	.2132E+01	.2059E+01	.8400E+00	.8187E+00	.8219E+00	.8031E+00	.8269E+00
.8109E+00	.8437E+00	.8295E+00	.8608E+00	.8461E+00	.8751E+00	.8621E+00	.8888E+00	.8767E+00	.9022E+00
.8908E+00	.3416E+01	.3281E+01	.1899E+01	.1836E+01	.1733E+01	.1677E+01	.7737E+01	.6388E+01	.4533E+01
.4394E+01	.4158E+01	.4068E+01	.3075E+01	.2957E+01	.1597E+01	.1546E+01	.1461E+01	.1412E+01	.3750E+01
.3584E+01	.2626E+01	.2521E+01	.2311E+01	.2224E+01	.1331E+01	.1288E+01	.1232E+01	.1192E+01	.6115E+01
.5434E+01	.4389E+01	.4271E+01	.4075E+01	.3964E+01	.3258E+01	.3127E+01	.2040E+01	.1968E+01	.1138E+01
.1103E+01	.1066E+01	.1032E+01	.5641E+01	.5142E+01	.3610E+01	.3444E+01	.2940E+01	.2818E+01	.1825E+01
.1762E+01	.9960E+00	.9656E+00	.9409E+00	.9123E+00	.4266E+01	.4168E+01	.3972E+01	.3840E+01	.2513E+01
.2411E+01	.1655E+01	.1599E+01	.1540E+01	.1482E+01	.8875E+00	.8601E+00	.8473E+00	.8216E+00	.8178E+00
.7940E+00	.5035E+01	.4749E+01	.3105E+01	.2978E+01	.2194E+01	.2110E+01	.1395E+01	.1345E+01	.8020E+00
.7809E+00	.8132E+00	.7948E+00	.8318E+00	.8143E+00	.8488E+00	.8331E+00	.4158E+01	.4053E+01	.3843E+01
.3691E+01	.3388E+01	.3229E+01	.2797E+01	.2674E+01	.1948E+01	.1874E+01	.1275E+01	.1229E+01	.1183E+01
.1142E+01	.8636E+00	.8475E+00	.8775E+00	.8630E+00	.8916E+00	.8778E+00	.4670E+01	.4492E+01	.2397E+01
.2297E+01	.1747E+01	.1683E+01	.1095E+01	.1057E+01	.1171E+02	.4544E+01	.4397E+01	.4041E+01	.3927E+01
.3246E+01	.3093E+01	.2954E+01	.2827E+01	.2104E+01	.2019E+01	.1590E+01	.1530E+01	.1020E+01	.9842E+00
.9615E+00	.9279E+00	.3607E+01	.3420E+01	.2649E+01	.2524E+01	.1458E+01	.1400E+01	.1339E+01	.1287E+01
.9043E+00	.8730E+00	.1115E+02	.9149E+01	.4352E+01	.4252E+01	.3915E+01	.3798E+01	.2855E+01	.2730E+01
.2284E+01	.2185E+01	.1850E+01	.1777E+01	.1225E+01	.1179E+01	.8541E+00	.8239E+00	.8173E+00	.7891E+00
.3430E+01	.3242E+01	.3052E+01	.2907E+01	.1666E+01	.1601E+01	.1130E+01	.1088E+01	.7883E+00	.7610E+00
.7828E+00	.7587E+00	.8001E+00	.7783E+00	.8186E+00	.7995E+00	.9016E+01	.7982E+01	.4233E+01	.4145E+01
.3798E+01	.3670E+01	.2510E+01	.2385E+01	.1988E+01	.1904E+01	.1522E+01	.1462E+01	.1050E+01	.1008E+01
.8350E+00	.8153E+00	.8515E+00	.8337E+00	.8669E+00	.8499E+00	.3259E+01	.3081E+01	.2721E+01	.2597E+01
.1394E+01	.1335E+01	.9784E+00	.9413E+00	.8794E+00	.8628E+00	.7973E+01	.7289E+01	.4126E+01	.4043E+01
.3669E+01	.3515E+01	.2880E+01	.2745E+01	.2145E+01	.2048E+01	.1756E+01	.1684E+01	.1270E+01	.1216E+01
.9192E+00	.8837E+00	.3097E+01	.2931E+01	.2372E+01	.2257E+01	.1589E+01	.1524E+01	.1166E+01	.1117E+01
.8673E+00	.8322E+00	.7284E+01	.6742E+01	.4021E+01	.3941E+01	.3514E+01	.3348E+01	.2772E+01	.2639E+01
.2590E+01	.2466E+01	.1878E+01	.1796E+01	.1454E+01	.1392E+01	.1078E+01	.1032E+01	.8201E+00	.7883E+00
.3970E+01	.3890E+01	.2044E+01	.1951E+01	.1689E+01	.1617E+01	.1329E+01	.1268E+01	.1003E+01	.9610E+00
.7823E+00	.7507E+00	.7620E+00	.7330E+00	.6734E+01	.6341E+01	.2878E+01	.2730E+01	.2248E+01	.2135E+01
.7608E+00	.7335E+00	.7818E+00	.7577E+00	.8021E+00	.7791E+00	.8209E+00	.7989E+00	.3868E+01	.3785E+01
.3277E+01	.3124E+01	.2615E+01	.2485E+01	.2456E+01	.2332E+01	.1798E+01	.1716E+01	.1512E+01	.1442E+01
.1201E+01	.1146E+01	.9305E+00	.8905E+00	.8355E+00	.8147E+00	.8517E+00	.8318E+00	.8668E+00	.8478E+00
.6296E+01	.6030E+01	.2750E+01	.2608E+01	.1948E+01	.1856E+01	.1106E+01	.1054E+01	.8758E+00	.8366E+00
.6134E+01	.5910E+01	.3761E+01	.3673E+01	.3133E+01	.2988E+01	.1599E+01	.1525E+01	.1372E+01	.1304E+01
.1026E+01	.9777E+00	.2462E+01	.2334E+01	.2320E+01	.2195E+01	.2087E+01	.1978E+01	.1250E+01	.1188E+01
.8204E+00	.7828E+00	.5884E+01	.5721E+01	.3649E+01	.3555E+01	.2996E+01	.2858E+01	.2570E+01	.2436E+01
.1692E+01	.1610E+01	.1433E+01	.1362E+01	.1144E+01	.1088E+01	.9467E+00	.9016E+00	.7786E+00	.7424E+00
.2361E+01	.2235E+01	.1823E+01	.1729E+01	.7439E+00	.7093E+00	.7308E+00	.6986E+00	.7416E+00	.7124E+00
.5703E+01	.5571E+01	.3528E+01	.3430E+01	.2864E+01	.2732E+01	.2456E+01	.2327E+01	.2187E+01	.2062E+01
.1970E+01	.1864E+01	.1509E+01	.1433E+01	.1298E+01	.1229E+01	.1045E+01	.9909E+00	.8797E+00	.8361E+00
.7608E+00	.7328E+00	.7821E+00	.7553E+00	.8019E+00	.7762E+00	.8203E+00	.7958E+00	.8366E+00	.8132E+00
.8518E+00	.8301E+00	.1614E+01	.1532E+01	.8299E+00	.7879E+00	.5556E+01	.5438E+01	.3434E+01	.3335E+01
.2239E+01	.2115E+01	.1176E+01	.1112E+01	.9659E+00	.9149E+00	.2723E+01	.2598E+01	.2333E+01	.2209E+01
.1885E+01	.1780E+01	.1722E+01	.1628E+01	.1347E+01	.1275E+01	.5448E+01	.5340E+01	.3334E+01	.3234E+01
.2052E+01	.1933E+01	.1072E+01	.1011E+01	.8963E+00	.8476E+00	.7774E+00	.7364E+00	.1423E+01	.1345E+01
.1224E+01	.1152E+01	.5326E+01	.5222E+01	.2585E+01	.2463E+01	.2214E+01	.2096E+01	.2093E+01	.1976E+01
.1520E+01	.1436E+01	.9829E+00	.9264E+00	.8362E+00	.7897E+00	.7341E+00	.6949E+00	.5264E+01	.5164E+01
.3184E+01	.3081E+01	.1954E+01	.1837E+01	.1775E+01	.1671E+01	.1625E+01	.1534E+01	.1108E+01	.1041E+01
.7042E+00	.6665E+00	.6986E+00	.6628E+00	.7172E+00	.6841E+00	.7405E+00	.7086E+00	.7622E+00	.7316E+00

.7822E+00	.7530E+00	.8009E+00	.7727E+00	.8181E+00	.7912E+00	.8343E+00	.8085E+00	.1265E+01	.1187E+01
.9085E+00	.8547E+00	.5149E+01	.5052E+01	.3082E+01	.2977E+01	.2452E+01	.2335E+01	.1990E+01	.1875E+01
.7771E+00	.7318E+00	.2066E+01	.1953E+01	.1330E+01	.1250E+01	.1146E+01	.1069E+01	.9986E+00	.9340E+00
.5037E+01	.4942E+01	.1826E+01	.1711E+01	.1663E+01	.1562E+01	.1532E+01	.1439E+01	.1417E+01	.1332E+01
.8352E+00	.7831E+00	.7327E+00	.6894E+00	.4981E+01	.4888E+01	.2927E+01	.2818E+01	.2324E+01	.2210E+01
.9181E+00	.8577E+00	.1958E+01	.1847E+01	.1855E+01	.1743E+01	.1177E+01	.1096E+01	.1023E+01	.9519E+00
.7816E+00	.7315E+00	.4873E+01	.4782E+01	.2822E+01	.2712E+01	.2241E+01	.2129E+01	.1256E+01	.1171E+01
.8488E+00	.7919E+00	.6876E+00	.6446E+00	.7578E+00	.7250E+00	.7769E+00	.7453E+00	.7952E+00	.7642E+00
.8117E+00	.7819E+00	.1701E+01	.1589E+01	.1556E+01	.1457E+01	.1438E+01	.1346E+01	.1334E+01	.1247E+01
.9357E+00	.8681E+00	.6624E+00	.6209E+00	.6646E+00	.6253E+00	.6887E+00	.6505E+00	.7117E+00	.6755E+00
.7339E+00	.6983E+00	.4769E+01	.4678E+01	.2718E+01	.2605E+01	.1853E+01	.1744E+01	.1757E+01	.1647E+01
.1048E+01	.9673E+00	.7266E+00	.6780E+00	.2118E+01	.2008E+01	.7820E+00	.7270E+00	.4664E+01	.4569E+01
.1086E+01	.1001E+01	.9509E+00	.8765E+00	.8497E+00	.7861E+00	.4609E+01	.4512E+01	.2559E+01	.2449E+01
.1750E+01	.1643E+01	.1577E+01	.1469E+01	.1450E+01	.1353E+01	.1346E+01	.1255E+01	.1250E+01	.1161E+01
.1158E+01	.1071E+01	.6797E+00	.6320E+00	.2001E+01	.1893E+01	.1632E+01	.1524E+01	.7246E+00	.6713E+00
.4496E+01	.4395E+01	.2467E+01	.2355E+01	.9652E+00	.8825E+00	.8591E+00	.7893E+00	.7789E+00	.7185E+00
.7682E+00	.7327E+00	.7852E+00	.7507E+00	.6408E+00	.5938E+00	.6842E+00	.6430E+00	.7061E+00	.6660E+00
.7265E+00	.6881E+00	.7461E+00	.7086E+00	.4381E+01	.4276E+01	.1896E+01	.1790E+01	.1632E+01	.1527E+01
.1470E+01	.1367E+01	.9948E+00	.9043E+00	.6773E+00	.6252E+00	.6216E+00	.5760E+00	.6324E+00	.5888E+00
.6570E+00	.6139E+00	.2331E+01	.2220E+01	.1521E+01	.1417E+01	.1335E+01	.1241E+01	.1241E+01	.1149E+01
.1151E+01	.1060E+01	.1062E+01	.9723E+00	.8663E+00	.7885E+00	.7837E+00	.7171E+00	.7209E+00	.6619E+00
.4261E+01	.4149E+01	.4198E+01	.4079E+01	.1545E+01	.1442E+01	.8839E+00	.7985E+00	.2196E+01	.2087E+01
.1759E+01	.1653E+01	.1367E+01	.1269E+01	.7847E+00	.7113E+00	.7208E+00	.6569E+00	.6710E+00	.6137E+00
.6305E+00	.5785E+00	.4059E+01	.3920E+01	.1414E+01	.1314E+01	.1245E+01	.1152E+01	.9002E+00	.8076E+00
.7552E+00	.7164E+00	.1135E+01	.1041E+01	.1049E+01	.9554E+00	.9643E+00	.8707E+00	.7943E+00	.7144E+00
.6963E+00	.6524E+00	.7157E+00	.6730E+00	.7340E+00	.6921E+00	.3899E+01	.3743E+01	.2064E+01	.1956E+01
.1657E+01	.1553E+01	.1430E+01	.1330E+01	.7167E+00	.6472E+00	.6499E+00	.6029E+00	.6711E+00	.6256E+00
.1335E+01	.1238E+01	.1270E+01	.1175E+01	.8016E+00	.7148E+00	.6589E+00	.5963E+00	.6211E+00	.5645E+00
.5901E+00	.5378E+00	.6224E+00	.5739E+00	.3718E+01	.3545E+01	.1978E+01	.1870E+01	.1157E+01	.1062E+01
.5765E+00	.5257E+00	.5942E+00	.5444E+00	.3620E+01	.3441E+01	.1557E+01	.1454E+01	.1050E+01	.9533E+00
.9663E+00	.8701E+00	.8054E+00	.7110E+00	.7078E+00	.6320E+00	.1320E+01	.1221E+01	.8635E+00	.7670E+00
.6503E+00	.5827E+00	.3414E+01	.3227E+01	.1852E+01	.1743E+01	.1235E+01	.1138E+01	.1176E+01	.1082E+01
.7066E+00	.6248E+00	.6065E+00	.5446E+00	.5787E+00	.5217E+00	.7205E+00	.6754E+00	.1456E+01	.1355E+01
.6980E+00	.6506E+00	.3200E+01	.3009E+01	.1047E+01	.9504E+00	.7053E+00	.6171E+00	.6388E+00	.5657E+00
.6559E+00	.6053E+00	.6749E+00	.6253E+00	.1744E+01	.1636E+01	.1219E+01	.1121E+01	.9457E+00	.8483E+00
.5980E+00	.5314E+00	.6309E+00	.5786E+00	.3032E+01	.2837E+01	.8496E+00	.7510E+00	.7733E+00	.6757E+00
.7043E+00	.6096E+00	.6376E+00	.5594E+00	.6052E+00	.5509E+00	.1352E+01	.1251E+01	.1123E+01	.1025E+01
.1068E+01	.9727E+00	.5592E+00	.4967E+00	.5787E+00	.5232E+00	.2858E+01	.2663E+01	.5338E+00	.4752E+00
.5517E+00	.4949E+00	.1616E+01	.1509E+01	.1128E+01	.1030E+01	.9471E+00	.8499E+00	.6223E+00	.5385E+00
.5789E+00	.5068E+00	.5265E+00	.4690E+00	.2685E+01	.2496E+01	.8518E+00	.7531E+00	.6747E+00	.6214E+00
.1248E+01	.1147E+01	.1035E+01	.9373E+00	.9844E+00	.8878E+00	.7610E+00	.6619E+00	.6142E+00	.5251E+00
.5417E+00	.4742E+00	.6519E+00	.5966E+00	.1521E+01	.1415E+01	.6748E+00	.5772E+00	.6170E+00	.5226E+00
.5632E+00	.4861E+00	.5187E+00	.4555E+00	.6285E+00	.5711E+00	.2437E+01	.2258E+01	.1037E+01	.9383E+00
.6044E+00	.5451E+00	.8474E+00	.7483E+00	.5533E+00	.4717E+00	.5272E+00	.4551E+00	.5799E+00	.5188E+00
.2277E+01	.2106E+01	.1144E+01	.1044E+01	.7574E+00	.6573E+00	.5549E+00	.4924E+00	.1396E+01	.1291E+01
.9250E+00	.8267E+00	.8780E+00	.7804E+00	.5401E+00	.4539E+00	.4990E+00	.4310E+00	.5297E+00	.4664E+00
.2125E+01	.1959E+01	.6544E+00	.5546E+00	.5082E+00	.4316E+00	.6274E+00	.5662E+00	.9219E+00	.8225E+00
.5766E+00	.4789E+00	.5231E+00	.4321E+00	.4770E+00	.4123E+00	.4987E+00	.4345E+00	.6045E+00	.5412E+00
.1977E+01	.1819E+01	.1304E+01	.1199E+01	.1041E+01	.9398E+00	.7460E+00	.6455E+00	.5162E+00	.4204E+00
.4945E+00	.4137E+00	.4739E+00	.4099E+00	.5813E+00	.5158E+00	.8365E+00	.7369E+00	.4740E+00	.4011E+00
.7720E+00	.6727E+00	.6457E+00	.5444E+00	.5496E+00	.4816E+00	.1788E+01	.1640E+01	.8346E+00	.7342E+00
.4718E+00	.3864E+00	.4545E+00	.3852E+00	.5253E+00	.4565E+00	.1196E+01	.1091E+01	.4551E+00	.3779E+00
.9264E+00	.8249E+00	.6525E+00	.5511E+00	.5467E+00	.4468E+00	.4581E+00	.3686E+00	.4932E+00	.4235E+00
.5703E+00	.4996E+00	.1645E+01	.1505E+01	.7318E+00	.6313E+00	.4694E+00	.3998E+00	.6689E+00	.5682E+00
.4768E+00	.3780E+00	.4431E+00	.3495E+00	.4343E+00	.3530E+00	.4287E+00	.3547E+00	.5377E+00	.4645E+00

.7307E+00	.6292E+00	.5502E+00	.4491E+00	.4389E+00	.3688E+00	.5141E+00	.4404E+00	.1509E+01	.1376E+01
.1069E+01	.9637E+00	.8379E+00	.7359E+00	.4268E+00	.3292E+00	.4116E+00	.3404E+00	.4906E+00	.4169E+00
.4117E+00	.3264E+00	.4081E+00	.3300E+00	.4098E+00	.3387E+00	.6259E+00	.5240E+00	.5856E+00	.4834E+00
.5425E+00	.4405E+00	.4591E+00	.3846E+00	.1381E+01	.1255E+01	.4527E+00	.3524E+00	.5019E+00	.4243E+00
.9671E+00	.8619E+00	.6256E+00	.5234E+00	.3873E+00	.2980E+00	.3840E+00	.3081E+00	.4285E+00	.3533E+00
.7266E+00	.6238E+00	.3776E+00	.2951E+00	.4690E+00	.3907E+00	.5402E+00	.4376E+00	.4394E+00	.3384E+00
.3700E+00	.2773E+00	.3993E+00	.3232E+00	.4472E+00	.3687E+00	.4801E+00	.3778E+00	.4506E+00	.3490E+00
.3761E+00	.2761E+00	.8655E+00	.7602E+00	.3532E+00	.2668E+00	.3538E+00	.2734E+00	.3712E+00	.2942E+00
.4162E+00	.3369E+00	.5195E+00	.4170E+00	.3423E+00	.2458E+00	.1102E+01	.9850E+00	.6155E+00	.5120E+00
.3383E+00	.2597E+00	.3436E+00	.2656E+00	.3858E+00	.3056E+00	.4256E+00	.3434E+00	.3502E+00	.2496E+00
.3236E+00	.2243E+00	.3269E+00	.2370E+00	.3286E+00	.2443E+00	.7559E+00	.6508E+00	.4248E+00	.3229E+00
.3558E+00	.2747E+00	.3929E+00	.3098E+00	.3752E+00	.2738E+00	.3424E+00	.2416E+00	.3122E+00	.2299E+00
.4305E+00	.3285E+00	.3441E+00	.2431E+00	.2996E+00	.2066E+00	.3270E+00	.2447E+00	.3612E+00	.2772E+00
.5073E+00	.4040E+00	.2929E+00	.2047E+00	.6443E+00	.5395E+00	.3307E+00	.2456E+00	.2753E+00	.1751E+00
.2720E+00	.1762E+00	.2763E+00	.1897E+00	.2897E+00	.2055E+00	.3405E+00	.2535E+00	.8007E+00	.6901E+00
.3245E+00	.2233E+00	.2653E+00	.1740E+00	.3012E+00	.2150E+00	.4212E+00	.3186E+00	.2531E+00	.1552E+00
.2593E+00	.1735E+00	.2634E+00	.1779E+00	.3091E+00	.2211E+00	.5333E+00	.4290E+00	.3244E+00	.2231E+00
.2665E+00	.1659E+00	.2505E+00	.1502E+00	.2729E+00	.1855E+00	.2469E+00	.1465E+00	.2430E+00	.1427E+00
.2373E+00	.1432E+00	.2392E+00	.1486E+00	.2788E+00	.1896E+00	.2253E+00	.1256E+00	.2309E+00	.1416E+00
.2458E+00	.1570E+00	.2496E+00	.1591E+00	.4231E+00	.3197E+00	.3148E+00	.2130E+00	.2250E+00	.1245E+00
.2091E+00	.1127E+00	.2106E+00	.1171E+00	.2501E+00	.1580E+00	.5491E+00	.4425E+00	.2095E+00	.1184E+00
.2216E+00	.1297E+00	.2191E+00	.1184E+00	.1743E+00	.7439E-01	.1922E+00	.9896E-01	.2199E+00	.1266E+00
.3381E+00	.2356E+00	.1777E+00	.7753E-01	.1803E+00	.8211E-01	.1714E+00	.7492E-01	.1728E+00	.7919E-01
.1748E+00	.8125E-01	.1834E+00	.8927E-01	.1914E+00	.9682E-01	.2145E+00	.1134E+00	.1520E+00	.5202E-01
.1563E+00	.5624E-01	.1452E+00	.4518E-01	.1501E+00	.5066E-01	.1518E+00	.5518E-01	.1581E+00	.6247E-01
.1640E+00	.6797E-01	.3080E+00	.2050E+00	.2181E+00	.1168E+00	.1409E+00	.4254E-01	.1558E+00	.5877E-01
.1306E+00	.3048E-01	.1298E+00	.2987E-01	.1316E+00	.3418E-01	.1263E+00	.2614E-01	.1228E+00	.2458E-01
.1252E+00	.2682E-01	.1274E+00	.2894E-01	.1293E+00	.2904E-01	.1102E+00	.1053E-01	.1104E+00	.1104E-01
.1000E+00	.0000E+00	.1000E+00	.0000E+00	.1000E+00	.0000E+00	.1000E+00	.0000E+00	.0000E+00	.0000E+00



CUMULATIVE TIME

.2184E+01 .3035E+01 .4218E+01 .5862E+01 .8146E+01 .1132E+02 .1573E+02 .2186E+02 .3037E+02 .4220E+02
 .5863E+02 .8147E+02 .1132E+03 .1573E+03 .2186E+03 .3037E+03 .4220E+03 .5864E+03 .8147E+03 .1132E+04

CUMULATIVE SALT WATER ENTRY INTO WELL

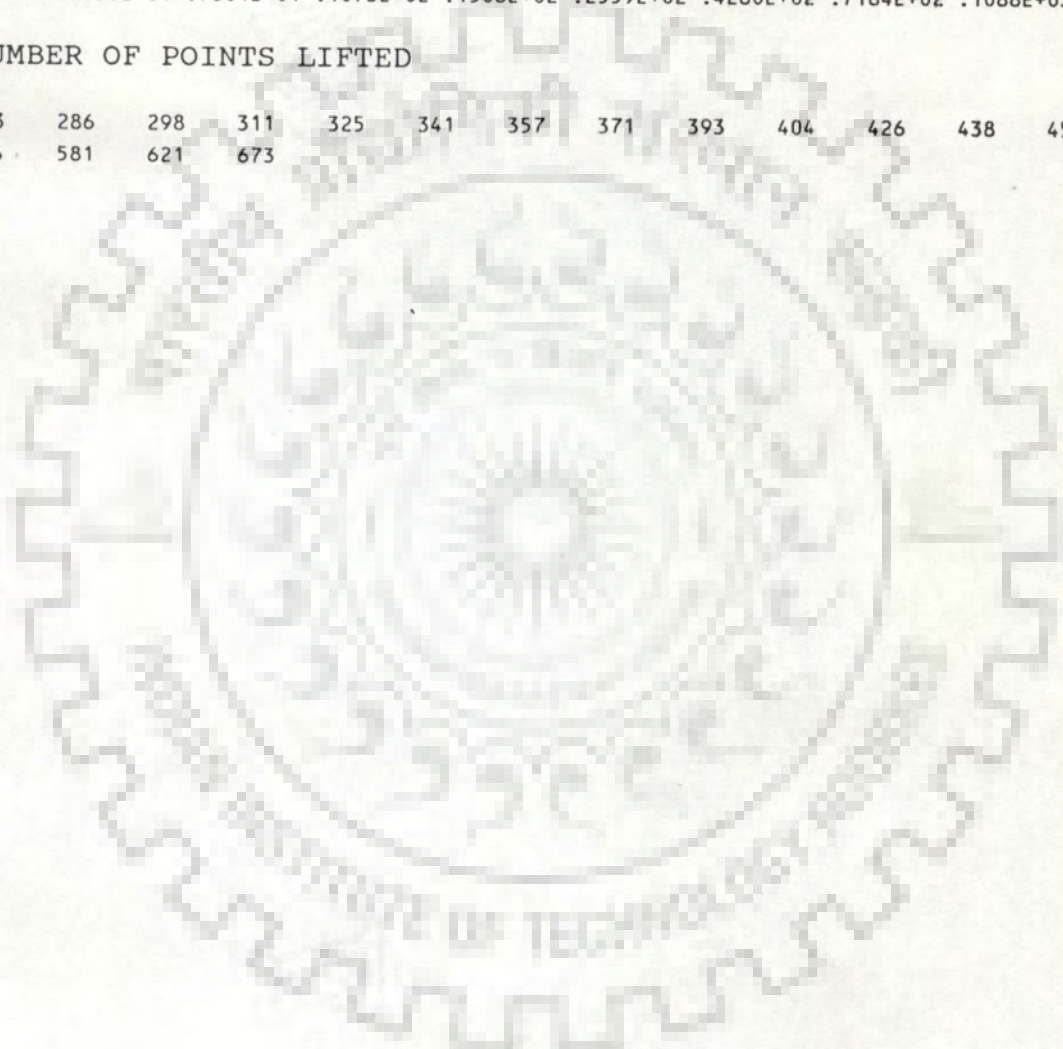
.0000E+00 .0000E+00 .0000E+00 .0000E+00 .0000E+00 .0000E+00 .0000E+00 .0000E+00 .0000E+00 .0000E+00
 .0000E+00 .0000E+00 .0000E+00 .0000E+00 .0000E+00 .0000E+00 .9111E-21 .9111E-21 .9111E-21 .1689E-13

CUMULATIVE SALT WATER LIFTING INTO SUSPENSION

.4320E-01 .6957E-01 .1096E+00 .1787E+00 .2941E+00 .4724E+00 .7417E+00 .1139E+01 .1719E+01 .2551E+01
 .3720E+01 .5350E+01 .7604E+01 .1073E+02 .1506E+02 .2559E+02 .4280E+02 .7184E+02 .1088E+03 .1816E+03

NUMBER OF POINTS LIFTED

273	286	298	311	325	341	357	371	393	404	426	438	459	474	49
544	581	621	673											



CUMULATIVE TIME

.1573E+04 .2186E+04 .3037E+04 .4220E+04 .5864E+04 .8147E+04 .1132E+05 .1152E+05 .1728E+05 .2304E+05

CUMULATIVE SALT WATER ENTRY INTO WELL

.2004E-09 .2231E-07 .3488E-07 .4661E-07 .2390E-03 .6670E-02 .1411E+00 .1411E+00 .2020E+02 .3962E+02

CUMULATIVE SALT WATER LIFTING INTO SUSPENSION

.2950E+03 .4060E+03 .5660E+03 .7560E+03 .1024E+04 .1376E+04 .1816E+04 .1841E+04 .2502E+04 .3124E+04

NUMBER OF POINTS LIFTED

745 821 926 1041 1208 1414 1682 1729 2064 2393



CUMULATIVE TIME

.1573E+04 .2186E+04 .3037E+04 .4220E+04 .5864E+04 .8147E+04 .1132E+05 .1152E+05 .1728E+05 .2304E+05

CUMULATIVE SALT WATER ENTRY INTO WELL

.2578E-15 .5068E-12 .6965E-12 .2810E-10 .1899E-07 .3076E-05 .5975E-05 .1708E-03 .3400E-01 .6099E+00

CUMULATIVE SALT WATER LIFTING INTO SUSPENSION

.1630E+03 .2843E+03 .3756E+03 .5388E+03 .7032E+03 .9450E+03 .1270E+04 .1271E+04 .1718E+04 .2097E+04

NUMBER OF POINTS LIFTED

636 708 771 874 989 1116 1322 1359 1617 1840



Dr. C. S. Murthy
 Director
 IIT Bombay

CUMULATIVE TIME

.2880E+05 .3456E+05 .4032E+05 .4320E+05 .5184E+05 .5760E+05 .6336E+05 .6912E+05 .7488E+05

CUMULATIVE SALT WATER ENTRY INTO WELL

.3703E+01 .1045E+02 .1820E+02 .2341E+02 .3838E+02 .5417E+02 .6629E+02 .7062E+02 .9233E+02

CUMULATIVE SALT WATER LIFTING INTO SUSPENSION

.2430E+04 .2705E+04 .2936E+04 .3058E+04 .3373E+04 .3616E+04 .3807E+04 .4021E+04 .4177E+04

NUMBER OF POINTS LIFTED

2043 2212 2364 2459 2694 2852 2990 3128 3233



Examiners
Board

CUMULATIVE TIME
.2916E+03 .4052E+03

CUMULATIVE SALT WATER ENTRY INTO WELL
.0000E+00 .0000E+00

CUMULATIVE SALT WATER LIFTING INTO SUSPENSION
.8666E-01 .1733E+00

NUMBER OF POINTS LIFTED
35 44

X-COORDINATES

.1399E+01 .2592E+01 .3370E+01 .3996E+01 .4538E+01 .5020E+01 .5459E+01 .5865E+01 .6247E+01 .6606E+01
.6945E+01 .7268E+01 .7578E+01 .7876E+01 .8163E+01 .8441E+01 .8709E+01 .8969E+01 .9222E+01 .9468E+01
.1500E+00 .1500E+00 .1500E+00 .1500E+00 .1500E+00 .1414E+01 .1414E+01 .1500E+00 .1500E+00 .1500E+00
.1500E+00 .1424E+01 .1425E+01 .1500E+00 .1500E+00 .2615E+01 .2615E+01 .1500E+00 .1500E+00 .1440E+01
.1440E+01 .1500E+00 .1500E+00 .1500E+00

Y-COORDINATES

.3381E-01 .1239E-01 .6465E-02 .4695E-02 .3143E-02 .2368E-02 .2119E-02 .1782E-02 .1552E-02 .1231E-02
.1016E-02 .9943E-03 .9776E-03 .9617E-03 .9463E-03 .9313E-03 .9169E-03 .9030E-03 .8894E-03 .7761E-03
.8521E-01 .8371E-01 .7237E-01 .7172E-01 .6059E-01 .3090E-01 .2079E-01 .6220E-01 .5128E-01 .4957E-01
.3887E-01 .2254E-01 .1246E-01 .4100E-01 .3045E-01 .1172E-01 .1716E-02 .2116E-01 .1096E-01 .1000E-01
.0000E+00 .1000E-01 .2000E-01 .0000E+00

CUMULATIVE TIME
.1768E+04 .1882E+04 .1995E+04

CUMULATIVE SALT WATER ENTRY INTO WELL
.0000E+00 .0000E+00 .0000E+00

CUMULATIVE SALT WATER LIFTING INTO SUSPENSION
.1040E+01 .1127E+01 .1170E+01

NUMBER OF POINTS LIFTED
130 138 144

X-COORDINATES

.1209E+01 .2484E+01 .3295E+01 .3935E+01 .4491E+01 .4978E+01 .5422E+01 .5832E+01 .6218E+01 .6579E+01
.6922E+01 .7245E+01 .7559E+01 .7857E+01 .8144E+01 .8423E+01 .8693E+01 .8954E+01 .9208E+01 .9454E+01
.1500E+00 .1500E+00 .1500E+00 .1500E+00 .1500E+00 .1226E+01 .1230E+01 .1500E+00 .1500E+00 .1500E+00
.1500E+00 .1240E+01 .1246E+01 .1500E+00 .1500E+00 .2507E+01 .2510E+01 .1500E+00 .1500E+00 .1263E+01

.1268E+01	.1500E+00	.1500E+00	.1500E+00	.1500E+00	.1500E+00	.1279E+01	.1282E+01	.1500E+00	.1500E+00
.1500E+00	.1500E+00	.1293E+01	.1296E+01	.3325E+01	.3325E+01	.1500E+00	.1500E+00	.2532E+01	.2534E+01
.1500E+00	.1500E+00	.1500E+00	.1500E+00	.1315E+01	.1317E+01	.1500E+00	.1500E+00	.3969E+01	.3969E+01
.1500E+00	.1500E+00	.1328E+01	.1329E+01	.1500E+00	.1500E+00	.1500E+00	.1500E+00	.1340E+01	.1343E+01
.2557E+01	.2557E+01	.1500E+00	.1500E+00	.1500E+00	.1500E+00	.1500E+00	.1500E+00	.1360E+01	.1361E+01
.1500E+00	.1500E+00	.3356E+01	.3356E+01	.4528E+01	.4528E+01	.1500E+00	.1500E+00	.1372E+01	.1374E+01
.1500E+00	.1500E+00	.2579E+01	.2580E+01	.1500E+00	.1500E+00	.1500E+00	.1500E+00	.1390E+01	.1391E+01
.1500E+00	.1500E+00	.1500E+00	.1500E+00	.1402E+01	.1403E+01	.5020E+01	.5020E+01	.1500E+00	.1500E+00
.1500E+00	.1500E+00	.4001E+01	.4002E+01	.1418E+01	.1419E+01	.2605E+01	.2605E+01	.1500E+00	.1500E+00
.5465E+01	.5465E+01	.1500E+00	.1500E+00	.3384E+01	.3384E+01	.1500E+00	.1500E+00	.1435E+01	.1435E+01
.1500E+00	.1500E+00	.1500E+00	.1500E+00						

Y-COORDINATES

.1756E+00	.5905E-01	.3264E-01	.2413E-01	.1662E-01	.1269E-01	.1114E-01	.9605E-02	.8183E-02	.6775E-02
.5478E-02	.5216E-02	.5173E-02	.4931E-02	.4791E-02	.4652E-02	.4515E-02	.4378E-02	.4243E-02	.4008E-02
.9033E+00	.8787E+00	.7432E+00	.7380E+00	.6654E+00	.1698E+00	.1583E+00	.6743E+00	.6135E+00	.6052E+00
.5567E+00	.1585E+00	.1469E+00	.5652E+00	.5239E+00	.5773E-01	.4761E-01	.4928E+00	.4603E+00	.1416E+00
.1301E+00	.4573E+00	.4889E+00	.4272E+00	.4249E+00	.3973E+00	.1298E+00	.1186E+00	.3952E+00	.3698E+00
.3684E+00	.3448E+00	.1185E+00	.1075E+00	.3207E-01	.2206E-01	.3434E+00	.3217E+00	.4699E-01	.3687E-01
.3213E+00	.3012E+00	.3006E+00	.2816E+00	.1025E+00	.9175E-01	.2809E+00	.2625E+00	.2365E-01	.1364E-01
.2619E+00	.2443E+00	.9223E-01	.8137E-01	.2436E+00	.2268E+00	.2263E+00	.2100E+00	.8215E-01	.7148E-01
.3675E-01	.2674E-01	.2100E+00	.1943E+00	.1943E+00	.1793E+00	.1796E+00	.1651E+00	.6794E-01	.5741E-01
.1653E+00	.1515E+00	.2199E-01	.1189E-01	.1623E-01	.6124E-02	.1519E+00	.1386E+00	.5882E-01	.4839E-01
.1391E+00	.1262E+00	.2702E-01	.1701E-01	.1269E+00	.1144E+00	.1152E+00	.1032E+00	.4579E-01	.3561E-01
.1038E+00	.9211E-01	.9278E-01	.8119E-01	.3734E-01	.2716E-01	.1257E-01	.2566E-02	.8186E-01	.7050E-01
.7117E-01	.6003E-01	.1339E-01	.3388E-02	.2524E-01	.1514E-01	.1602E-01	.6013E-02	.5047E-01	.3972E-01
.1097E-01	.9630E-03	.4015E-01	.2959E-01	.1181E-01	.1811E-02	.3001E-01	.1964E-01	.1376E-01	.3736E-02
.1991E-01	.9731E-02	.1000E-01	.0000E+00						



CUMULATIVE TIME

.1573E+03 .2186E+03 .3000E+03 .3600E+03 .4800E+03

CUMULATIVE SALT WATER ENTRY INTO WELL

.1072E+02 .2223E+02 .3934E+02 .4950E+02 .8688E+02

CUMULATIVE SALT WATER LIFTING INTO SUSPENSION

.1059E+03 .1425E+03 .1904E+03 .2248E+03 .2938E+03

CUMULATIVE SALT WATER ENTRY BELOW INTERFACE

.0000E+00 .0000E+00 .0000E+00 .0000E+00 .0000E+00

CUMULATIVE SALT WATER LIFTING INTO SUSP. (DIFF)

.2790E+02 .3324E+02 .3899E+02 .4270E+02 .5072E+02

DRAW DOWN

20.3572900

CUMULATIVE TIME

.9600E+03 .1440E+04

CUMULATIVE SALT WATER ENTRY INTO WELL

.8688E+02 .8688E+02

CUMULATIVE SALT WATER LIFTING INTO SUSPENSION

.2953E+03 .2970E+03

CUMULATIVE SALT WATER ENTRY BELOW INTERFACE

.2393E+01 .8665E+01

CUMULATIVE SALT WATER LIFTING INTO SUSP. (DIFF)

.5217E+02 .5389E+02

DRAW DOWN

6.8335670

REFERENCES

1. Ackermann, N.L., and Chang, Y.Y., (1971), " Saltwater interface during ground water pumping ", J. Hydraul. Div., Proc. ASCE, Vol. 97, No.HY2, PP. 223-232.
2. Ackermann, N.L., and Sridurongkatum, P., (1964)," Salt water interface near a fresh-water canal ", J. Hydraul. Div., Proc. ASCE, Vol.90, No.HY6, PP. 97-116.
3. Andrews, R. W., (1981), " Salt-water intrusion in the Costa de Hermosillo, Mexico; A numerical analysis of water management proposals", Ground Water, Vol.19, No.6, PP. 635-647.
4. Appelo, C.A.J., and Willemsen, A., (1987), "Geochemical calculations and observations on saltwater intrusions, 1. A combined geochemical / mixing cell model," J. Hydrol., Vol.94, PP. 313-330.
5. Basak, P., and Rajagopalan, S.P., (1982), "Effect of non-Darcy flow on computing seawater intrusion lengths", J.Hydrol, Vol. 58, PP. 83-87.
6. Bear, J., (1979), " Hydraulics of ground water", McGraw-Hill New York.
7. Bear, J., and Dagan, G. (1964a), " Moving interface in coastal aquifer, " J. Hydraul. Div., Proc. ASCE, Vol. 90, No. HY4, PP. 193-216.
8. Bear, J. and Dagan, G., (1964b), " Some exact solutions of interface problems by means of the hodograph method", J. Geophys. Res., Vol. 69, No.8, PP. 1563-1572.
9. Bear, J., Shamir, U. Gamliel, A., and Shapiro, A.M., (1985)," Motion of the seawater interface in a coastal aquifer by the

- method of successive steady states", J. Hydrol., Vol. 76, PP. 119-132.
10. Bear, J. and Kapuler, I., (1981), "A numerical solution for the movement of an interface in a layered coastal aquifer", J. Hydrol., Vol. 50, PP. 273-298.
 11. Bennett, G.D., and Giusti, E.V., (1971), "Coastal ground water flow near Ponce, Puerto Rico, U.S. Geol. Surv., Prof. Pap. 750-D, PP. D206-D211.
 12. Bennett, G.D., Mundryoff, M.J. and Amjad Hussain, S., (1968), "Electric analog studies of brine coning beneath fresh-water wells in the Punjab Region, West Pakistan", U.S. Geol. Surv. Water Supply Pap. 1608-J, PP. J1-J31.
 13. Bruch, J.C., JR. (1970), "Two-dimensional dispersion experiments in porous medium", Water Resour. Res., Vol.6, No.3, PP. 791-800.
 14. Bush, P.W., (1988), "Simulation of saltwater movement in the Floridan aquifer system, Hilton Head Island, South Carolina", U.S. Geol. Surv. Water Supply Pap. 2331.
 15. Cat, V.M., (1986), "Numerical simulation of saltwater transport towards a pumped well", M.E.Thesis, Dept. of Hydrology, University of Roorkee, Roorkee, India.
 16. Chahill, J.M., (1968), "Hydraulic sand model study of the cyclic flow of saltwater in a coastal aquifer", U.S. Geol. Surv. Prof. Pap. 575-B, PP. 240-244.
 17. Chahill, J. M. (1973), "Hydraulic sand model studies of miscible-fluid flow", U.S. Geol. Surv. Jour. Res., Vol.1, PP. 243-250.
 18. Chandler, R.L. and McWhorter, D.B., (1975), "Upconing of the saltwater -freshwater interface beneath of pumping well",

Ground water, Vol. 13, No.4, PP. 354-359.

19. Charmonmon, S., (1965), "A solution of the pattern of fresh-water flow in an unconfined coastal aquifer", J. Geophys. Res., Vol. 70, No.12, PP. 2813-2819.
20. Collins, M.A. and Gelhar, L.W., (1971), "Sea water intrusion in layered aquifers", Water Resour. Res., Vol.7, No.4, PP. 971-979.
21. Collins, M.A., Gelhar, L.W. and Wilson, J.L., (1972), "Hele-Shaw model of long Island aquifer system", J. Hydraul. Div., Proc. ASCE., Vol.98, No.HY9, PP. 1701-1713.
22. Columbus, N., (1965), "Viscous model study of sea water intrusion in water table aquifers", Water Resour. Res., Vol.1, No.2, PP. 313-323.
23. Contractor, D.N., and Srivastava, R., (1990), " Simulation of saltwater intrusion in the Northern Guam Lens using a microcomputer", J. Hydrol., Vol.138, PP. 87-106.
24. Cooper, H.H., (1959), "A hypothesis concerning the dynamic balance of fresh water and saltwater in a coastal aquifer," J.Geophys. Res., Vol.64, No.4, PP. 461-467.
25. Dagan, G. and Bear, J., (1968), "Solving the problem of local interface upconing in a coastal aquifer by the method of small perturbations", J. Hydraul. Res., Vol.6, No.1, PP. 15-44.
26. Detournay, C. and Strak, O.D.L., (1988) ," A new approximate technique for hodograph method in ground flow and its application to coastal aquifers" ,Water Resour. Res., Vol.24, No.9, PP. 1471-1481.
27. Diersch, H.J., Prochnow, D., and Thiele, M., (1984), "Finite-element analysis of dispersion-affected saltwater

- upconing below a pumping well", *Appl. Math. Modelling*, Vol.8, PP. 305-312.
28. Frind, E.O., (1982a), "Simulation of long-term transient density-dependent transport in groundwater", *Adv. Water Resour.*, Vol.5, PP. 73-88.
 29. Frind, E.O., (1982b), "Seawater intrusion in continuous coastal aquifer aquitard systems", *Adv. Water Resour.*, Vol.5, PP.89-97.
 30. Garde, R.J., and Mirajgaoker, A.S., (1983), "Engineering fluid mechanics", Nem Chan & Bros, Roorkee, India, PP.274-275.
 31. Glover, R.E., (1959), "The pattern of fresh-water flow in a coastal aquifer", *J. Geophys. Res.*, Vol. 64, No.4, PP. 457-459.
 32. Gupta, A.D., (1983), "Steady interface upconing beneath a coastal infiltration gallery", *Ground Water*, Vol.21, No.4, PP. 465-474.
 33. Gupta, A.D., (1985a), "Simulated saltwater movement in the Nakon Luang aquifer, Bangkok, Thailand", *Ground Water*, Vol.23, No.4, PP.512-522.
 34. Gupta, A.D., (1985b), "Approximation of saltwater interface fluctuation in an unconfined coastal aquifer", *Ground Water*, Vol.23, No.6, PP. 783-794.
 35. Gupta, A.D. and Gaikwad, V.P., (1987), "Interface upconing due to a horizontal well in unconfined aquifer", *Ground Water*, Vol.25, No.4, PP. 466-474.
 36. Hantush, M.S., (1968), "Unsteady movement of freshwater in thick unconfined saline aquifers", *Bull. Int. Assoc. Sci. Hydrol.*, Vol.13, No.2, PP.40-60.
 37. Harleman, D.R.F., and Rumer, R.R., (1963), "Longitudinal and lateral

- dispersion in an isotropic porous medium", *J. of Fluid Mechanics*, Vol. 16, PP. 385-394.
38. Haubold, R.G. (1975), "Approximation for steady interface beneath a well pumping fresh water overlying saltwater", *Ground Water*, Vol.13, No.3, PP. 254-259.
 39. Henry, H.R., (1959), "Saltwater intrusion into fresh water aquifers", *J. Geophys. Res.*, Vol. 64, No.11, PP. 1911-1919.
 40. Hoque, M.M., (1987), "Simulation of saltwater upconing in Inland aquifer", *J. Indian Water Resour. Soci.*, Vol.7, No.1, PP. 21-42.
 41. Hubbert, M.K., (1940), "The theory of ground water motion", *J. Geol.*, Vol.48, No.8, PP.785-944.
 42. Huyakorn, P.S., Andersen, P.F., Mercer, J.W., and White, H.O. JR., (1987), "Saltwater intrusion in aquifers; development and testing of three-dimensional finite element model", *Water Resour. Res.*, Vol.23, No.2, PP. 293-312.
 43. Inouchi, K., Kishi, Y., and Kakinuma, T., (1985), "The regional unsteady interface between freshwater and saltwater in a confined coastal aquifer", *J. Hydrol.*, Vol.77, PP. 307-331.
 44. Isaacs, L.T., (1985), "Estimating interface advance due to abrupt changes in replenishment in unconfined coastal aquifer", *J. Hydrol.*, Vol.78, PP. 279-289.
 45. Isaacs, L.T. and Hunt, B., (1986), "A simple approximation for a moving interface in a coastal aquifer", *J. Hydrol.*, Vol. 83, PP.29-43.
 46. Jacob, C.E., (1950), "Flow of ground water", in H.Rous (ed), *Engineering Hydraulic*, Wiley, New York, Chap.5, PP. 321-386.

47. Johnston, R.H., (1983), "The saltwater-freshwater interface in the Tertiary limestone aquifer, southeast Atlantic outer-continental shelf of the U.S.A", *J.Hydrol.*, Vol.61, PP.239-249.
48. Kakinuma, T., Kishi, Y. and Inouchi, K., (1988), "The behaviour of groundwater with dispersion in coastal aquifers", *J.Hydrol.*, Vol.98, PP. 225-248.
49. Kashef, A.I., (1970), "Model studies of saltwater intrusion", *Water Resour. Bull.*, Vol.6, No.6, PP. 944-967.
50. Kashef, A.I., and Smith, J.C., (1975), "Expansion of salt-water zone due to well discharge", *Water Resour. Bull.*, Vol.11, No.6, PP.1107-1120.
51. Kashef, A.I., (1983a), "Salt-water intrusion in the Nile Delta", *Ground Water*, Vol.21, No.2, PP. 160-167.
52. Kashef, A.I., (1983b), "Harmonizing Ghyben-Herzberg interface with rigorous solutions", *Ground Water* Vol.21, No.2 PP. 153-159.
53. Kemblowshi, M., (1985), "Saltwater-freshwater transient upconing - An implicit boundary - element solution", *J. Hydrol.*, Vol.78, PP.35-47.
54. Khaleel, R., and Reddell, D.L. (1985), "Miscible displacement in porous media : MOC solution", *J. of Irrigation and Drainage Engineering*, Vol 111, No. 1, PP. 45-64.
55. Kishi, Y. and Fukuo, Y., (1977), "Studies on salinization of ground water, I. Theoretical consideration on the three-dimensional movement of the saltwater interface caused by the pumpage of confined ground water in fan-shaped alluvium", *J.Hydrol.*, Vol.35, PP.1-29.

56. Kishi, Y., Fukuo, Y., Kakinuma, T., and Ifuku, M., (1982), " The regional steady interface between freshwater and saltwater in a coastal aquifer," J.Hydrol. Vol. 58, PP.63-82.
57. Kohout, F.A., (1960), "Cyclic flow of saltwater in the Biscayne aquifer of southeastern Florida", J. Geophys. Res., Vol.65, No.7, PP. 2133-2141.
58. Konikow, L.F. and Bredehoeft, J.D., (1978), "Computer model of two-dimensional solute transport and dispersion in ground water", U.S. Geol.Survey, Book 7, Chap. C2.
59. Kruseman, G.P., and De Ridder, (1983), "Analysis and evaluation of pumping test data", ILRI, Netherlands PP.97-103.
60. Ledoux, E., Sauvagnac, S., and Rivera, A., (1990) "A compatible single-phase /two phase numerical model; I. Modeling the transient saltwater / freshwater interface motion", Ground Water, Vol. 28, No.1, PP.79-87.
61. Lee, C.-H and Cheng, R.T-sh., (1974), "On seawater encroachment in coastal aquifers", Water Ressour. Res., Vol. 10, No.5, PP. 1039-1043.
62. Lusczynski, N.J. and Swarzenski, W.V., (1960), "Position of the saltwater body in the Magothy formation in the Gedarhurst-Woodmere area of Southwestern Nassau country, Long Island, N.Y.", Econ. Geol., Vol. 55, PP.1739-1750.
63. Lusczynski, N.J. and Swarzenski, W.V. (1962), "Fresh and salty ground water in Long Island, N.Y.", J.Hydraul. Div., Proc. ASCE, Vol.88, No.4, PP. 173-194.
64. McElwee, C.D., (1985), "A model study of salt-water intrusion to a river using the sharp interface approximation", Ground Water, Vol.23, No.4, PP. 465-475.

65. McElwee, C and Kemblowski, M., (1990), "Theory and application of an approximate model of saltwater upconing in aquifers", J.Hydrol., Vol.115, PP. 139 - 163.
66. Mehnert, E., and Jennings, A.A., (1985), "The effect of salinity - dependent hydraulic conductivity on saltwater intrusion episodes", J.Hydrol., Vol.80, PP. 283-297.
67. Mercer, J.W., Larson, S.P. and Faust, C.R., (1980), "Simulation of salt-water interface motion", Ground Water, Vol.18, No.4, PP. 374-385.
68. Mualem, Y. and Bear, J., (1974), "The shape of the interface in steady flow in a stratified aquifer", Water Resour. Res., Vol.10, No.6, PP. 1207-1215.
69. Muskat, M., (1937), "The flow of Homogeneous fluid through porous media", McGraw-Hill Book Company, New York.
70. Nuthrown, D.A., (1976), "Optimal pumping regimes in an unconfined coastal aquifer", J. Hydrol., Vol.31, PP. 271-280.
71. Panigrahi, B.K., Gupta, A.D., and Arbhabhirama, A., (1980)", Approximation for salt-water intrusion in unconfined coastal aquifer", Ground Water, Vol.18, No.2, PP. 147-151.
72. Pinder, G.F. and Cooper, H.H.JR., (1970), "A numerical technique for calculating the transient position of the saltwater front", Water Resour. Res., Vol.6, No.3, PP. 875-882.
73. Polo, J.F., and Ramis, F.J.R., (1983), "Simulation of saltwater - freshwater interface motion", Water Resour. Res., Vol.19, No.1, PP. 61-68.
74. Reilly, T.E., (1990), "Simulation of dispersion in layered coastal aquifer system", J. Hydrol. Vol.114, PP. 211-228.

75. Reilly, T.E., Frimpter, M.H., LeBlanc, D.R., and Goodman, A.S., (1987)", Analysis of steady - state salt - water upconing with application at Truro well field, Cape Cod, Massachusetts", Ground Water, Vol.25, No.2, PP.194-206.
76. Reilly, T.E., and Goodman, A.S., (1987)", Analysis of saltwater upconing beneath a pumping well", J.Hydrol., Vol.89, PP.169-204.
77. Remson, I., Hornberger, G.M., and Molz, F.J., (1971), " Numerical methods in subsurface hydrology", John Wiley, New York.
78. Rubin, H. and Pinder, G.F., (1977), " Approximate analysis of upconing", Adv. Water Resour., Vol.1, No.2, PP. 79-101.
79. Rushton, K.R., and Chan, Y.K., (1976), " A numerical model for pumping test analysis", Proc. Instn. Civ. Engrs., Part 2, Vol.61, PP. 281-296.
80. Rushton, K.R., and Redshaw, S.C., (1979), "Seepage and ground water flow; Numerical analysis by analogy and digital methods", Wiley - Interscience, New York, PP. 32-33.
81. Rumer, JR. R.R., and Harleman, D.R.F., (1963), "Intruded salt-water wedge in porous media", J. Hydraul. Div., Proc. ASCE, Vol.89, No. HY6, PP. 193-220.
82. Rumer, JR., R.R., and Shiau, J.C., (1968), "Saltwater interface in a layered coastal aquifer", Water Resour. Res., Vol.4, No.6, PP.1235-1247.
83. Sahni, B.M., (1973), "Skimming of freshwater afloat upon saltwater", International symposium of development of ground water resources, held from Nov. 26-29, Vol.2, Madras, India, Session IV, PP. 31-42.

84. Scheidegger, A.E.,(1961), "General theory of dispersion in porous media", J. Geophys. Res.,Vol.66, No.10, PP. 3273-3278.
85. Schmorak, S., and Mercado, A., (1969)," Upconing of freshwater - seawater interface below pumping wells, field study " Water Resour. Res., Vol.5, No.6, PP. 1290-1311.
86. Sagol,G. and Pinder, G.F., (1976), "Transient simulation of saltwater intrusion in Southeastern Florida", Water Resour. Res., Vol.12, No.1, PP. 65-70.
87. Segol, G., Pinder, G.F., and Gray, W.G., (1975)", A Galerkin-finite element technique for calculating the transient position of the saltwater front", Water Resour. Res., Vol.11, No.2, PP. 343-347.
88. Shamir, U., and Dagan, G., (1971),"Motion of the seawater interface in coastal aquifers; A numerical solution", Water Resour. Res., Vol.7, No.3, PP. 644-657.
89. Shamir U., and Harleman, D.R.F.,(1967), "Numerical solutions for dispersion in porous medium", Water Resour. Res., Vol.3, No.2, PP. 557-581.
90. Shechter, M., and Schwarz, J. (1970), "Optimal planning of a coastal collector",Water Resour. Res., Vol.6, No.4, PP.1017-1024.
91. Sherif, M.M.,Singh, V.P. and Amer, A.M., (1988), "A two-dimensional finite element model for dispersion (2D-FED) in coastal aquifers", J.Hydrol. Vol.103, PP 11-36.
92. Sikkema,P.C. and Van Dam, J.C.,(1982)," Analytical formulate for the shape of the interface in a semi - confined aquifer", J.Hydrol.,Vol.56, PP.201-220.

93. Srimal, G.K., (1985), "Modelling of saltwater entry into a pumped well", M.E.Theis, Dept. of Hydrology, University of Roorkee, Roorkee, India.
94. Strack, O.D.L., (1976), "A single-potential solution for regional interface problems in coastal aquifers", Water Resour. Res., Vol.12, No.6, PP. 1165-1174.
95. Stringfield, V.T., Warren, M.A., and Cooper, H.H.,JR., (1941)", Artesian in the coastal area of Georgia and Northeastern Florida", Econ. Geol., Vol.36, No.7, PP. 698-711.
96. Todd, D.K., (1980), "Ground water hydrology", 2ed., Wiley, New York.
97. Trescoff, P.C., Pinder, G.F., and Larson, S.P., (1976), "Finite - difference model for aquifer simulation in two dimensions with results of numerical experiments", U.S. Geol. Survey, Chap. C1, Book 7.
98. Van Dam, J.C., and Sikkema, P.C., (1982), " Approximate solution of the problem of the shape of the interface in a semi-confined aquifer", J.Hydrol., Vol.56, PP.231-237.
99. Vandenberg, A., (1975), "Simultaneous pumping of fresh and saltwater from a coastal aquifer", J.Hydrol., Vol.24, PP.37-43.
100. Van der Veer, P., (1977a), "Analytical solution for steady interface flow in a coastal aquifer involving a phreatic surface with precipitation", J.Hydrol., Vol.34, PP. 1-11.
101. Van der Veer, P.(1977b), "Analytical solution for a two-fluid flow in a coastal aquifer involving a phreatic surface with precipitation", J. Hydrol., Vol.35, PP.271-278.

102. Van der Veer P., (1978), "Exact solutions for two-dimensional groundwater flow problems involving a semi-pervious boundary", J. Hydrol. Vol.37, PP. 159-168.
103. Vappicha, V.N., and Nagaraja, S.H., (1976), "An approximate solution for the transient interface in a coastal aquifer", J.Hydrol., Vol.31, PP.161-173.
104. Volker, R.E., and Rushton, K.R.,(1982), "An assessment of the importance of some parameters for seawater intrusion in aquifers and a comparison of dispersive and sharp-interface modelling approaches", J.Hydrol., Vol.56, PP. 239-250.
105. Voss, C.I., and Souza, W.R., (1987), "Variable density flow and solute transport simulation of regional aquifers containing a narrow fresh water - saltwater transition zone", Water Resour. Res., Vol.23, No.10, PP. 1851-1866.
106. Wang, M., and Cheng, R.T., (1975), "A study of convective - dispersion equation by isoparametric finite elements", J.Hydrol. Vol.24, PP.45-56.
107. Warrick, A.W., Biggar, J.W., and Nielsen, D.R., (1971), "Simultaneous solute and water transfer for an unsaturated soil", Water Resour. Res., Vol.7, No.5, PP. 1216-1225.
108. Wirojanagud, P., and Charbeneau, R.J., (1985), "Saltwater upconing in unconfined aquifers", J.Hydraul. Eng. Vol.111, No.3, PP. 417-434.